RECONSTRUCTING PAST ANTARCTIC ICE FLOW PATHS IN THE ROSS EMBAYMENT, ANTARCTICA USING SAND PETROGRAPHY, PARTICLE SIZE AND DETRITAL ZIRCON PROVENANCE

Andrea J. Schilling

Submitted to the faculty of the University Graduate School
in partial fulfillment of the requirements
for the degree
Master of Science
in the Department of Earth Sciences,
Indiana University

March 2010

Accepted by the Faculty of Indiana University, in partial fulfillment of the requirements for the degree of Master of Science.

Kathy Licht, PhD

R. Jeffrey Swope, PhD

Master's Thesis Committee

Joseph Pachut, Jr., PhD

ACKNOWLEDGEMENTS

This product could have not been accomplished without the help of many people.

I first must thank my advisor, Dr. Kathy Licht, without whom this project would not have been possible. Dr. Licht brought me into the Antarctic world and allowed me so many great opportunities; for that I am very grateful. Kathy is truly a remarkable person and I feel very blessed to have her as a mentor and friend. Thank you, Kathy, for having so much confidence in me.

I also am very appreciative to Dr. Jeffrey Swope for his time, support and critiques. Dr. Swope's passion and enthusiasm for science is contagious. Thank you for allowing me my first bit of research (all those black rocks!).

I also want to thank all of the faculty and staff, Dr. Pachut in particular, and the Earth Science department for their input and support.

A huge thanks to all my friends, fellow graduate and undergraduate students at IUPUI for sharing these past few years.

To Matthew Hennessy, for being a great lab partner and always being there to make me laugh! Thank you, Matt, for all of your support, understanding and of course, your voice of reason.

Last, but definitely not least, I want to thank my family. My parents, Steve and Carla Schilling, have always been there for me with unlimited support and encouragement. Without their love and constant support I would not be where I am today. Thank you, Mom and Dad, for believing in me. To my brother, Chris, who motivates me by his dedication. We are happy to have you home. To my sister, Maggie, who inspires me by her ambition and resilience. Thank you for always being there.

This research was funded by the IUPUI Research Support Funds Grant.

ABSTRACT

Andrea J. Schilling

Reconstructing past Antarctic ice flow paths in the Ross Embayment, Antarctica using sand petrography, particle size and detrital zircon provenance

Tills for this study were analyzed from sites in East Antarctica (EA), West Antarctica (WA) and along a transect in the Ross Sea. Particle size, sand petrography, and detrital zircons were used to provide new information on the subglacial geology of Antarctica, as well as assisting in the reconstruction of Last Glacial Maximum (LGM) ice flow paths. Statistical analyses using the Kolmogorov-Smirnov (K-S test) reveal that EA and WA zircon age distributions are distinct at a P-value <0.05. This makes it possible to trace the unique signatures from EA and WA into the Ross Sea.

The majority of Bindschadler and Whillans Ice Stream samples are dominated by polymict grains and silt and clay, while Kamb is dominated by sand and only three of the four cores are polymict rich. WA ice streams (Kamb, Bindschadler, and Whillans, all contain Ross age (550-500 Ma) and Grenville age (1100-1000 Ma) populations. Kamb and Bindschadler contain a young zircons age population (~100 Ma), whereas Whillians Ice Streams is missing the ~100 Ma age populations but contains a ~230 Ma age population.

The presence of the low sand, the felsic-intermediate igneous lithic fragments and unique U-Pb ages observed in till samples taken from Mount Howe and Davis Nunatak indicate that subglacial material is being transported from East Antarctic sites and deposited at Mount Howe and Davis Nunatak. All EA samples collected at the head and middle of major EA outlet glaciers contain grains whose age of formation is consistent with the Ross Orogeny and all samples showed small age populations scattered

throughout the Proterozoic. The most noteworthy peaks occur from the Permian through the Triassic. EA outlet glacier samples, Beardmore Glacier (BG), Davis Nunatak (DN), Bates Nunatak (BN), and Cloudmaker (CM) (all where Beacon Group rocks have been mapped) match age populations from previous published Beacon samples of ~240-270 Ma. This may suggest that the signature from the Beacon Supergroup may be identifiable. These outlet samples are a representation of material being transported into the TAM. The fingerprint of each outlet glacier will be altered as it crosses the TAM, resulting in more Ross age material. Three anomalously young zircons (19.4± 0.9, 25± 0.9 and 23.1± 0.5) were found at the head of the Scott Glacier from Mt. Howe (MH).

All of the Ross Sea samples contain age populations consistent with the Ross Orogeny; however the samples show spatial variability in the age distribution of the Mesozoic grains. The Central Eastern and Eastern Ross Sea has a ~100 Ma population which is consistent with the age populations seen at Kamb and Bindschadler Ice Streams. This suggests that the ice flow of the West Antarctic Ice Sheet (WAIS) was confined to the region during the Last Glacial Maximum (LGM). The Ross Sea also displays a spatial geographic boundary at the 170° with the presence of polymict rich till, as well as clay type (smectite and illite). More research needs to be done in order to determine the significance of the clay type with respect to polymict formation and preservation.

Kathy Licht, PhD

TABLE OF CONTENTS

List of Tables

List of Figures

List of Appendices

INTRODUCTION

Antarctica is divided by the Transantarctic Mountains (TAM) into the larger, slow-flowing East Antarctic Ice Sheet (EAIS) and the smaller, less stable West Antarctic Ice sheet (WAIS) that contains areas of fast moving ice called ice streams (Alley and Bindschadler, 2001) (Fig. 1). These ice streams are 40 km-wide areas of ice that flow up to two orders of magnitude faster than the surrounding ice. Warming temperatures and rising sea level may increase the instability of the WAIS, escalating the potential for a catastrophic collapse of the ice sheet. A total collapse would result in about 6m of sea level rise, causing irreversible damage to coastal cities around the world (Alley and Bindschadler, 2001). Constraining the behavior and extent of the WAIS during the Last Glacial Maximum (LGM), approximately 17,000 years ago, is essential to developing accurate models of ice sheet behavior. Till provenance as determined by coarse sand fraction, mineral composition, and further constrained by U/Pb ages of detrital zircons is one method for constraining past ice movements and thus models. U/Pb ages of detrital zircons can also be used to learn about the geology of ice covered regions.

Zircons are resistant to physical and chemical weathering, found in an array of rock types, and contain a variety of elements such as, U, Th, Pb, and Hf, making them ideal for geochronology and provenance studies (Reiners, et al., 2004). Zircon U-Pb geochronology procedure is the most commonly used technique and is based on the radioactive decay series of ^{238}U into ^{206}Pb ($t_{1/2}$= 4.5 billion years) which gives insight into the age of zircon crystallization or high grade metamorphism (>900°C). Zircons are also used in the Double Dating Technique. As ^{238}U is being broken down in zircons to form ^{206}Pb, radiogenic He is also being produced as a decay product. The U-Th-He system has a closure temperature for He around 170°C to190°C (Reiners, et al., 2004) and therefore, can be affected by shallow burial. When the zircon has reached its closure temperature, the He stops diffusing out of the mineral and the concentration begins to build up. Measuring this concentration gives the age since it cooled below 170°C to190°C and so is used to gain information about the timing and rate of exhumation for that zircon.

This project describes sand petrography, particle size, U-Th-Pb, and U-Th-He detrital zircon data of till samples from the Ross Embayment of Antarctica. Specifically, samples from beneath West Antarctic (WA) ice streams, samples from moraines at the head of East Antarctic (EA) outlet glaciers (Strickland Nunatak, Mt. Howe, Davis Nunatak, and Beardmore Glacier) from the mouth (Karo Hills) and mid-glacier (Cloudmaker) and from a transect along the front of the Ross Ice Shelf were evaluated (Fig. 1). Upstream or source area samples were compared to the Ross Sea samples to identify similarities and differences. This was done in order to place constraints on the area of convergence between the two ice sheets which extended across the Ross Sea during the LGM, thus providing additional constraints on the size of the WAIS relative to the EAIS at the LGM with implication for the past extent of WA ice streams.

Physical Setting

Antarctica is 98% covered by ice, holds about 70% of the world's fresh water, and is extremely important to global climate and ocean circulation patterns. It is divided by the 3,500 km long Transantarctic Mountains (TAM) into two segments, East and West Antarctica (Goodge, 2006). East Antarctica is a stable, land-based ice sheet, primarily resting on bedrock above sea level, while West Antarctica is a potentially unstable, marine-based ice sheet, grounded below sea level over large areas. The majority of the EAIS that drains into the Ross Embayment flows via outlet glaciers through the TAM, whereas most of the ice in WA draining into the Ross Sea occurs through fast moving ice streams unconstrained by bedrock (Fahnestock and Bamber, 2001). The glacial till transported from these regions gives a window to what is under the EAIS and the WAIS (e.g., Licht et al., 2005; Farmer et al., 2006).

The East Antarctic shield is thought to be one of the oldest geologic terrains on Earth (Goodge et al., 1999). The EA craton began its formation in the Early Archean and concluded in the Middle Proterozoic (e.g., Borg et al., 1987; Elliot, 1975; Grikurov, 1982; Black et al., 1983). Much of what is known about the geology of EA relies on exposures found in the TAM and other small outcrops around the EAIS perimeter. In the TAM, the major units exposed consist of the Nimrod, Beardmore, Byrd, Granite Harbor Intrusive, Beacon, Ferrar, and McMurdo Volcanics Groups, which vary in age from the Precambrian to the Quaternary (Tingey, 1991).

Much of West Antarctica formed as a rift basin much later in the Mesozoic and Cenozoic, with its displacement totaling several hundred kilometers between Marie Byrd Land and EA (Winberry and Anandakrishnan, 2004). The majority of the West Antarctic Rift Basin is occupied with basin fill sediments shed from adjacent areas of the TAM and Marie Byrd Land (Denton and Hughes, 2002). The major outcrop exposures in Marie Byrd Land are the Marie Byrd Land Volcanics group that range in age from the Cretaceous to the Cenozoic (Tingey, 1991).

The TAM rocks exposed are adjacent to WA and date in age from the Neoproterozoic to the Paleozoic, which are younger than the East Antarctic shield and older than the WA basin (e.g. Goodge and Fanning, 2002). Due to the different age terrains of WA and EA, the detrital zircon ages in till derived from these regions are expected to be distinctly different. In the WA basin, we expect to find younger aged zircons in areas near Marie Byrd Land and a mix of ages typical of Marie Byrd Land and of TAM in sediment from the sites closer to the TAM. The EA sample sites were selected at the head of the glaciers, rather than the mouth, in an effort to chacterize the distribution of material from the EA interior relative to the TAM rocks. This sampling approach should maximize the possibility of differentiating between the two ice sheets.

Geologic History

East Antarctica

The first known orogenic event was the Napier Orogeny which occurred approximately 4000 Ma (Fig. 2; Table 1) (Sobotovich et al., 1976; Grikurov, 1982; Kamenev, 1982; and Ravich, 1982; Anderson, 1999). This orogeny has been associated with the formation of the cratonic core of Antarctica. Following the Napier Orogeny was the Rayner Orogeny (~3500 Ma) (Fig. 2; Table 1) which began to thicken the crust of East Antarctica (Grikurov, 1982; Ravich, 1982a and b; Anderson, 1999). Evidence from the Napier and Rayner Orogenies can be observed in Enderby and Kemp Lands in East Antarctica (Tingey, 1991). U-Pb ages from zircons found in this these rock units range from 3800 Ma to 1980 Ma (Tingey, 1991).

The Humbolt Orogeny followed the Rayner Orogeny about 3000 Ma (Fig. 2)(Grikurov, 1982). Rocks affected by this orogeny are observed in Queen Maud Land and in MacRobertson Land (Fig. 2; Table 1). The Insel Orogeny about 2650 Ma is linked to the formation of new crust from the re-working of older crust and is characterized by amphibolite grade metamorphism (Fig. 2; Table 1). Exposures of rock affected by this orogeny can also be seen in Queen Maud Land as well as the southern Prince Charles Mountains (Tingey, 1991; Anderson, 1999). Approximately 2000-1700 Ma, the Early Ruker Orogeny occurred and is associated with many sediment filled non-magmatic intracratonic basins located in the Prince Charles Mountains (Fig. 2; Table 1) (Grikurov, 1982; Tingey, 1982; Anderson, 1999).

Transantarctic Mountains

In the central TAM, from the Byrd to the Reedy Glacier, the major rock units exposed are (from Precambrian to Quaternary) the Nimrod, Beardmore, La Gorce, Byrd, Wyatt, Ackerman, Granite Harbor Intrusive, Beacon, Ferrar, and McMurdo Volcanics (Tingey, 1991). The Nimrod Group (3150-3000 Ma) outcrops at the head of the Nimrod Glacier and is a high-grade metamorphic complex composed of schist, banded quartzofeldpathic to mafic gneiss, amphibolite, and areas of ultramafic rocks (Goodge et al., 2001). This rock unit probably forms the basement of the TAM and is a result of the Humbolt Orogeny (~3150-3000 Ma) which was then metamorphosed by the Insel Orogeny (~2500 Ma). Further magmatism and metamorphism occurred during the Nimrod Orogeny (1730-1720 Ma), followed by a time of quiescence and clastic sedimentation after ~1700 Ma (Goodge and Fanning, 2002). Age data within the Nimrod Group reveals a Precambrian history overprinted by younger Ross events. The pre-Ross zircon ages of 3290-3060 Ma have been obtained from gneisses and schist (Bennett and Fanning, 1993; Goodge and Fanning, 1999) as well as whole-rock Nd-model ages of 3100-2720 Ma (Borg et al., 1990; Borg and DePaolo, 1994). The Upper Precambrian Beardmore Group overlies the Nimrod Group and consists of peltic schist, hornfels, conglomerate, phyllite, marble and metagraywacke (Myrow et al., 2002; Goodge et al., 2002). Detrital zircon ages from this the Beardmore Group range from 2810-610 Ma (Goodge et al., 2004). The La Gorce Formation, found in the Queen Maud and Horlick Mountains around Scott Glacier, consists of a sequence of folded greywacke and aluminum rich metamorphic rocks (Stump, 1995). It is thought that this sequence is equivalent in age to the Beardmore Group (upper Precambrian) (Stump, 1995).

The period of quiescence, since 1700 Ma, ended ~1000 Ma with the Late Ruker Orogeny, equivalent to the Grenville Orogeny, and is associated with the formation of Rodina, which caused widespread plutonism and metamorphism (Grikurov, 1982; Anderson, 1999; Li et al., 2008). The uplift associated with this orogeny is associated with magmatic re-working and partial melting of metamorphic and plutonic basement rocks, as well as metamorphism along the initial Pacific margin in East Antarctica. Following the Late Ruker Orogeny was the Beardmore Orogeny (633-620 Ma) which can be seen as old folded rock units in the central TAM (Elliot, 1975). Igneous activity, coupled with the Beardmore Orogeny, is seen mainly as pyroclastics that overly greywacke units found in Queen Maud Land, the Horlick Mountains and the Theil Mountains (Anderson, 1999).

The Ross Orogeny (550-500 Ma) is associated with the formation of Gondwana, when the paleo- Pacific plate subducted beneath the East Antarctic craton (e.g., Borg et al. 1990; Stump, 1995). Sediments that accumulated within basins underwent metamorphism, deformation, and felsic igneous intrusions, which termed the Granite Harbor Intrusives. The Granite Harbor Intrusive Complex (Cambrian-Ordovician) is observed in outcrops along the TAM. U-Pb ages of 520-500 Ma were found for the

Granite Harbor Intrusives in the central TAM (Borg et al., 1990; Tonarini and Rocchi, 1994). Rb-Sr ages range from 470 and 510 Ma in the Granite Harbor Intrusives located in southern Victoria Land (Tonarini and Rocchi, 1994). This formation also includes gabbro, granite, granodiorite, and quartz monzonite (Borg, 1983; Stump, 1995). Effects of the Ross Orogeny can be observed throughout the TAM. The Ross Orogeny ceased by ~500 Ma and was followed by a time of quiescence and erosion (Borg, 1983; Stump, 1995).

At the surface of the Cambrian collisional margin, carbonate siliclastic sediments were deposited to form the Byrd Group. The Shackleton Limestone is the lowermost unit of the Cambrian Byrd Group and includes limestone, oolitic limestone, and marble and the upper unit includes quartzite, shale, sandstone, and conglomerates (Goodge et al., 2004). The Bryd group and consists of sedimentary and metasedimentary rock units derived from eroding Granite Harbor Intrusives and older units. Above the Byrd group and localized near Scott Glacier, the Wyatt formation (~526 Ma), a massive, silicic porphyry, intrudes the La Gorce Formation (619-581 Ma) (Stump, 1995; Stump et al., 2007). The Ackerman Formation, a clastic sequence, overlays the Wyatt Formation. The Ackerman Formation has been difficult to date but is correlated with porphyry formations in the Thiel Mountains which have been dated at ~500 Ma (Stump, 1995).

The Beacon Supergroup (Devonian- Middle Triassic) represents a time of mostly clastic sedimentation and consists of tillites, glacial fluvial sediments, and a sequence of sandstone, shale, and coal which is intruded by the Jurassic Ferrar dolerite sills (Tingey, 1991; Barrett, 1991). The Ferrar Group also consists of basalt, tuff, and volcanic conglomerates and has U-Pb age of ~183.6+/-1.8 Ma (Encarnación, 1996). Lastly, the

McMurdo Volcanic Group, dated ~30 Ma (Behrendt et al., 1996), is a widespread volcanic complex extending from eastern Victoria Land into the western Ross Sea and includes rhyolites and basalts and is associated with rifting and the formation the bulk of the WA basin (Kyle, 1990). As an exception to the ~30 Ma basalts, Cenozoic olivine basalts (~19 Ma) have been found in EA at the head of Scott Glacier at Sheridan Bluff (Stump et al., 1980).

West Antarctica

Most of West Antarctica is a rift basin formed in the Middle Cretaceous through the Cenozoic with horizontal displacement totaling several hundred kilometers between Marie Byrd Land and EA (Fig. 2) (Winberry and Anandakrishnan, 2004). Major extension began in the Cretaceous about 105 Ma (Siddoway, 2008). Arc magmatism is recorded in Marie Byrd Land at this time. A latter period of major extension also occurred throughout the Cenozoic, with 150 km of extension recorded in the Eocene-Oligocene time (Siddoway, 2008). During the Eocene, the TAM were being uplifted and shedding sediments into the rift basin (tenBrink et al., 1997; Fitzgerald, 2002; Siddoway, 2008). The present day West Antarctic Rift Basin is occupied by thick basin fill sediments, up to 600 m, shed from adjacent areas of the TAM and Marie Byrd Land (Rooney et al., 1991; Denton and Hughes, 2002). The major rock outcrop exposures in WA are limited to Marie Byrd Land and consist of the Paleozoic Swanson Formation, and Ford Granodiorite, the Mesozoic Byrd Coast Granites, and the Cretaceous to Cenozoic Marie Byrd Land Volcanics (Tingey, 1991). The immature metasediments of the Swanson Formation have been dated by detrital zircons as being ~500 Ma (Pankhurst et al., 1998). The Swanson Formation is intruded by the Ford Granodiorite which has been dated at ~375 Ma (Pankhurst et al., 1998). The Byrd Coast Granite was emplaced following the Ford Granodiorite from 124-95 Ma (Siddoway, 2008; Pankhurst et al., 1998). The Mount Prince Granite was emplaced along the Ruppert and Hobbs Coasts, and has been dated at ~110 Ma (Mukasa and Dalziel, 2000). Edward VII Peninsula Granites formed next from 95-100 Ma (Weaver et al., 1994). Ages found in the Marie Byrd Land Volcanics range from 25-30 Ma (Tingey, 1991) and are composed of basaltic flows overlain by felsic and intermediate flows, which are overlain by basaltic cinder cones and tuff cones (Le Masurier and Rex, 1991).

Summary of Geologic Setting

The rock exposures in the TAM range in age from the Neoproterozoic to Lower Mesozoic, and are likely much younger than the East Antarctic shield, but largely older than the bedrock within the WA basin (Goodge and Fanning, 2002). The detrital zircon ages found in a sedimentary rock unit do not necessarily reflect the depositional ages of the unit. The zircons can be older or younger depending on the environment in which they reside. For example, detrital zircons can be younger than its depositional age if the rocks were subsequently metamorphosed to temperatures >900°C (Lee et al., 1997). More commonly, most detrital zircons are older than the depositional age because they have been eroded from older rock units

Due to the different ages of WA and EA, the detrital zircon ages for rocks collected in the terrains are expected to have distinct age ranges and patterns. In the WA basin, we expect to find Mesozoic to Cenozoic detrital zircons derived from igneous rocks, as well as ages associated with Late Mesozoic crustal extension and the Cenozoic volcanic rocks in areas near Marie Byrd Land. Intermediate ages are expected from

TAM sediment in the sites closer to the TAM. In East Antarctica, we expected to find mostly Archean to Cambrian aged detrital zircons which would be associated with the creation of the EA craton and the uplift of the TAM. An exception to this would be the Beacon Supergroup because it is siliclastic sediments accumulated by erosion of East and West Antarctic terrains.

PREVIOUS RESEARCH

Previous studies have emphasized the value and importance of determining Antarctica's glacial history over the past 50,000 years. Stuvier et al. (1981) attempted to model past ice flow paths of EAIS and WAIS at the LGM. They suggested that the majority of the ice flow into the Ross Sea was a result of WAIS expansion (Fig. 3). Licht and Fastook (1998) presented a more balanced model of past ice flow paths, suggesting that the EAIS and the WAIS contributed about equally to the maximum extent of ice at the LGM (Fig. 3). The data collection in this proposed provenance study will be useful to distinguishing between these two models of ice flow.

Anderson et al. (1992) used sand petrography and heavy mineral separations to characterize variability in sediment composition between parallel troughs on the seafloor. They found that each trough was identifiably different, which suggested that the ice in each trough flowed from a seperate area of different composition, making it possible to trace each trough back onto the continent; however this study lacked samples from these potential source areas. Later work by Shipp et al. (1999) and Mosola and Anderson (2006) used multibeam and sidescan sonar data to identify megascale glacial lineations in the Ross Sea providing indirect evidence that streaming ice extended into the Ross Sea during the LGM. The results of these studies suggest that specific LGM ice stream flow paths may be constrained by examining the composition of the source area, the downstream deposits, and the glacial morphology of the Ross Sea floor.

More recent work provides further constraints on ice flow with the addition of samples from the East and West Antarctic source areas (Licht et al., 2005; Farmer et al., 2006). They analyzed coarse sand fractions and the Sm-Nd isotopic signature of the <63 μm fraction of till from EA outlet glacier samples and from beneath the WA ice streams and found these source tills to be distinctly different. The source area tills were then compared to the Ross Sea tills to determine its provenance. Both the sand and isotopic datasets suggested a confluence of West and East Antarctic ice in the central Ross Sea. However, only four samples were available from the WA ice streams and no samples were available for several of the major EA outlet glaciers.

Detrital zircon analyses have been used in EA to study till provenance and movements down one outlet glacier, but have not yet been attempted on WA till samples. Palmer (2008) used detrital zircons from till samples collected from Byrd Glacier, EA, and from the Ross Sea, to determine if U-Th-Pb zircon age distributions could be traced downstream. One central Ross Sea site, ELT27-14, was identified as a statistical match to Byrd Glacier, while an adjacent sample, NBP94-07-39 showed a very different age distribution (Fig. 4). This suggests that these two Ross Sea samples are from different source areas and thus are tentatively interpreted to represent a boundary between the EAIS and WAIS. However, no data were available from WA to confirm this hypothesis.

METHODS

Sample Acquisition

Till samples were collected from EA and WA sites in order to define the distinguishing characteristics of each source area. Nine sub-ice stream samples were selected from Whillans, Kamb, and Bindschadler ice stream sediment cores (Fig. 1; Table 2) collected in the 1992-1999 field seasons by researchers at the California Institute of Technology (Kamb and Engelhardt). Each till sample integrated material over a 2-5cm interval. Six EA samples, collected in 2006-2007, were selected from the head of the Reedy, Scott and Beardmore Glaciers. These may provide an example of what is being eroded upstream from the unexposed bedrock of EA. An additional sample was taken from a moraine at the mouth of Scott Glacier (Karo Hills) and another sample was taken from a moraine in the middle of Beardmore Glacier (Cloudmaker). The sites are modern ice cored moraines. At each site, material was collected a few centimeters beneath the surface to minimize the effects of wind erosion (deflation). Nine LGM- age till samples from six Ross Sea cores that were collected in seafloor troughs along a transect near the Ross Ice Shelf front (Fig. 1), were obtained from the Antarctic Research Facility at Florida State University. Each of these sample integrated material over a 2-5 cm interval.

Detrital Zircon Separation

Samples were separated into magnetic and non-magnetic mineral fractions using a Frantz Isodynamic Magnetic Separator model L-1 in the PRIME lab at Purdue University. This was done in order to eliminate the magnetic minerals, many which have a density of >2.85g/ml, that complicate the following process.

The 0.063-0.149 mm non-magnetic fraction from till samples were separated using a lithium heteropolytungstates (LST) heavy mineral separation technique. The LST used for these separations, supplied by Central Chemical Consulting, has a density of 2.85 g/ml and viscosity of about 11 cP. Approximately 25-30ml of LST was placed in a labeled plastic centrifuge tube with the entire non-magnetic 0.063-0.149mm fraction. The solution was shaken and allowed to sit overnight. After settling, the bottom portion of the centrifuge tube was placed in liquid nitrogen in order to freeze and isolate the dense grains. The unfrozen material (<2.85 g/ml) was poured over a 25 micron sieve in a funnel and allowed to drain into a beaker labeled 'light'. The frozen material (> 2.85g/ml) was thawed and poured into a 25 micron sieve in a funnel and allowed to drain into a beaker labeled 'heavy'. The light and heavy material was allowed to dry and the heavy material was sent to the Arizona LaserChron Center where zircons were handpicked. A second group of samples (0.063-0.149 mm fraction) were sent to the Arizona LaserChron Center and heavy mineral and zircon separation was done using heavy liquids at their facility (Gehrels et al., 2008). All zircons were mounted in 2.54 cm diameter epoxy plugs, sanded through 1/3 of the thickness of the zircon crystals, then polished with 9 micron grit and photographed (Gehrels et al., 2006).

U-Th-Pb Analysis

U and Pb isotopic compositions of zircons were analyzed by laser ablation multicollector inductively coupled plasma mass spectrometry (LA-MC-ICPMS) at the Arizona LaserChron Center following the method of Gehrels et al. (2006). The analyses involve ablation of zircon with a New Wave/Lambda Physik DUV193 Excimer laser (operating at a wavelength of 193 nm) using a spot diameter of 20 microns. Helium carries the ablated material into the plasma source of a GVI Isoprobe ICP-MS, which contains a flight tube of adequate width that U, Th, and Pb isotopes are measured at the same time. All measurements are made in static mode, using 10^{11} ohm faraday detectors for ^{238}U, ^{232}Th, ^{208}Pb, and ^{206}Pb, a 10^{12} ohm faraday collector for ^{207}Pb, and an ion-counting channel for ^{204}Pb. Ion yields are ~1.0 mv per ppm. Each analysis consists of one 20-second integration with the laser off (for backgrounds), 20 one-second integrations with the laser firing, and a 30 second wait to flush out the previous sample and prepare for the next. The resulting ablation pit is ~15 microns in depth.

Common Pb correction was done by using the measured ^{204}Pb and assuming an initial Pb composition from Stacey and Kramers (1975) (Gehrels et al., 2006). Uncertainties of 1.0% for $^{206}Pb/^{204}Pb$, 0.3% for $^{207}Pb/^{204}Pb$ and 2.0% for $^{208}Pb/^{204}$ Pb are used for the composition of the common Pb. Measuring ^{204}Pb accurately can be difficult because of the high amount of ^{204}Hg present in the argon plasma gas. Our measurement of ^{204}Pb is not affected by the occurrence of ^{204}Hg because the backgrounds are measured on peaks, and any of the background of ^{204}Hg and ^{204}Pb is subtracted.

Every fifth measurement a standard, a Sri Lanka zircon crystal, was used with known age of 564 ± 4 Ma (2-sigma error) was used to correct for the fractionation of Pb isotopes, generally ~2% (Gehrels et al., 2006). The uncertainty resulting from the calibration correction is generally 1-2% (2-sigma) for both $^{206}Pb/^{207}Pb$ and $^{206}Pb/^{238}U$ ages. Interpreted ages are based on $^{206}Pb/^{238}U$ for < 1000 Ma grains and on $^{206}Pb/^{207}Pb$ for > 1000 Ma grains (Gehrels et al., 2006). Analyses that are > 30% discordant (by comparing $^{206}Pb/^{238}U$ and $^{206}Pb/^{207}Pb$ ages) are not considered further.

The resulting interpreted ages for either sample are shown on normalized probability diagrams. For most detrital zircon samples (n ≥ 100), significant age populations are only defined as clusters with three or more overlapping analyses (Gehrels et al., 2006). Normalized probability plots are formed by calculating a normal distribution for each age from the data, summing the probability distribution of all accepted analyses, and dividing the area under the curve by the number of analyses. The peak heights are a function of the number of grains at a particular age and the precision associated with that analysis.

The interpreted ages are also analyzed using the Kolmogorov-Smirnov test (K-S test). This is a statistical test used to compare distributions to determine their similarity. The K-S test compares the cumulative distribution functions (Fig. 5). Specifically, the K-S test compares the maximum probability difference between two cumulative distribution functions or the maximum vertical differences between the curves. If this observed difference, D_{obs}, is greater than some critical value, D_{crit}, the null hypothesis, that the populations are statistically similar, is accepted and the two samples most likely came from the same population. The critical value, D_{crit}, depends on the number of samples in the distribution (n) and the desired confidence level (α) (Guynn, 2006). This test was used to compare age population distributions to determine if they are statistically different at a 95% level of confidence.

The "P" value gives the probability that two samples were drawn from the same population. The null hypothesis was accepted when the "P" value exceeded 0.05.

U-Th/He Analysis

Double dating with U-Th-He was done on 27 individual zircon grains selected from three U-Pb populations (Grenville, Ross, and ~230Ma) to examine differences or similarities in their cooling ages. Twenty seven zircons, >60um width, were retrieved out of the epoxy pucks following the U/Pb analysis. The epoxy pucks were covered with a layer of alcohol to help in controlling the movement of the crystals and a clay pin tool was used to gently push the crystals up and out of the epoxy. Each zircon crystal was photographed and the length, width, and height were documented. The crystal was then carefully turned over 90 degrees using tweezers and the width, length, and height were documented for a second time. The abrasion index, a value of 1-5, for each crystal was documented, as well as important observations of grain shape that would affect the alpha correction for each crystal (i.e. broken crystal tip, inclusions, etc). Each crystal was placed in a 1mm Nb tube, sealed completely and placed in a stainless steel planchet. Each Nb tube was heated at least two times to 1200-1300°C for 15 minutes in order to insure that ^{4}He was quantitatively extracted and yielded less than 1-2% in the second re-extraction (Reiners et al., 2004). The Fish Canyon Tuff standard (28 Ma) was run after every four laser extractions (approximately every 2 samples). The Nb foil packets were spiked with a low U-Th solution and dissolved. U and Th were then measured by isotopic dilution on a single collector sector ICP-MS and ^{3}He/^{4}He ratio was determined (Reiners et al., 2004).

Sand Petrography Analysis

Grain mounts were prepared using approximately a 3 g representative sub-sample of the 500-2000 um sand fraction from each till sample. A 0.91 mL Buehler Epo-thin® resin/11 mL Buehler Epo-thin® hardener mixture was combined to produce the resin compound and was poured over the sand grains housed in the ice cube tray and allowed to harden for twenty-four hours, to form ‘pucks’. The pucks containing the sand grains were removed from the ice cube trays and the bottom-side of each puck was polished using 600 and 1000 grit silicon carbide polishing compound, exposing the sand grains.

Once exposed and polished, the puck was cemented to a standard thin section slide using a 3/8-gram resin to 1/8-gram hardener ratio of Epo-thin® low-viscosity epoxy and allowed to set for approximately twenty-four hours. The excess sample pucks were removed using a Buehler ® Petrothin and polished with 1000 grit silicon carbide to approximately 30um.

Point counts were made using a Leitz® Laborlux 11 POL S petrographic microscope fitted with a Leitz® Wetzlar point counting stage. Every grain in each slide was counted (~300 grains per slide) using the Indiana Point Counting Method (Suttner, 1974) in order to account for lithology and mineralogy of each sample (Table 3).

Particle Size Analysis

Approximately two grams of the bulk till sample was used for particle size analysis. Each sample was sieved in order to remove the >2000 µm size fraction. In order to remove the organic material from the < 2000 µm material, five mL of 35% H_2O_2 was added to the material and was heated on a hot plate on low heat for 15 minutes and on high heat for 15 minutes. This heating procedure was done approximately three times. After cooking, 8 mL of 25-g/mL magnesium chloride was added to the sample. The sample was then wet sieved through a 125 µm sieve. The > 125 µm material was examined under a Leica MZ95 stereoscope and any remaining organic matter was removed by hand. The entire sample was placed in a 600 mL beaker, rinsed with deionized water, and allowed to settle for twenty-four hours. After settling, the water was siphoned off and the remaining sediment was recombined in a 50 mL centrifuge tube and centrifuged for ~15 minutes at 8000 rpm. After centrifuging, water was decanted and 20 mL of a 25g/mL sodium metaphosphate dispersant was added. The samples were split using an ELE sample splitter into 1/4 or 1/8 splits depending on the size fraction present and analyzed on the Malvern Mastersizer 2000 Laser Particle Size Analyzer three times and averaged to limit any inconsistencies.

RESULTS

East Antarctica

Particle Size

Particle size was determined from four new East Antarctic (EA) sample sites (expanding the much larger regional dataset (Fig. 6; Table 4)). Two EA sites, Strickland Nunatak and Beardmore Glacier, have >70% sand, Davis Nunatak has 47% sand and Mount Howe has only 20% sand. All sites but Strickland Nunatak are mapped as Beacon Supergroup. Downstream, Karo Hills has 82% sand and Cloudmaker has 65% sand. Karo Hills and Cloudmaker have similar amounts of silt but Cloudmaker has more clay than Karo Hills. Samples from Mount Howe and Karo Hills were compared to samples from Byrd Glacier. Mount Howe and Lonewolf and Lonewolf 2 (Palmer, 2008) are both mapped as Beacon Supergroup (Doumani and Minshew, 1965; Grindley and Laird, 1969) and both were observed to have thicker till accumulations than other sites on EA plateau. Lonewolf and Lonewolf 2 have 30-46% sand content and 34-42% silt content (Palmer, 2008), while Mount Howe has 33-44% silt content and 35-40% clay content (Kramer, 2008). Karo Hills' particle distribution is similar to Byrd Glacier lateral moraine sites that are also mapped as Granite Harbor Intrusive, such as Crazy Jim (CJ) and Horny Bluff (HB), with the majority of the sample being composed of sand with minor amounts of silt and clay (Palmer, 2008).

Sand Petrography

Strickland Nunatak is mapped as an unknown metamorphic (Davis and Blankenship, 2005) and sand petrography from two samples shows that this site is dominated by quartzite and quartz (Fig. 7; Table 5 (Kramer, 2008)). Mount Howe is mapped as Beacon Supergroup (Doumani and Minshew, 1965) and >80% of both till samples is split between felsic/intermediate igneous lithics and sedimentary rock fragments plus quartzite. Both Mt. Howe samples contain sand-sized polymicts. Polymicts are clay sized balls of till that have been associated with streaming ice (Kramer, 2008). Minor amounts mafic igneous grains are observed in Mount Howe samples. The bedrock adjacent to Karo Hills is Granite Harbor Intrusive and is composed mainly of quartz, other metamorphics, and felsic and intermediate igneous lithic fragments (Stump et al., 1980; Stump et al., 2007). Beardmore Glacier (individual site) is dominated by siltstone, sandstone, limestone and quartzite lithic grains and is mapped as Beacon Supergroup (Borg et al., 1990; Goodge, et al, 2002). Davis Nunatak is dominated by siltstone, sandstone, quartzite, and felsic and intermediate lithic grains but is mapped as just Beacon Supergroup (Borg et al., 1990; Tingey, 1991). Cloudmaker is solely composed of siltstone, sandstone, and polymict and is mapped as Beacon Supergroup (Barrett, 1991; Goodge, et al., 2002).

U-Th-Pb

A total of 661 detrital zircons were analyzed from 6 East Antarctic sample sites (Fig. 8; Appendix A). Replicate sample sets were analyzed from Strickland Nunatak and Mount Howe. The two samples from Strickland Nunatak were collected on the same moraine, while Mount Howe samples were collected on different moraines. Sample 1691 was collected on the outermost moraine and sample 1690 was collected on the next inner moraine. Strickland Nunatak and Mount Howe were analyzed using the K-S test and Strickland Nunatak was found to have a p-value of 0.375 and Mount Howe samples had a p-value of 0.173 (Table 6). Therefore, the sites were combined to increase the number grains from each location.

All EA samples contain grains whose age of formation is consistent with the Ross Orogeny (~500 Ma) and all samples showed small age populations scattered throughout the Archean and Proterozoic (Figs. 8 and 9). Noteworthy peaks occur from the Permian through the Triassic (~240-270 Ma) at all sites where Beacon is mapped (Beardmore Glacier, Davis Nunatak, Cloudmaker, Mount Howe). Three anomalously young zircons (19.4± 0.9, 25± 0.9 and 23.1± 0.5) were found at the head of the Scott Glacier from Mt. Howe.

West Antarctica

Particle Size

The particle size data collected for Bindschadler and Whillans Ice Stream tills are very similar (Fig. 6; Table 4). These tills are dominated by a high percentage of silt size material (34-42%), and typically have <26% sand size material. In contrast, and as noted by Kramer (2008), three of the four Kamb Ice Stream samples are >78% sand.

Sand Petrography

The majority of Bindschadler and Whillans Ice Stream till samples are dominated by polymict grains (Fig. 10). Bindschadler contained 60-68% polymicts and Whillans contained 68-81% polymicts (Table 5). The second most abundant category at Bindschadler was 9-19% quartz grains and 8-15% quartz at Whillans. Kamb Ice Stream till was dominated by quartz (26-30%) and felsic and intermediate igneous grains (18-30%). Three samples from Kamb (1771, 1772, and 1773) contained <2% polymict grains, while one sample (1774) contained ~ 28% polymict grains (Kramer, 2008).

U-Th-Pb

A total of 549 detrital zircons were analyzed from Whillans, Kamb and Bindschadler ice streams (Fig. 11; Appendix A). There were multiple samples from each ice stream. Kamb 1772 and Kamb 1773 showed some variability with the main difference being that Kamb 1773 contained more Mesozoic grains than Kamb 1772 (Appendix A). However, the other samples are statistically indistinguishable between the sites, showing that the ice streams do not contain significant down core variability (Table 7). For between site comparisons, all data from a given ice stream were combined to make a single age distribution (Fig. 11). Each ice stream contained a significant age population at the Grenville Orogeny (1300-1000 Ma) as well as a peak at the Ross Orogeny (~500 Ma). Kamb and Bindschadler Ice Stream contain a ~100 Ma peak while Whillans Ice Stream does not contain a peak at this age (Fig. 11).

Ross Sea and RISP

Particle Size

The particle size data collected from the Ross Sea till shows similar results between sample sites (Fig. 6; Table 4). Samples are dominated by the silt size fraction (37-54%), followed by clay size (26-39%), and smaller amounts of the sand size fraction (10-29%).

Sand Petrography

The sand petrography data collected form the Ross Sea varies spatially from the Eastern Ross Sea to the Western Ross Sea (Fig. 12; Tables 5 and 8). The Eastern Ross Sea and RISP samples are dominated by quartz, quartzite, and felsic to intermediate igneous lithic grains with no mafic grains observed. The Western Ross Sea samples are dominated by polymict grains (33-67%) with lesser amounts of quartz, felsic and intermediate grains, and metamorphic lithic grains.

U-Th-Pb

A total of 502 detrital zircons were analyzed from 6 cores in the Ross Sea (Fig. 13; Appendix A). All of the Ross Sea samples contain age populations consistent with the Ross Orogeny (~500 Ma); however the samples show spatial variability in the content of Mesozoic grains. The Eastern and East Central Ross Sea have a ~100 Ma age population which is consistent with the age populations seen at Kamb and Bindschadler Ice Streams. This peak is absent in the cores west of the 180° longitude.

Between Site Kolmogorov-Smirnov Analysis

Statistical analyses using the Kolmogorov-Smirnov (K-S test) reveal that EA and WA zircon age distributions are distinct at a P-value <0.05 (Table 9). Because ice streams do not show variability down core, U-Pb data were combined to increase the number of grains per ice stream. The K-S test was applied and shows that each ice stream is distinguishable from one another (Table 10). It was also determined that there was no significant variability down core in the Ross Sea samples (Table 11). Therefore, the U-Pb data were combined for each core to increase the number of grains representing that core.

Mount Howe and Karo Hills, both of which are part of Scott Glacier, were tested with the K-S test. It was found that Mount Howe and Karo Hills have a p-value of 0.00 and so could be distinguished from eachother (Table 12). Assuming that the material from Mount Howe is a representation of the subglacial material and that Karo Hills is a representation of what is being eroded from the local bedrock, the two sites were combined to form a sample for Scott Glacier. This sample was then compared to cores in the Ross Sea (Table 13). The Scott Glacier sample is indistinguishable from 3 of the 4 cores in the Western Ross Sea.

Beardmore, Davis Nunatak, and Cloudmaker, all which are part of Beardmore Glacier, were tested with the K-S test. Beardmore and Davis Nunatak are assumed to be a representation of the subglacial material and that Cloudmaker is a representation of what is being eroded from the local bedrock mid glacier. No sample exists at the mouth of Beardmore Glacier. The samples were combined and compared to cores in the Ross Sea (Table 14). The Beardmore Glacier sample is indistinguishable from 2 of the 4 cores in the Western Ross Sea.

U-Th/He Analysis

A part of this study was using zircon double dating to determine provenance (Campbell et al., 2005). U-Th/He was used in combination with U-Pb ages to identify subgroups within three significant U-Pb age populations. Grains from Kamb Ice Stream, Whillians Ice Stream, Beardmore Glacier, Mt. Howe, Strickland Nunatak and Davis Nunatak were selected for use in this pilot study (Fig. 14; Table 15). Of the grains with U-Pb age 1000-1100 Ma, two subgroups were identified with U-Th/He ages of ~280-330 Ma and 85-162 Ma. The subgroups for U-Pb age of 500-600 Ma were less distinct but cluster at 240 Ma, 110-160 Ma, and a single grain at 65 Ma. Finally, for the grains with a U-Pb age ~250 Ma, all clustered with U-Th/He ages of 137-170 Ma.

The Ross Embayment He and U-Pb ages were plotted against the Prydz bay area He and U-Pb ages (Fig. 15) (data compliments of Peter Reiners). These areas have similar U-Pb ages but the Ross Embayment U-Th/He ages are much younger than the Prydz Bay U-Th/He ages.

DISCUSSION

What is the bedrock source of the till?

Some East Antarctic (EA) sites are consistent with locally derived material (rock types exposed at the nearest outcrop), while others contain evidence for a non-local component. The high sand fraction of sample sites along Strickland Nunatak and Beardmore Glacier indicates an immature sediment, probably derived from a near by source of material. Downstream sites, Karo Hills and Cloudmaker, also contain high sand content, suggesting that the material is locally derived. Strickland Nunatak, Beardmore Glacier, Cloudmaker, and Karo Hills sand petrography is mostly similar to the mapped rock types. In contrast, the low sand content of EA samples from Davis Nunatak and Mount Howe suggests that the till from these samples are derived, at least partially, from material eroded subglacially from the interior of EA. Mount Howe and Davis Nunatak are both mapped as Beacon Supergroup, and both contain felsic to mafic igneous lithic grains in the sand fraction. This indicates a different rock type upstream beneath the East Antarctic Ice Sheet (EAIS). The petrographic data combined with zircon ages 500-600 Ma suggest there are more buried Ross-aged granites which are widely seen throughout the Transantarctic Mountains (TAM). Mount Howe zircon data also contains an unique ~25 Ma age peak (Fig. 8). Sheridan Bluff has the most 'interior' Cenozoic basalts of anywhere in the Ross Embayment but this site is downstream from Mount Howe. The evidence from detrital zircons (~23 Ma) age plus observations of vesicular basalt (Townsend et al., 2009) suggest that Cenozoic basalt is buried upstream of Mount Howe. Davis Nunatak zircon data contains a ~677 Ma peak (Fig. 8) that is not found else where in EA, also suggesting the material found at Davis Nunatak is non-locally derived.

One complication to using zircons to identify subglacial rock types is the possibility of getting recycled grains out of the Beacon Supergroup. Elliot and Fanning (2008) studied three bedrock samples collected from the Beacon Supergroup at Shackleton Glacier and found a common age peak of ~247-268 Ma (Fig. 16). EA samples from Beardmore Glacier, Davis Nunatak, Cloudmaker, and Mount Howe have been mapped as Beacon Supergroup and all contain a common peak of ~240-270 Ma. Elliot and Fanning (2008) linked these ages to West Antarctic (WA) bedrock, which implies it is derived from the West Antarctic foreland basin in the Permian-Triassic (Collinson et al., 1994; Elliot and Fanning, 2008). Interestingly, the WA till samples lack this as a dominant peak. With more sampling it may be possible to identify the Beacon signature in tills throughout samples in Antarctica.

The WA basin is filled with up to 600m of sediment (Rooney et al., 1991). The provenance of tills described in this study can help identify the origin of the sediments filling up the WA basin. Through the K-S test, WA ice streams zircon ages were found to be statistically distinct at a P-value <0.05. This contradicted with what was seen in the visual curve of the age peaks as well as the overlap and similarity analysis. The overlap and similarity analysis was done on the ice streams to determine how they were different to one another (Table 16; Fig. 17). The analysis showed that the ice streams did have ages that overlapped but the distribution of those ages were different and therefore, failed the K-S test. Each ice stream contained a significant age peak at the Grenville Orogeny (1300-1000 Ma) as well as a peak at the Ross Orogeny (550-500 Ma). However, Kamb and Bindschadler Ice Streams contain a ~100 Ma peak while Whillans Ice Stream does not contain a peak at this age. Mukasa and Dalziel (2000) found 101-110 Ma U-Pb ages in granitoids and felsic and intermediate dike swarms along the Ruppert and Hobbs coasts of western Marie Byrd Land. The zircon ages found in Kamb and Bindschadler and in the Ruppert and Hobbs coasts suggest that the bedrock from Marie Byrd Land, or the sediments shed from it, extend further under the ice to the catchment of these two ice streams. Bindschadler Ice Stream contains many more Mesozoic and Cenozoic grains than Whillans Ice Stream (Fig. 17, 18). Whillans Ice Stream contains a Ross Age peak at ~520 Ma similar to that of SN and KH. Taken together, the older grains and ~520 age peak, is evidence of a TAM source for Whillans Ice Stream. These differences in sand petrography, amount of ploymicts and quartz, and U-Pb age suggest that with high enough sampling density, it may be possible to trace each WA ice stream fingerprint into the Ross Sea.

Bindschadler and Whillans Ice Stream are dominated by a high percentage of silt size material suggesting that the till seen is likely a result of a glacial deposit formed under a previous glacial time (Tulaczyk et al., 1998). In contrast, three of the four Kamb Ice Stream samples are >78% sand, suggesting a closer source of material for Kamb Ice Stream (Kramer, 2008). It may also suggest the process of sorting took place by way of water at the bed of Kamb Ice Stream.

Downstream Transport

Tracking similarities from source areas, EA and WA, to the Ross Sea is one way to help understand downstream transport. Through the use of the K-S test on zircon ages, it was found that Mount Howe was statistically similar to one core in the Western Ross Sea and Karo Hills was not considered similar to any Ross Sea core. Mount Howe, which is at the head of Scott Glacier, and Karo Hills, which is at the mouth of Scott Glacier, were combined in an attempt to determine the signature for Scott Glacier. This signature was compared to the signature in the Ross Sea. The K-S test showed that Scott Glacier was similar to two of the three cores in the Western Ross Sea (Table 13). Interesting, Scott Glacier was considered 'not similar' to the core ELT27-14. ELT 27-14 is very close in location to ELT 32-21 and ELT 32-20, which were shown to be statistically similar to one another through the K-S test. The overlap and similarity analysis was also used to determine the distinguishing difference between ELT27-14 and Scott Glacier (Table 17; Fig. 19). The analyses showed ELT27-14 to have a high overlap with Scott Glacier (0.814) and a high similarity of those overlaps (0.796). This finding suggests that the reason ELT27-14 failed the K-S test was a result of ELT 27-14 and Scott Glacier have a different distribution of ages.

Since creating a simple mixture of the two sites, the head of the glacier and side of the glacier, may create a better match to Ross Sea tills it appears that the subglacial load of Scott Glacier may be a mix of EA interior plus locally eroded material. A similar pattern was observed for the entire Beardmore Glacier. Beardmore Glacier (individual site), Davis Nunatak, and Cloudmaker were combined to create a signature for Beardmore Glacier. The combined Beardmore Glacier zircon distribution was found to be significantly similar through the K-S test to one core in the Western Ross Sea, ELT 27-14. Because ELT32-20 and ELT32-21 very close in location to ELT 27-14, the overlap and similarity analyses were used to determine the missing component in ELT32-20 and ELT32-21 (Table 18; Fig. 20). It was found that ELT32-20 and ELT32-21 has a very high overlap with Beardmore Glacier (0.875- 0.756) and those overlaps were found to be very similar (0.803-0.806). This suggests that the distribution of ages at Beardmore Glacier and ELT32-20 and ELT32-21 are different, which is why the cores failed the K-S test.

The combining of samples to form an entire glacier assumes a simplistic approach by combining all grains from each sample site. This approach also assumes an accurate and complete representation of the Transantarctic Mountains geology by the downstream samples, Karo Hills and Cloudmaker in this case. Geochemistry modeling and additional sampling would assist in determining more of the EA signature.

What is the source of till at the LGM in the Ross Sea?

Comparisons of the percent quartz, feldspar (plagioclase and k-spar), and mafic igneous lithic fragments within the coarse sand fraction revealed a pattern between sample locations (Fig. 21). The pattern shows that East Antarctica, Western Ross Sea and three Central Ross Sea samples have a more mafic component which is absent in West Antarctica, Eastern Ross Sea, and the remaining Central Ross Sea samples. A comparison of percent quartz, feldspar, and mafic igneous lithic fragments within the coarse sand fraction from Palmer (2008), Kramer (2008), and this study show a similar pattern, where the mafic component is only seen in East Antarctica, Western Ross Sea, and a few in the Central Ross Sea samples (Fig. 22). Conversely, the West Antarctica ice streams were found to contain 80-90% quartz (Kramer, 2008). The Central Ross Sea plots between the two groups, suggesting that the Central Ross Sea is receiving input from both East Antarctic Ice Sheet and West Antarctic Ice Sheet. This finding supports the proposed model by Licht and Fastook (1998) and Denton and Hughes (2002) that there was a convergence of West Antarctica and East Antarctica ice in the Central Ross Sea at the Last Glacial Maximum (Fig. 3).

Through the K-S test comparing various till samples age distributions it was found that the West Antarctic ice streams are statistically different from the Eastern Ross Sea (with the exception of core NBP99-02-17). Because the sand petrography from previous studies and this study suggested otherwise, a cumulative probability plot was done on the ice stream and Eastern Ross Sea data (Fig. 17). It was found was found that proportions of the young ~100 Ma peaks are different between sites. Core NBP94-07-39 has 50% of its ages below ~500 Ma, while NBP94-07-63 has only 30% of its data below 500Ma and 25% of its data below 250 Ma. Bindschadler has higher proportions of older grains than the other samples. Although the proportion of the ~100 year old peaks is different between ice streams and the Ross Sea (Fig. 18), these distinctive peaks suggest that the ice flow of the West Antarctic Ice Sheet was confined to the Eastern Ross Sea region during the Last Glacial Maximum. This finding is consistent with the ice flow model proposed Licht and Fastook (1998) and Denton and Hughes (2002) (Fig. 3).

Through the K-S test, the Ross Sea cores NBP99-02-17 and ELT 32-20 were found to be statistically not dissimilar in zircon age distribution to nearly every sample (Table 9). Preliminary analysis suggests that these samples are statistically not dissimilar nearly every other sample because they contain a very broad ~500 Ma peak, covering approximately 100 million years (Fig. 13; Table 9). Because of the extremely broad peaks and the amount of ~500 Ma grains all of the samples contain, it is logical that the samples would be statistically similar. Therefore, these particular cores are deemed not useful for this study.

Velocity

Polymicts have been suspected to form in the presence of water under streaming ice, due to their abundance beneath the West Antarctic ice streams (Kramer, 2008). Whillians and Bindschadler ice streams contain >59% polymicts. Three samples from Kamb only contained <2% and one sample contained ~27%. Kramer (2008) suggested that the small percentage of polymicts noted within Kamb Ice Stream was an indication of its shutdown approximately 200 years ago.

The Ross Sea sand petrography indicates a sharp boundary in the abundance of polymicts (Fig. 12). The Eastern Ross Sea (with the exception of core NBP94-07-39) contain only 1-4% polymict, while the Western Ross Sea tills contain 8-61% polymict (Table 5). This division in the Ross Sea at 170° could be a result of a clay type coming from West Antarctica compared to East Antarctica. A study by Balshaw (1981) found a geographic boundary of clay type in Ross Sea tills. Sites East of 170° were composed of the clay mineral, smectitie and sites west of 170° were dominated by illite. These observations suggest that the type of clay, in addition to water at the bed, may be the culprit in the formation and/or preservation of these polymicts. However, the formation and preservation of polymicts remains unresolved.

CONCLUSION

Zircons are resistant to physical and chemical weathering, found in an array of rock types, and have been proven to be very useful in this provenance study. The patterns and distributions of age populations, tested with statistical analyses, provide important information related to provenance. By combining zircon ages from East Antarctica sites to create an entire glacier signature and statistically testing the data was useful in determining ice flow directions. This is also useful in determining more of the subglacial geology of East Antarctica. It is important to understand that the statistical tests do not capture everything so looking at the tests to determine if it makes geological sense is essential.

It is important to identify unique peaks in a population. For example, the overall pattern of the West Antarctic ice streams would have yielded limited results in 'matching' the Eastern Ross Sea, but the ~100 Ma peak identified in Kamb and Bindschadler Ice streams was important in reflecting ice flow direction into the Eastern Ross Sea. The double dating technique, which incorporates the U-Pb and U-He, may further assist in separating and identifying unique zircon signatures of the till.

The presence of the low sand, the felsic-intermediate igneous lithic fragments and unique U-Pb ages observed in till samples taken from Mount Howe and Davis Nunatak indicate that subglacial material is being transported from East Antarctic sites and deposited at Mount Howe and Davis Nunatak. West Antarctic ice stream samples have been associated with cores confined in the Eastern Ross Sea at the Last Glacial Maximum (LGM). Specifically, because of the presence of unique young (~100 Ma) peaks seen the samples of Bindschadler and Kamb Ice Stream, as well as those from cores in the Eastern

Ross Sea. The potential combining of the U-Pb ages at the mouth and heads of East Antarctic Glaciers to better define the source of the Ross Sea tills was demonstrated by combining samples to form representations of entire glaciers such as, Scott Glacier and Beardmore Glacier.

The spatial geographic boundary of the polymict rich till samples, found in the Ross Sea, and the clay types could prove to be a useful province tool. More research needs to be done in order to determine the significance of the clay type with respect to polymict formation and preservation. Analysis of clay may also serve to better demonstrate the estimate the extent of West and East Antarctic ice at the LGM.

Table 1: Geologic Events in Antarctica.

Global Orogenic Event	Antarctic Tectonic Event	Age	Location	Reference
	WA Volcanism	30-25 Ma	Marie Byrd Land	Tingey, 1991
	Uplift of TAM*	55-34 Ma	TAM*	ten Brink et al., 1997; Fitzgerald, 2002; Siddoway, 2008
	WA Extension	83-70 Ma	Marie Byrd Land	Siddoway, 2008
Gondwana Break up (~130 Ma)	WA Extension	105-90 Ma	Marie Byrd Land	Siddoway, 2008
Gondwana Formation (~500 Ma)	Ross Orogeny	550-500 Ma	TAM*	Borg et al. 1990; Stump, 1995
Pan-African Orogeny (500-700 Ma)	Beardmore Orogeny	633-620 Ma	Central TAM*	Elliot, 1975
Formation of Rodinia (750-1100 Ma)	Late Ruker Orogeny	~1000 Ma	TAM*	Grikurov, 1982; Licht et al. 2008
Grenville Orogeny (1000-1300 Ma)	Nimrod Orogeny	1730-1720 Ma	TAM*	Goodge et al., 2001
Wopmay Orogeny (1800-1900 Ma) Trans-Hudson Orogeny (1900-2000 Ma)	Early Ruker Orogeny	2000-1700 Ma	Prince Charles Mountains	Grikurov, 1982; Tingey, 1982; Anderson, 1999
	Insel Orogeny	~2650 Ma	Queen Maud Land and S. Prince Charles Mountains	Tingey, 1991; Anderson, 1999
	Humbolt Orogeny	~3000 Ma	Queen Maud Land and MacRobertson Land	Grikurov, 1982
	Rayner Orogeny	~3500 Ma	Enderby and Kemp Lands	Grikurov, 1982; Ravich, 1982b; Anderson, 1999
	Napier Orogeny	4000+-200Ma	Enderby and Kemp Lands	Sobotovich et al., 1976; Grikurov, 1982; Kamenev, 1982; Ravich, 1982; Anderson, 1999

*TAM= Transantarctic Mountains

Table 2: Latitude , longitude and sampling information for the Ross Sea, West Antarctic Ice Streams, and East Antarctica samples.

Ross Sea Samples						
Site Name	**SAL #**	**Latitude**	**Longitude**	**Sampling Depth (cm)**	**Water Depth (m)**	
NBP94-07-39	278	-77.924	-177.982	53	694	
NBP99-02-17	141	-77.716	-161.862	105	715	
NBP94-07-63	142	-77.327	-169.181	113	582	
NBP94-07-63	164	-77.327	-169.181	53	582	
NBP99-02-04	296	-78.151	-168.58	53	618	
ELT 32-20	1638	-77.585	174.918	65	728	
ELT 32-21	1640	-77.933	178.013	56	680	
RISP 78-14	222	-82.22	-168.38	100	587	
ELT 27-14	1634	-77.8	177.333	48	761	
ELT-27-14	1635	-77.8	177.333	64	761	
ELT 27-14	1637	-77.8	177.333	167	761	
West Antarctic Ice Stream Samples						
Site Name	**SAL #**	**Latitude**	**Longitude**	**Sampling Depth (cm)**	**Elevation (mamsl)**	
Whillians IS	1744	-83.45	-137.76	30-40	334	
Whillians IS	1750	-83.45	-137.76	110-120	334	
Whillians IS	1755	-83.45	-137.76	180-190	527	
Kamb IS	1771	82.43	-135.95	180-190	527	
Kamb IS	1772	82.43	-135.95	140-150	527	
Kamb IS	1773	82.43	-135.95	40-50	527	
Kamb IS	1774	82.43	-135.95	30-40	527	
Bindschadler IS	1775	-81.067	-140.005	<100	493	
Bindschadler IS	1776	-81.067	-140.005	<100	493	
East Antarctic Glacier Samples						
Site Name	**SAL #**	**Latitude**	**Longitude**	**Sampling Depth (cm)**	**Elevation (m)**	**Adjacent Bedrock**
Strickland Nunatak	1659	-86.488	-124.719	Surface	2086	Unnamned Metamorphic
Strickland Nunatak	1660	-86.488	-124.719	Surface	2086	Unamned Metamorphic
Mt. Howe	1690	-87.351	-149.926	Surface	2401	Beacon Supergroup
Mt. Howe	1691	-87.351	-149.926	Surface	2401	Beacon Supergroup
Davis Nunatak	1694	-85.631	-167.303	Surface	2379	Beacon Supergroup
Beardmore Glacier	1654	-85.308	-164.749	Surface	2247	Beacon Supergroup
Cloudmaker	183	-85.407	-166.235	30-60cm	~2200	Ferrar Dolerite and Beacon Supergroup
Karo Hills	1700	-85.007	-154.007	Surface	111	Granite Harbor Intrusive

Table 3: Point count classification scheme.	
Sedimentary Lithic Fragments	Lithic Fragment mineral classification criteria
Silt/Sandstone	Grains with distinct boundaries sand/silt size grains May contain some matrix
Mudstone	Contain silt and clay-sized particles Difficult to determine exact composition
Claystone	No discernable grain boundaries
Polymict	Lithic fragment consists of unspecified clast surrounded by fine- grained matrix may or may not be lithified
Intrusive Igneous Fragments	Large crystals and obvious boundaries
Felsic	Quartz + K-spar ± plagioclase, biotite, hornblende, muscovite
Intermediate	± Quartz + > 50% plagioclase + minor K-spar ± hornblende, biotite, clinopyroxene
Mafic	> 50% plagioclase + orth/clinopyroxene ± olivine, iron oxide
Extrusive Igneous Fragments	± Large crystals with matrix of smaller elongate angular crystals
Basalt ± Andesite ± Rhyolite	Multiple zoned and/or twinned plagioclase ± fibrous glass ± opaque minerals ± volcanic glass ± clinopyroxene
Metamorphic Fragments	
Quartzite	Intergrowth of quartz crystals
Marble	Twinned calcite
Schist	Grains that exhibit fabric

Table 4: Particle Size data from East Antarctica, West Antarctica, and the Ross Sea.

East Antarctica										
	Location	SN* 1659	SN* 1660	MH* 1690	MH* 1691	KH 1700	DN 1694	BG 1654	CM 183	
Total % Sand		**79.0**	**91.3**	**27.1**	**20.1**	**82.1**	**46.8**	**72.4**	**65.1**	
Total % Silt		**13.4**	**6.5**	**33.1**	**44.5**	**11.9**	**21.8**	**16.7**	**15.1**	
Total % Clay		**7.6**	**2.3**	**39.8**	**35.5**	**6.0**	**31.4**	**10.9**	**19.8**	
West Antarctica										
	Location	WIS 1744*	WIS 1750*	WIS 1755*	KIS 1771*	KIS 1772*	KIS 1773*	KIS 1774*	BIS 1775*	BIS 1776*
Total % Sand		**20.7**	**41.0**	**25.1**	**83.8**	**78.4**	**83.1**	**19.5**	**26.0**	**22.3**
Total % Silt		**41.6**	**34.4**	**35.9**	**13.2**	**17.0**	**14.4**	**53.0**	**41.4**	**42.3**
Total % Clay		**37.7**	**24.6**	**39.1**	**3.1**	**4.6**	**2.6**	**27.5**	**32.5**	**35.4**
Ross Sea		**141**	**142**	**278**	**1640**	**1634**	**1637**	**1638**	**222**	
	Location	NBP99-02-17***	NBP94-07-63***	NBP94-07-39	ELT32-21**	ELT27-14**	ELT27-14**	ELT32-20**	RISP***	
Total % Sand		**20.9**	**28.4**	**29.4**	**21.6**	**11.4**	**9.8**	**18.6**	**21.8**	
Total % Silt		**40.2**	**36.8**	**38.7**	**45.5**	**54.3**	**52.6**	**51.7**	**52.0**	
Total % Clay		**39.0**	**34.8**	**32.0**	**33.0**	**34.4**	**37.6**	**29.7**	**26.2**	
***= Data from Kramer (2008)**										
****= Data from Palmer (2008)**										
*****= Data from Lederer (2003)**										

Table 5. Percentage data from point counts made on each thin section

Location	Depth (cm)	Sample ID	Counted by		qtz	pyrox	kspar	plag	biot	chlor	opq	other/ unk.	poly	silt/s.s.	mudst	extr	maf	int	fel	meta	n =
West Antarctic Samples																					
Whillans Ice Stream	10-20	SAL 1755	KLK		11.9	0.0	0.0	3.1	0.0	0.0	0.3	0.0	68.3	0.0	0.0	0.0	0.0	0.0	7.8	8.6	360
89-1-4	30-40	SAL 1754	KLK		13.4	0.0	0.0	2.5	0.0	0.0	0.0	0.0	72.8	0.0	0.0	0.0	0.0	0.0	3.3	8.0	276
	40-50	SAL 1753	KLK		12.3	0.0	0.0	3.0	0.0	0.0	0.3	0.0	72.0	0.0	0.0	0.0	0.0	0.0	7.3	5.3	400
	80-90	SAL 1752	KLK		11.5	0.0	0.0	1.6	0.0	0.0	0.3	0.0	65.9	0.0	0.0	0.0	0.0	0.0	4.9	15.7	364
	110-120	SAL 1751	KLK		13.1	0.0	0.0	1.4	0.2	0.0	0.0	0.0	76.0	0.0	0.0	0.0	0.0	0.0	4.5	4.8	420
	130-140	SAL 1750	KLK		8.4	0.0	0.0	1.7	0.3	0.0	0.6	0.0	79.2	0.0	0.0	0.0	0.0	0.0	3.5	6.4	346
	140-150	SAL 1747	KLK		12.4	0.0	0.0	1.7	0.6	0.0	0.0	0.0	72.1	0.0	0.0	0.0	0.0	0.0	3.4	9.8	348
	150-160	SAL 1745	KLK		11.2	0.0	0.0	2.0	0.0	0.0	0.0	0.0	74.8	0.0	0.0	0.0	0.3	0.0	3.9	7.8	357
	160-170	SAL 1744	KLK		15.5	0.0	0.0	1.0	0.0	0.0	0.0	0.0	73.4	0.0	0.0	0.0	0.0	0.0	2.8	7.2	387
	180-190	SAL 1743	KLK		12.0	0.0	0.0	1.1	0.0	0.0	0.4	0.0	81.3	0.0	0.0	0.0	0.0	0.0	2.2	3.0	267
				Average	12.2	0.0	0.0	1.9	0.1	0.0	0.2	0.0	73.6	0.0	0.0	0.0	0.0	0.0	4.4	7.6	
				STNDEV	1.8	0.0	0.0	0.7	0.2	0.0	0.2	0.0	4.6	0.0	0.0	0.0	0.1	0.0	1.8	3.5	
Kamb Ice Stream	30-40	SAL 1774	KLK		26.8	0.0	3.8	0.6	0.0	0.0	0.0	0.0	27.9	0.0	0.0	0.0	0.0	0.5	18.2	22.2	308
96-3-1	40-50	SAL 1773	KLK		30.3	0.0	5.1	2.4	2.0	0.0	0.0	0.0	0.3	0.0	0.0	0.0	0.0	2.7	23.1	34.0	294
	140-150	SAL 1772	KLK		29.2	0.0	4.8	1.3	2.2	0.0	0.0	0.0	1.3	0.0	0.0	0.0	0.0	2.6	28.2	30.1	312
	180-190	SAL 1771	KLK		30.0	0.0	4.0	2.2	2.2	0.0	0.0	0.0	1.4	0.0	0.0	0.1	0.0	4.0	25.6	30.7	277
				Average	29.0	0.0	4.4	1.6	1.6	0.0	0.0	0.0	7.8	0.0	0.0	0.0	0.0	2.4	23.8	29.3	
				STNDEV	1.6	0.0	0.6	0.8	1.1	0.0	0.0	0.0	13.5	0.0	0.0	0.1	0.0	1.4	4.2	5.0	
Bindschadler Ice Stream		SAL 1775	AJS		19.1	0.0	0.0	0.0	0.0	0.0	2.5	0.0	59.9	5.1	1.9	0.0	0.0	0.0	6.4	5.1	196
98-2-1-1		SAL 1776	AJS		9.2	0.0	1.6	1.6	0.0	0.5	1.6	0.0	67.6	4.3	0.0	0.0	0.0	0.0	4.3	9.2	210
				Average	14.1	0.0	0.8	0.8	0.0	0.3	2.1	0.0	63.7	4.7	1.0	0.0	0.0	0.0	5.3	7.1	
				STNDEV	7.0	0.0	1.1	1.1	0.0	0.4	0.7	0.0	5.4	0.5	1.4	0.0	0.0	0.0	1.4	2.9	
Reedy Glacier																					
Quartz Hills		SAL 1628	KLK		19.1	0.0	6.4	19.9	2.8	0.8	0.0	0.4	0.0	0.0	0.0	0.0	0.0	0.0	48.6	1.2	251
Quartz Hills		SAL 1629	KLK		11.9	0.0	10.3	18.4	2.2	0.5	0.0	0.0	0.0	0.0	0.0	0.0	0.0	0.0	55.7	1.1	185
Quartz Hills		SAL 1630	KLK		25.3	0.0	20.9	23.2	4.7	1.3	0.0	0.0	0.0	0.0	0.0	0.0	0.0	0.0	24.0	0.3	383
Quartz Hills		SAL 1631	KLK		21.7	0.0	24.5	11.1	2.9	1.3	0.0	0.3	0.0	0.0	0.0	0.0	0.0	0.0	37.3	0.3	314
				Average	19.5	0.0	15.5	18.2	3.1	1.0	0.0	0.2	0.0	0.0	0.0	0.0	0.0	0.0	41.4	0.7	
				STNDEV	5.7	0.0	8.6	5.1	1.1	0.4	0.0	0.2	0.0	0.0	0.0	0.0	0.0	0.0	13.8	0.5	
Caloplaca Hills		SAL 1632	KLK		15.2	0.0	8.7	12.2	10.4	0.0	0.0	0.9	0.0	0.0	0.0	0.0	0.0	0.0	49.1	3.0	230
Metavolcanic Mountain A		SAL 1643	KLK		9.1	0.0	7.5	0.0	0.4	0.0	0.0	0.0	0.0	0.0	0.0	0.0	0.0	2.8	73.6	6.7	254
Metavolcanic Mountain B		SAL 1644	KLK		7.4	0.0	13.3	0.0	1.8	0.0	0.0	0.0	0.0	0.0	0.0	0.0	0.0	1.0	63.3	13.3	392
Metavolcanic Mountain C		SAL 1645	KLK		5.6	0.0	10.1	0.0	0.0	0.0	0.0	0.0	0.0	0.0	0.0	0.0	0.0	0.7	75.7	8.0	288
				Average	7.3	0.0	10.3	0.0	0.7	0.0	0.0	0.0	0.0	0.0	0.0	0.0	0.0	1.5	70.9	9.3	
				STNDEV	1.8	0.0	2.9	0.0	0.9	0.0	0.0	0.0	0.0	0.0	0.0	0.0	0.0	1.1	6.7	3.5	
Mims Spur A		SAL 1646	KLK		13.4	0.0	6.9	4.9	15.4	0.0	0.0	0.0	0.0	0.0	0.0	0.0	0.0	2.8	29.7	27.6	246
Mims Spur B		SAL 1647	KLK		9.3	0.0	5.7	4.8	15.0	0.0	0.0	0.0	0.0	0.0	0.0	0.0	0.0	1.3	40.1	23.8	227
Mims Spur C		SAL 1648	KLK		14.7	0.0	6.1	3.5	5.6	1.3	0.0	0.0	0.0	0.0	0.0	0.0	0.0	0.9	47.2	20.8	231
				Average	12.5	0.0	6.2	4.4	12.0	0.4	0.0	0.0	0.0	0.0	0.0	0.0	0.0	1.7	39.0	24.1	
				STNDEV	2.9	0.0	0.6	0.8	5.5	0.7	0.0	0.0	0.0	0.0	0.0	0.0	0.0	1.0	8.8	3.4	
Strickland Nunatak A		SAL 1658	KLK		8.4	0.0	0.0	0.0	0.0	0.0	0.0	0.0	0.0	0.0	0.0	0.0	0.0	0.0	0.0	91.6	334
Strickland Nunatak B		SAL 1659	KLK		11.3	0.0	0.0	0.0	0.0	0.0	0.0	0.0	0.0	0.0	0.0	0.0	0.0	0.0	0.0	88.7	284
Strickland Nunatak C		SAL 1660	KLK		13.6	0.0	0.3	0.0	0.0	0.0	0.0	0.0	0.0	0.0	0.0	0.0	0.0	0.0	0.0	86.1	287
				Average	11.1	0.0	0.1	0.0	0.0	0.0	0.0	0.0	0.0	0.0	0.0	0.0	0.0	0.0	0.0	88.8	
				STNDEV	2.6	0.0	0.2	0.0	0.0	0.0	0.0	0.0	0.0	0.0	0.0	0.0	0.0	0.0	0.0	2.8	
Quonset Glacier A		SAL 1684	KLK		29.8	0.0	9.1	17.4	6.1	0.6	0.0	0.0	0.0	0.0	0.0	0.0	0.0	2.8	34.4	0.0	363
Quonset Glacier B		SAL 1685	KLK		29.0	0.0	4.6	21.3	2.6	0.0	0.0	0.0	0.0	0.0	0.0	0.0	0.0	4.9	37.6	0.0	348
Quonset Glacier C		SAL 1686	KLK		29.6	0.0	6.6	19.8	4.9	0.9	0.0	0.0	0.0	0.0	0.0	0.0	0.0	1.7	36.5	0.0	348
				Average	29.5	0.0	6.8	19.5	4.5	0.5	0.0	0.0	0.0	0.0	0.0	0.0	0.0	3.1	36.2	0.0	
				STNDEV	0.4	0.0	2.3	2.0	1.8	0.4	0.0	0.0	0.0	0.0	0.0	0.0	0.0	1.6	1.6	0.0	

Table 5 cont. Percentage data from point counts made on each thin section

Location	Depth (cm)	Sample ID	Counted by		qtz	pyrox	kspar	plag	biot	chlor	opq	other/ unk.	poly	silt/s.s.	mudst	extr	maf	int	fel	meta	n=
Scott Glacier																					
Mt. Howe		SAL 1690	AJS		4.6	0.0	0.0	0.0	0.0	0.0	5.3	0.0	6.1	17.6	6.9	0.0	3.1	9.9	29.0	17.6	151
Mt. Howe		SAL 1691	AJS		6.0	0.0	0.0	1.8	3.2	0.9	0.9	0.0	10.1	10.1	1.4	0.0	3.7	17.0	9.6	35.3	253
Karo Hills		SAL 1700	AJS		34.6	0.4	1.9	4.6	2.3	1.2	1.2	0.0	0.8	10.8	0.4	0.0	0.0	0.0	12.3	17.3	260
				Average	15.1	0.1	0.6	2.2	1.8	0.7	2.5	0.0	5.7	12.8	2.9	0.0	2.2	9.0	17.0	23.4	
				STNDEV	17.0	0.2	1.1	2.3	1.7	0.6	2.5	0.0	4.7	4.1	3.5	0.0	2.0	8.5	10.5	10.3	
Beardmore Glacier																					
Davis Nunatak		SAL 1694	AJS		8.4	0.0	0.4	0.0	1.2	4.4	6.4	0.0	4.4	20.4	7.2	0.0	0.0	11.2	15.2	20.8	316
Beardmore Glacier		SAL 1654	AJS		4.0	1.1	0.0	0.0	0.0	0.0	0.0	0.0	9.2	56.9	0.0	0.0	0.0	0.6	10.3	17.8	233
Cloudmaker		SAL 183	AJS		0.0	0.0	0.0	0.0	0.0	0.0	0.0	0.0	8.3	91.7	0.0	0.0	0.0	0.0	0.0	0.0	12
				Average	4.1	0.4	0.1	0.0	0.4	1.5	2.1	0.0	7.3	56.3	2.4	0.0	0.0	3.9	8.5	12.9	
				STNDEV	4.2	0.7	0.2	0.0	0.7	2.5	3.7	0.0	2.6	35.6	4.2	0.0	0.0	6.3	7.8	11.2	
RISP Samples																					
RISP 78-8	42 - 44	SAL 219	KLK		45.9	0.0	0.0	0.5	0.0	0.0	0.0	0.0	6.5	0.5	13.7	8.2	0.5	0.0	19.1	1.1	183
RISP 78-14	82 - 84	SAL 223	KLK		52.6	0.0	0.4	0.7	0.0	0.0	0.0	0.0	7.5	0.3	11.2	1.7	0.0	0.0	17.3	1.8	146
RISP 78-44	99-101	SAL 222	KLK		57.9	0.0	0.7	1.4	0.0	0.0	0.0	0.0	1.4	0.0	10.7	1.4	0.0	0.0	13.6	2.9	140
				Average	52.1	0.0	0.4	0.9	0.0	0.0	0.0	0.0	5.1	0.3	11.9	3.8	0.2	0.0	16.7	1.9	
				STNDEV	6.0	0.0	0.4	0.5	0.0	0.0	0.0	0.0	3.3	0.3	1.6	3.8	0.3	0.0	2.8	0.9	
Central Ross Sea Samples																					
NBP94-07-39	52-54	SAL 278	AJS		1.7	0.0	0.0	0.0	0.0	0.0	0.0	0.0	79.9	14.5	3.9	0.0	0.0	0.0	0.0	0.0	179
NBP94-07-39	100-102	SAL 282	EFP		2.8	0.0	0.7	0.7	0.0	0.0	1.4	0.7	92.3	0.7	0.0	0.0	0.0	0.0	0.0	0.7	142
NBP95-01-11	48-50	SAL 537	EFP		17.3	1.3	7.2	6.5	0.0	0.0	1.3	1.0	30.1	3.6	1.0	0.3	0.3	10.1	7.8	12.1	405
NBP95-01-11	100-120	SAL 538	EFP		18.6	0.2	4.7	12.1	0.0	0.0	0.4	0.9	32.2	2.0	0.7	1.6	0.7	6.7	11.2	8.0	374
NBP95-01-17	48-50	SAL 540	EFP		25.0	0.8	3.3	4.9	0.0	0.0	0.8	0.3	23.4	1.1	1.4	0.5	0.0	4.9	19.0	13.1	375
NBP95-01-17	100-102	SAL 543	EFP		14.7	0.0	6.4	4.4	0.7	0.0	0.7	0.5	30.1	2.7	0.5	0.5	0.5	6.1	17.6	13.7	324
NBP95-01-17	153-155	SAL 534	EFP		20.7	0.3	5.2	5.8	0.3	0.0	0.3	0.3	22.4	5.5	0.3	0.0	1.2	5.0	20.7	11.1	320
ELT32-21	54-58	SAL 1640	AJS		15.2	0.1	4.8	5.4	0.0	0.0	0.3	0.6	33.0	6.1	1.2	0.3	1.7	4.3	9.5	17	1090
ELT32-21	104-108	SAL 1641	EFP		14.2	0.1	3.3	2.6	0.0	0.0	0.0	0.0	50.7	3.7	2.2	0.4	2.2	2.5	5.6	12	957
ELT32-21	154-160	SAL 1642	EFP		2.1	0.0	1.1	0.6	0.0	0.0	0.2	0.2	87.4	1.3	0.2	0.0	0.2	0.6	1.6	5	1238
				Average	13.2	0.3	3.7	4.3	0.1	0.0	0.6	0.4	48.1	4.1	1.1	0.4	0.7	4.0	9.3	9.2	
				STNDEV	8.3	0.4	2.4	3.6	0.2	0.0	0.5	0.3	27.7	4.1	1.2	0.5	0.8	3.3	7.8	5.7	
Western Ross Sea Samples																					
NBP94-01-02	50-52	SAL 372	EFP		13.5	0.3	8.3	4.0	0.0	0.0	2.0	1.3	37.3	1.0	0.7	10.0	1.7	4.0	5.6	10.2	303
NBP94-01-02	111-116	SAL 1633	EFP		1.7	0.2	0.6	0.1	0.0	0.0	0.3	0.0	90.9	0.8	0.2	1.2	0.9	0.7	0.9	1.6	903
NBP94-01-02	150-152	SAL 374	EFP		19.2	0.0	5.3	7.3	0.7	0.0	5.3	1.3	9.3	2.0	2.6	11.3	9.3	4.6	7.9	13.6	151
ELT32-13	49-51	SAL 406	EFP		42.0	1.0	16.0	17.0	1.0	0.0	9.0	1.0	83.0	18.0	3.0	76.0	8.0	16.0	46.0	24.0	268
ELT32-13	100-102	SAL 407	EFP		46.0	0.0	9.0	24.0	1.0	0.0	10.0	1.3	47.0	6.0	1.0	23.0	4.0	3.0	26.0	17.0	212
ELT32-13	149-151	SAL 408	EFP		21.0	0.0	6.0	9.0	0.0	0.0	3.0	0.0	15.0	7.0	1.0	21.0	4.0	8.0	17.0	13.0	121
ELT32-20	54-58	SAL 1640	EFP		30.1	0.0	4.2	3.2	0.5	0.5	0.5	0.0	8.8	4.6	13.9	0.0	3.7	0.9	15.7	13.4	267
ELT32-20	64-69	SAL 1638	EFP		5.8	0.4	2.4	2.4	0.0	0.0	0.0	0.2	61.0	1.8	0.6	0.2	7.2	3.6	5.2	8.9	497
ELT32-20	132-134	SAL 1639	EFP		0.0	0.0	0.6	0.3	0.0	0.0	0.1	0.1	96.7	0.3	0.0	0.2	0.5	0.5	0.3	0.4	1188
ELT27-14	47-50	SAL 1634	EFP		9.4	0.6	3.1	2.0	0.0	0.0	0.0	0.6	65.3	1.1	0.3	0.3	2.0	2.8	3.7	8.5	352
ELT27-14	63-66	SAL 1635	EFP		10.3	0.2	1.4	4.2	0.0	0.0	0.3	0.0	65.5	0.3	0.5	1.6	3.1	1.6	2.6	8.2	621
ELT27-14	105-109	SAL 1636	EFP		18.9	0.6	1.7	0.9	0.0	0.0	0.3	0.3	55.9	1.7	1.4	0.0	4.9	0.0	5.4	8.0	349
ELT27-14	164-170	SAL 1637	EFP		9.9	0.0	3.3	1.7	0.0	0.0	0.3	0.2	67.1	0.3	0.2	0.7	2.1	1.2	5.3	7.7	605
				Average	17.5	0.3	4.8	5.9	0.2	0.0	2.4	0.5	54.1	3.5	2.0	11.2	4.0	3.6	10.9	10.3	
				STNDEV	14.4	0.3	4.3	7.1	0.4	0.1	3.5	0.5	29.4	4.9	3.7	21.1	2.8	4.3	12.9	6.2	

Table 5 cont. Percentage data from point counts made on each thin section.

Location	Depth (cm)	Sample ID	Counted by		qtz	pyrox	kspar	plag	biot	chlor	opq	other/ unk.	poly	silt/s.s.	mudst	extr	maf	int	fel	meta	n=
Eastern Ross Sea Samples																					
NBP9407-63	52-54	SAL 164	AJS		34.5	0.0	3.2	5.0	0.5	0.9	3.6	0.0	2.7	7.7	12.7	0.0	0.0	0.5	15.5	13.2	290
NBP9407-63	112-114	SAL 142	AJS		60.0	0.0	2.3	3.3	0.0	0.4	0.0	0.0	3.7	0.0	7.0	0.0	0.0	0.0	5.6	5.6	217
NBP9902-04	10-12	SAL 138	JRL		69.0	0.0	1.2	1.2	0.0	0.0	0.6	5.4	0.0	0.0	3.0	3.7	0.0	0.6	10.4	0.0	164
NBP9902-04	52-54	SAL 296	AJS		25.1	0.0	2.9	1.0	1.4	3.4	1.0	0.0	0.5	11.6	10.1	0.0	0.0	11.6	11.1	18.8	249
NBP9902-04	97-99	SAL 169	JRL		64.1	0.5	2.0	1.5	0.0	0.0	1.5	3.5	0.0	0.0	4.6	1.5	0.0	0.0	9.7	2.0	195
NBP9902-05	105-107	SAL 177	JRL		78.8	0.0	5.6	7.1	0.6	0.0	0.6	0.0	0.0	0.3	0.6	0.0	0.0	0.0	6.2	0.3	354
NBP9902-08	103-105	SAL 178	JRL		65.6	0.0	1.6	3.6	0.0	0.0	0.3	1.0	0.0	1.0	3.3	0.7	0.0	0.0	16.0	3.9	305
NBP9902-17	104-106	SAL 141	AJS		66.5	0.0	2.6	2.6	0.0	0.0	0.0	0.0	4.2	0.0	7.9	0.0	0.0	0.0	6.3	12.2	196
				Average	58.0	0.1	2.7	3.2	0.3	0.6	1.0	1.2	1.4	2.6	6.2	0.7	0.0	1.6	10.1	7.0	
				STNDEV	18.3	0.2	1.4	2.1	0.5	1.2	1.2	2.1	1.8	4.5	4.0	1.3	0.0	4.1	4.0	6.9	

Note: Point count data are the 500-2000 micron sand-fraction of each West Antarctic, East Antarctic, RISP, and Ross Sea sample analyzed. Mineral and lithic fragment percentages have been rounded to the nearest tenth of a percent, therefore the percentages do not always sum to exactly 100% for each sample. SAL numbers correspond to sample numbers assigned in the IUPUI Sediment Analysis Labratory. In order to demonstrate reproducibility and calculate error, several samples have been counted multiple times. Where this is the case, the average petrographic composition of till form an entire area (i.e. West Antarctica) has been calculated using the average values form the sample replicates. Note qtz= quartz, pyrox= pyroxene, k-spar= potassium feldspar, biot= biotite, chlor= chlorite, opq= opaques, unk=unknown, silt=siltstone, s.s= sandstone, mud st= mud stone, clay st= clay stone, extr= extrusive volcanic, maf= mafic intrusive, int= intermediate intrusive, fel= felsic intrusive, and meta= metamorphic. n= number or point counts for the thin section. AJS= Andrea Schilling, KLK= Kate Kramer, EFP= Emerson Palmer, and JRL= Jason Lederer.

Table 6: K-S P-values from all EA sample sites. Shaded areas indicate P value >0.05.

	K-S P-values using error in the CDF							
	SN 1659	SN 1660	MH 1690	MH 1691	KH 1700	DN 1694	BG 1654	CM 183
SN 1659		**0.375**	0.000	0.007	0.000	0.001	**0.173**	0.000
SN 1660	**0.375**		**0.070**	**0.180**	**0.182**	**0.118**	**0.371**	0.006
MH 1690	0.000	**0.070**		**0.173**	0.000	0.024	**0.278**	0.031
MH 1691	0.007	**0.180**	**0.173**		0.002	**0.602**	**0.256**	0.000
KH 1700	0.000	**0.182**	0.000	0.002		0.005	0.000	0.000
DN 1694	0.001	**0.118**	0.024	**0.602**	0.005		0.023	0.000
BG 1654	**0.173**	**0.371**	**0.278**	**0.256**	0.000	0.023		0.033
CM 183	0.000	0.006	0.031	0.000	0.000	0.000	0.033	

Table 7: K-S P-values from all WA sample sites. Shaded areas indicate P value >0.05.

	K-S P-values using error in the CDF								
	Bindschadler 1775	Bindschadler 1776	Kamb 1771	Kamb 1772	Kamb 1773	Kamb 1774	Whillans 1744	Whillans 1750	Whillans 1755
Bindschadler 1775		**0.814**	0.001	0.000	**0.091**	**0.234**	**0.059**	**0.367**	**0.307**
Bindschadler 1776	**0.814**		0.019	0.001	**0.081**	**0.652**	**0.354**	**0.658**	**0.307**
Kamb 1771	0.001	0.019		**0.674**	**0.349**	**0.390**	**0.066**	0.041	**0.355**
Kamb 1772	0.000	0.001	**0.674**		0.045	**0.058**	0.013	0.006	**0.076**
Kamb 1773	**0.091**	**0.081**	**0.349**	0.045		**0.644**	**0.095**	**0.061**	**0.998**
Kamb 1774	**0.234**	**0.652**	**0.390**	**0.058**	**0.644**		**0.957**	**0.821**	**0.944**
Whillans 1744	**0.059**	**0.354**	**0.066**	0.013	**0.095**	**0.957**		**0.934**	**0.291**
Whillans 1750	**0.367**	**0.658**	0.041	0.006	**0.061**	**0.821**	**0.934**		**0.159**
Whillans 1755	**0.307**	**0.307**	**0.355**	**0.076**	**0.998**	**0.944**	**0.291**	**0.159**	

Table 8: Average point count % differences with Lederer 2003 data from the Ross Sea samples.

Sample ID	qtz	pyrox	kspar	plag	biot	chlor	opq	other/ unk.	poly	silt/s.s.	mudst	extr	maf	int	fel	meta	n
SAL 142 (2009)	60.0	0.0	2.3	3.3	0.0	0.4	0.0	0.0	3.7	0.0	7.0	0.0	0.0	0.0	5.6	5.6	217.0
SAL 142 (2003)	75.3	0.0	1.3	3.9	0.4	0.0	0.9	3.0	0.0	0.0	0.9	2.6	0.0	0.0	7.4	0.0	231
st. dev.	10.8	0.0	0.7	0.4	0.3	0.3	0.6	2.1	2.6	0.0	4.3	1.8	0.0	0.0	1.3	4.0	
% Difference (total)	15.3	0	1	0.6	0.4	0.4	0.9	3	3.7	0	6.1	0	0	0	1.8	5.6	
SAL 141 (2009)	66.5	0.0	2.6	2.6	0.0	0.0	0.0	0.0	4.2	0.0	7.9	0.0	0.0	0.0	6.3	12.2	188
SAL 141 (2003)	76.0	0.0	0.5	0.0	0.0	0.0	0.5	0.5	0.0	2.0	6.6	0.0	0.0	0.0	6.1	1.5	196
st. dev.	6.7	0.0	1.5	1.8	0.0	0.0	0.4	0.4	3.0	1.4	0.9	0.0	0.0	0.0	0.1	7.6	
% Difference (total)	9.5	0.0	2.1	2.6	0.0	0.0	0.0	0.0	4.2	2.0	1.3	0.0	0.0	0.0	0.2	10.7	

Table 9. K-S values using error for East Antarctica, West Antarctica and the Ross Sea

K-S P-values using error in the CDF																
	Bind-schadler	Kamb	Whillians	Strick-land	Mt Howe	Karo Hills	Davis	Beard-more	Cloud-maker	NBP 99-02-17	NBP94-07-63	NBP94-07-39	ELT 32-21	ELT 27-14	ELT 32-20	RISP (222)
Bindschadler		0.000	0.039	0.001	**0.086**	0.000	**0.121**	**0.174**	0.001	**0.981**	0.000	0.000	**0.232**	0.027	**0.567**	0.040
Kamb	0.000		0.039	0.000	0.000	0.000	**0.053**	0.000	0.000	**0.058**	0.001	0.000	0.000	0.000	0.008	**0.883**
Whillians	0.039	0.039		0.005	0.002	**0.124**	0.021	0.003	0.000	**0.264**	0.000	0.000	**0.105**	0.012	**0.134**	**0.125**
Strickland	0.001	0.000	0.005		0.001	0.000	0.002	**0.135**	0.000	0.011	0.000	0.000	**0.157**	0.023	**0.105**	0.003
Mt Howe	**0.086**	0.000	0.002	0.001		0.000	**0.051**	**0.543**	0.001	**0.506**	0.000	0.001	0.011	0.033	**0.389**	0.008
Karo Hills	0.000	0.000	**0.124**	0.000	0.000		0.005	0.000	0.000	0.033	0.000	0.000	0.000	0.000	0.005	0.023
Davis	**0.121**	**0.053**	0.021	0.002	**0.051**	0.005		0.028	0.000	**0.635**	**0.051**	0.002	0.033	0.008	**0.375**	**0.501**
Beardmore	**0.174**	0.000	0.003	**0.135**	**0.543**	0.000	0.028		0.031	**0.211**	0.000	0.001	**0.181**	**0.379**	**0.259**	0.002
Cloudmaker	0.001	0.000	0.000	0.000	0.001	0.000	0.000	0.031		0.003	0.000	0.000	0.000	0.008	0.000	0.000
NBP99-02-17	**0.981**	**0.058**	**0.264**	0.011	**0.506**	0.033	**0.635**	**0.211**	0.003		0.001	0.015	**0.331**	**0.082**	**0.908**	**0.125**
NBP94-07-63	0.000	0.001	0.000	0.000	0.000	0.000	**0.051**	0.000	0.000	0.001		**0.105**	0.000	0.000	0.000	**0.268**
NBP94-07-39	0.000	0.000	0.000	0.000	0.001	0.000	0.002	0.001	0.000	0.015	**0.105**		0.000	0.000	0.017	**0.067**
ELT32-21	**0.232**	0.000	**0.105**	**0.157**	0.011	0.000	0.033	**0.181**	0.000	**0.331**	0.000	0.000		**0.109**	**0.392**	0.048
ELT27-14	0.027	0.000	0.012	0.023	0.033	0.000	0.008	**0.379**	0.008	**0.082**	0.000	0.000	**0.109**		**0.497**	0.001
ELT32-20	**0.567**	0.008	**0.134**	**0.105**	**0.389**	0.005	**0.375**	**0.259**	0.000	**0.908**	0.000	0.017	**0.392**	**0.497**		**0.051**
RISP (222)	0.040	**0.883**	**0.125**	0.003	0.008	0.023	**0.501**	0.002	0.000	**0.125**	**0.268**	**0.067**	0.048	0.001	**0.051**	

Table 10: K-S P-values from all WA ice streams. Shaded areas indicate P value >0.05.

	K-S P-values using error in the CDF		
	Whillans	Bindschadler	Kamb
Whillans		0.034	0.042
Bindschadler	0.034		0.000
Kamb	0.042	0.000	

Table 11: K-S P-values from all Ross Sea sample sites.Shaded areas indicate P value >0.05.

	K-S P-values using error in the CDF			
	NBP94-07-63 (SAL 142)	NBP94-07-63 (SAL 164)		
NBP94-07-63 (SAL 142)		**0.811**		
NBP94-07-63 (SAL 164)	**0.811**			
	K-S P-values using error in the CDF			
	NBP94-07-39 (SAL 278)	NBP94-07-39 (SAL 282)		
NBP94-07-39 (SAL 278)		**0.325**		
NBP94-07-39 (SAL 282)	**0.325**			
	K-S P-values using error in the CDF			
	ELT32-21 (SAL 1640)	ELT32-21 (SAL 1641)		
ELT32-21 (SAL 1640)		**0.717**		
ELT32-21 (SAL 1641)	**0.717**			
	K-S P-values using error in the CDF			
	ELT27-14 (SAL 1634)	ELT27-14 (SAL 1635)	ELT27-14 (SAL 1636)	ELT27-14 (SAL 1637)
ELT27-14 (SAL 1634)		**0.845**	**0.968**	**0.694**
ELT27-14 (SAL 1635)	**0.845**		**0.868**	**0.683**
ELT27-14 (SAL 1636)	**0.968**	**0.868**		**0.665**
ELT27-14 (SAL 1637)	**0.694**	**0.683**	**0.665**	
	K-S P-values using error in the CDF			
	ELT32-20 (SAL 1638)	ELT32-20 (SAL 1639)		
ELT32-20 (SAL 1638)		**0.099**		
ELT32-20 (SAL 1639)	**0.099**			

Table 12. K-S P-values from MH and KH sample sit

	K-S P-values using error in the CDF			
	KH	Mt Howe		
KH		0.000		
Mt Howe	0.000			

Table 13: K-S P-values from Scott Glacier and Ross Sea sample sites. Shaded areas indicate P values >0.05.

	K-S P-values using error in the CDF							
	Scott Glacier	NBP99-02-17	NBP94-07-63	NBP94-07-39	ELT32-21	ELT27-14	ELT32-20	NBP94-01-02
Scott Glacier		**0.570**	0.000	0.000	**0.312**	0.016	**0.963**	**0.321**
NBP99-02-17	**0.570**		0.001	0.015	**0.331**	**0.082**	**0.908**	**0.387**
NBP94-07-63	0.000	0.001		**0.105**	0.000	0.000	0.000	0.000
NBP94-07-39	0.000	0.015	**0.105**		0.000	0.000	0.017	0.001
ELT32-21	**0.312**	**0.331**	0.000	0.000		**0.109**	**0.392**	**0.565**
ELT27-14	0.016	**0.082**	0.000	0.000	**0.109**		**0.497**	**0.600**
ELT32-20	**0.963**	**0.908**	0.000	0.017	**0.392**	**0.497**		**0.708**
NBP94-01-02	**0.321**	**0.387**	0.000	0.001	**0.565**	**0.600**	**0.708**	

Table 14: K-S P- values from Beardmore Glacier and Ross Sea sample sites. Shaded areas indicate P values >0.05

	K-S P-values using error in the CDF							
	Beardmore Glacier	NBP99-02-17	NBP94-07-63	NBP94-07-39	ELT32-21	ELT27-14	ELT32-20	NBP94-01-02
Beardmore Glacier		**0.165**	0.000	0.000	0.002	**0.378**	0.032	**0.558**
NBP99-02-17	**0.165**		0.001	0.015	**0.335**	**0.080**	**0.910**	**0.384**
NBP94-07-63	0.000	0.001		**0.122**	0.000	0.000	0.000	0.000
NBP94-07-39	0.000	0.015	**0.122**		0.000	0.000	0.017	0.001
ELT32-21	0.002	**0.335**	0.000	0.000		**0.101**	**0.392**	**0.597**
ELT27-14	**0.378**	**0.080**	0.000	0.000	**0.101**		**0.488**	**0.599**
ELT32-20	0.032	**0.910**	0.000	0.017	**0.392**	**0.488**		**0.701**
NBP94-01-02	**0.558**	**0.384**	0.000	0.001	**0.597**	**0.599**	**0.701**	

Table 15: Helium and U-Pb age data for selected samples in East Antarcitca and West Antarctica.

Grain	Location	Age picked from He	upper err	lower err	U/Pb age	Ma + -	Sampling Depth (cm)
1654-2	Davis Nunatak	153.28	43.67	3.27	530.3	5.8	Surface
1654-10	Davis Nunatak	137.03	33.92	2.76	246.5	6.4	Surface
1654-12	Davis Nunatak	146.44	6.48	36.89	595.1	5.1	Surface
1660-6	Strickland Nunatak	336.85	6.97	70.09	1034.0	42.6	Surface
1690-7	Mt. Howe	139.29	43.16	3.46	559.6	5.0	Surface
1690-17	Mt. Howe	151.18	25.49	3.05	488.2	7.1	Surface
1690-20	Mt. Howe	125.25	40.35	2.70	967.6	5.9	Surface
1691-2	Mt. Howe	153.19	3.69	33.36	275.8	3.0	Surface
1691-6	Mt. Howe	125.91	27.76	2.62	534.7	4.5	Surface
1691-13	Mt. Howe	129.09	35.35	2.59	599.5	6.8	Surface
1694-3	Beardmore Glacier	168.13	3.02	30.07	589.3	4.6	Surface
1694-9	Beardmore Glacier	149.03	23.35	2.51	524.2	7.0	Surface
1694-14	Beardmore Glacier	169.97	2.87	32.90	257.8	1.5	Surface
1694-18	Beardmore Glacier	123.43	42.88	2.29	1056.8	96.9	Surface
1694-23	Beardmore Glacier	151.03	37.52	2.69	528.6	4.6	Surface
1744-20	Whillians Ice Stream	68.67	14.95	1.33	528.1	19.6	30-40
1744-21	Whillians Ice Stream	281.16	106.16	5.32	1035.7	76.0	30-40
1744-26	Whillians Ice Stream	171.90	53.42	3.11	580.4	38.9	30-40
1744-35	Whillians Ice Stream	85.34	25.68	1.62	1048.4	74.0	30-40
1755-41	Whillians Ice Stream	157.13	2.78	35.84	1010.0	62.1	180-190
1755-44	Whillians Ice Stream	245.84	50.68	3.95	536.7	13.4	180-190
1771-19	Kamb Ice Stream	240.49	4.22	39.60	511.9	9.1	180-190
1771-30	Kamb Ice Stream	317.51	68.44	5.64	1099.8	68.3	180-190
1771-66	Kamb Ice Stream	314.69	6.53	57.44	1022.3	38.9	180-190
1772-19	Kamb Ice Stream	147.18	25.91	2.42	488.5	13.7	140-150
1772-37	Kamb Ice Stream	109.47	18.66	1.91	558.3	5.4	140-150
1773-5	Kamb Ice Stream	162.62	40.52	2.86	1114.9	22.8	40-50

Table 16: Overlap and Similarity analyses of U-Th ages of zircons from WA.

Overlap		
Whillans	**Whillans**	
Bindschadler	0.732	**Bindschadler**
Kamb	0.779	0.893
Similarity of overlaps		
Whillans	**Whillans**	
Bindschadler	0.782	**Binschadler**
Kamb	0.883	0.825

Table 17: Overlap and similarity analyses of Scott Glacier and the Ross Sea.

Overlap								
Scott Glacier	**Scott Glacier**							
NBP99-02-17	0.798	**NBP99-02-17**						
NBP94-07-63	0.468	0.602	**NBP94-07-63**					
NBP94-07-39	0.476	0.600	0.720	**NBP94-07-39**				
ELT32-21	0.860	0.838	0.573	0.545	**ELT32-21**			
ELT27-14	0.814	0.793	0.487	0.493	0.730	**ELT27-14**		
ELT32-20	0.804	0.805	0.540	0.587	0.788	0.752	**ELT32-20**	
NBP94-01-02	0.716	0.842	0.626	0.661	0.782	0.726	0.714	**NBP94-01-02**
RISP (222)	0.306	0.408	0.700	0.536	0.377	0.394	0.388	0.449
Similarity								
Scott Glacier	**Scott Glacier**							
NBP99-02-17	0.744	**NBP99-02-17**						
NBP94-07-63	0.647	0.738	**NBP94-07-63**					
NBP94-07-39	0.549	0.599	0.649	**NBP94-07-39**				
ELT32-21	0.834	0.790	0.776	0.590	**ELT32-21**			
ELT27-14	0.796	0.723	0.591	0.501	0.776	**ELT27-14**		
ELT32-20	0.787	0.733	0.619	0.563	0.768	0.782	**ELT32-20**	
NBP94-01-02	0.800	0.791	0.644	0.580	0.869	0.784	0.745	**NBP94-01-02**
RISP (222)	0.559	0.550	0.707	0.496	0.681	0.523	0.500	0.558

Table 18: Overlap and similarity analyses of Beardmore Glacier and the Ross Sea.

Overlap									
Beardmore Glacier	**Beardmore Glacier**								
NBP99-02-17	0.854	**NBP99-02-17**							
NBP94-07-63	0.496	0.602	**NBP94-07-63**						
NBP94-07-39	0.495	0.600	0.720	**NBP94-07-39**					
ELT32-21	0.875	0.838	0.573	0.545	**ELT32-21**				
ELT27-14	0.781	0.793	0.487	0.493	0.730	**ELT27-14**			
ELT32-20	0.756	0.805	0.540	0.587	0.788	0.752	**ELT32-20**		
NBP94-01-02	0.763	0.842	0.626	0.661	0.782	0.726	0.714	**NBP94-01-02**	
RISP (222)	0.326	0.408	0.700	0.536	0.377	0.394	0.388	0.449	
Similarity									
Beardmore Glacier	**Beardmore Glacier**								
NBP99-02-17	0.777	**NBP99-02-17**							
NBP94-07-63	0.628	0.738	**NBP94-07-63**						
NBP94-07-39	0.495	0.599	0.649	**NBP94-07-39**					
ELT32-21	0.803	0.790	0.776	0.590	**ELT32-21**				
ELT27-14	0.777	0.723	0.591	0.501	0.776	**ELT27-14**			
ELT32-20	0.720	0.733	0.619	0.563	0.768	0.782	**ELT32-20**		
NBP94-01-02	0.806	0.791	0.644	0.580	0.869	0.784	0.745	**NBP94-01-02**	
RISP (222)	0.489	0.550	0.707	0.496	0.681	0.523	0.500	0.558	**RISP (222)**

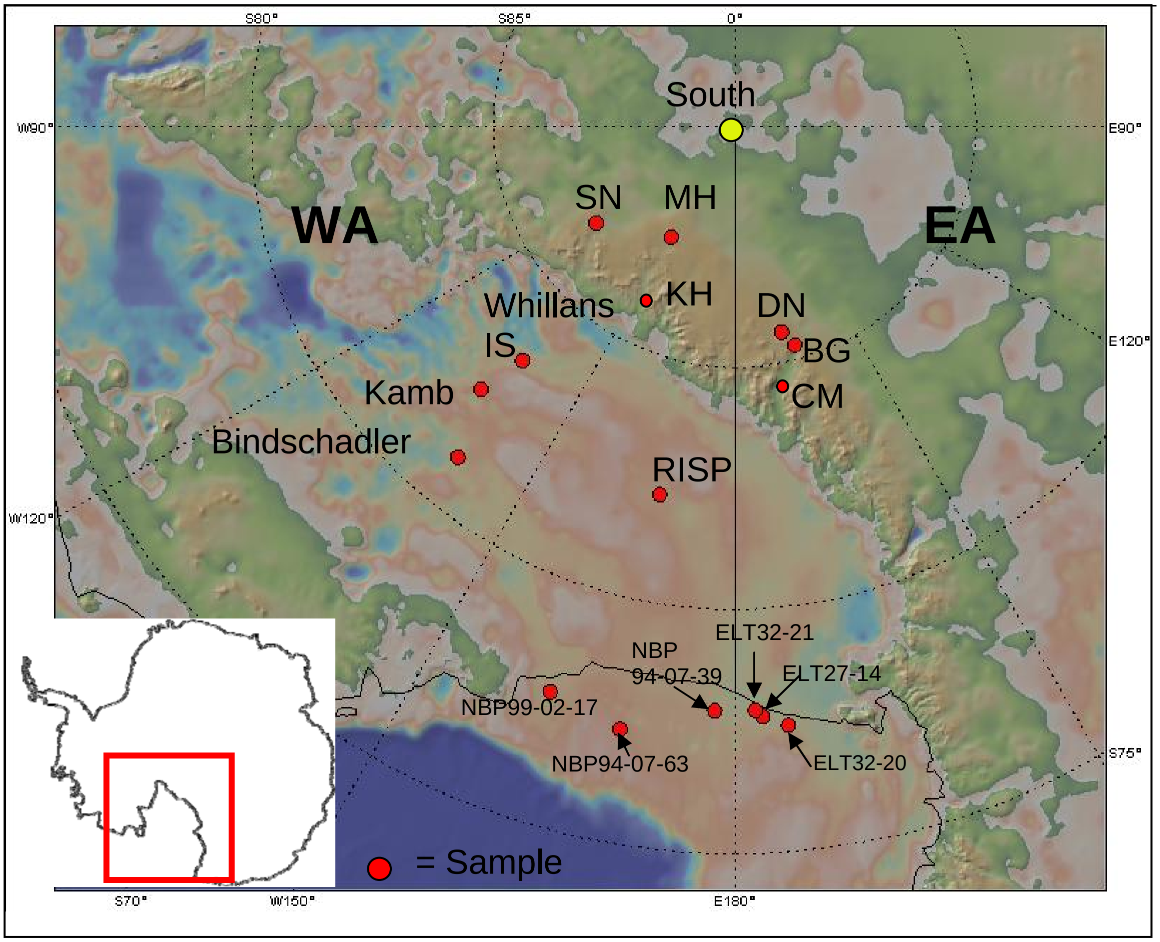

Figure 1. Shaded relief map showing sample site locations. (WA= West Antarctica; EA= East Antarctica; IS= Ice Stream; SN= Strickland Nunatak; MH= Mount Howe; KH= Karo Hills; DN= Davis Nunatak; BG= Beardmore Glacier; CM= Cloudmaker; RISP= Ross Ice Shelf Project.

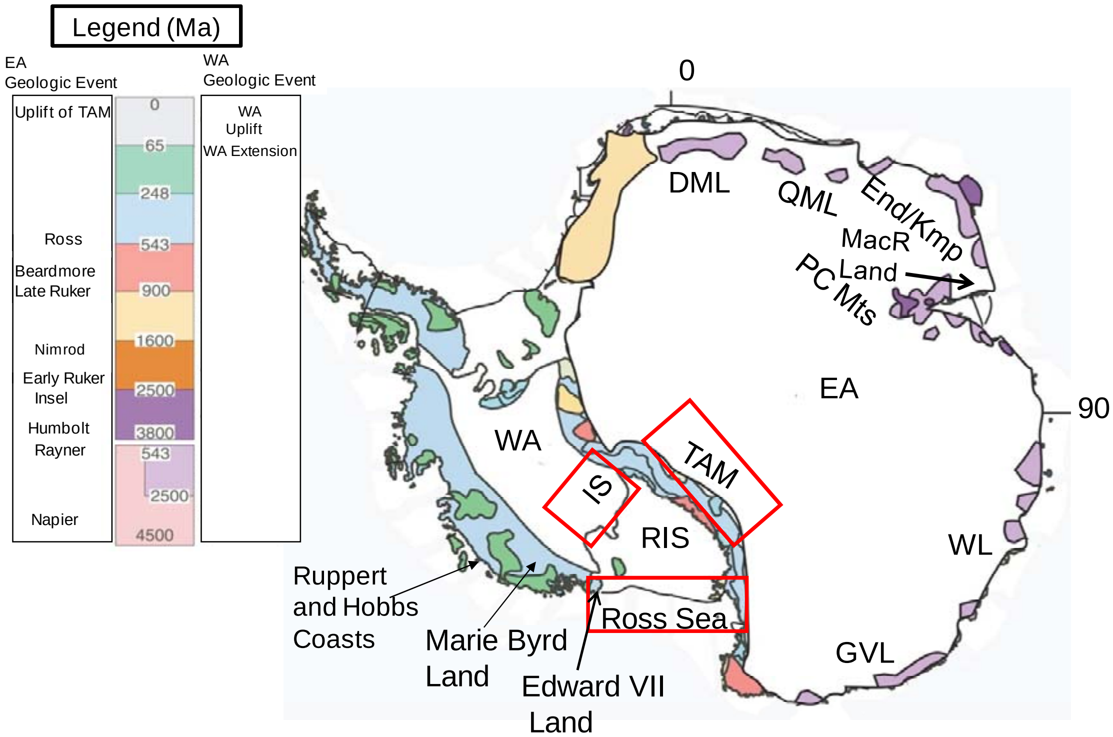

Figure 2. Bedrock geology map of Antarctica. WA= West Antarctica, EA= East Antarctica, IS= Ice Streams, TAM= Transantarctic Mountains, RIS= Ross Ice Shelf, GVL= George V Land, WL= Wilkes Land, PC= Prince Charles, DML= Dronning Maud Land, QML= Queen Maud Land, End/Kmp= Enderby and Kemp Lands, Mac R Land= MacRobertson Land. Red boxes indicate sample locations for this study (Modified by Roy et al., 2007).

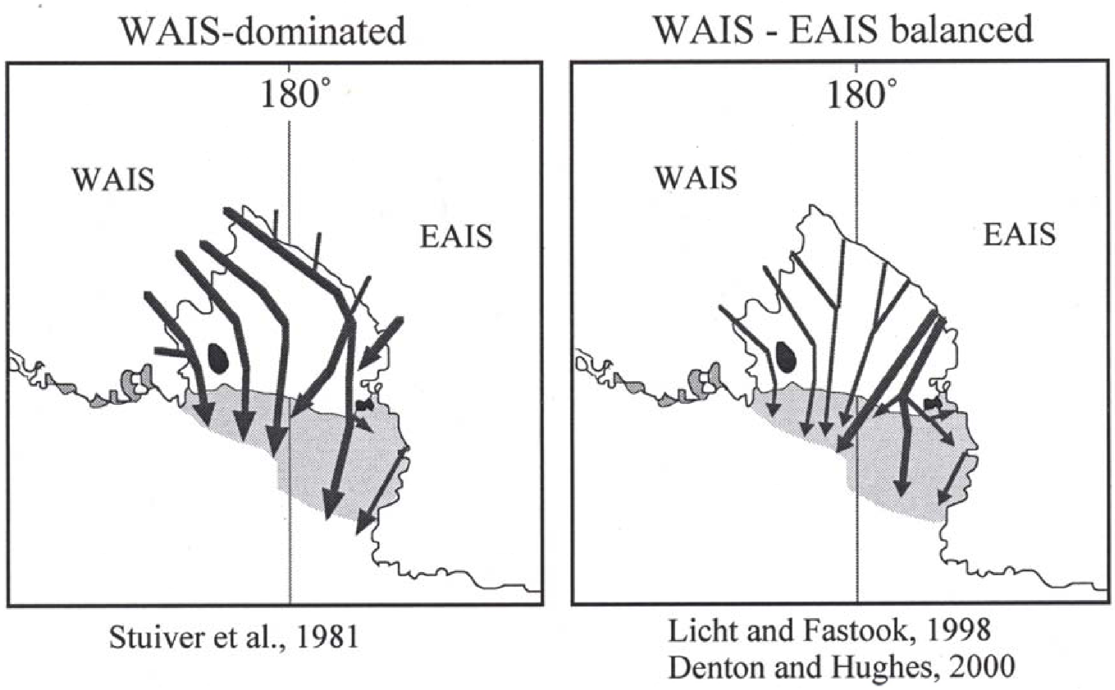

Figure 3. Paleo ice-flow models of Stuiver et al. (1981) and Licht and Fastook (1998) (Taken from Licht et al., 2005).

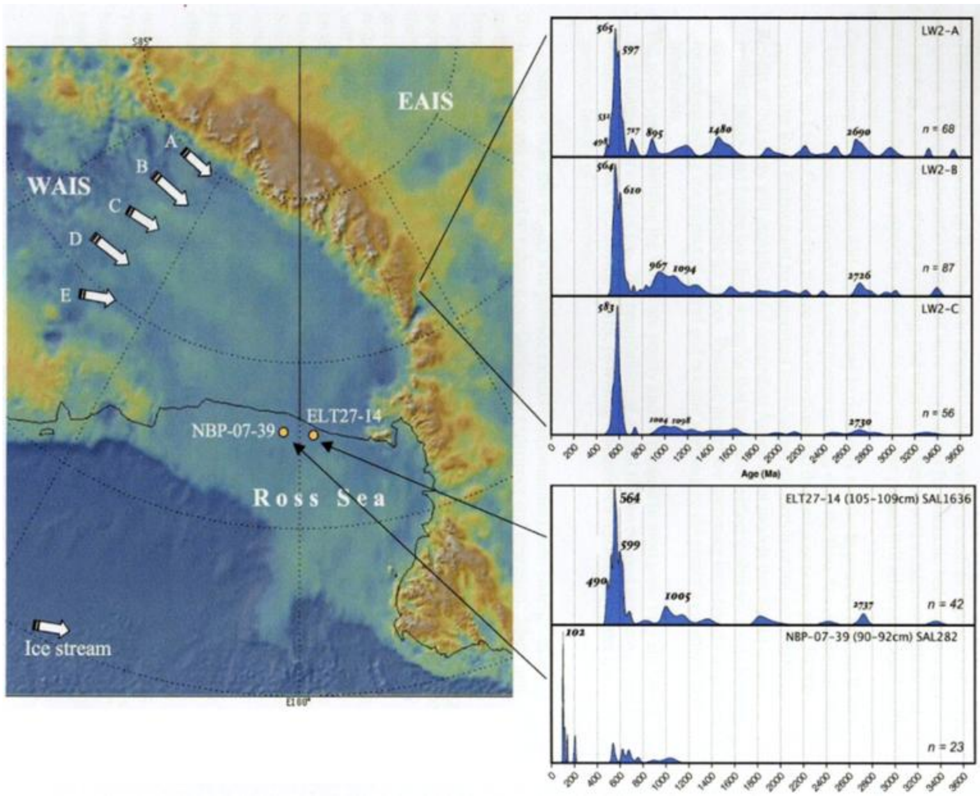

Figure 4. Detrital zircon analysis from Ross Sea samples, showing a distinct age boundary between East Antarctica and West Antarctica concentrated in the central Ross Sea (Palmer and Licht, 2007).

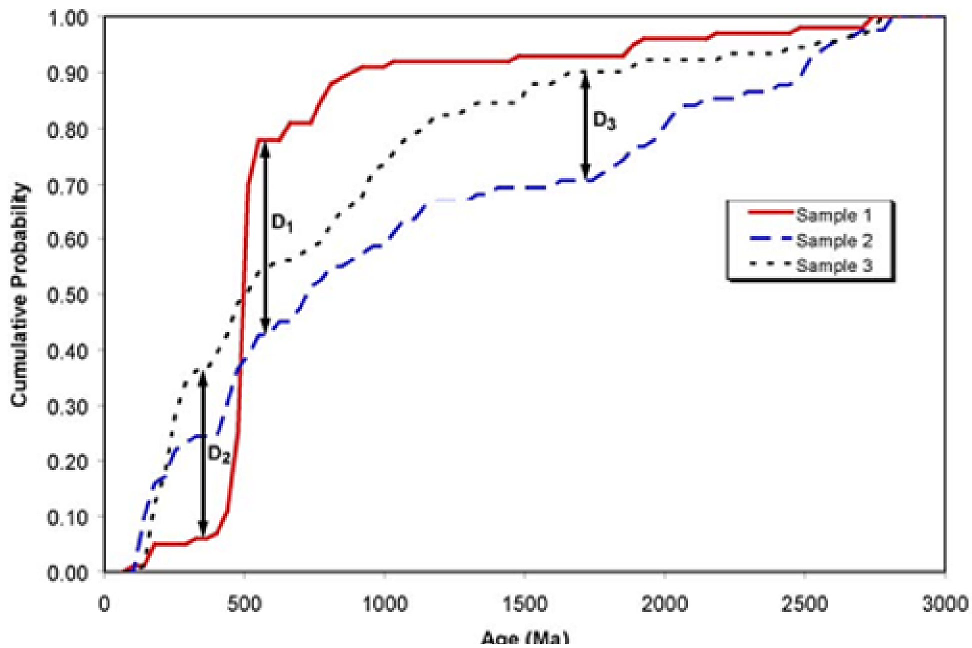

Figure 5. The maximum difference, D, between several cumulative distribution functions. D_1 is the maximum distance between Sample 1 and Sample 2, D_2 between Sample 1 and Sample 3 and D_3 between Sample 2 and Sample 3 (Guynn, 2006).

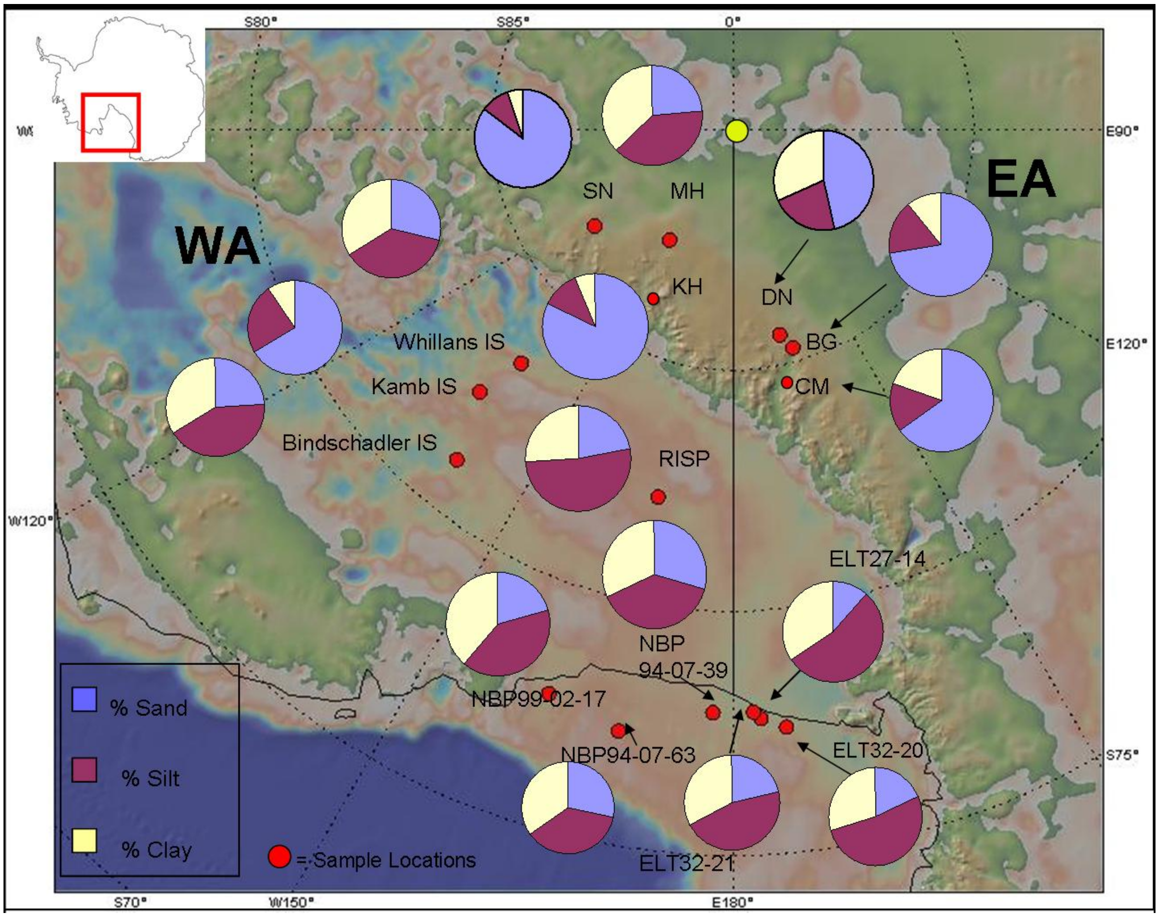

Figure 6. Particle size data from WA ice streams, EA outlet glaciers, and in the Ross Sea.

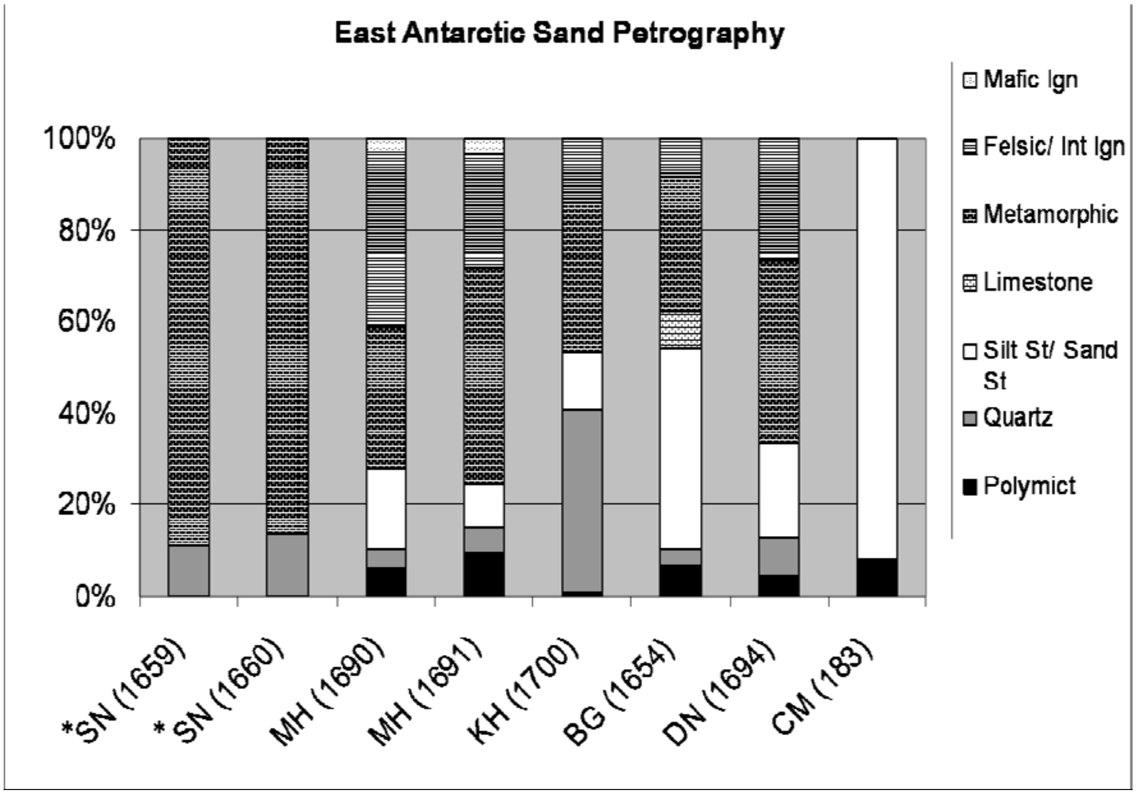

Figure 7. Sand petrography data from EA outlet Glaciers. * = data from Kramer (2008).

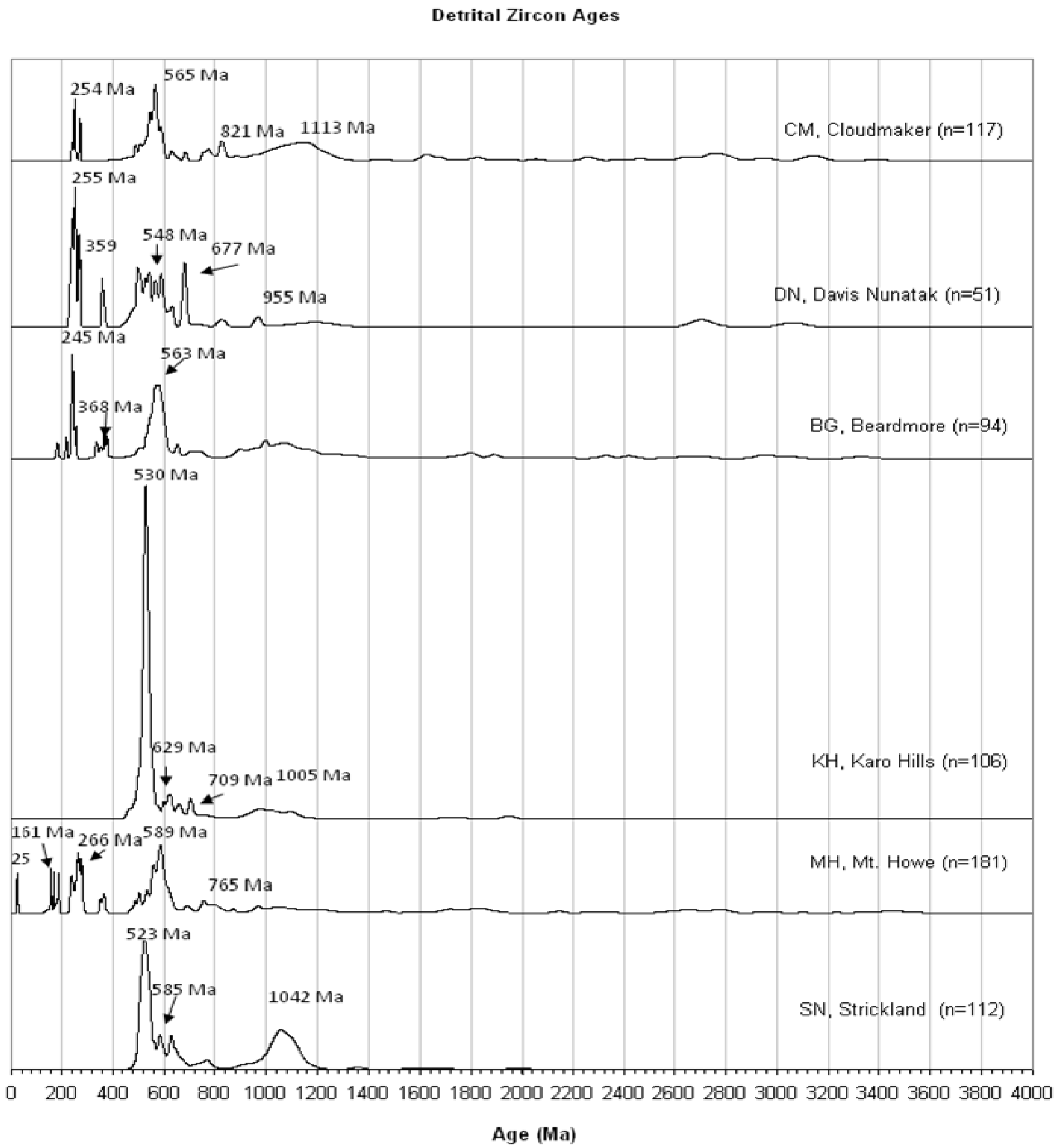

Figure 8. Normalized probability plot of detrital zircon ages in EA. Peaks significant in this study are labeled.

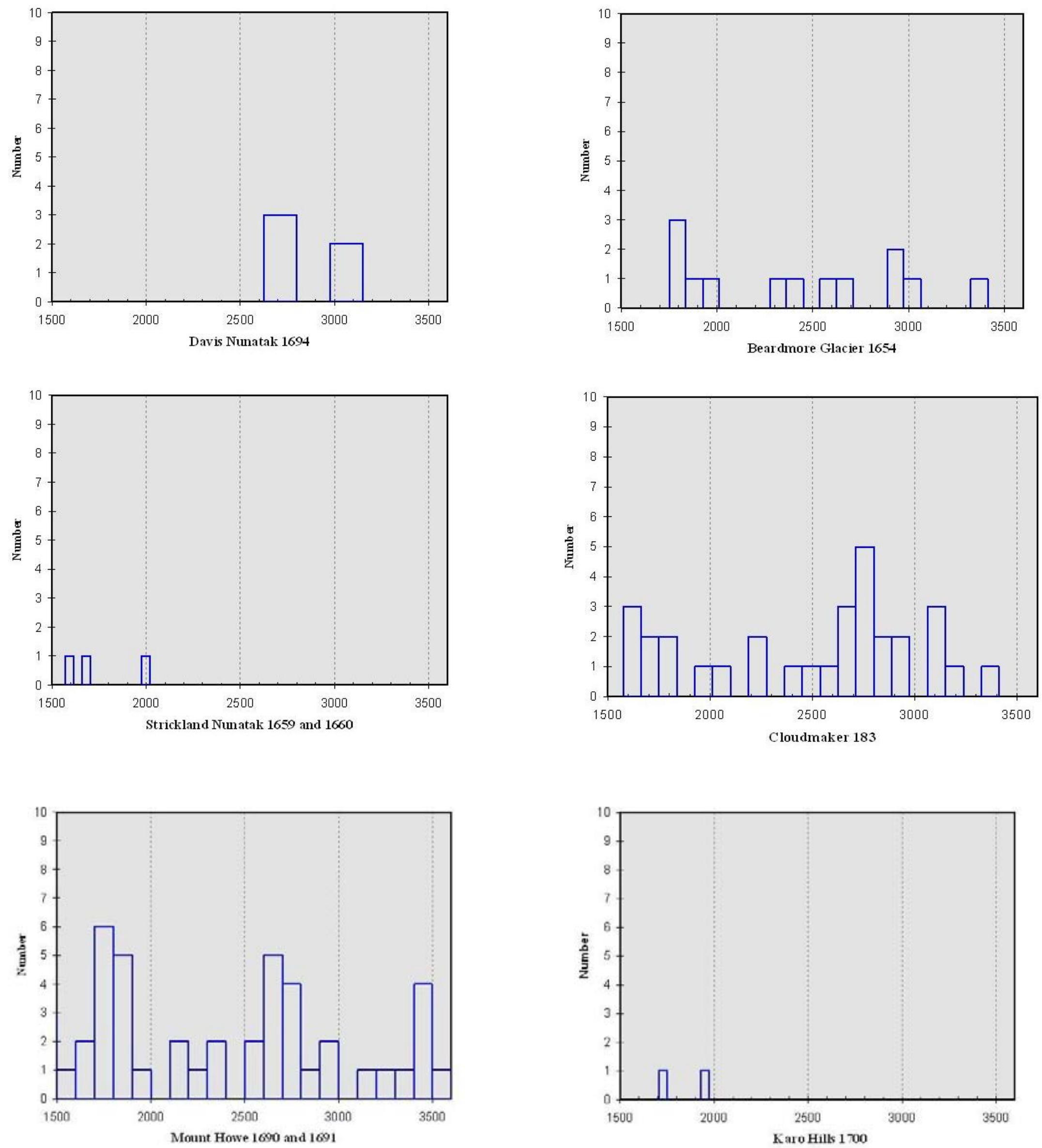

Figure 9. Histogram showing ages > 1500 Ma from EA sites.

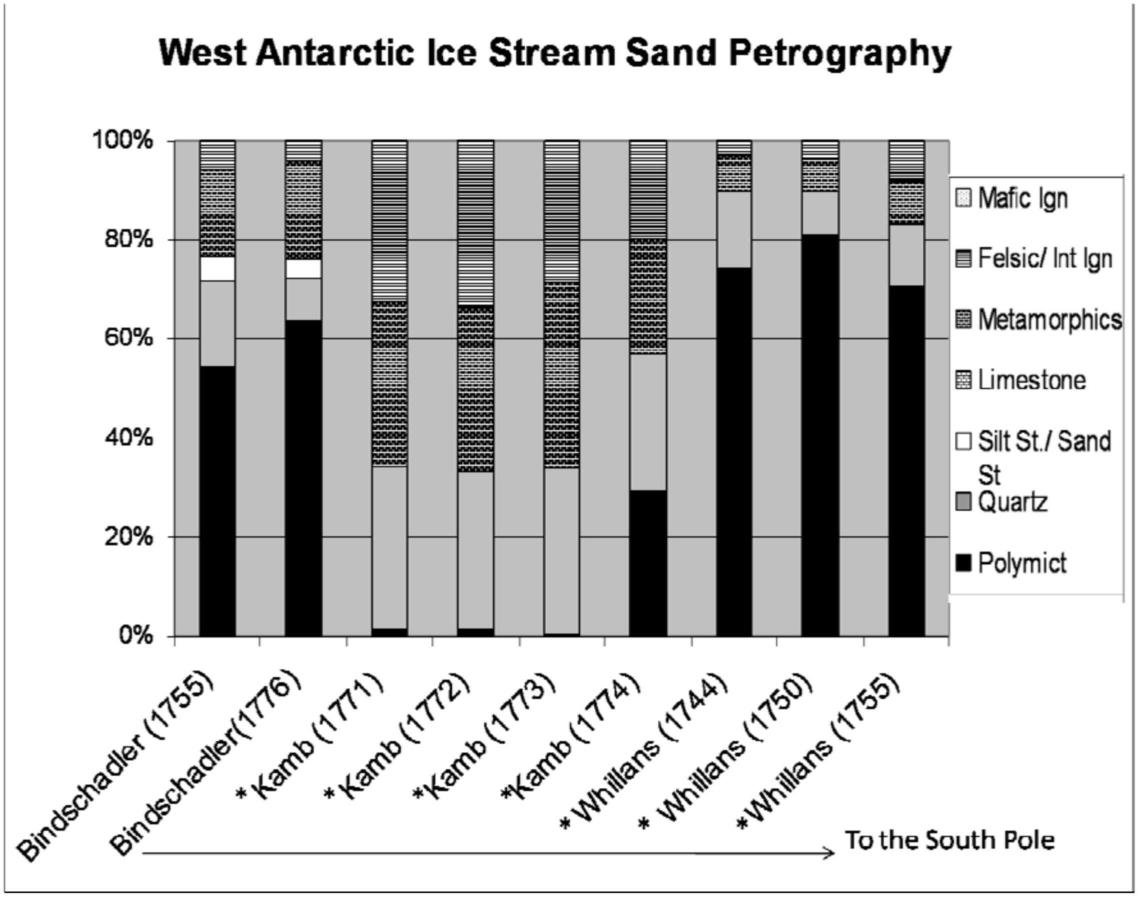

Figure 10. Sand Petrography from West Antarctic Ice Streams. *= data from Kramer (2008).

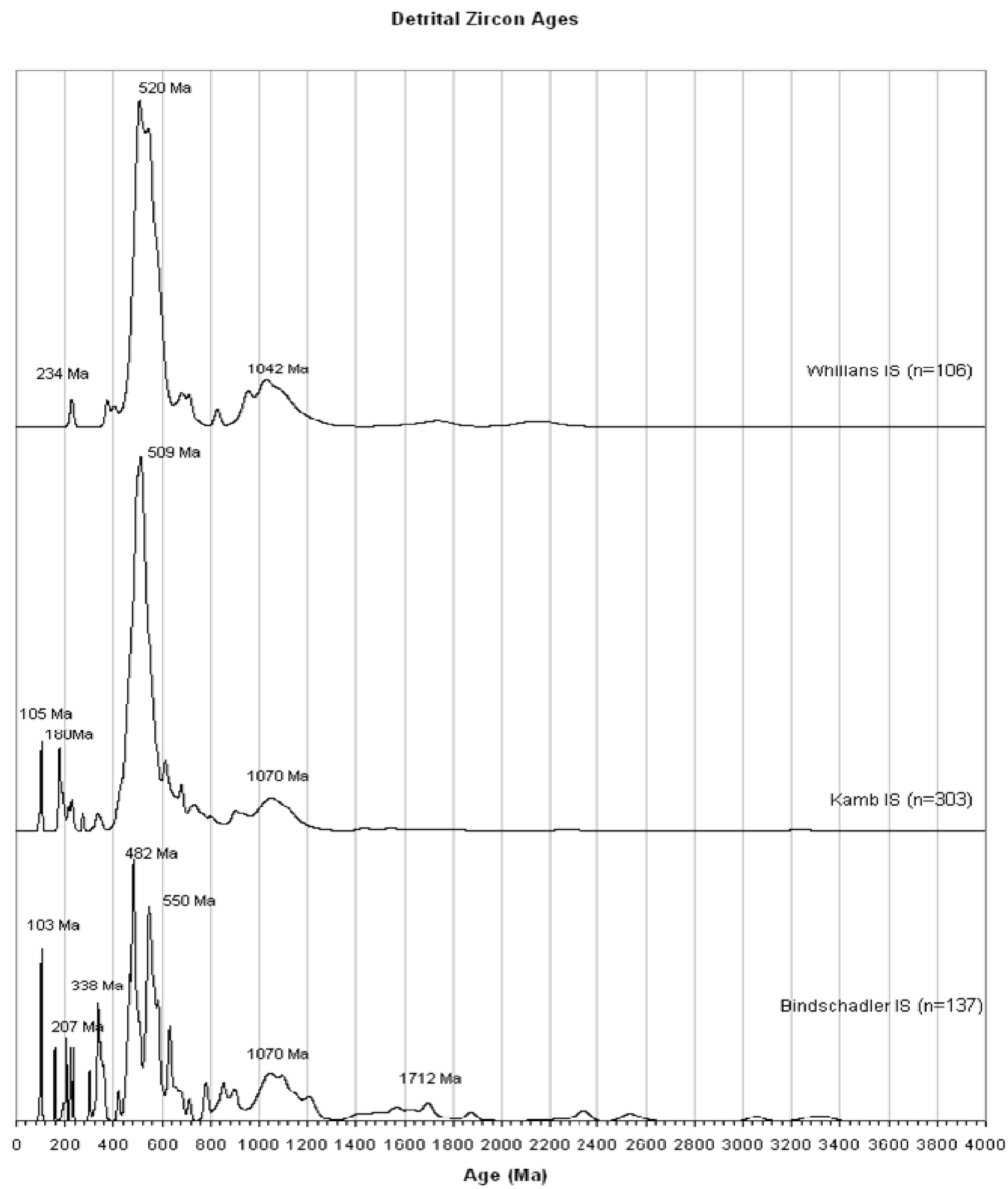

Figure 11. Normalized probability plot of detrital zircon ages in WA Ice Streams (IS= Ice stream).

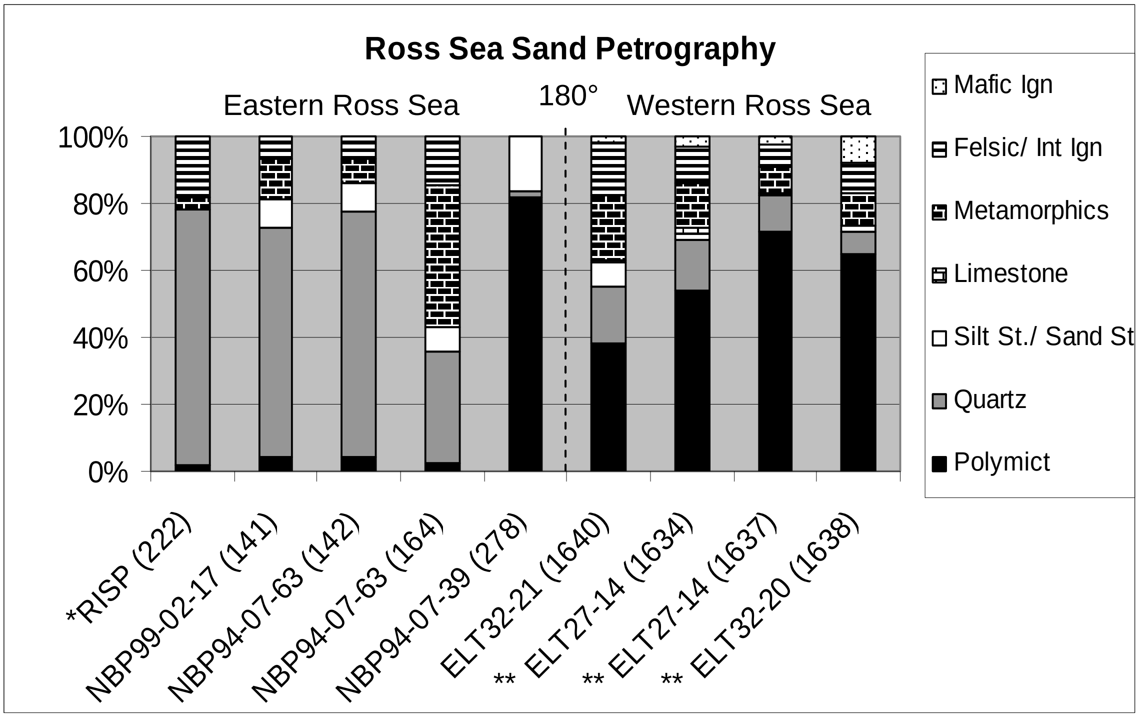

Figure 12. Sand petrography data from the Ross Sea. *= data from Kramer (2008). **= data from Palmer (2008).

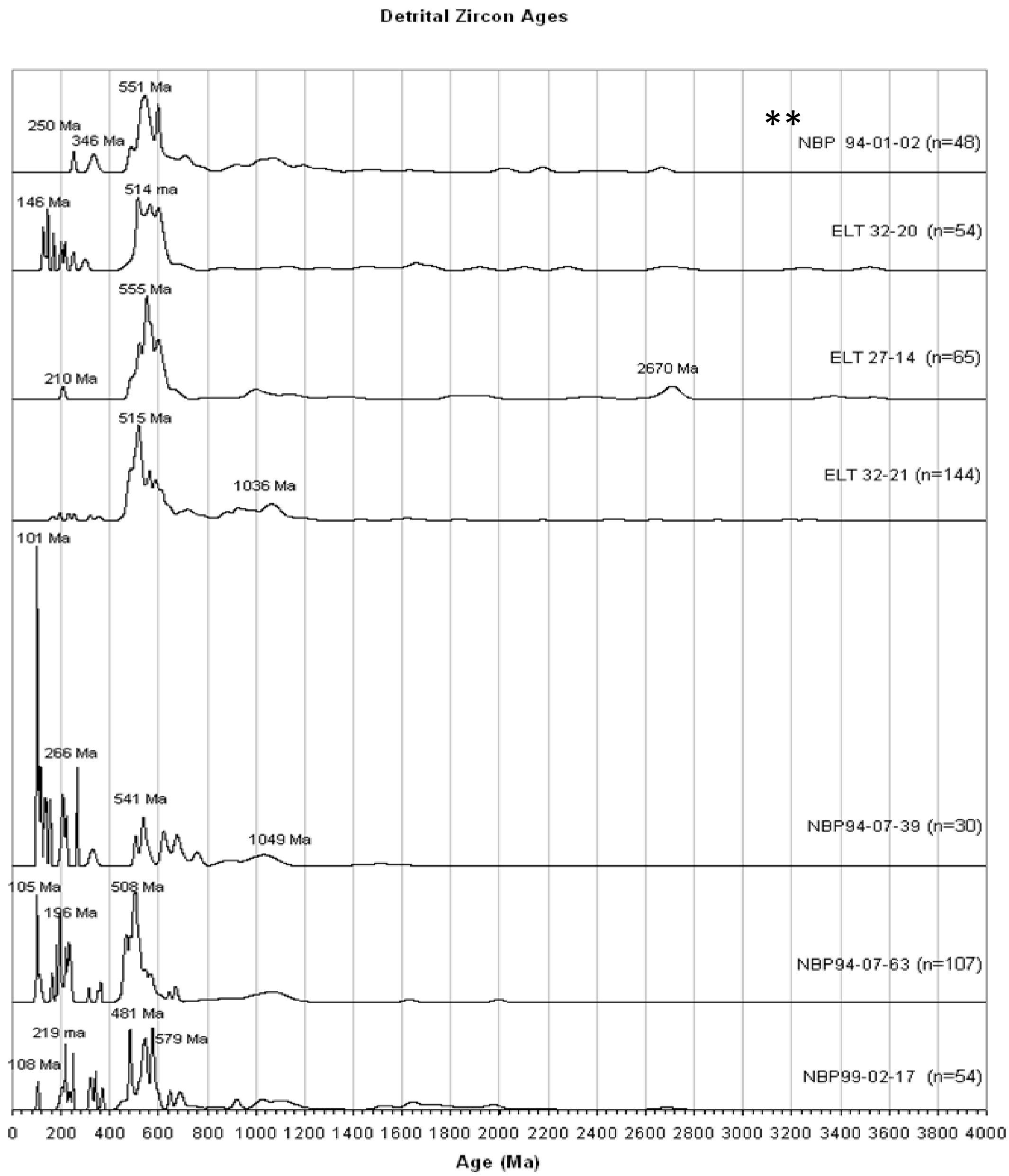

Figure 13. Normalized probability plots of detrital zircon ages in the Ross Sea. **= data from Palmer (2008)

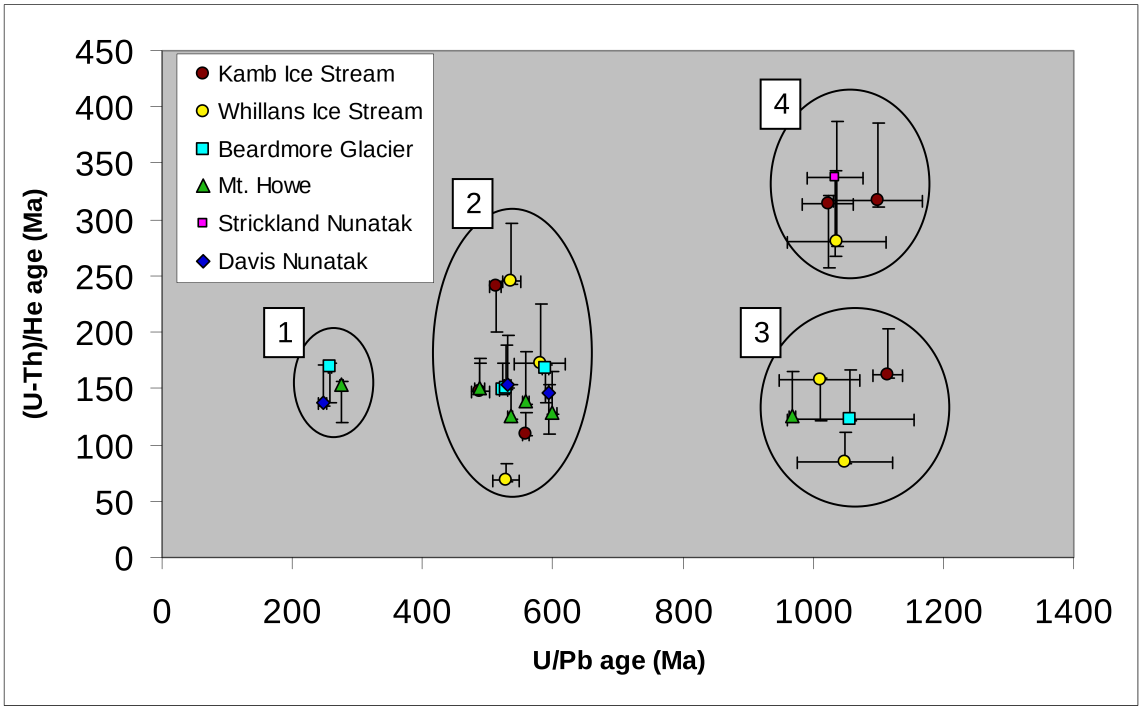

Figure 14. U-Th/He and U-Pb data for select EA and WA sample sites. Age groupings are labeled in the white boxes.

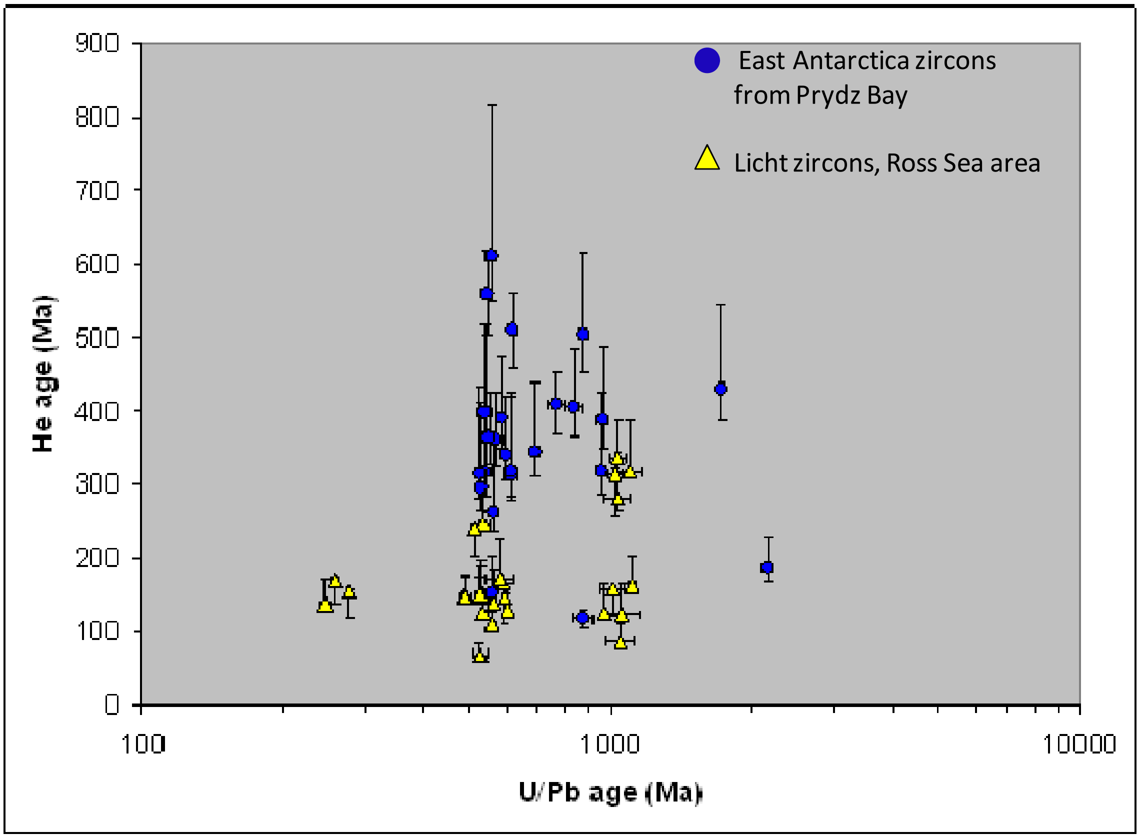

Figure 15. U-Pb and He age data for the Ross Embayment and the Prydz bay area (Prydz data compliments of Peter Reiners).

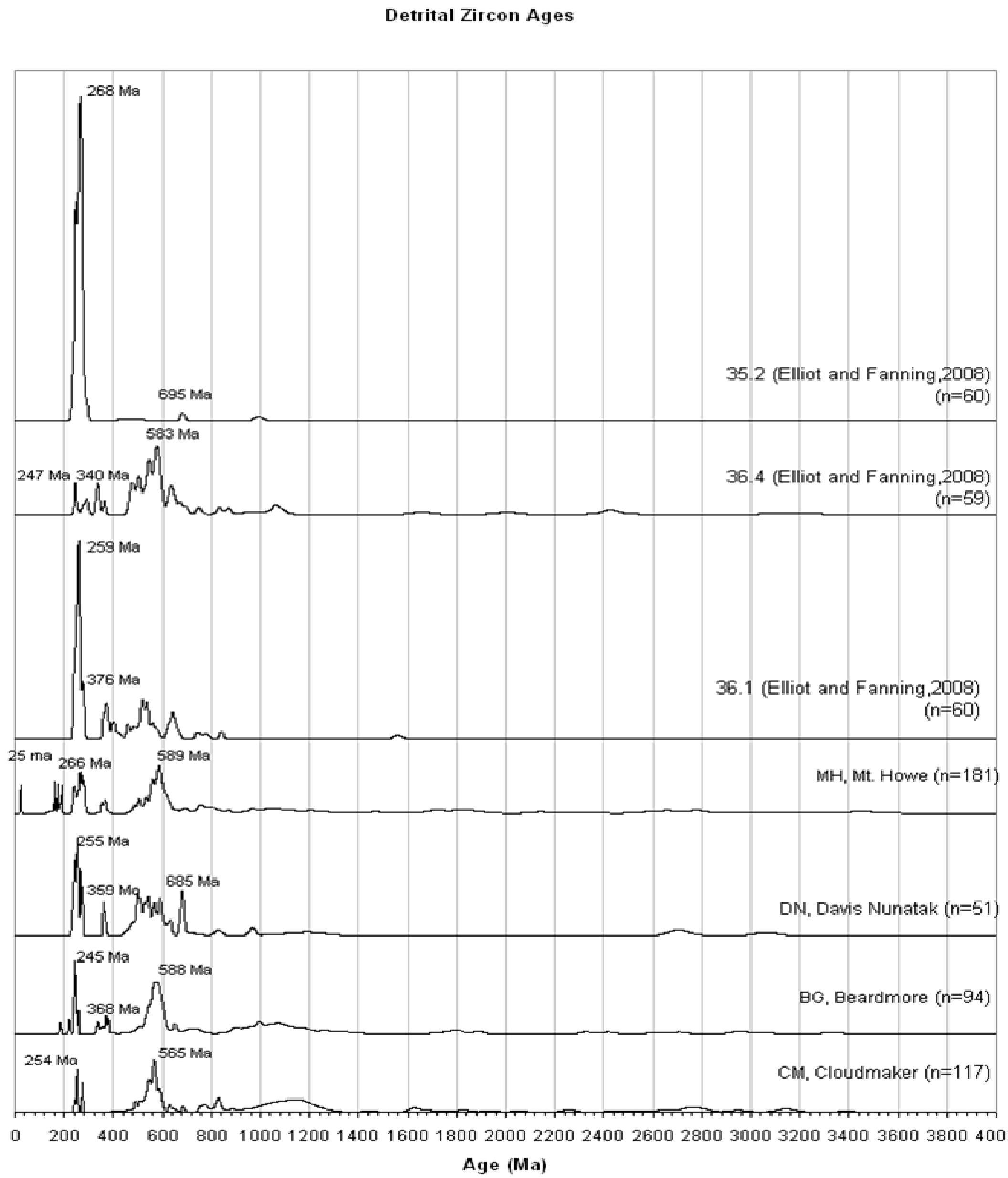

Figure 16. Normalized probability plots of detrital zircon ages from EA and Elliot and Fanning (2008) from Beacon Supergroup.

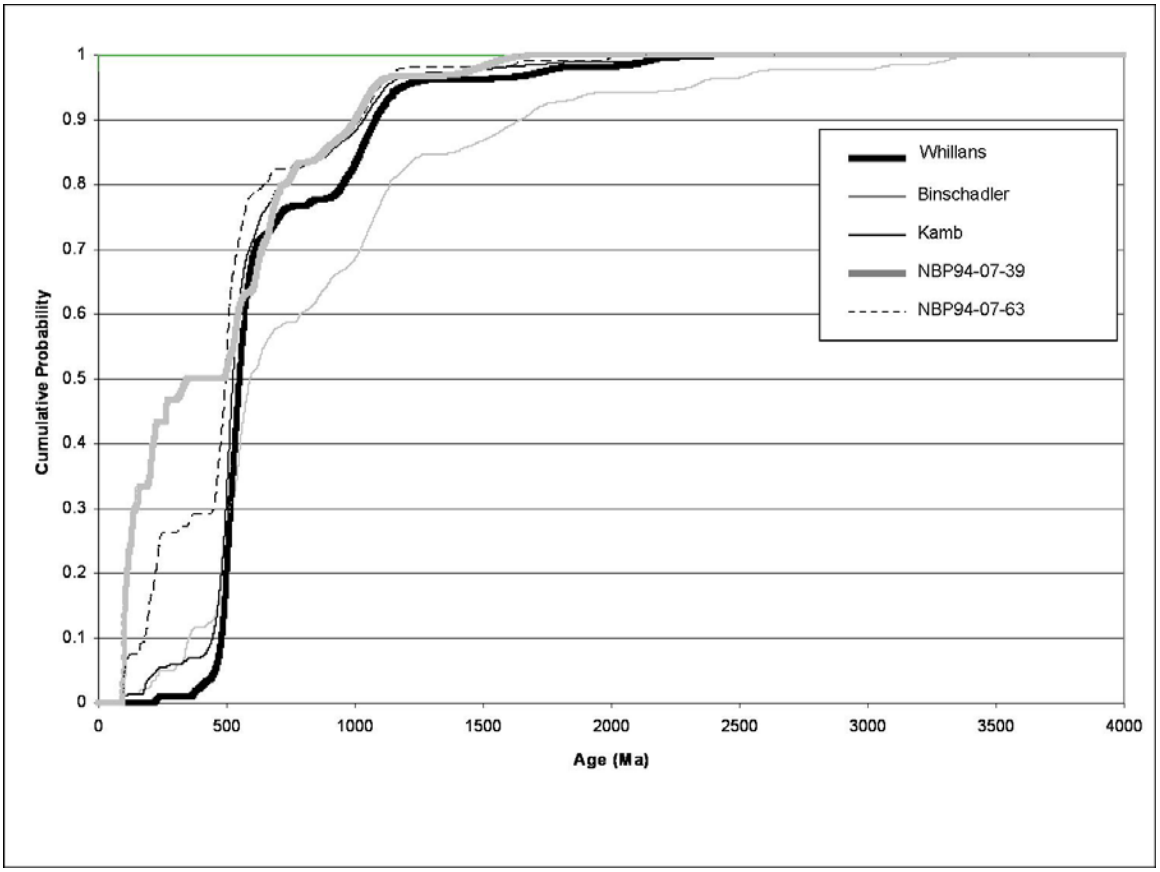

Figure 17. Cumulative Probability plot of WA ice streams and Ross Sea cores, NBP94-07-39 and NBP94-07-63.

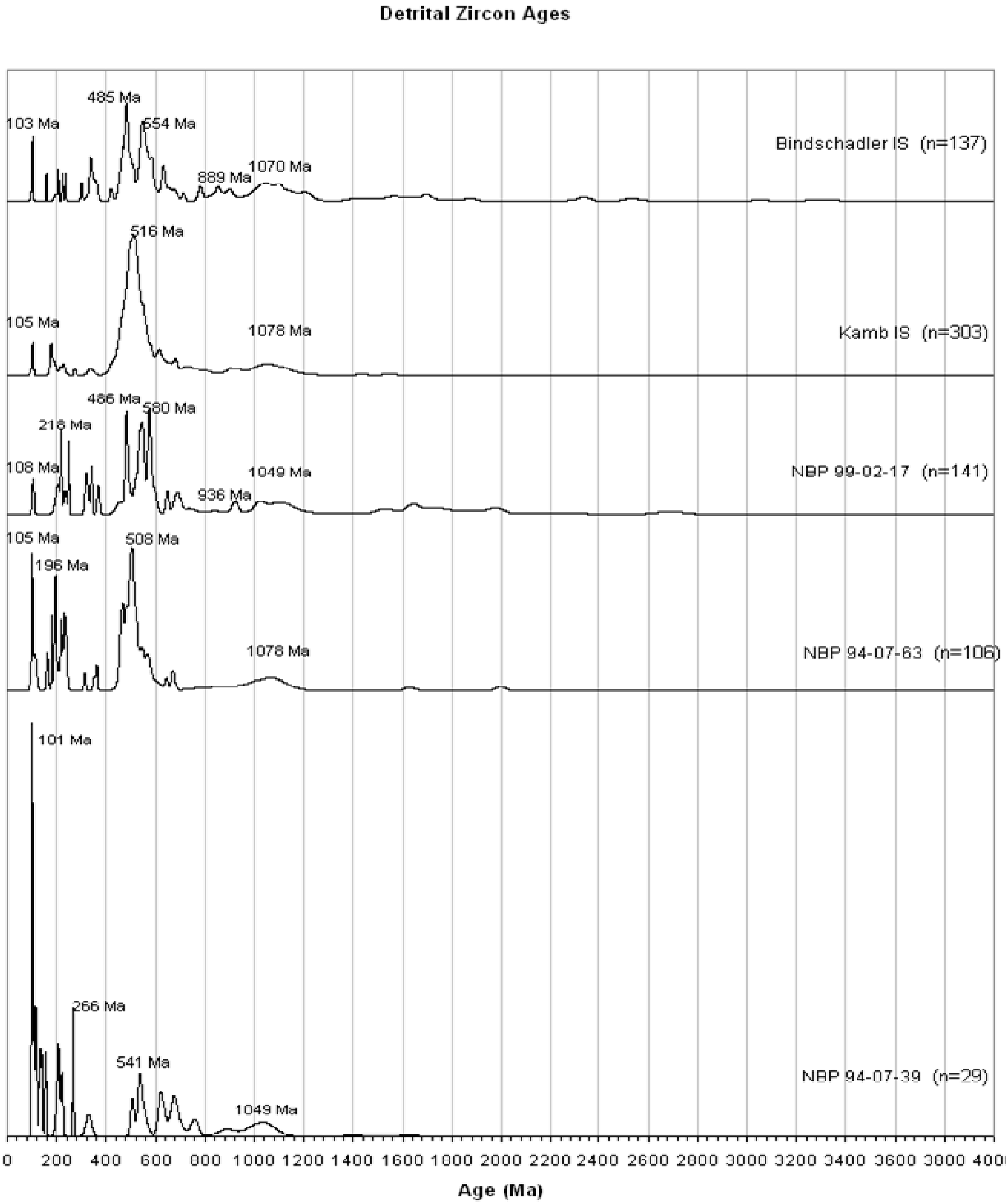

Figure 18. Normalized probability plot of Kamb Ice stream, Bindschadler Ice Stream and the Eastern Ross Sea cores.

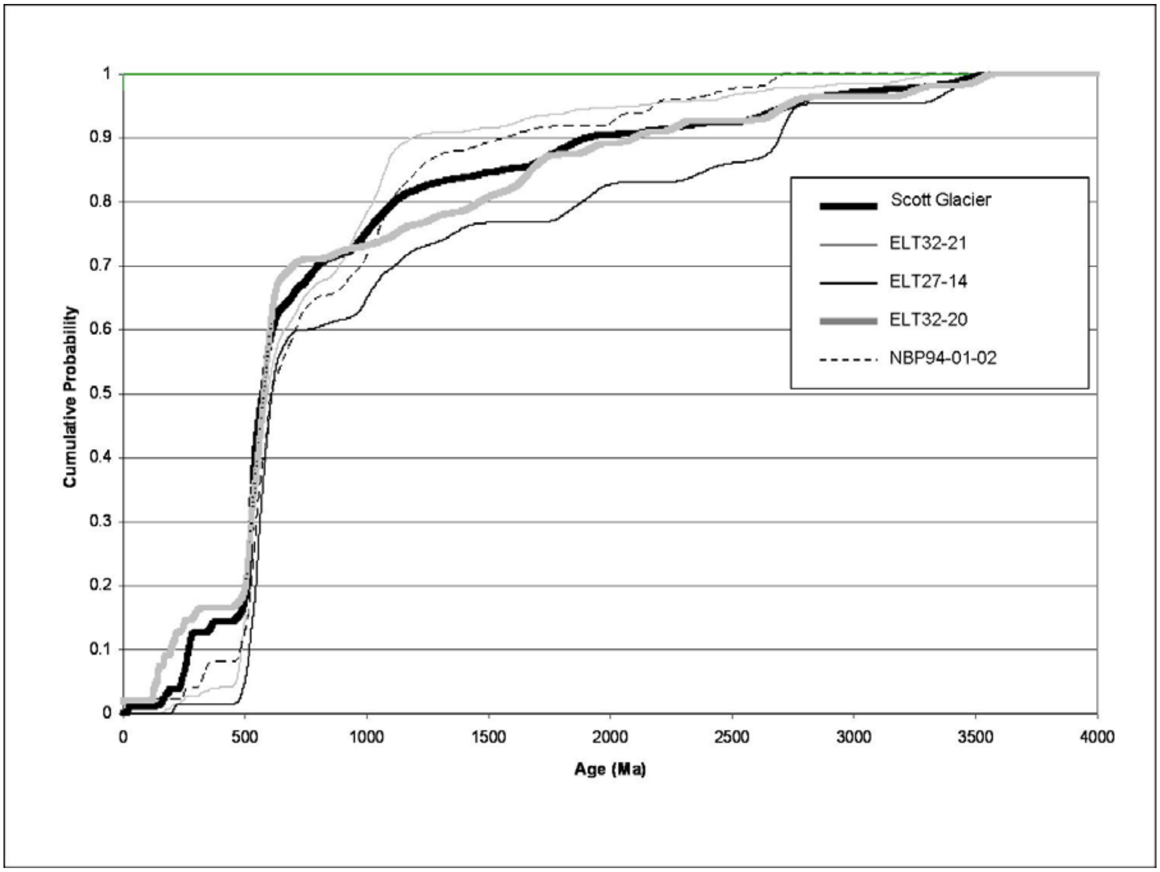

Figure 19. Cumulative probability plot of Scott Glacier and Central/Western Ross Sea cores.

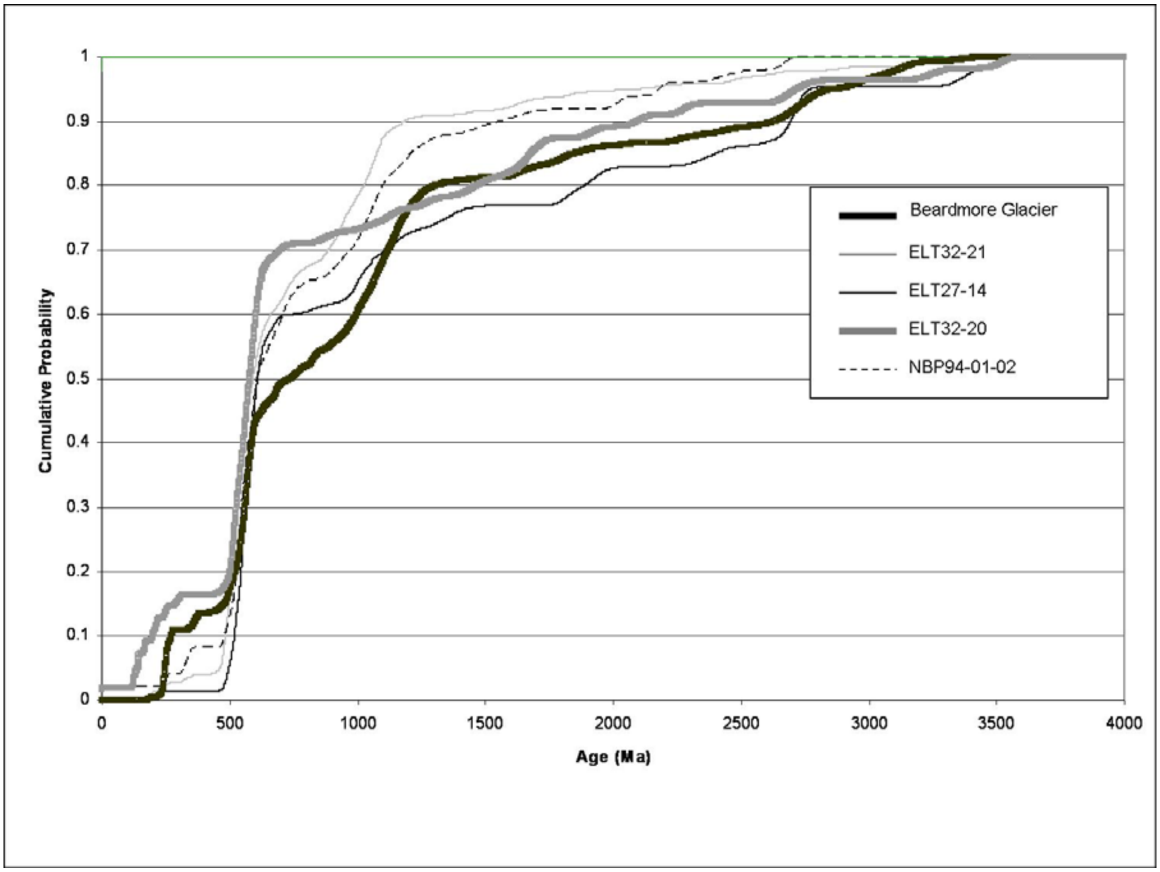

Figure 20. Cumulative probability plot of Beardmore Glacier and Eastern Ross Sea.

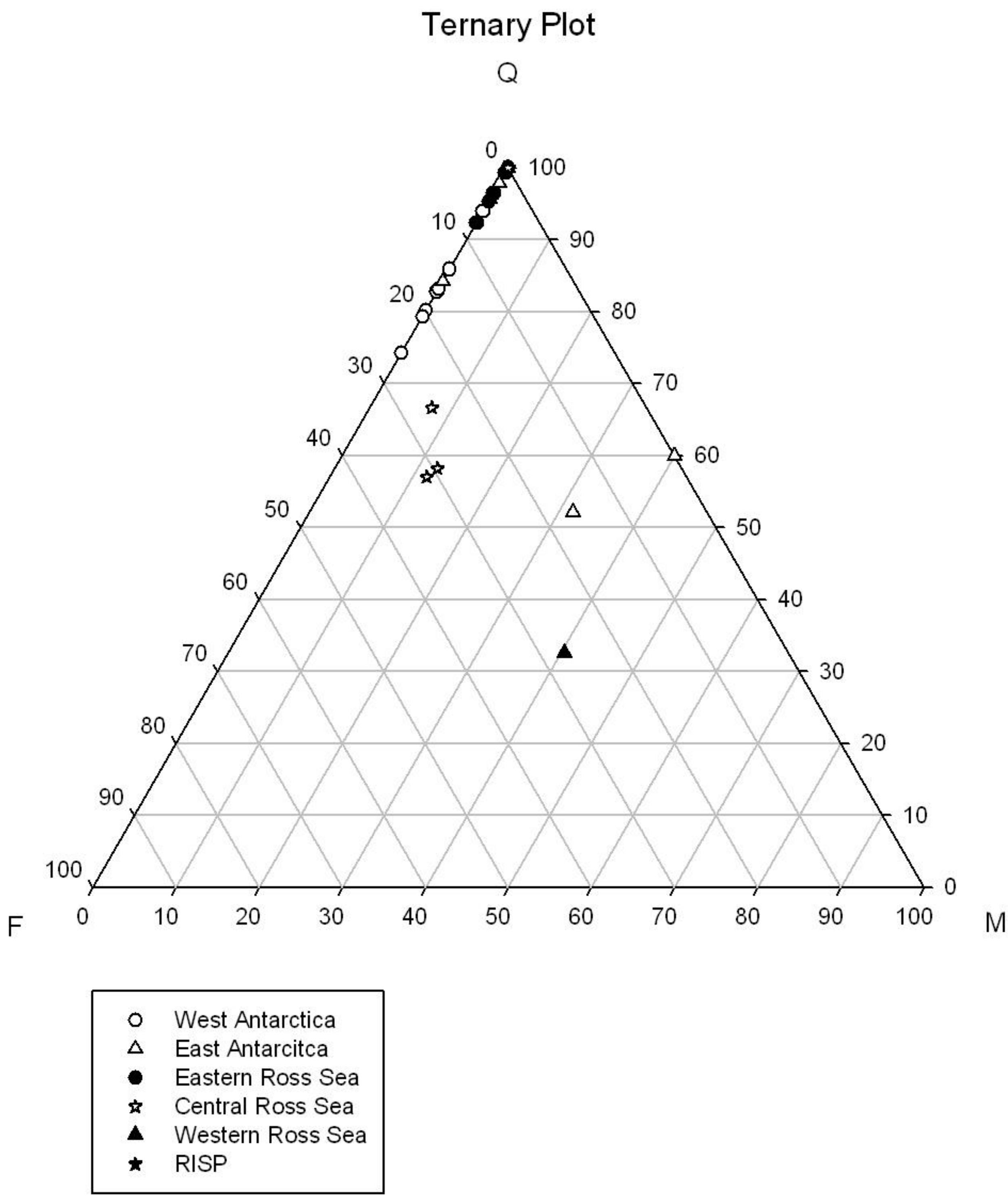

Figure 21. QFM diagram of samples identified in this study. (Additional data from Palmer (2008) and Kramer (2008)). Q= Quartz, F= Feldspar (plag + k-spar), and M= Mafic lithic fragments

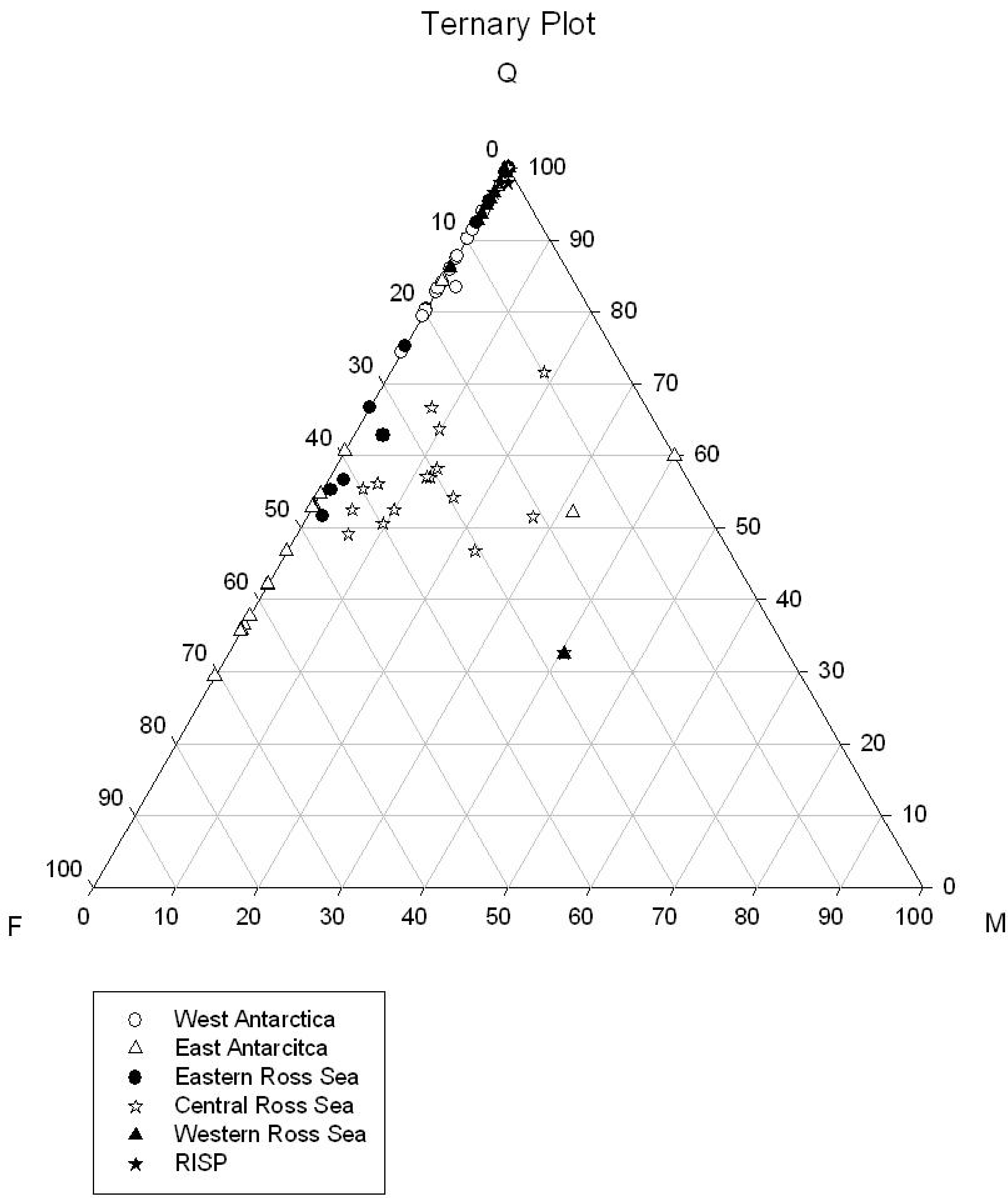

Figure 22. QFM diagram of data from all samples from Palmer (2008), Kramer (2008), and this study. Q= Quartz, F= Feldspar (plag + k-spar), and M= Mafic lithic fragment

Appendix A: U-Pb detrital zircon geochronologic analyses by Laser-Ablation Multicollector ICP Mass Spectrometry

			Isotope ratios							Apparent ages (Ma)							
U (ppm)	206Pb 204Pb	U/Th	206Pb* 207Pb*	± (%)	207Pb* 235U*	± (%)	206Pb* 238U	± (%)	error corr.	206Pb* 238U*	± (Ma)	207Pb* 235U	± (Ma)	206Pb* 207Pb*	± (Ma)	**Best age (Ma)**	± (Ma)
Bindschadler (SAL 1775)																	
438	8770	2.3	15.9751	3.5	0.584	3.7	0.068	1.3	0.3	421.7	5.3	466.7	13.8	694.6	73.7	421.7	5.3
144	14285	1.4	17.1173	3.9	0.622	4.3	0.077	1.9	0.4	479.8	8.6	491.3	16.7	545.5	84.4	479.8	8.6
480	35030	2.8	12.4455	3.1	2.140	3.5	0.193	1.6	0.5	1138.5	16.8	1161.8	24.4	1205.6	61.9	1205.6	61.9
100	51405	3.5	13.3865	3.3	1.936	3.4	0.188	0.6	0.2	1110.1	6.5	1093.5	22.8	1060.5	67.3	1060.5	67.3
397	7925	2.8	15.3473	2.8	0.476	5.1	0.053	4.2	0.8	332.7	13.7	395.2	16.5	779.4	58.2	332.7	13.7
837	6190	2.2	13.5772	17.0	0.561	17.1	0.055	1.4	0.1	346.5	4.6	452.0	62.4	1032.0	346.4	346.5	4.6
182	16683	3.5	17.2127	5.0	0.620	5.1	0.077	1.0	0.2	480.4	4.7	489.7	20.0	533.4	110.6	480.4	4.7
419	41040	1.2	16.7577	1.0	0.784	2.2	0.095	2.0	0.9	586.7	11.2	587.7	10.0	591.8	22.1	586.7	11.2
277	38100	14.4	16.2693	4.6	0.876	5.8	0.103	3.6	0.6	633.8	21.6	638.6	27.7	655.6	99.2	633.8	21.6
144	16968	3.0	17.2648	2.0	0.629	2.7	0.079	1.9	0.7	488.7	9.0	495.5	10.7	526.8	43.0	488.7	9.0
187	14535	1.6	16.9112	1.8	0.710	2.4	0.087	1.6	0.7	538.5	8.5	545.0	10.1	572.0	38.1	538.5	8.5
468	10926	1.7	16.6188	5.5	0.637	5.8	0.077	1.8	0.3	477.2	8.2	500.7	22.8	609.8	118.6	477.2	8.2
189	18927	1.7	17.4196	2.6	0.698	2.8	0.088	1.1	0.4	544.5	5.8	537.3	11.7	507.2	56.5	544.5	5.8
704	13533	2.2	12.5329	4.3	1.972	4.5	0.179	1.4	0.3	1063.0	13.4	1106.1	30.5	1191.8	85.0	1191.8	85.0
553	32202	8.5	14.5310	1.5	1.245	1.6	0.131	0.5	0.3	794.6	3.7	821.1	8.9	893.3	31.0	893.3	31.0
228	20355	1.4	17.9653	2.5	0.590	2.6	0.077	0.8	0.3	477.1	3.7	470.5	9.9	438.9	55.8	477.1	3.7
207	59280	2.2	10.4830	1.5	3.581	1.7	0.272	0.7	0.4	1552.1	10.1	1545.2	13.5	1535.8	28.8	1535.8	28.8
210	131811	6.5	3.7798	2.6	18.315	6.0	0.502	5.5	0.9	2622.7	117.4	3006.4	58.3	3274.1	41.2	3274.1	41.2
141	19401	1.4	16.7384	3.7	0.808	4.1	0.098	1.6	0.4	603.0	9.2	601.2	18.4	594.3	81.0	603.0	9.2
85	12702	2.6	17.5781	6.4	0.680	6.7	0.087	1.9	0.3	536.3	10.0	527.0	27.5	487.2	141.3	536.3	10.0
343	17124	1.8	19.7301	4.7	0.260	4.9	0.037	1.3	0.3	235.5	3.0	234.7	10.2	226.5	108.7	235.5	3.0
198	36594	4.1	13.5044	1.5	1.741	2.4	0.171	2.0	0.8	1014.9	18.4	1023.8	15.8	1042.8	29.5	1042.8	29.5
547	31500	1.3	17.3528	4.0	0.639	4.2	0.080	1.2	0.3	498.5	5.6	501.5	16.7	515.6	88.8	498.5	5.6
86	10701	0.9	16.8379	4.8	0.758	4.9	0.093	1.0	0.2	571.0	5.5	573.1	21.5	581.4	104.2	571.0	5.5
154	2418	1.5	17.2847	33.1	0.126	33.5	0.016	5.4	0.2	100.6	5.4	120.1	38.0	524.2	744.3	100.6	5.4
136	12708	2.9	17.2828	17.5	0.638	17.8	0.080	3.3	0.2	495.7	15.9	500.8	70.5	524.5	386.1	495.7	15.9
249	34668	2.3	14.2906	1.6	1.396	2.4	0.145	1.7	0.7	870.8	13.9	887.0	13.9	927.6	33.1	927.6	33.1
305	58575	2.0	13.1220	0.7	1.944	2.2	0.185	2.1	1.0	1094.4	20.6	1096.4	14.5	1100.6	13.4	1100.6	13.4
206	45561	3.2	13.7027	1.8	1.665	2.6	0.165	1.8	0.7	987.0	16.5	995.2	16.3	1013.3	37.3	1013.3	37.3
227	19017	2.2	16.0868	2.0	0.884	2.1	0.103	0.7	0.3	633.0	4.3	643.3	10.0	679.7	42.1	633.0	4.3

Appendix A Cont.: U-Pb detrital zircon geochronologic analyses by Laser-Ablation Multicollector ICP Mass Spectrometry

					Isotope ratios							**Apparent ages (Ma)**					
U (ppm)	206Pb 204Pb	U/Th	206Pb* 207Pb*	± (%)	207Pb* 235U*	± (%)	206Pb* 238U	± (%)	error corr.	206Pb* 238U*	± (Ma)	207Pb* 235U	± (Ma)	206Pb* 207Pb*	± (Ma)	**Best age** (Ma)	± (Ma)
Bindschadler (SAL 1775) Cont.																	
232	102477	1.5	6.6622	1.3	9.152	1.4	0.442	0.6	0.4	2360.5	12.5	2353.3	12.9	2347.0	21.5	2347.0	21.5
400	12522	3.7	16.6767	1.4	0.717	3.5	0.087	3.2	0.9	536.0	16.7	548.8	14.9	602.3	29.9	536.0	16.7
73	34521	3.0	6.7431	2.0	8.961	2.5	0.438	1.5	0.6	2342.7	30.2	2334.0	23.1	2326.4	34.4	2326.4	34.4
345	188481	5.6	3.6269	1.7	25.705	2.3	0.676	1.6	0.7	3329.7	41.1	3335.4	22.8	3338.8	26.9	3338.8	26.9
127	22188	2.3	13.7309	1.3	1.678	1.7	0.167	1.0	0.6	996.1	9.5	1000.2	10.6	1009.2	26.3	1009.2	26.3
156	34398	2.6	13.0365	1.8	1.999	2.1	0.189	1.1	0.5	1116.1	11.4	1115.3	14.1	1113.6	35.4	1113.6	35.4
139	12045	2.3	18.4978	6.1	0.574	6.3	0.077	1.5	0.2	478.2	7.1	460.5	23.3	373.5	137.2	478.2	7.1
358	26790	2.2	14.8414	1.5	1.294	2.5	0.139	2.0	0.8	840.7	15.4	843.2	14.1	849.5	30.8	849.5	30.8
227	52566	1.1	12.4461	0.8	2.300	1.5	0.208	1.3	0.8	1216.3	14.0	1212.4	10.7	1205.5	16.3	1205.5	16.3
54	23082	1.4	8.7227	1.2	5.389	2.1	0.341	1.7	0.8	1891.1	27.7	1883.1	17.6	1874.3	21.0	1874.3	21.0
702	55776	5.2	16.8123	0.7	0.771	1.4	0.094	1.2	0.9	579.5	6.8	580.5	6.2	584.7	15.5	579.5	6.8
169	21615	0.8	13.5083	1.3	1.824	1.5	0.179	0.9	0.6	1059.7	8.6	1054.0	10.1	1042.2	25.7	1042.2	25.7
284	18396	2.5	13.4993	2.0	1.613	4.6	0.158	4.1	0.9	945.1	36.4	975.2	28.9	1043.6	41.2	1043.6	41.2
215	25092	4.3	16.9080	3.1	0.738	4.0	0.091	2.6	0.6	558.5	13.6	561.3	17.3	572.4	67.1	558.5	13.6
138	15654	0.8	17.3224	3.0	0.722	3.4	0.091	1.6	0.5	559.4	8.7	551.6	14.4	519.5	65.0	559.4	8.7
56	7482	1.1	16.1361	5.3	0.922	5.5	0.108	1.3	0.2	660.6	8.1	663.5	26.8	673.2	114.3	660.6	8.1
140	24543	4.2	14.7037	5.1	0.867	10.6	0.092	9.3	0.9	570.2	50.8	634.0	50.0	868.9	105.6	570.2	50.8
31	6639	2.1	13.3394	4.5	1.919	4.5	0.186	0.5	0.1	1097.6	5.1	1087.6	30.4	1067.6	90.9	1067.6	90.9
321	12441	2.3	17.3245	2.9	0.626	3.4	0.079	1.8	0.5	488.1	8.3	493.6	13.3	519.2	63.5	488.1	8.3
68	14925	1.0	14.4325	2.8	1.451	3.0	0.152	1.0	0.3	911.6	8.8	910.3	18.0	907.3	57.7	907.3	57.7
99	23274	1.6	12.8279	1.1	2.086	1.3	0.194	0.6	0.5	1143.3	6.7	1144.1	8.7	1145.7	21.7	1145.7	21.7
310	98154	1.3	5.8749	2.7	11.408	3.3	0.486	1.8	0.5	2553.7	37.5	2557.1	30.4	2559.7	45.7	2559.7	45.7
423	3096	6.2	13.5928	10.0	0.488	10.1	0.048	0.9	0.1	302.7	2.8	403.3	33.5	1029.6	203.0	302.7	2.8
456	42366	1.9	17.6346	1.8	0.576	2.1	0.074	1.2	0.5	458.3	5.2	462.0	7.9	480.1	39.4	458.3	5.2
290	30273	3.1	11.2666	1.5	2.551	3.6	0.208	3.3	0.9	1220.4	36.5	1286.6	26.4	1398.9	29.0	1398.9	29.0
61	20358	2.0	10.3018	1.0	3.702	1.4	0.277	0.9	0.7	1574.3	13.0	1571.8	11.2	1568.6	19.5	1568.6	19.5
427	12825	5.1	13.5177	2.5	1.223	3.5	0.120	2.5	0.7	729.7	16.9	810.9	19.6	1040.8	50.9	1040.8	50.9
437	12645	2.0	13.6048	3.7	1.440	4.4	0.142	2.5	0.6	856.7	19.7	905.9	26.4	1027.8	74.0	1027.8	74.0

Appendix A Cont.: U-Pb detrital zircon geochronologic analyses by Laser-Ablation Multicollector ICP Mass Spectrometry

			Isotope ratios							Apparent ages (Ma)							
U (ppm)	206Pb 204Pb	U/Th	206Pb* 207Pb*	± (%)	207Pb* 235U*	± (%)	206Pb* 238U	± (%)	error corr.	206Pb* 238U*	± (Ma)	207Pb* 235U	± (Ma)	206Pb* 207Pb*	± (Ma)	**Best age (Ma)**	± (Ma)
Bindschadler (SAL 1775) Cont.																	
431	66180	2.7	17.0823	0.6	0.716	1.1	0.089	0.9	0.9	548.0	4.9	548.4	4.7	550.0	12.5	548.0	4.9
280	26451	2.0	17.6760	2.6	0.586	2.7	0.075	0.9	0.3	467.3	3.9	468.6	10.2	474.9	57.3	467.3	3.9
248	37119	1.3	17.1139	3.0	0.735	3.5	0.091	1.8	0.5	563.1	9.7	559.7	14.9	546.0	65.0	563.1	9.7
456	20256	1.6	16.7241	5.7	0.652	5.9	0.079	1.7	0.3	490.3	8.2	509.4	23.7	596.1	122.6	490.3	8.2
517	10572	1.6	15.8817	2.6	0.789	3.1	0.091	1.7	0.5	560.5	9.2	590.4	14.1	707.1	55.9	560.5	9.2
153	35823	3.7	14.6336	0.8	1.285	3.7	0.136	3.6	1.0	824.1	27.7	839.0	20.9	878.8	16.4	878.8	16.4
84	21375	1.2	13.1778	2.3	1.830	4.0	0.175	3.2	0.8	1039.2	31.1	1056.4	26.1	1092.0	46.3	1092.0	46.3
342	26282	1.4	16.3283	1.9	0.939	2.6	0.111	1.9	0.7	679.7	12.1	672.3	13.0	647.8	39.9	679.7	12.1
425	2778	0.2	16.6791	15.0	0.258	15.6	0.031	4.3	0.3	198.3	8.4	233.2	32.5	601.9	325.6	198.3	8.4
140	19592	2.7	16.8428	3.1	0.781	3.3	0.095	1.1	0.3	587.6	5.9	586.2	14.6	580.8	67.6	587.6	5.9
133	2532	2.4	16.3502	6.5	0.662	6.8	0.078	2.1	0.3	486.8	9.7	515.6	27.4	644.9	138.8	486.8	9.7
121	12072	2.0	17.0917	6.5	0.440	7.8	0.055	4.3	0.6	342.6	14.4	370.5	24.2	548.9	142.0	342.6	14.4
350	86888	2.2	12.3322	1.0	2.342	1.4	0.210	1.0	0.7	1226.2	11.5	1225.3	10.2	1223.6	19.5	1223.6	19.5
168	72402	1.8	4.3393	1.5	18.774	1.7	0.591	0.8	0.5	2992.8	19.4	3030.3	16.2	3055.2	23.5	3055.2	23.5
173	6402	3.1	17.1200	5.8	0.606	5.9	0.075	0.6	0.1	467.6	2.5	480.9	22.4	545.2	127.5	467.6	2.5
598	19272	1.8	18.8654	2.3	0.393	2.7	0.054	1.4	0.5	338.0	4.7	336.9	7.9	329.1	53.2	338.0	4.7
478	53704	2.8	18.7748	2.4	0.416	3.4	0.057	2.5	0.7	355.0	8.5	353.0	10.2	340.0	53.4	355.0	8.5
419	30314	3.3	18.8014	2.5	0.409	4.8	0.056	4.1	0.9	350.0	14.0	348.3	14.1	336.8	55.8	350.0	14.0
79	4772	2.2	16.9522	10.9	0.660	11.3	0.081	2.9	0.3	503.2	14.1	514.8	45.8	566.7	239.0	503.2	14.1
155	7762	1.5	17.9431	2.4	0.598	2.5	0.078	0.6	0.3	483.3	3.0	476.2	9.6	441.7	54.2	483.3	3.0
293	59886	2.6	9.7128	2.4	4.304	2.5	0.303	0.8	0.3	1707.0	11.2	1694.1	20.9	1678.1	44.7	1678.1	44.7
496	49372	3.9	16.7960	2.5	0.725	3.0	0.088	1.7	0.6	545.8	8.9	553.8	12.9	586.8	54.0	545.8	8.9
444	12292	2.5	13.1343	2.1	1.986	2.6	0.189	1.4	0.6	1116.9	14.8	1110.7	17.4	1098.7	42.6	1098.7	42.6
237	27308	2.9	14.9288	2.2	1.192	2.3	0.129	0.7	0.3	782.2	5.2	796.7	12.6	837.3	45.3	782.2	5.2
201	21814	2.9	10.9627	2.3	2.632	5.2	0.209	4.6	0.9	1224.8	51.3	1309.5	38.0	1451.2	44.6	1451.2	44.6
53	1876	1.3	8.9615	7.6	4.153	7.9	0.270	2.2	0.3	1540.4	30.4	1664.8	64.7	1825.4	137.5	1825.4	137.5
Bindschadler (SAL 1776)																	
368	37070	2.6	16.5502	3.6	0.622	7.1	0.075	6.1	0.9	463.9	27.3	490.8	27.6	618.7	78.0	463.9	27.3
724	11265	1.2	20.4032	1.9	0.109	2.2	0.016	1.1	0.5	103.4	1.2	105.3	2.2	148.4	44.0	103.4	1.2
233	20825	2.0	17.2663	4.5	0.584	5.0	0.073	2.3	0.5	455.0	10.2	467.0	18.8	526.6	97.9	455.0	10.2
125	7098	2.4	19.3614	13.1	0.411	13.2	0.058	1.6	0.1	361.8	5.7	349.6	39.0	269.9	300.8	361.8	5.7

Appendix A Cont.: U-Pb detrital zircon geochronologic analyses by Laser-Ablation Multicollector ICP Mass Spectrometry

			Isotope ratios									Apparent ages (Ma)					
U (ppm)	206Pb 204Pb	U/Th	206Pb* 207Pb*	± (%)	207Pb* 235U*	± (%)	206Pb* 238U	± (%)	error corr.	206Pb* 238U*	± (Ma)	207Pb* 235U	± (Ma)	206Pb* 207Pb*	± (Ma)	**Best age** (Ma)	± (Ma)
Bindschadler (SAL 1776) Cont.																	
67	6704	2.0	16.6921	7.0	0.714	7.8	0.086	3.4	0.4	534.3	17.5	547.0	33.1	600.2	152.4	534.3	17.5
69	8776	1.7	13.1104	2.7	1.922	2.8	0.183	0.5	0.2	1081.9	5.0	1088.7	18.5	1102.3	54.5	1102.3	54.5
155	16996	2.0	17.4910	2.7	0.709	3.0	0.090	1.3	0.4	555.3	6.8	544.2	12.7	498.2	60.2	555.3	6.8
712	83450	2.0	9.6057	0.8	4.101	1.1	0.286	0.8	0.7	1620.1	10.7	1654.5	9.2	1698.5	15.5	1698.5	15.5
407	75432	0.5	16.6403	2.4	0.854	2.5	0.103	0.6	0.3	632.1	3.9	626.7	11.5	607.0	51.1	632.1	3.9
548	14782	14.4	16.0389	3.1	0.910	3.4	0.106	1.4	0.4	648.8	8.4	657.2	16.4	686.1	66.4	648.8	8.4
506	48730	4.9	15.9101	2.1	1.014	2.4	0.117	1.0	0.4	713.6	6.9	711.1	12.0	703.3	45.2	713.6	6.9
465	45132	12.3	17.3012	1.4	0.700	1.6	0.088	0.8	0.5	542.6	4.3	538.7	6.8	522.1	30.8	542.6	4.3
308	64112	3.8	13.4237	1.4	1.780	1.7	0.173	0.8	0.5	1030.2	7.9	1038.2	10.8	1054.9	29.0	1054.9	29.0
146	20094	14.5	16.4538	4.6	0.770	4.7	0.092	0.9	0.2	566.4	4.7	579.5	20.7	631.3	99.2	566.4	4.7
395	29520	6.8	14.0499	2.9	1.326	4.7	0.135	3.7	0.8	817.1	28.6	857.2	27.4	962.5	59.3	817.1	28.6
93	4960	1.5	22.9140	28.0	0.197	28.1	0.033	1.3	0.0	207.3	2.7	182.3	46.9	-130.9	705.1	207.3	2.7
298	20188	18.2	15.0337	2.7	1.019	3.1	0.111	1.5	0.5	679.4	9.8	713.6	15.7	822.7	55.7	679.4	9.8
74	28286	2.7	10.8105	1.6	3.315	2.4	0.260	1.8	0.7	1489.5	23.7	1484.6	18.9	1477.7	31.1	1477.7	31.1
108	14214	1.8	17.6186	5.6	0.737	5.8	0.094	1.2	0.2	579.8	6.7	560.4	24.9	482.2	124.8	579.8	6.7
366	25322	1.5	17.4370	1.4	0.652	1.5	0.082	0.6	0.4	510.5	2.8	509.5	6.2	505.0	31.7	510.5	2.8
641	46000	48.6	9.6786	2.1	4.187	2.4	0.294	1.1	0.5	1661.1	16.0	1671.5	19.5	1684.6	39.0	1684.6	39.0
656	72124	12.0	16.6151	1.5	0.858	1.6	0.103	0.5	0.3	634.5	3.0	629.2	7.3	610.3	31.8	634.5	3.0
660	47568	3.8	16.7165	1.8	0.838	2.3	0.102	1.4	0.6	624.1	8.3	618.3	10.5	597.1	38.4	624.1	8.3
592	121150	2.2	12.6082	1.3	2.171	2.0	0.199	1.6	0.8	1167.5	16.6	1171.9	14.0	1180.0	25.5	1180.0	25.5
88	12684	2.6	13.3433	4.3	1.797	4.4	0.174	1.1	0.2	1033.5	10.4	1044.3	28.9	1067.0	86.4	1067.0	86.4
178	89822	1.2	10.1692	2.7	3.861	2.8	0.285	0.8	0.3	1615.3	11.0	1605.6	22.3	1592.8	49.7	1592.8	49.7
198	78914	2.9	5.9854	1.8	11.215	2.3	0.487	1.5	0.6	2557.0	30.6	2541.2	21.6	2528.5	30.4	2528.5	30.4
310	614	1.5	11.1434	7.8	0.910	8.0	0.074	2.1	0.3	457.3	9.2	656.9	38.9	1420.0	148.6	457.3	9.2
523	129878	2.8	13.5309	2.1	1.791	2.4	0.176	1.3	0.5	1043.7	12.5	1042.2	15.9	1038.9	41.8	1038.9	41.8
250	49732	4.1	13.0599	2.4	2.052	2.6	0.194	0.9	0.3	1145.2	8.9	1133.1	17.6	1110.0	48.6	1110.0	48.6
244	1072	1.0	14.7607	11.3	0.331	11.4	0.035	0.5	0.0	224.6	1.2	290.5	28.7	860.8	236.2	224.6	1.2
831	12738	0.7	19.4407	4.8	0.177	5.0	0.025	1.4	0.3	159.3	2.2	165.8	7.6	260.6	109.3	159.3	2.2

Appendix A Cont.: U-Pb detrital zircon geochronologic analyses by Laser-Ablation Multicollector ICP Mass Spectrometry

			Isotope ratios							Apparent ages (Ma)							
U (ppm)	206Pb 204Pb	U/Th	206Pb* 207Pb*	± (%)	207Pb* 235U*	± (%)	206Pb* 238U	± (%)	error corr.	206Pb* 238U*	± (Ma)	207Pb* 235U	± (Ma)	206Pb* 207Pb*	± (Ma)	**Best age (Ma)**	± (Ma)
Bindschadler (SAL 1776) Cont.																	
428	42616	1.8	16.0228	10.1	0.799	10.9	0.093	4.2	0.4	572.1	22.7	596.0	49.3	688.2	216.2	572.1	22.7
171	76140	2.6	17.9447	6.3	0.576	6.5	0.075	1.9	0.3	466.1	8.5	462.0	24.3	441.5	139.6	466.1	8.5
311	68768	6.4	14.0363	4.6	1.367	5.3	0.139	2.6	0.5	839.8	20.8	874.8	31.1	964.4	93.8	839.8	20.8
211	6024	3.5	16.4526	3.4	0.754	3.5	0.090	0.7	0.2	555.2	3.5	570.4	15.2	631.5	73.6	555.2	3.5
287	10206	14.6	14.7123	1.9	1.208	2.4	0.129	1.4	0.6	781.7	10.0	804.4	13.2	867.6	40.3	781.7	10.0
515	20944	19.6	16.0791	2.5	0.749	3.5	0.087	2.4	0.7	539.8	12.3	567.6	15.1	680.7	54.2	539.8	12.3
307	69104	2.7	14.1761	3.1	1.460	3.2	0.150	0.6	0.2	901.8	5.2	914.2	19.2	944.1	64.2	901.8	5.2
384	8656	1.2	9.2394	3.9	3.876	8.8	0.260	7.9	0.9	1488.4	104.7	1608.7	71.1	1769.9	71.6	1769.9	71.6
450	11764	2.8	17.2089	4.0	0.627	4.1	0.078	0.5	0.1	485.4	2.3	494.0	15.9	533.9	88.4	485.4	2.3
604	32892	3.8	17.5098	3.9	0.649	4.0	0.082	0.9	0.2	510.6	4.6	507.9	15.9	495.8	85.4	510.6	4.6
250	30928	2.0	13.3196	2.6	1.831	2.6	0.177	0.5	0.2	1049.7	5.0	1056.5	17.1	1070.6	51.3	1070.6	51.3
275	23996	1.9	17.9558	5.0	0.602	5.1	0.078	0.7	0.1	486.5	3.3	478.5	19.4	440.1	112.3	486.5	3.3
73	6200	6.7	17.8476	13.7	0.695	13.8	0.090	2.1	0.2	555.4	11.1	535.9	57.6	453.5	304.3	555.4	11.1
506	27262	2.0	18.6227	2.9	0.398	3.1	0.054	1.0	0.3	337.9	3.2	340.5	8.9	358.4	65.9	337.9	3.2
1028	286	11.6	7.1427	4.4	1.556	7.3	0.081	5.9	0.8	499.6	28.2	952.7	45.2	2227.2	75.8	2227.2	75.8
684	18226	17.5	16.3528	4.6	0.804	4.7	0.095	0.8	0.2	587.3	4.4	599.2	21.2	644.6	99.4	587.3	4.4
340	37136	1.5	17.3696	2.6	0.707	2.9	0.089	1.2	0.4	549.6	6.2	542.7	12.0	513.5	57.2	549.6	6.2
227	1494	2.3	13.9499	5.8	0.797	6.0	0.081	1.5	0.2	500.1	7.0	595.3	26.8	977.0	117.8	500.1	7.0
156	10564	3.2	17.7699	4.4	0.658	4.7	0.085	1.9	0.4	525.1	9.4	513.7	19.1	463.3	96.7	525.1	9.4
139	38622	3.7	10.0182	1.4	3.878	1.5	0.282	0.7	0.4	1600.4	9.8	1609.2	12.5	1620.7	25.8	1620.7	25.8
291	69426	5.5	14.1149	2.6	1.383	2.7	0.142	0.7	0.2	853.7	5.3	881.8	15.9	953.0	53.4	853.7	5.3
136	7490	1.9	16.8045	2.7	0.777	4.6	0.095	3.8	0.8	583.0	20.9	583.6	20.6	585.7	59.6	583.0	20.9
Kamb (SAL 1771)																	
289	34635	5.8	17.3653	3.7	0.654	5.4	0.082	4.0	0.7	510.2	19.7	510.9	21.9	514.0	81.1	510.2	19.7
81	11355	1.7	17.9583	5.5	0.671	7.0	0.087	4.4	0.6	540.5	22.8	521.6	28.6	439.8	121.5	540.5	22.8
472	63460	4.5	16.6449	4.4	0.671	5.2	0.081	2.8	0.5	502.0	13.3	521.2	21.1	606.4	94.8	502.0	13.3
129	25460	3.3	16.8844	4.4	0.816	10.0	0.100	9.0	0.9	613.7	52.9	605.6	45.8	575.4	95.5	613.7	52.9
629	22430	2.0	18.9687	5.4	0.208	7.6	0.029	5.3	0.7	181.5	9.5	191.5	13.2	316.7	122.8	181.5	9.5
630	101045	16.6	14.0890	4.5	1.517	5.8	0.155	3.6	0.6	929.0	31.0	937.2	35.3	956.7	92.5	929.0	31.0
383	52470	6.3	14.6089	6.5	1.047	6.8	0.111	2.2	0.3	678.0	14.3	727.3	35.5	882.2	133.7	678.0	14.3
332	14460	2.0	16.2238	3.7	0.572	4.7	0.067	2.9	0.6	419.8	11.9	459.2	17.5	661.5	79.4	419.8	11.9

Appendix A Cont.: U-Pb detrital zircon geochronologic analyses by Laser-Ablation Multicollector ICP Mass Spectrometry

					Isotope ratios							Apparent ages (Ma)					
U (ppm)	206Pb 204Pb	U/Th	206Pb* 207Pb*	± (%)	207Pb* 235U*	± (%)	206Pb* 238U	± (%)	error corr.	206Pb* 238U*	± (Ma)	207Pb* 235U	± (Ma)	206Pb* 207Pb*	± (Ma)	**Best age** (Ma)	± (Ma)
Kamb (SAL 1771) Cont.																	
555	48450	4.6	17.1187	15.9	0.592	16.0	0.074	2.0	0.1	457.4	8.6	472.3	60.6	545.4	349.5	457.4	8.6
479	46165	2.9	17.7235	10.7	0.571	11.1	0.073	2.9	0.3	456.7	13.0	458.8	40.8	469.0	236.6	456.7	13.0
209	19315	2.4	17.1209	4.4	0.650	4.5	0.081	1.1	0.2	500.5	5.3	508.6	18.0	545.1	95.1	500.5	5.3
924	103905	6.7	16.2340	2.5	0.846	6.1	0.100	5.6	0.9	612.0	32.9	622.4	28.6	660.2	53.0	612.0	32.9
443	33785	3.7	17.6592	5.4	0.557	6.4	0.071	3.4	0.5	443.9	14.7	449.3	23.1	477.0	118.8	443.9	14.7
178	24335	3.0	16.7964	7.0	0.698	7.9	0.085	3.7	0.5	526.3	18.8	537.8	33.0	586.8	151.5	526.3	18.8
121	27975	2.0	17.7924	6.8	0.641	7.7	0.083	3.7	0.5	512.4	18.2	503.0	30.7	460.4	150.5	512.4	18.2
85	11225	1.8	17.8534	7.2	0.638	7.4	0.083	1.9	0.3	511.9	9.1	501.3	29.3	452.8	159.1	511.9	9.1
211	71145	4.1	13.8843	2.0	1.352	4.6	0.136	4.1	0.9	823.1	32.0	868.6	26.9	986.6	41.1	823.1	32.0
280	45620	4.2	16.9568	3.7	0.769	4.3	0.095	2.2	0.5	582.5	12.4	579.2	19.1	566.1	80.8	582.5	12.4
87	22760	1.0	16.7544	4.9	0.923	5.1	0.112	1.5	0.3	685.3	9.8	664.0	25.0	592.2	106.3	685.3	9.8
139	28165	1.4	17.3723	4.4	0.683	4.5	0.086	1.0	0.2	532.5	4.9	528.9	18.6	513.1	97.2	532.5	4.9
82	17995	5.0	17.6682	6.7	0.656	7.6	0.084	3.6	0.5	520.1	17.9	512.0	30.7	475.9	149.3	520.1	17.9
358	115480	3.6	13.4527	3.0	1.820	3.2	0.178	0.9	0.3	1053.8	8.4	1052.8	20.7	1050.6	61.3	1050.6	61.3
84	29530	0.8	17.1474	8.9	0.709	9.9	0.088	4.5	0.5	544.7	23.5	544.1	41.9	541.7	194.3	544.7	23.5
178	32280	2.2	17.7087	9.1	0.578	9.8	0.074	3.7	0.4	461.5	16.7	463.1	36.6	470.9	201.9	461.5	16.7
584	87965	2.6	14.1835	3.7	1.334	6.9	0.137	5.8	0.8	828.8	45.4	860.5	40.0	943.1	75.0	828.8	45.4
172	30030	3.9	13.1269	3.4	1.833	5.6	0.175	4.5	0.8	1037.0	43.1	1057.4	37.1	1099.8	68.3	1099.8	68.3
205	29090	2.0	16.6224	5.2	0.761	5.6	0.092	2.1	0.4	565.6	11.3	574.4	24.5	609.3	111.8	565.6	11.3
435	14950	1.4	20.3854	6.2	0.190	6.7	0.028	2.7	0.4	178.4	4.8	176.4	10.9	150.4	144.6	178.4	4.8
376	54835	3.6	16.0837	5.1	0.868	5.7	0.101	2.6	0.5	621.7	15.3	634.4	27.1	680.1	109.7	621.7	15.3
148	32590	2.3	17.8590	7.9	0.672	8.9	0.087	4.1	0.5	538.0	21.2	521.9	36.3	452.1	175.6	538.0	21.2
353	48700	1.2	16.6466	4.9	0.782	4.9	0.094	0.8	0.2	581.6	4.3	586.6	22.0	606.2	105.6	581.6	4.3
163	21450	7.8	18.3545	7.3	0.612	7.3	0.081	0.9	0.1	504.6	4.3	484.6	28.2	391.0	162.9	504.6	4.3
363	33550	1.4	17.7043	5.3	0.545	6.6	0.070	3.9	0.6	435.7	16.4	441.4	23.6	471.4	118.0	435.7	16.4
173	37705	10.0	17.6356	4.0	0.697	4.0	0.089	0.7	0.2	550.5	3.9	537.0	16.8	480.0	87.8	550.5	3.9
212	15905	0.8	16.5192	3.2	0.692	3.4	0.083	1.4	0.4	513.5	6.8	534.0	14.3	622.8	68.2	513.5	6.8
74	14070	1.3	17.0300	12.0	0.661	12.1	0.082	2.0	0.2	506.2	9.8	515.5	49.1	556.7	261.7	506.2	9.8
89	8895	1.3	18.5480	23.4	0.323	23.4	0.044	1.8	0.1	274.6	4.8	284.6	58.2	367.4	532.9	274.6	4.8
270	43560	7.5	16.9066	6.2	0.452	6.8	0.055	2.8	0.4	347.6	9.6	378.6	21.6	572.5	135.5	347.6	9.6
59	22355	0.9	16.1949	8.8	0.952	8.8	0.112	0.8	0.1	683.3	5.2	679.1	43.6	665.4	187.8	683.3	5.2

Appendix A Cont.: U-Pb detrital zircon geochronologic analyses by Laser-Ablation Multicollector ICP Mass Spectrometry

U (ppm)	206Pb 204Pb	U/Th	206Pb* 207Pb*	± (%)	207Pb* 235U*	± (%)	206Pb* 238U	± (%)	error corr.	206Pb* 238U*	± (Ma)	207Pb* 235U	± (Ma)	206Pb* 207Pb*	± (Ma)	**Best age** (Ma)	± (Ma)
					Isotope ratios							**Apparent ages (Ma)**					
Kamb (SAL 1771) Cont.																	
71	45975	2.2	12.4229	4.9	1.764	5.7	0.159	2.9	0.5	950.7	25.9	1032.2	37.1	1209.2	96.7	1209.2	96.7
47	14335	1.7	16.7444	8.0	0.653	8.1	0.079	1.2	0.1	492.1	5.7	510.4	32.5	593.5	173.6	492.1	5.7
406	3700	0.7	13.9191	17.0	0.278	17.1	0.028	2.1	0.1	178.3	3.7	248.9	37.8	981.5	348.4	178.3	3.7
633	35350	3.0	13.1097	3.4	1.431	7.6	0.136	6.7	0.9	822.3	52.0	902.0	45.2	1102.4	68.5	822.3	52.0
878	25550	3.0	20.4981	3.5	0.102	5.6	0.015	4.3	0.8	97.0	4.1	98.6	5.2	137.5	82.8	97.0	4.1
707	39290	3.5	16.6145	4.6	0.596	7.9	0.072	6.4	0.8	447.4	27.8	475.0	30.0	610.3	99.7	447.4	27.8
653	1955	1.6	10.7406	6.7	0.889	7.3	0.069	3.0	0.4	431.5	12.4	645.7	35.0	1490.0	127.1	431.5	12.4
307	6320	2.6	19.0564	7.4	0.113	7.7	0.016	1.9	0.2	100.1	1.9	108.9	7.9	306.2	169.7	100.1	1.9
217	17700	0.8	17.7071	8.0	0.592	8.6	0.076	3.2	0.4	472.2	14.8	472.0	32.5	471.0	176.5	472.2	14.8
610	80940	4.8	16.9638	5.7	0.613	6.7	0.075	3.7	0.5	468.8	16.5	485.5	26.0	565.2	123.6	468.8	16.5
288	32445	2.1	17.7930	5.1	0.579	5.8	0.075	2.8	0.5	464.5	12.3	463.8	21.6	460.3	113.4	464.5	12.3
355	35330	3.7	13.4006	3.3	1.644	5.5	0.160	4.5	0.8	955.6	39.8	987.2	35.0	1058.4	65.7	1058.4	65.7
299	28005	3.4	16.6176	3.8	0.726	4.6	0.088	2.5	0.5	540.8	12.8	554.3	19.5	609.9	82.8	540.8	12.8
145	78615	6.2	15.7555	10.1	0.947	10.2	0.108	1.5	0.1	662.4	9.3	676.6	50.5	724.0	214.7	662.4	9.3
90	22755	1.6	18.0462	8.2	0.680	8.2	0.089	1.1	0.1	549.6	5.7	526.7	33.8	428.9	182.0	549.6	5.7
307	47950	4.3	17.4612	4.5	0.655	7.7	0.083	6.2	0.8	513.7	30.7	511.5	30.8	501.9	98.2	513.7	30.7
197	98765	8.1	13.6419	1.9	1.801	2.0	0.178	0.5	0.3	1057.3	5.1	1045.9	13.0	1022.3	38.9	1022.3	38.9
123	56670	3.8	16.9984	5.8	0.828	6.6	0.102	3.1	0.5	626.6	18.3	612.5	30.1	560.8	126.3	626.6	18.3
328	25980	3.2	16.6313	7.1	0.606	9.2	0.073	5.8	0.6	454.5	25.6	480.8	35.2	608.2	153.9	454.5	25.6
342	38015	2.6	17.2333	5.2	0.582	8.4	0.073	6.6	0.8	452.4	29.0	465.5	31.4	530.8	112.9	452.4	29.0
265	17710	1.1	17.6129	4.2	0.545	7.4	0.070	6.1	0.8	433.5	25.6	441.4	26.6	482.8	93.7	433.5	25.6
287	37520	1.3	18.2350	5.7	0.581	6.5	0.077	3.1	0.5	477.4	14.4	465.3	24.3	405.7	127.9	477.4	14.4
417	65170	43.6	16.9717	7.3	0.709	9.5	0.087	6.0	0.6	539.1	31.1	543.9	40.0	564.2	160.1	539.1	31.1
61	62600	1.5	3.8687	2.7	23.512	2.7	0.660	0.6	0.2	3266.0	14.6	3248.4	26.5	3237.5	42.0	3237.5	42.0
51	87170	2.2	16.8782	9.2	0.737	9.9	0.090	3.7	0.4	556.9	19.6	560.7	42.6	576.2	199.7	556.9	19.6
162	25825	1.2	17.1077	4.0	0.680	4.2	0.084	1.0	0.2	522.4	5.2	526.9	17.1	546.8	88.1	522.4	5.2
58	14850	1.1	16.7052	15.6	0.702	15.7	0.085	1.7	0.1	526.6	8.3	540.3	66.0	598.6	340.5	526.6	8.3
306	28630	1.7	17.1227	3.7	0.690	4.1	0.086	1.9	0.4	529.6	9.4	532.5	17.1	544.9	80.5	529.6	9.4
90	12060	3.2	18.0266	8.2	0.603	8.6	0.079	2.7	0.3	489.4	12.5	479.3	33.0	431.3	183.3	489.4	12.5
185	34340	2.3	17.6380	5.0	0.592	5.8	0.076	2.9	0.5	470.5	13.2	472.1	21.9	479.7	110.6	470.5	13.2
109	389745	4.9	14.3726	14.4	1.072	17.4	0.112	9.9	0.6	682.9	63.8	739.8	91.9	915.9	297.7	682.9	63.8

Appendix A Cont.: U-Pb detrital zircon geochronologic analyses by Laser-Ablation Multicollector ICP Mass Spectrometry

					Isotope ratios							Apparent ages (Ma)					
U (ppm)	206Pb 204Pb	U/Th	206Pb* 207Pb*	± (%)	207Pb* 235U*	± (%)	206Pb* 238U	± (%)	error corr.	206Pb* 238U*	± (Ma)	207Pb* 235U	± (Ma)	206Pb* 207Pb*	± (Ma)	**Best age** (Ma)	± (Ma)
217	91410	2.2	13.4993	3.9	1.868	5.2	0.183	3.5	0.7	1082.5	35.2	1069.7	34.6	1043.6	77.7	1043.6	77.7
154	39245	2.7	14.1045	4.0	1.450	4.8	0.148	2.7	0.6	891.5	22.6	909.8	28.8	954.5	81.0	891.5	22.6
340	13030	1.2	20.1436	3.9	0.195	4.5	0.028	2.1	0.5	180.6	3.8	180.5	7.4	178.3	92.1	180.6	3.8
428	40835	2.2	17.0619	4.9	0.639	5.1	0.079	1.5	0.3	490.6	7.0	501.7	20.3	552.6	107.2	490.6	7.0
1343	16560	2.0	17.4242	6.1	0.547	6.4	0.069	2.0	0.3	430.7	8.1	442.9	23.0	506.6	134.4	430.7	8.1
292	34515	1.9	16.9638	4.4	0.697	7.3	0.086	5.8	0.8	530.1	29.5	536.8	30.3	565.2	95.4	530.1	29.5
85	26950	1.6	17.5843	14.5	0.717	14.6	0.091	1.8	0.1	564.3	9.9	549.1	62.0	486.4	321.4	564.3	9.9
51	13750	2.4	17.6226	16.2	0.641	16.2	0.082	1.0	0.1	507.8	4.8	503.1	64.4	481.6	359.6	507.8	4.8
323	45820	3.6	17.7730	3.5	0.665	4.1	0.086	2.2	0.5	530.3	11.1	517.8	16.6	462.8	76.7	530.3	11.1
208	11165	0.5	22.4396	11.9	0.182	12.5	0.030	3.9	0.3	187.9	7.2	169.6	19.5	-79.4	291.5	187.9	7.2
209	39725	1.9	16.7637	5.4	0.825	5.5	0.100	0.8	0.2	616.1	4.9	610.7	25.3	591.0	118.1	616.1	4.9
156	97255	1.3	17.5601	7.8	0.606	8.5	0.077	3.3	0.4	479.1	15.4	480.9	32.7	489.5	173.2	479.1	15.4
26	8670	3.6	19.3470	13.3	0.651	13.5	0.091	2.7	0.2	563.4	14.7	509.0	54.3	271.6	305.2	563.4	14.7
203	95005	6.8	13.7501	2.3	1.732	3.3	0.173	2.4	0.7	1027.0	22.9	1020.4	21.4	1006.3	46.5	1006.3	46.5
357	39740	2.4	14.6086	19.7	0.841	19.7	0.089	0.7	0.0	550.0	3.7	619.4	91.7	882.3	411.2	550.0	3.7
165	24385	1.8	16.2281	3.2	0.880	4.0	0.104	2.5	0.6	635.2	14.9	640.9	19.2	661.0	68.7	635.2	14.9
114	24720	2.6	13.0790	1.7	1.838	6.1	0.174	5.8	1.0	1036.3	55.8	1059.3	39.9	1107.1	33.0	1107.1	33.0
336	39760	1.5	17.1926	2.2	0.640	2.7	0.080	1.5	0.6	495.1	7.3	502.5	10.6	535.9	47.7	495.1	7.3
152	22000	2.1	16.8473	5.9	0.731	6.1	0.089	1.3	0.2	551.8	6.6	557.4	26.0	580.2	128.8	551.8	6.6
512	70575	5.1	17.2672	1.5	0.700	3.1	0.088	2.7	0.9	541.9	13.9	538.9	12.8	526.5	32.0	541.9	13.9
378	59355	2.4	13.7179	0.9	1.612	2.3	0.160	2.1	0.9	958.8	18.6	974.8	14.4	1011.1	19.2	1011.1	19.2
279	30900	1.4	16.3374	1.6	0.845	4.1	0.100	3.7	0.9	614.8	21.9	621.7	18.9	646.6	35.0	614.8	21.9
345	42565	1.8	17.5703	2.1	0.662	3.1	0.084	2.3	0.7	522.2	11.4	516.0	12.6	488.2	46.8	522.2	11.4
83	15770	7.6	16.2395	6.1	0.792	6.5	0.093	2.3	0.3	574.9	12.4	592.3	29.4	659.5	131.8	574.9	12.4
340	59615	6.9	17.5623	1.9	0.655	2.6	0.083	1.7	0.7	516.8	8.6	511.7	10.4	489.2	42.4	516.8	8.6
363	50270	3.2	15.3652	1.7	1.054	3.3	0.117	2.8	0.9	716.1	19.0	731.0	17.1	777.0	36.2	716.1	19.0
156	17240	1.2	17.8642	4.7	0.575	5.1	0.074	2.1	0.4	463.0	9.2	461.0	19.0	451.5	104.5	463.0	9.2
761	23625	4.4	12.9166	2.1	1.771	2.3	0.166	1.1	0.5	989.4	9.7	1034.8	15.1	1132.0	41.2	1132.0	41.2
292	6700	0.6	18.0783	7.2	0.276	7.4	0.036	1.9	0.3	228.9	4.3	247.3	16.3	425.0	160.1	228.9	4.3
276	40960	1.6	17.2801	3.7	0.618	4.4	0.078	2.4	0.6	481.3	11.3	488.9	17.2	524.8	81.2	481.3	11.3
565	63560	0.7	16.7277	2.4	0.727	2.8	0.088	1.5	0.5	545.1	8.0	555.0	12.2	595.6	51.8	545.1	8.0
192	68570	3.6	15.3668	3.0	1.188	3.4	0.132	1.6	0.5	801.6	12.4	795.1	19.0	776.8	63.6	801.6	12.4

Appendix A Cont.: U-Pb detrital zircon geochronologic analyses by Laser-Ablation Multicollector ICP Mass Spectrometry

					Isotope ratios							Apparent ages (Ma)					
U (ppm)	206Pb 204Pb	U/Th	206Pb* 207Pb*	± (%)	207Pb* 235U*	± (%)	206Pb* 238U	± (%)	error corr.	206Pb* 238U*	± (Ma)	207Pb* 235U	± (Ma)	206Pb* 207Pb*	± (Ma)	**Best age** (Ma)	± (Ma)
Kamb (SAL 1771) Cont.																	
161	20645	1.7	17.5294	6.8	0.653	7.3	0.083	2.8	0.4	514.4	13.6	510.6	29.3	493.3	149.5	514.4	13.6
264	38490	1.2	17.9265	3.3	0.592	5.1	0.077	3.8	0.8	478.2	17.6	472.3	19.1	443.7	74.1	478.2	17.6
371	13945	2.7	15.6708	11.4	0.737	11.9	0.084	3.5	0.3	518.3	17.6	560.4	51.4	735.4	242.1	518.3	17.6
257	38525	3.8	14.8963	2.7	1.147	3.4	0.124	2.1	0.6	753.0	15.2	775.7	18.5	841.8	55.4	753.0	15.2
605	16400	0.6	16.4399	4.1	0.726	4.9	0.087	2.7	0.6	534.9	14.1	554.0	21.1	633.1	88.3	534.9	14.1
251	40495	2.0	17.5840	7.2	0.617	9.1	0.079	5.5	0.6	488.1	25.8	487.8	35.2	486.5	159.6	488.1	25.8
375	89070	6.0	14.1013	2.5	1.541	3.7	0.158	2.7	0.7	943.6	23.9	947.0	22.9	955.0	52.0	943.6	23.9
160	19840	1.2	17.3074	5.7	0.689	6.0	0.086	2.0	0.3	534.6	10.5	532.1	25.0	521.4	124.6	534.6	10.5
639	43170	1.6	17.3002	1.7	0.621	4.1	0.078	3.8	0.9	483.4	17.5	490.2	16.1	522.3	38.0	483.4	17.5
322	43105	1.3	17.2427	2.1	0.639	2.8	0.080	1.9	0.7	495.6	8.8	501.7	11.0	529.6	45.2	495.6	8.8
161	10440	1.7	16.0207	4.8	0.724	5.2	0.084	2.1	0.4	520.9	10.4	553.2	22.2	688.5	102.1	520.9	10.4
83	15835	1.5	17.4282	5.2	0.688	6.2	0.087	3.3	0.5	537.6	17.1	531.7	25.7	506.1	115.2	537.6	17.1
111	16955	2.0	17.4689	6.4	0.681	6.7	0.086	2.2	0.3	533.6	11.3	527.4	27.7	500.9	140.4	533.6	11.3
193	28095	6.1	17.7756	3.6	0.635	5.1	0.082	3.6	0.7	506.9	17.4	498.9	20.1	462.5	80.8	506.9	17.4
5189	22795	13.8	16.6349	3.8	0.689	4.6	0.083	2.6	0.6	514.5	12.8	532.0	18.9	607.7	81.1	514.5	12.8
220	63660	2.2	13.8632	2.2	1.713	3.0	0.172	2.0	0.7	1024.3	18.9	1013.3	18.9	989.7	44.2	989.7	44.2
Kamb (SAL 1772)																	
144	15365	1.9	17.3845	6.6	0.639	7.6	0.081	3.6	0.5	499.8	17.5	501.9	30.0	511.6	145.9	499.8	17.5
262	19675	3.6	15.2203	3.4	0.976	8.4	0.108	7.6	0.9	659.7	47.9	691.6	42.0	796.9	71.5	659.7	47.9
177	17400	2.0	16.5614	5.3	0.737	7.0	0.089	4.5	0.7	546.9	23.8	560.7	30.0	617.2	114.0	546.9	23.8
210	23845	2.1	17.2705	3.7	0.634	5.9	0.079	4.6	0.8	492.7	21.8	498.7	23.2	526.0	81.0	492.7	21.8
364	35910	2.9	16.7952	5.4	0.757	7.4	0.092	5.0	0.7	568.3	27.1	572.0	32.2	586.9	117.3	568.3	27.1
101	17090	2.1	16.0107	5.0	1.048	5.2	0.122	1.4	0.3	740.0	9.7	727.7	27.0	689.8	106.8	740.0	9.7
94	8515	2.1	17.4124	9.9	0.651	10.4	0.082	3.1	0.3	509.5	15.2	509.2	41.5	508.1	217.6	509.5	15.2
333	36800	1.7	17.3586	1.7	0.697	3.1	0.088	2.5	0.8	542.4	13.1	537.1	12.8	514.9	38.3	542.4	13.1
451	33670	1.4	17.1730	2.5	0.644	3.1	0.080	1.8	0.6	497.4	8.7	504.8	12.3	538.4	54.8	497.4	8.7
160	15620	3.4	16.9487	7.4	0.671	9.3	0.083	5.6	0.6	511.1	27.3	521.4	37.9	567.1	162.1	511.1	27.3
187	21630	2.0	16.6497	4.4	0.676	6.0	0.082	4.0	0.7	505.9	19.5	524.4	24.4	605.8	95.5	505.9	19.5
327	33930	11.8	17.3242	2.1	0.689	2.4	0.087	1.2	0.5	535.0	6.3	532.0	10.0	519.2	45.7	535.0	6.3
222	35280	4.9	15.7306	4.6	1.057	5.3	0.121	2.7	0.5	734.3	18.6	732.6	27.8	727.3	97.6	734.3	18.6
715	95695	4.5	16.2843	1.9	0.883	3.4	0.104	2.9	0.8	639.7	17.7	642.8	16.4	653.6	39.7	639.7	17.7

Appendix A Cont.: U-Pb detrital zircon geochronologic analyses by Laser-Ablation Multicollector ICP Mass Spectrometry

			Isotope ratios								Apparent ages (Ma)							
U (ppm)	206Pb 204Pb	U/Th	206Pb* 207Pb*	± (%)	207Pb* 235U*	± (%)	206Pb* 238U	± (%)	error corr.	206Pb* 238U*	± (Ma)	207Pb* 235U	± (Ma)	206Pb* 207Pb*	± (Ma)	**Best age** (Ma)	± (Ma)
Kamb (SAL 1772) Cont.																	
286	31285	2.8	17.8990	3.0	0.568	3.6	0.074	2.0	0.6	458.3	8.8	456.4	13.3	447.1	67.2	458.3	8.8
219	25855	2.1	18.0210	3.5	0.602	4.5	0.079	2.9	0.6	488.5	13.7	478.7	17.4	432.0	77.8	488.5	13.7
98	10455	1.7	17.6886	10.2	0.646	10.4	0.083	1.9	0.2	513.1	9.4	505.9	41.6	473.4	227.3	513.1	9.4
210	12570	2.2	16.9222	5.0	0.632	5.8	0.078	2.9	0.5	481.9	13.7	497.6	23.0	570.5	109.9	481.9	13.7
309	31585	4.6	17.5703	2.0	0.672	3.2	0.086	2.5	0.8	529.6	12.7	521.9	13.0	488.2	44.0	529.6	12.7
101	15730	1.4	16.1475	4.2	0.827	4.9	0.097	2.4	0.5	596.1	13.6	612.1	22.4	671.6	90.7	596.1	13.6
256	9580	1.0	15.7301	11.6	0.606	14.5	0.069	8.8	0.6	431.1	36.7	481.2	55.7	727.4	245.9	431.1	36.7
566	54655	2.3	17.1140	2.9	0.586	6.1	0.073	5.4	0.9	452.6	23.6	468.3	23.0	546.0	62.9	452.6	23.6
96	11645	1.0	17.6958	6.2	0.588	7.5	0.075	4.2	0.6	468.6	18.8	469.3	28.0	472.5	137.0	468.6	18.8
783	51770	4.4	17.2984	1.9	0.562	6.3	0.071	6.0	1.0	439.2	25.6	452.8	23.1	522.5	41.3	439.2	25.6
1097	70520	21.7	17.2763	1.9	0.680	2.9	0.085	2.2	0.8	527.3	11.2	527.0	12.0	525.3	41.2	527.3	11.2
302	27730	2.0	16.8069	2.8	0.690	6.0	0.084	5.3	0.9	520.7	26.6	532.9	25.0	585.4	61.5	520.7	26.6
255	23470	1.9	17.5210	4.1	0.611	6.2	0.078	4.7	0.7	482.0	21.6	484.2	23.9	494.4	90.4	482.0	21.6
149	19730	1.9	17.5968	1.8	0.636	3.1	0.081	2.5	0.8	503.1	11.9	499.8	12.1	484.9	40.8	503.1	11.9
314	37000	2.8	17.9059	2.9	0.586	4.9	0.076	3.9	0.8	472.7	17.9	468.2	18.3	446.3	64.7	472.7	17.9
253	38545	1.7	17.5567	2.8	0.647	3.9	0.082	2.8	0.7	510.0	13.6	506.4	15.6	489.9	61.0	510.0	13.6
607	83240	1.5	13.4233	1.7	1.732	4.6	0.169	4.3	0.9	1004.3	39.9	1020.4	29.6	1055.0	33.2	1055.0	33.2
239	25390	3.4	17.8103	3.3	0.617	5.2	0.080	4.0	0.8	494.4	19.0	488.0	20.2	458.2	74.1	494.4	19.0
152	22570	2.4	17.1258	2.4	0.728	2.6	0.090	1.0	0.4	558.3	5.4	555.6	11.1	544.5	52.4	558.3	5.4
395	41960	8.4	17.2453	3.5	0.685	4.1	0.086	2.1	0.5	529.6	10.8	529.5	16.8	529.2	76.1	529.6	10.8
484	64725	5.8	17.0640	2.5	0.728	4.1	0.090	3.3	0.8	556.2	17.5	555.4	17.6	552.4	53.9	556.2	17.5
560	42255	4.8	14.0511	4.8	0.986	8.2	0.100	6.6	0.8	617.3	38.9	696.7	41.2	962.3	98.1	617.3	38.9
763	62220	1.7	16.8277	3.9	0.694	5.8	0.085	4.3	0.7	524.2	21.6	535.2	24.1	582.7	84.1	524.2	21.6
79	9845	5.6	18.2628	6.5	0.638	7.3	0.085	3.4	0.5	522.9	17.1	501.0	29.0	402.3	145.4	522.9	17.1
139	6985	2.2	14.5435	20.0	0.772	20.1	0.081	2.5	0.1	504.7	12.1	581.0	89.2	891.5	416.0	504.7	12.1
465	51220	1.7	17.2462	3.4	0.589	4.0	0.074	2.2	0.5	458.5	9.5	470.4	15.2	529.1	75.2	458.5	9.5
226	25300	2.4	16.5489	4.5	0.734	5.2	0.088	2.6	0.5	544.0	13.3	558.6	22.3	618.9	97.8	544.0	13.3
189	16935	1.3	16.8578	5.8	0.603	6.8	0.074	3.5	0.5	458.3	15.7	478.9	26.1	578.8	126.9	458.3	15.7
277	24180	3.3	16.4069	4.5	0.706	6.4	0.084	4.5	0.7	519.7	22.4	542.1	26.8	637.5	97.6	519.7	22.4
194	19020	2.4	16.4905	10.5	0.686	10.8	0.082	2.6	0.2	508.5	12.8	530.5	44.6	626.5	226.1	508.5	12.8
595	11780	1.1	18.4888	4.1	0.241	6.7	0.032	5.3	0.8	205.4	10.7	219.6	13.3	374.6	92.8	205.4	10.7

Appendix A Cont.: U-Pb detrital zircon geochronologic analyses by Laser-Ablation Multicollector ICP Mass Spectrometry

					Isotope ratios							Apparent ages (Ma)					
U (ppm)	206Pb 204Pb	U/Th	206Pb* 207Pb*	± (%)	207Pb* 235U*	± (%)	206Pb* 238U	± (%)	error corr.	206Pb* 238U*	± (Ma)	207Pb* 235U	± (Ma)	206Pb* 207Pb*	± (Ma)	**Best age** (Ma)	± (Ma)
Kamb (SAL 1772) Cont.																	
417	11370	5.0	16.0712	4.4	0.659	6.4	0.077	4.6	0.7	477.2	21.2	514.1	25.8	681.8	94.5	477.2	21.2
757	37605	4.3	14.0152	4.6	1.034	7.6	0.105	6.0	0.8	644.1	36.7	720.8	39.1	967.5	94.8	644.1	36.7
523	20715	1.3	19.9002	3.2	0.236	3.8	0.034	2.0	0.5	216.3	4.3	215.5	7.4	206.6	75.3	216.3	4.3
267	24800	1.6	16.9613	1.2	0.671	2.3	0.083	2.0	0.9	511.4	9.7	521.4	9.4	565.5	25.4	511.4	9.7
280	24385	1.7	17.0217	3.0	0.682	3.7	0.084	2.2	0.6	521.0	11.1	527.9	15.2	557.8	64.8	521.0	11.1
662	42690	13.5	16.6401	2.3	0.689	3.9	0.083	3.2	0.8	514.8	15.6	532.1	16.3	607.0	50.6	514.8	15.6
244	41115	3.0	13.4518	1.1	1.712	2.6	0.167	2.4	0.9	995.9	21.8	1013.2	16.8	1050.7	22.8	1050.7	22.8
311	28160	5.4	17.2970	2.0	0.643	3.0	0.081	2.3	0.8	500.0	10.9	504.1	12.0	522.7	43.8	500.0	10.9
188	17220	2.1	16.7751	6.1	0.662	9.4	0.081	7.1	0.8	499.2	33.9	515.7	37.9	589.5	133.3	499.2	33.9
160	10925	3.7	14.2404	27.3	0.801	28.1	0.083	6.9	0.2	512.2	33.8	597.2	127.6	934.9	569.7	512.2	33.8
952	63510	2.1	16.0640	1.3	0.865	2.3	0.101	1.9	0.8	618.7	11.3	632.6	10.8	682.7	27.4	618.7	11.3
579	56780	1.1	17.2637	3.5	0.627	4.2	0.079	2.4	0.6	487.4	11.2	494.4	16.5	526.9	76.3	487.4	11.2
806	149460	2.8	10.4439	1.6	3.457	2.1	0.262	1.3	0.6	1499.5	16.9	1517.6	16.2	1542.8	30.5	1542.8	30.5
407	46805	7.8	15.9178	2.2	0.920	4.7	0.106	4.2	0.9	650.9	25.8	662.5	23.0	702.2	47.3	650.9	25.8
458	51080	2.3	17.3212	4.4	0.642	7.2	0.081	5.7	0.8	499.9	27.3	503.4	28.5	519.6	96.6	499.9	27.3
Kamb (SAL 1773)																	
286	31515	4.0	17.4480	3.9	0.661	4.3	0.084	1.8	0.4	517.6	9.1	515.0	17.3	503.6	85.2	517.6	9.1
298	21025	2.7	16.9463	3.2	0.679	3.5	0.083	1.5	0.4	516.5	7.3	526.0	14.4	567.4	69.1	516.5	7.3
225	20540	2.2	16.8331	2.8	0.681	3.1	0.083	1.4	0.4	515.0	6.9	527.5	13.0	582.0	61.4	515.0	6.9
168	44515	2.9	13.0276	1.1	1.970	1.6	0.186	1.1	0.7	1100.6	11.3	1105.5	10.8	1114.9	22.8	1114.9	22.8
1856	3580	1.1	13.6577	2.9	0.537	3.8	0.053	2.4	0.6	334.2	7.8	436.6	13.4	1020.0	59.5	334.2	7.8
1881	3840	0.9	13.0831	15.9	0.558	16.7	0.053	5.1	0.3	332.3	16.5	449.9	60.9	1106.5	320.6	332.3	16.5
301	32080	2.3	16.4187	1.8	0.784	3.9	0.093	3.5	0.9	575.7	19.2	588.0	17.5	635.9	38.8	575.7	19.2
172	14535	4.5	16.8280	1.4	0.678	2.1	0.083	1.6	0.7	512.7	7.7	525.7	8.7	582.7	31.0	512.7	7.7
144	15725	5.2	14.8709	2.7	1.096	3.1	0.118	1.6	0.5	720.2	11.0	751.4	16.7	845.4	56.0	720.2	11.0

Appendix A Cont.: U-Pb detrital zircon geochronologic analyses by Laser-Ablation Multicollector ICP Mass Spectrometry

			Isotope ratios							Apparent ages (Ma)							
U (ppm)	206Pb 204Pb	U/Th	206Pb* 207Pb*	± (%)	207Pb* 235U*	± (%)	206Pb* 238U	± (%)	error corr.	206Pb* 238U*	± (Ma)	207Pb* 235U	± (Ma)	206Pb* 207Pb*	± (Ma)	**Best age** (Ma)	± (Ma)
Kamb (SAL 1773) Cont.																	
1446	179210	35.6	15.1501	1.2	1.089	2.9	0.120	2.7	0.9	728.8	18.3	748.2	15.4	806.6	25.5	728.8	18.3
241	57015	2.1	11.0617	1.4	2.927	2.4	0.235	1.9	0.8	1359.8	23.4	1389.0	17.9	1434.0	26.7	1434.0	26.7
1585	67015	4.5	18.9723	3.5	0.265	4.5	0.037	2.8	0.6	231.2	6.2	239.0	9.5	316.2	80.5	231.2	6.2
223	25520	2.1	17.3112	3.7	0.613	4.4	0.077	2.3	0.5	478.1	10.7	485.5	17.0	520.9	82.2	478.1	10.7
262	21685	2.2	17.0696	4.0	0.656	5.4	0.081	3.6	0.7	503.6	17.6	512.4	21.6	551.6	86.3	503.6	17.6
893	71080	1.6	17.4922	2.2	0.601	4.0	0.076	3.4	0.8	473.7	15.4	477.9	15.4	498.0	48.7	473.7	15.4
218	17460	2.0	16.7128	3.9	0.671	4.7	0.081	2.7	0.6	503.9	13.2	521.2	19.2	597.6	83.5	503.9	13.2
934	82180	1.5	13.2843	2.1	1.503	5.5	0.145	5.1	0.9	871.9	41.7	931.7	33.6	1075.9	41.2	1075.9	41.2
166	4460	0.9	21.1163	11.6	0.194	12.3	0.030	4.2	0.3	188.3	7.8	179.6	20.3	67.2	276.6	188.3	7.8
141	12260	1.7	17.2271	5.0	0.674	6.5	0.084	4.1	0.6	521.2	20.5	523.1	26.4	531.6	109.5	521.2	20.5
556	44755	1.8	17.2054	2.2	0.639	4.0	0.080	3.3	0.8	494.8	15.8	501.9	15.8	534.3	48.0	494.8	15.8
333	23600	0.7	17.4531	3.4	0.634	4.6	0.080	3.1	0.7	497.8	14.7	498.7	18.1	502.9	75.0	497.8	14.7
367	34835	6.5	17.3844	2.8	0.602	3.9	0.076	2.7	0.7	471.6	12.1	478.5	14.8	511.6	62.3	471.6	12.1
63	8010	2.4	13.7620	6.3	1.286	7.6	0.128	4.2	0.6	778.3	30.9	839.4	43.3	1004.6	128.0	778.3	30.9
723	38145	5.7	17.0297	1.8	0.633	3.2	0.078	2.6	0.8	484.9	12.1	497.7	12.5	556.7	39.7	484.9	12.1
317	26500	1.4	17.2198	1.8	0.619	4.3	0.077	3.9	0.9	479.7	18.1	488.9	16.7	532.5	40.0	479.7	18.1
256	78015	5.0	9.1114	2.7	4.759	3.4	0.314	2.0	0.6	1762.6	30.8	1777.6	28.5	1795.3	49.9	1795.3	49.9
88	20340	4.0	13.4450	4.3	1.694	5.5	0.165	3.6	0.6	985.4	32.4	1006.2	35.4	1051.7	85.8	1051.7	85.8
311	34045	2.6	16.8717	5.3	0.704	5.6	0.086	1.7	0.3	532.9	8.4	541.4	23.4	577.0	115.7	532.9	8.4
246	16735	2.4	16.4184	1.7	0.722	2.3	0.086	1.7	0.7	531.5	8.4	551.7	9.9	635.9	35.6	531.5	8.4
270	23145	1.6	17.3030	4.7	0.636	4.9	0.080	1.2	0.2	495.4	5.6	500.1	19.2	521.9	103.6	495.4	5.6
455	44350	3.4	13.0759	3.3	1.750	3.8	0.166	1.8	0.5	989.6	16.9	1027.0	24.3	1107.5	65.6	1107.5	65.6
164	20675	3.1	13.0211	3.9	1.805	4.0	0.170	0.7	0.2	1014.4	6.9	1047.1	26.1	1115.9	78.5	1115.9	78.5
179	39570	3.5	13.1979	3.0	1.795	4.5	0.172	3.4	0.8	1022.1	32.4	1043.7	29.6	1089.0	59.3	1089.0	59.3
122	9505	1.8	16.8286	10.3	0.633	10.7	0.077	2.9	0.3	480.0	13.5	498.2	42.0	582.6	223.2	480.0	13.5
136	10460	1.8	16.9700	4.6	0.662	5.9	0.081	3.7	0.6	504.8	18.0	515.7	23.8	564.4	99.7	504.8	18.0
337	21785	1.7	17.0059	3.3	0.657	5.1	0.081	3.8	0.8	502.0	18.5	512.6	20.4	559.8	72.7	502.0	18.5
358	34395	3.3	15.9100	2.8	0.862	3.9	0.099	2.7	0.7	611.3	15.7	631.3	18.1	703.3	58.6	611.3	15.7
622	82525	9.7	13.9369	2.4	1.348	5.2	0.136	4.6	0.9	823.7	35.2	866.9	30.1	978.9	49.7	823.7	35.2
211	25280	1.3	16.7945	4.7	0.781	5.1	0.095	1.8	0.4	585.6	10.0	585.9	22.6	587.0	102.9	585.6	10.0
226	26080	21.1	16.1567	3.7	0.791	8.9	0.093	8.1	0.9	571.7	44.1	592.0	39.8	670.4	79.2	571.7	44.1
242	9570	0.8	20.1797	8.6	0.187	9.0	0.027	2.5	0.3	174.4	4.4	174.4	14.4	174.1	201.6	174.4	4.4

Appendix A Cont.: U-Pb detrital zircon geochronologic analyses by Laser-Ablation Multicollector ICP Mass Spectrometry

			Isotope ratios							Apparent ages (Ma)							
U (ppm)	206Pb 204Pb	U/Th	206Pb* 207Pb*	± (%)	207Pb* 235U*	± (%)	206Pb* 238U	± (%)	error corr.	206Pb* 238U*	± (Ma)	207Pb* 235U	± (Ma)	206Pb* 207Pb*	± (Ma)	**Best age** (Ma)	± (Ma)
Kamb (SAL 1773) Cont.																	
389	67210	5.1	13.0869	2.9	1.824	3.4	0.173	1.9	0.6	1029.4	18.0	1054.2	22.5	1105.9	57.2	1105.9	57.2
418	55695	45.7	15.1950	5.5	0.923	11.7	0.102	10.4	0.9	624.6	61.8	664.1	57.3	800.3	114.9	624.6	61.8
268	49180	3.9	14.0322	3.2	1.521	3.6	0.155	1.7	0.5	927.7	14.9	938.8	22.2	965.0	65.2	927.7	14.9
580	86985	6.6	13.3184	2.7	1.639	4.1	0.158	3.0	0.7	947.5	26.6	985.4	25.6	1070.7	54.3	1070.7	54.3
595	48100	78.3	17.1820	1.4	0.645	2.0	0.080	1.3	0.7	498.5	6.4	505.5	7.8	537.3	31.5	498.5	6.4
140	2240	1.5	19.1283	25.3	0.118	25.3	0.016	1.4	0.1	105.0	1.5	113.6	27.2	297.6	585.4	105.0	1.5
343	51170	3.7	14.2434	9.9	1.163	13.5	0.120	9.3	0.7	731.2	64.2	783.2	74.1	934.4	202.7	731.2	64.2
173	12555	1.6	17.6440	6.4	0.604	6.8	0.077	2.3	0.3	479.6	10.5	479.5	26.0	478.9	142.1	479.6	10.5
324	11095	1.2	19.1189	6.1	0.255	10.2	0.035	8.1	0.8	223.7	17.8	230.4	21.0	298.7	140.3	223.7	17.8
244	19085	1.0	16.8775	3.0	0.653	3.3	0.080	1.4	0.4	495.8	6.8	510.4	13.3	576.3	65.0	495.8	6.8
156	37480	0.8	9.8367	2.6	3.878	3.1	0.277	1.7	0.6	1574.6	24.0	1609.1	25.0	1654.6	47.8	1654.6	47.8
360	34635	1.6	17.5588	3.3	0.646	4.0	0.082	2.3	0.6	509.5	11.2	505.9	16.1	489.6	73.5	509.5	11.2
550	5400	1.3	10.1855	45.4	0.952	46.3	0.070	9.2	0.2	438.1	39.1	679.1	233.3	1589.8	898.1	1589.8	898.1
838	38345	0.8	16.3659	7.0	0.736	7.8	0.087	3.5	0.4	539.8	18.1	560.0	33.7	642.8	150.5	539.8	18.1
851	25530	10.2	16.4091	3.8	0.669	6.1	0.080	4.7	0.8	494.2	22.5	520.4	24.7	637.2	82.1	494.2	22.5
96	22415	1.8	13.3641	3.9	1.828	4.4	0.177	2.1	0.5	1051.8	20.3	1055.7	28.9	1063.9	77.9	1063.9	77.9
206	20500	2.5	17.8572	5.0	0.620	5.1	0.080	1.1	0.2	497.9	5.3	489.8	19.9	452.3	111.3	497.9	5.3
717	44355	2.9	13.0459	3.2	1.512	7.3	0.143	6.6	0.9	861.9	53.2	935.2	44.9	1112.2	64.7	1112.2	64.7
939	85415	5.5	14.7347	2.4	0.996	5.9	0.106	5.4	0.9	652.2	33.2	701.9	29.7	864.5	49.6	652.2	33.2
124	27930	1.6	12.9398	2.6	1.914	3.9	0.180	2.9	0.7	1064.7	28.7	1085.8	26.0	1128.4	51.5	1128.4	51.5
217	19500	1.8	17.0023	4.0	0.692	4.9	0.085	2.8	0.6	527.8	14.3	533.9	20.3	560.3	86.8	527.8	14.3
342	33510	6.1	16.8347	3.5	0.690	3.6	0.084	1.1	0.3	521.5	5.4	532.9	15.1	581.8	75.4	521.5	5.4
312	54625	2.1	13.6411	2.1	1.547	3.5	0.153	2.9	0.8	918.1	24.5	949.3	21.7	1022.5	41.5	1022.5	41.5
191	16645	2.1	17.4585	3.6	0.669	5.2	0.085	3.8	0.7	524.0	19.0	520.0	21.3	502.3	79.6	524.0	19.0
720	22460	1.8	15.8281	2.4	0.811	3.9	0.093	3.1	0.8	574.1	16.8	603.2	17.7	714.2	51.4	574.1	16.8
162	16165	1.4	17.8272	4.2	0.604	5.7	0.078	3.8	0.7	484.5	17.7	479.6	21.7	456.1	93.6	484.5	17.7
200	7525	1.4	19.8758	7.4	0.210	7.9	0.030	2.7	0.3	192.5	5.1	193.8	14.0	209.4	172.6	192.5	5.1
146	15085	3.1	17.8896	4.5	0.647	7.4	0.084	5.8	0.8	519.5	29.1	506.5	29.4	448.3	100.6	519.5	29.1
255	42420	3.5	13.6655	1.9	1.628	4.0	0.161	3.4	0.9	964.4	30.8	981.2	24.9	1018.8	39.3	1018.8	39.3
610	50690	1.3	17.3738	2.9	0.631	3.5	0.079	2.0	0.6	492.8	9.3	496.4	13.9	513.0	64.6	492.8	9.3
659	66070	12.0	16.7518	2.6	0.754	3.6	0.092	2.4	0.7	564.9	13.2	570.5	15.5	592.5	55.9	564.9	13.2

Appendix A Cont.: U-Pb detrital zircon geochronologic analyses by Laser-Ablation Multicollector ICP Mass Spectrometry

			Isotope ratios							Apparent ages (Ma)							
U (ppm)	206Pb 204Pb	U/Th	206Pb* 207Pb*	± (%)	207Pb* 235U*	± (%)	206Pb* 238U	± (%)	error corr.	206Pb* 238U*	± (Ma)	207Pb* 235U	± (Ma)	206Pb* 207Pb*	± (Ma)	**Best age (Ma)**	± (Ma)
Kamb (SAL 1773) Cont.																	
123	24250	1.3	13.8739	2.5	1.559	3.8	0.157	2.8	0.8	939.1	24.8	953.9	23.4	988.1	50.9	939.1	24.8
440	38165	5.1	17.3045	2.7	0.601	4.4	0.075	3.5	0.8	468.5	15.6	477.6	16.7	521.7	59.0	468.5	15.6
819	70625	1.5	17.4289	2.3	0.654	2.8	0.083	1.7	0.6	512.1	8.3	511.0	11.4	506.0	50.6	512.1	8.3
673	93115	8.6	13.4253	1.2	1.687	3.8	0.164	3.6	0.9	980.6	32.7	1003.8	24.2	1054.7	24.4	1054.7	24.4
222	36785	1.7	15.0833	2.5	1.161	2.9	0.127	1.4	0.5	770.5	10.4	782.2	15.9	815.8	53.1	770.5	10.4
510	45150	1.8	17.0949	1.5	0.651	2.2	0.081	1.7	0.8	500.6	8.0	509.2	8.9	548.4	31.7	500.6	8.0
284	21270	1.4	17.1149	2.6	0.631	3.6	0.078	2.6	0.7	486.4	12.1	496.9	14.3	545.9	56.3	486.4	12.1
248	6420	4.0	13.6879	9.8	0.880	9.9	0.087	1.2	0.1	539.7	6.1	640.8	47.1	1015.5	199.6	539.7	6.1
637	32300	3.3	13.7436	2.6	1.183	6.5	0.118	5.9	0.9	718.8	40.3	792.9	35.6	1007.3	52.3	718.8	40.3
490	45875	3.8	16.6031	2.6	0.752	4.9	0.091	4.1	0.8	559.0	22.0	569.5	21.2	611.8	56.2	559.0	22.0
159	18595	1.6	16.8248	4.6	0.738	7.7	0.090	6.2	0.8	555.8	33.2	561.2	33.4	583.1	99.7	555.8	33.2
173	30630	3.3	13.5647	3.1	1.600	6.0	0.157	5.1	0.9	942.6	45.0	970.4	37.6	1033.8	63.5	1033.8	63.5
254	24250	3.1	17.2473	2.5	0.673	2.8	0.084	1.2	0.4	521.0	6.2	522.5	11.2	529.0	54.0	521.0	6.2
217	23075	2.5	17.3090	3.5	0.677	4.6	0.085	3.0	0.6	525.5	15.0	524.7	18.8	521.2	76.4	525.5	15.0
299	50230	3.5	13.4104	1.5	1.654	5.8	0.161	5.6	1.0	961.5	50.0	991.0	36.7	1056.9	30.0	1056.9	30.0
442	53200	3.5	16.8596	2.3	0.751	2.5	0.092	0.9	0.3	566.5	4.6	568.9	10.7	578.6	50.2	566.5	4.6
340	26375	2.7	17.4866	3.6	0.601	3.9	0.076	1.6	0.4	473.5	7.2	477.8	15.0	498.7	79.5	473.5	7.2
136	12730	1.8	16.9439	5.8	0.669	6.0	0.082	1.5	0.3	509.2	7.5	520.0	24.2	567.7	125.4	509.2	7.5
194	17385	2.0	17.6806	4.5	0.641	4.6	0.082	1.1	0.2	509.4	5.5	503.1	18.3	474.4	99.0	509.4	5.5
281	25170	4.7	17.0684	3.4	0.678	4.4	0.084	2.8	0.6	519.2	13.8	525.3	18.1	551.8	74.9	519.2	13.8
197	41505	3.4	14.1380	1.9	1.447	2.8	0.148	2.0	0.7	892.1	16.5	908.8	16.7	949.6	39.8	892.1	16.5
134	14590	2.7	17.5784	8.5	0.659	8.9	0.084	2.8	0.3	520.1	13.8	514.0	36.0	487.2	187.3	520.1	13.8
897	97035	6.3	15.7787	1.9	0.970	2.2	0.111	1.1	0.5	678.7	7.1	688.5	10.8	720.9	39.5	678.7	7.1
57	12140	2.9	13.3608	2.2	1.713	2.5	0.166	1.2	0.5	989.8	10.7	1013.3	16.2	1064.3	45.0	1064.3	45.0
611	21815	1.0	16.9027	3.1	0.641	4.3	0.079	2.9	0.7	487.8	13.7	503.1	16.9	573.0	67.7	487.8	13.7
498	44710	2.6	16.9146	6.9	0.676	7.0	0.083	1.1	0.2	513.4	5.5	524.2	28.5	571.5	149.4	513.4	5.5
Kamb (SAL 1774)																	
159	35980	4.7	13.8618	2.5	1.641	3.0	0.165	1.7	0.5	984.7	15.2	986.3	19.2	989.9	51.7	989.9	51.7
185	13655	2.5	16.6392	5.8	0.663	6.8	0.080	3.5	0.5	496.1	16.5	516.3	27.4	607.1	125.9	496.1	16.5
128	20830	2.5	16.2737	2.2	0.903	3.4	0.107	2.6	0.8	652.7	15.8	653.2	16.3	655.0	48.0	652.7	15.8
89	8655	1.2	16.3408	7.6	0.649	8.4	0.077	3.6	0.4	477.6	16.5	507.8	33.6	646.1	163.7	477.6	16.5

Appendix A Cont.: U-Pb detrital zircon geochronologic analyses by Laser-Ablation Multicollector ICP Mass Spectrometry

U (ppm)	206Pb 204Pb	U/Th	206Pb* 207Pb*	± (%)	207Pb* 235U*	± (%)	206Pb* 238U	± (%)	error corr.	206Pb* 238U*	± (Ma)	207Pb* 235U	± (Ma)	206Pb* 207Pb*	± (Ma)	**Best age** (Ma)	± (Ma)
					Isotope ratios					**Apparent ages (Ma)**							
Kamb (SAL 1774) Cont.																	
48	14125	2.5	12.5472	3.7	2.252	5.7	0.205	4.3	0.8	1201.7	47.3	1197.4	40.1	1189.5	73.5	1189.5	73.5
589	29760	3.6	16.4789	3.0	0.699	6.3	0.083	5.6	0.9	516.9	27.6	538.0	26.4	628.0	64.7	516.9	27.6
131	19920	1.5	16.2019	2.9	0.918	6.1	0.108	5.3	0.9	660.5	33.5	661.4	29.6	664.4	62.6	660.5	33.5
223	43280	3.6	16.7247	2.2	0.823	3.8	0.100	3.1	0.8	613.3	18.4	609.6	17.6	596.0	47.9	613.3	18.4
695	20995	1.1	16.2192	2.4	0.759	7.0	0.089	6.6	0.9	551.2	34.7	573.3	30.7	662.2	51.8	551.2	34.7
92	3550	2.1	15.0297	8.7	0.839	8.7	0.091	1.2	0.1	564.3	6.6	618.7	40.6	823.2	181.2	564.3	6.6
546	35670	1.9	15.9351	3.9	0.859	4.8	0.099	2.7	0.6	610.5	15.8	629.8	22.4	699.9	83.3	610.5	15.8
141	18575	2.6	16.5045	3.0	0.832	3.3	0.100	1.5	0.5	611.9	8.8	614.6	15.3	624.7	63.7	611.9	8.8
160	16930	2.0	17.7810	5.8	0.627	7.1	0.081	4.1	0.6	500.9	19.7	493.9	27.9	461.8	129.4	500.9	19.7
149	20160	2.2	17.0504	4.6	0.754	7.0	0.093	5.3	0.8	574.5	29.2	570.4	30.6	554.1	99.6	574.5	29.2
122	26785	1.5	14.2457	2.2	1.457	2.5	0.151	1.1	0.4	903.9	9.2	912.7	14.8	934.1	45.2	903.9	9.2
324	32570	1.6	16.9750	2.4	0.711	3.6	0.087	2.7	0.8	540.7	14.1	545.1	15.2	563.8	51.9	540.7	14.1
491	965	1.4	7.6669	15.9	1.313	16.3	0.073	3.6	0.2	454.4	15.8	851.6	94.3	2103.8	281.2	2103.8	281.2
623	56975	2.5	16.7039	3.6	0.750	4.2	0.091	2.2	0.5	560.8	11.8	568.4	18.5	598.7	78.6	560.8	11.8
315	19970	1.4	17.4123	4.4	0.622	4.8	0.079	1.8	0.4	487.7	8.4	491.3	18.6	508.1	97.6	487.7	8.4
147	18945	1.8	17.5970	4.6	0.709	5.1	0.090	2.1	0.4	558.2	11.3	544.0	21.3	484.8	101.7	558.2	11.3
174	19110	2.8	16.7402	7.0	0.696	7.3	0.085	1.8	0.2	523.1	8.9	536.5	30.3	594.0	152.8	523.1	8.9
150	13730	1.3	17.5531	5.9	0.603	8.9	0.077	6.6	0.7	476.5	30.3	478.9	33.9	490.3	131.3	476.5	30.3
125	2710	2.6	23.7888	29.0	0.097	29.1	0.017	2.9	0.1	106.6	3.1	93.7	26.1	-224.4	742.3	106.6	3.1
107	13505	1.3	17.0819	5.4	0.609	6.9	0.075	4.3	0.6	468.7	19.6	482.8	26.7	550.1	118.3	468.7	19.6
442	29675	1.7	16.8390	4.2	0.686	6.1	0.084	4.4	0.7	518.8	21.9	530.6	25.1	581.3	91.3	518.8	21.9
330	119615	6.8	6.9497	2.7	7.591	2.9	0.383	1.2	0.4	2088.5	21.9	2183.8	26.3	2274.6	45.8	2274.6	45.8
303	48725	2.9	13.3131	3.2	1.767	8.0	0.171	7.3	0.9	1015.2	68.6	1033.3	51.7	1071.5	63.9	1071.5	63.9
358	24365	4.3	15.2240	4.1	0.845	10.6	0.093	9.8	0.9	575.1	54.0	621.9	49.4	796.4	85.0	575.1	54.0

Appendix A Cont.: U-Pb detrital zircon geochronologic analyses by Laser-Ablation Multicollector ICP Mass Spectrometry

U (ppm)	206Pb/204Pb	U/Th	**Isotope ratios** 206Pb*/207Pb*	± (%)	207Pb*/235U*	± (%)	206Pb*/238U	± (%)	error corr.	**Apparent ages (Ma)** 206Pb*/238U*	± (Ma)	207Pb*/235U	± (Ma)	206Pb*/207Pb*	± (Ma)	**Best age** (Ma)	± (Ma)
Whillans (SAL 1744)																	
148	14016	4.0	16.8406	5.4	0.802	6.5	0.098	3.6	0.6	602.7	20.7	598.2	29.3	581.1	117.1	602.7	20.7
268	25272	1.4	16.9758	3.6	0.771	4.4	0.095	2.5	0.6	584.9	14.2	580.6	19.4	563.7	78.1	584.9	14.2
681	11036	2.8	12.5828	2.5	1.840	2.6	0.168	0.6	0.2	1000.7	5.7	1059.9	16.8	1183.9	49.1	1183.9	49.1
196	27156	1.9	15.9216	3.7	0.939	4.8	0.108	3.0	0.6	663.3	18.9	672.1	23.4	701.7	78.9	663.3	18.9
526	78792	2.3	13.3292	4.9	1.961	7.1	0.190	5.1	0.7	1119.2	52.2	1102.3	47.5	1069.1	98.5	1069.1	98.5
441	18060	1.8	16.8394	3.7	0.723	4.2	0.088	2.0	0.5	545.3	10.4	552.3	17.9	581.2	80.8	545.3	10.4
345	18820	1.3	16.9128	2.7	0.722	5.2	0.089	4.4	0.9	547.3	23.2	552.1	22.0	571.7	58.6	547.3	23.2
290	9360	1.3	16.4499	5.3	0.655	6.4	0.078	3.6	0.6	485.1	16.7	511.6	25.6	631.8	113.7	485.1	16.7
405	39336	3.6	13.4541	4.0	1.700	7.7	0.166	6.6	0.9	989.3	60.9	1008.5	49.5	1050.3	80.0	1050.3	80.0
224	14908	4.9	17.0770	2.5	0.697	4.7	0.086	4.0	0.9	533.6	20.6	536.9	19.7	550.7	54.1	533.6	20.6
712	14836	6.2	13.9883	2.3	1.153	2.8	0.117	1.6	0.6	713.1	10.7	778.6	15.1	971.4	46.4	713.1	10.7
270	16972	1.8	17.6626	4.0	0.693	6.2	0.089	4.7	0.8	548.5	24.8	534.8	25.8	476.6	88.8	548.5	24.8
281	19772	1.4	17.7420	4.0	0.686	8.7	0.088	7.8	0.9	545.3	40.5	530.4	36.1	466.7	89.1	545.3	40.5
1374	13476	4.8	15.6676	3.1	0.913	6.8	0.104	6.0	0.9	636.1	36.4	658.5	32.9	735.8	66.5	636.1	36.4
625	62248	2.0	17.5957	2.7	0.644	7.3	0.082	6.8	0.9	509.1	33.4	504.7	29.2	485.0	59.2	509.1	33.4
210	12172	1.7	17.1843	4.4	0.679	6.8	0.085	5.2	0.8	523.4	26.3	525.9	28.0	537.0	95.4	523.4	26.3
120	13680	2.7	17.6864	5.0	0.656	7.1	0.084	5.1	0.7	520.9	25.3	512.2	28.5	473.6	109.8	520.9	25.3
122	12992	2.3	17.4213	7.7	0.676	8.6	0.085	3.9	0.4	528.1	19.6	524.1	35.4	507.0	170.1	528.1	19.6
366	56968	4.7	13.5522	3.8	1.866	7.1	0.183	6.0	0.8	1085.4	60.2	1069.0	47.0	1035.7	76.0	1035.7	76.0
153	13720	3.2	17.0892	6.0	0.719	7.1	0.089	3.7	0.5	550.4	19.7	550.1	30.0	549.1	131.2	550.4	19.7
255	13308	1.6	16.7662	7.7	0.725	8.7	0.088	4.1	0.5	544.4	21.6	553.4	37.2	590.7	166.3	544.4	21.6
324	17144	2.0	17.2163	3.5	0.702	6.7	0.088	5.7	0.9	541.9	29.6	540.2	27.9	532.9	75.6	541.9	29.6
219	18452	1.4	17.9561	5.4	0.652	8.0	0.085	5.9	0.7	525.5	30.0	509.8	32.1	440.1	119.6	525.5	30.0
338	29092	1.5	16.5051	5.6	0.787	9.0	0.094	7.0	0.8	580.4	38.9	589.5	40.2	624.6	121.5	580.4	38.9
291	15676	1.2	17.4616	6.9	0.680	8.0	0.086	4.0	0.5	532.2	20.4	526.5	32.7	501.9	151.6	532.2	20.4
303	25516	2.8	17.3914	5.7	0.711	7.1	0.090	4.2	0.6	553.8	22.5	545.5	29.9	510.7	124.5	553.8	22.5
365	14076	2.9	15.3500	3.8	0.856	10.7	0.095	10.0	0.9	586.9	56.2	628.0	50.3	779.1	80.9	586.9	56.2
373	19184	1.5	16.1621	6.6	0.743	10.3	0.087	7.9	0.8	538.3	40.8	564.1	44.6	669.7	141.7	538.3	40.8
105	11868	2.3	17.9074	6.5	0.657	8.2	0.085	5.0	0.6	527.8	25.3	512.7	33.0	446.1	144.9	527.8	25.3
62	5768	1.2	18.4207	8.5	0.648	10.1	0.087	5.3	0.5	535.1	27.3	507.2	40.2	382.9	192.4	535.1	27.3
425	71292	2.9	13.4672	3.7	1.889	7.2	0.185	6.2	0.9	1091.8	62.5	1077.4	48.0	1048.4	74.0	1048.4	74.0

Appendix A Cont.: U-Pb detrital zircon geochronologic analyses by Laser-Ablation Multicollector ICP Mass Spectrometry

			Isotope ratios							Apparent ages (Ma)							
U (ppm)	206Pb 204Pb	U/Th	206Pb* 207Pb*	± (%)	207Pb* 235U*	± (%)	206Pb* 238U	± (%)	error corr.	206Pb* 238U*	± (Ma)	207Pb* 235U	± (Ma)	206Pb* 207Pb*	± (Ma)	**Best age** (Ma)	± (Ma)
Whillans (SAL 1750)																	
33	2408	1.2	18.3194	20.8	0.689	21.1	0.092	3.8	0.2	565.0	20.7	532.5	87.7	395.3	470.4	565.0	20.7
281	18176	3.0	16.9911	4.8	0.784	5.1	0.097	1.7	0.3	594.9	9.8	588.0	22.7	561.7	104.5	594.9	9.8
158	14676	4.1	16.9319	6.4	0.742	7.3	0.091	3.7	0.5	562.5	19.7	563.8	31.8	569.3	138.7	562.5	19.7
299	22316	1.3	17.4818	3.0	0.708	6.5	0.090	5.8	0.9	554.1	30.6	543.5	27.4	499.3	67.0	554.1	30.6
144	11024	1.2	18.0839	5.4	0.643	6.6	0.084	3.8	0.6	521.6	19.2	503.9	26.2	424.3	119.8	521.6	19.2
138	10840	1.7	16.8401	4.0	0.743	5.8	0.091	4.1	0.7	560.0	22.0	564.2	24.9	581.1	87.7	560.0	22.0
216	43704	0.9	9.3513	2.7	4.632	2.7	0.314	0.5	0.2	1761.0	7.7	1755.0	22.9	1747.8	49.5	1747.8	49.5
159	10504	0.9	17.2918	3.7	0.729	5.0	0.091	3.3	0.7	564.1	17.9	556.1	21.3	523.3	81.7	564.1	17.9
472	7384	1.6	12.5708	3.8	1.762	6.1	0.161	4.7	0.8	960.6	41.8	1031.8	39.3	1185.8	76.1	1185.8	76.1
459	6564	1.4	15.6095	5.1	0.671	7.8	0.076	6.0	0.8	471.8	27.1	521.2	31.9	743.7	107.2	471.8	27.1
224	9744	1.2	16.2291	6.3	0.847	6.9	0.100	2.7	0.4	612.6	15.6	623.0	31.9	660.9	135.5	612.6	15.6
389	20076	1.4	17.3558	3.5	0.709	3.8	0.089	1.4	0.4	551.1	7.3	544.2	16.0	515.2	77.6	551.1	7.3
1039	7668	2.1	13.8293	2.3	1.134	6.1	0.114	5.7	0.9	694.7	37.2	769.9	32.9	994.7	46.7	694.7	37.2
403	15928	0.7	16.4085	4.7	0.790	4.9	0.094	1.5	0.3	579.2	8.4	591.1	22.1	637.2	100.9	579.2	8.4
253	16352	0.9	13.4963	4.0	1.776	6.3	0.174	4.8	0.8	1033.3	45.9	1036.8	40.9	1044.0	81.7	1044.0	81.7
234	4596	1.2	14.5912	16.0	0.824	16.5	0.087	4.0	0.2	539.2	20.5	610.5	75.9	884.7	333.2	539.2	20.5
Whillans (SAL 1755)																	
305	34990	5.3	16.9178	4.3	0.716	5.5	0.088	3.5	0.6	542.7	18.1	548.2	23.4	571.1	93.4	542.7	18.1
135	24255	2.0	16.8648	4.8	0.747	6.5	0.091	4.5	0.7	563.6	24.0	566.5	28.4	577.9	104.0	563.6	24.0
1134	21490	1.5	17.0715	3.2	0.567	7.5	0.070	6.8	0.9	437.7	28.7	456.4	27.6	551.4	70.2	437.7	28.7
742	71255	2.7	17.3272	1.7	0.656	4.6	0.082	4.3	0.9	510.9	21.1	512.4	18.6	518.9	37.8	510.9	21.1
514	83100	3.4	16.9203	2.5	0.781	3.7	0.096	2.7	0.7	590.2	15.3	586.3	16.4	570.8	53.8	590.2	15.3
605	35395	1.4	20.2599	3.0	0.247	4.6	0.036	3.5	0.8	229.8	7.9	224.1	9.3	164.9	70.2	229.8	7.9
85	15030	1.8	17.9070	4.9	0.612	5.9	0.079	3.3	0.6	493.1	15.8	484.8	22.8	446.2	108.8	493.1	15.8
195	32405	3.1	16.2872	3.2	0.773	4.2	0.091	2.6	0.6	563.6	14.2	581.7	18.5	653.2	69.6	563.6	14.2
145	32835	2.2	16.4061	3.3	0.817	4.1	0.097	2.5	0.6	598.3	14.3	606.5	18.8	637.6	70.4	598.3	14.3
96	14680	2.1	17.2265	7.5	0.663	9.2	0.083	5.3	0.6	513.4	26.2	516.7	37.3	531.6	165.3	513.4	26.2
171	55625	1.9	17.4013	2.0	0.671	5.7	0.085	5.3	0.9	524.1	26.6	521.4	23.1	509.5	44.8	524.1	26.6
168	18280	1.0	17.3497	4.6	0.647	5.1	0.081	2.0	0.4	504.5	9.8	506.6	20.2	516.0	102.0	504.5	9.8
498	67730	1.1	16.8492	0.9	0.758	4.2	0.093	4.1	1.0	570.8	22.2	572.6	18.2	579.9	20.0	570.8	22.2
203	33425	2.0	17.6949	3.5	0.617	4.8	0.079	3.3	0.7	490.9	15.6	487.7	18.6	472.6	77.3	490.9	15.6

Appendix A Cont.: U-Pb detrital zircon geochronologic analyses by Laser-Ablation Multicollector ICP Mass Spectrometry

					Isotope ratios							Apparent ages (Ma)					
U (ppm)	206Pb 204Pb	U/Th	206Pb* 207Pb*	± (%)	207Pb* 235U*	± (%)	206Pb* 238U	± (%)	error corr.	206Pb* 238U*	± (Ma)	207Pb* 235U	± (Ma)	206Pb* 207Pb*	± (Ma)	**Best age** (Ma)	± (Ma)
Whillans (SAL 1755) Cont.																	
77	10735	0.9	18.2122	11.3	0.640	11.6	0.085	2.4	0.2	523.0	12.3	502.2	45.9	408.5	253.8	523.0	12.3
261	24960	1.8	18.6969	4.3	0.442	4.9	0.060	2.3	0.5	374.9	8.5	371.4	15.2	349.4	97.3	374.9	8.5
554	171225	7.9	13.7031	2.6	1.674	3.9	0.166	2.9	0.7	992.1	26.9	998.7	24.8	1013.3	52.3	1013.3	52.3
426	5050	1.3	15.0304	3.5	0.590	4.7	0.064	3.1	0.7	401.9	12.2	470.9	17.7	823.1	72.8	401.9	12.2
78	10990	1.3	17.7186	9.0	0.621	9.1	0.080	1.8	0.2	495.3	8.5	490.7	35.6	469.6	198.8	495.3	8.5
280	42815	1.4	17.5095	3.3	0.682	5.8	0.087	4.8	0.8	535.4	24.5	528.0	23.8	495.8	72.5	535.4	24.5
360	40185	2.0	17.7568	6.2	0.662	8.5	0.085	5.8	0.7	527.5	29.5	515.9	34.4	464.8	137.7	527.5	29.5
612	98475	9.9	15.3873	1.3	1.005	2.2	0.112	1.8	0.8	685.3	11.6	706.3	11.3	774.0	27.8	685.3	11.6
133	19140	3.5	16.7449	2.6	0.697	3.7	0.085	2.7	0.7	523.9	13.7	537.0	15.6	593.4	55.6	523.9	13.7
180	23590	2.8	12.9619	5.5	1.562	5.8	0.147	2.0	0.3	883.3	16.7	955.3	36.1	1125.0	109.0	1125.0	109.0
1271	15750	3.2	13.0312	1.6	1.612	5.0	0.152	4.8	0.9	914.2	40.5	975.0	31.4	1114.4	31.6	1114.4	31.6
314	29195	6.6	13.8889	4.0	1.361	4.2	0.137	1.5	0.3	828.2	11.3	872.3	24.7	985.9	80.4	828.2	11.3
509	64850	3.2	13.6044	1.1	1.636	1.4	0.161	0.8	0.6	964.6	7.2	984.1	8.8	1027.9	23.1	1027.9	23.1
115	18995	1.0	17.2547	3.4	0.660	6.2	0.083	5.2	0.8	511.9	25.5	514.9	25.1	528.0	74.8	511.9	25.5
103	12375	1.3	18.2349	4.5	0.590	5.8	0.078	3.7	0.6	484.0	17.3	470.6	22.0	405.7	101.3	484.0	17.3
195	27085	1.9	17.6346	3.3	0.642	3.7	0.082	1.6	0.4	508.4	7.8	503.3	14.5	480.1	72.8	508.4	7.8
202	24250	1.3	17.1941	5.9	0.616	6.7	0.077	3.2	0.5	477.0	14.5	487.3	25.8	535.8	128.4	477.0	14.5
130	17445	1.3	17.4479	3.8	0.639	5.5	0.081	4.0	0.7	501.0	19.2	501.5	21.7	503.6	82.9	501.0	19.2
170	58840	2.1	13.2255	1.1	1.928	2.8	0.185	2.6	0.9	1094.0	25.9	1090.9	18.8	1084.8	22.9	1084.8	22.9
143	24880	2.0	16.7115	6.7	0.655	8.0	0.079	4.3	0.5	492.4	20.2	511.5	32.1	597.7	146.1	492.4	20.2
200	31990	3.1	13.6619	1.1	1.680	2.8	0.167	2.6	0.9	992.8	23.5	1001.1	17.7	1019.4	22.2	1019.4	22.2
329	10570	0.8	16.0421	4.6	0.652	7.0	0.076	5.3	0.8	471.4	23.9	509.7	28.1	685.6	98.9	471.4	23.9
105	14395	2.5	17.9766	5.1	0.601	5.7	0.078	2.5	0.4	486.4	11.5	477.9	21.7	437.5	114.3	486.4	11.5
79	15320	2.2	17.8727	4.9	0.579	9.4	0.075	8.0	0.9	466.7	36.2	463.9	35.1	450.4	109.6	466.7	36.2
541	52000	1.3	13.7251	3.1	1.615	4.1	0.161	2.8	0.7	961.1	24.7	976.1	25.9	1010.0	62.1	1010.0	62.1
404	28255	6.3	13.7593	4.1	1.180	6.2	0.118	4.7	0.8	717.5	31.6	791.2	34.0	1005.0	82.8	717.5	31.6
95	16780	2.0	17.4411	6.9	0.652	8.6	0.083	5.2	0.6	511.2	25.5	510.0	34.5	504.4	151.5	511.2	25.5
347	5145	1.0	13.1597	16.6	0.910	16.8	0.087	2.6	0.2	536.7	13.4	656.9	81.4	1094.8	334.5	536.7	13.4
354	21430	2.0	16.7290	3.9	0.675	4.9	0.082	3.0	0.6	507.5	14.7	523.8	20.2	595.5	84.7	507.5	14.7
342	67395	1.0	13.4705	1.3	1.794	2.5	0.175	2.1	0.8	1041.3	20.2	1043.4	16.2	1047.9	27.0	1047.9	27.0
683	9990	5.6	13.4923	5.6	0.995	7.5	0.097	5.0	0.7	598.7	28.5	701.1	38.0	1044.6	113.0	598.7	28.5
321	76865	2.1	13.8782	2.5	1.564	3.5	0.157	2.5	0.7	942.5	22.1	956.1	21.9	987.5	50.5	942.5	22.1
148	21345	3.1	13.1749	2.8	1.880	3.3	0.180	1.7	0.5	1065.2	16.4	1074.2	21.9	1092.5	57.0	1092.5	57.0

Appendix A Cont.: U-Pb detrital zircon geochronologic analyses by Laser-Ablation Multicollector ICP Mass Spectrometry

					Isotope ratios							Apparent ages (Ma)					
U (ppm)	206Pb 204Pb	U/Th	206Pb* 207Pb*	± (%)	207Pb* 235U*	± (%)	206Pb* 238U	± (%)	error corr.	206Pb* 238U*	± (Ma)	207Pb* 235U	± (Ma)	206Pb* 207Pb*	± (Ma)	**Best age (Ma)**	± (Ma)
Whillans (SAL 1755) Cont.																	
281	44525	2.6	17.9900	3.5	0.619	4.4	0.081	2.6	0.6	500.6	12.5	489.1	16.9	435.9	78.2	500.6	12.5
363	61040	3.1	17.4326	2.6	0.720	3.7	0.091	2.6	0.7	561.4	14.2	550.5	15.7	505.5	56.6	561.4	14.2
631	40105	1.8	17.1646	1.2	0.671	3.8	0.084	3.6	1.0	517.5	17.8	521.6	15.4	539.5	25.5	517.5	17.8
198	31520	1.3	17.6288	4.4	0.640	5.5	0.082	3.3	0.6	507.3	16.1	502.6	21.9	480.8	98.2	507.3	16.1
85	790	0.6	9.7666	4.4	1.142	5.2	0.081	2.8	0.5	501.5	13.7	773.5	28.4	1667.9	81.7	1667.9	81.7
60	755	6.6	7.4695	4.1	1.564	5.8	0.085	4.0	0.7	524.4	20.2	956.2	35.7	2149.4	72.1	2149.4	72.1
92	24550	1.6	13.9199	1.6	1.592	7.1	0.161	6.9	1.0	960.5	61.9	966.9	44.4	981.4	32.0	981.4	32.0
96	830	5.9	7.4732	4.3	1.560	4.6	0.085	1.7	0.4	523.2	8.7	954.5	28.6	2148.6	74.7	2148.6	74.7
330	57620	1.7	14.2219	2.8	1.546	3.2	0.159	1.6	0.5	953.8	14.5	948.9	20.0	937.5	57.4	953.8	14.5
246	6955	2.2	15.7886	3.5	0.736	5.2	0.084	3.8	0.7	521.7	19.2	560.1	22.5	719.5	75.2	521.7	19.2
80	23420	1.8	13.1964	3.3	1.961	5.1	0.188	3.9	0.8	1108.6	40.0	1102.1	34.5	1089.2	66.0	1089.2	66.0
234	38075	15.9	16.2357	2.7	0.765	7.0	0.090	6.4	0.9	556.1	34.3	577.0	30.8	660.0	58.1	556.1	34.3
171	7695	1.6	17.5390	3.2	0.644	3.9	0.082	2.3	0.6	507.6	11.2	504.8	15.6	492.1	70.3	507.6	11.2
SN (SAL 1659)																	
395	9848	3.3	15.8246	3.5	0.793	4.8	0.091	3.3	0.7	561.6	17.8	592.9	21.6	714.7	73.9	561.6	17.8
75	5432	1.6	17.5939	7.3	0.682	7.5	0.087	1.4	0.2	537.6	7.4	527.7	30.8	485.2	162.3	537.6	7.4
123	25124	1.6	13.1580	4.3	1.944	4.7	0.185	1.9	0.4	1096.8	18.7	1096.2	31.5	1095.0	86.4	1095.0	86.4
511	52568	2.6	13.2553	2.0	1.939	2.5	0.186	1.6	0.6	1102.0	15.7	1094.7	17.0	1080.3	40.1	1080.3	40.1
473	33520	1.9	17.1680	2.6	0.729	5.4	0.091	4.7	0.9	560.3	25.3	556.1	23.1	539.1	57.1	560.3	25.3
317	45896	3.4	13.3715	3.9	1.759	6.0	0.171	4.6	0.8	1015.5	43.2	1030.6	39.1	1062.7	78.5	1062.7	78.5
524	35916	2.6	14.3091	2.1	1.235	6.3	0.128	5.9	0.9	777.3	43.1	816.5	35.1	925.0	43.7	777.3	43.1
466	82088	3.6	12.7424	1.6	2.138	3.8	0.198	3.5	0.9	1162.4	37.1	1161.2	26.4	1159.0	30.7	1159.0	30.7
198	11724	1.3	17.6920	2.4	0.629	3.9	0.081	3.0	0.8	500.7	14.5	495.7	15.1	472.9	53.7	500.7	14.5
232	22964	3.0	13.2315	2.7	1.833	3.4	0.176	2.1	0.6	1044.3	20.0	1057.2	22.2	1083.9	53.7	1083.9	53.7
116	23484	2.6	11.5101	1.1	2.778	1.2	0.232	0.5	0.4	1344.5	6.1	1349.7	9.2	1357.8	21.8	1357.8	21.8
168	12496	3.1	17.2257	4.6	0.672	4.8	0.084	1.1	0.2	519.3	5.7	521.6	19.4	531.7	101.3	519.3	5.7
427	29052	2.2	16.5390	3.9	0.787	4.1	0.094	1.2	0.3	581.4	6.7	589.4	18.3	620.2	84.7	581.4	6.7
215	33915	1.5	13.1688	2.4	1.993	2.8	0.190	1.5	0.5	1123.1	15.3	1113.0	19.2	1093.4	48.7	1093.4	48.7
210	16853	7.4	16.5844	3.5	0.741	3.7	0.089	1.0	0.3	550.1	5.3	562.8	15.9	614.3	76.5	550.1	5.3
702	82460	4.2	14.4529	1.1	1.272	2.0	0.133	1.6	0.8	806.9	12.1	833.3	11.1	904.4	23.5	904.4	23.5
326	39258	12.9	16.0663	2.7	0.833	5.4	0.097	4.7	0.9	596.9	27.0	615.0	25.1	682.4	57.4	596.9	27.0
378	31895	1.6	16.7586	3.7	0.696	5.0	0.085	3.3	0.7	523.2	16.6	536.1	20.7	591.7	80.3	523.2	16.6
236	14643	1.7	16.6897	2.6	0.786	2.6	0.095	0.7	0.3	586.1	3.7	589.1	11.8	600.6	55.3	586.1	3.7
177	8525	2.1	15.8240	3.3	0.773	3.7	0.089	1.6	0.4	548.2	8.6	581.7	16.3	714.8	69.8	548.2	8.6

Appendix A Cont.: U-Pb detrital zircon geochronologic analyses by Laser-Ablation Multicollector ICP Mass Spectrometry

					Isotope ratios							Apparent ages (Ma)					
U (ppm)	206Pb 204Pb	U/Th	206Pb* 207Pb*	± (%)	207Pb* 235U*	± (%)	206Pb* 238U	± (%)	error corr.	206Pb* 238U*	± (Ma)	207Pb* 235U	± (Ma)	206Pb* 207Pb*	± (Ma)	**Best age (Ma)**	± (Ma)
SN (SAL 1659) Cont.																	
195	12953	4.9	17.2308	2.1	0.681	2.5	0.085	1.2	0.5	526.6	6.1	527.5	10.1	531.1	46.8	526.6	6.1
414	30300	1.9	13.6951	2.6	1.786	5.2	0.177	4.5	0.9	1052.8	43.7	1040.4	33.7	1014.5	51.9	1014.5	51.9
699	63110	27.5	16.3090	1.0	0.867	1.2	0.103	0.7	0.6	629.1	4.3	633.8	5.9	650.3	21.7	629.1	4.3
288	41290	16.3	16.3039	3.1	0.774	4.8	0.092	3.7	0.8	564.8	19.8	582.3	21.1	651.0	65.7	564.8	19.8
327	15573	2.0	16.9639	2.0	0.696	3.7	0.086	3.2	0.8	529.4	16.1	536.2	15.6	565.2	43.8	529.4	16.1
111	11198	1.8	17.4037	6.6	0.680	6.7	0.086	0.7	0.1	530.6	3.8	526.6	27.4	509.2	145.8	530.6	3.8
564	80600	2.6	16.1593	2.0	0.904	2.5	0.106	1.5	0.6	648.9	9.2	653.6	12.1	670.1	43.1	648.9	9.2
250	27243	1.9	16.2290	1.5	0.810	2.9	0.095	2.4	0.8	587.3	13.7	602.6	13.1	660.9	32.9	587.3	13.7
142	22768	2.0	13.1334	1.6	1.990	1.8	0.190	0.7	0.4	1119.1	7.3	1112.2	12.1	1098.8	32.9	1098.8	32.9
340	55738	2.9	13.5489	0.9	1.780	1.2	0.175	0.8	0.6	1039.3	7.4	1038.3	7.9	1036.2	18.8	1036.2	18.8
423	58578	3.5	16.0464	1.5	0.944	3.1	0.110	2.6	0.9	671.7	16.8	674.8	15.0	685.1	32.7	671.7	16.8
530	60773	4.2	13.5141	2.1	1.813	2.8	0.178	1.9	0.7	1054.6	18.2	1050.3	18.2	1041.4	41.4	1041.4	41.4
241	25755	1.6	16.2902	1.8	0.869	2.6	0.103	1.9	0.7	630.3	11.5	635.2	12.4	652.8	38.7	630.3	11.5
476	18250	1.5	17.0130	1.8	0.741	1.9	0.091	0.7	0.4	564.2	3.7	563.1	8.2	558.9	38.3	564.2	3.7
459	58770	1.8	13.4591	1.5	1.818	1.6	0.177	0.5	0.3	1053.1	4.9	1051.9	10.4	1049.6	30.4	1049.6	30.4
307	25473	2.9	17.4203	1.9	0.688	2.1	0.087	0.9	0.4	537.4	4.8	531.7	8.9	507.1	42.4	537.4	4.8
389	26588	2.0	17.2677	1.3	0.666	1.4	0.083	0.5	0.4	516.7	2.5	518.5	5.5	526.4	27.7	516.7	2.5
110	22968	2.4	13.1813	2.5	1.946	3.3	0.186	2.2	0.6	1099.8	21.7	1097.0	22.2	1091.5	50.4	1091.5	50.4
270	36748	4.2	14.2704	1.7	1.462	5.0	0.151	4.7	0.9	908.2	39.6	914.7	30.0	930.5	34.9	930.5	34.9
122	17568	1.9	17.6071	4.1	0.659	4.2	0.084	0.6	0.1	520.5	3.0	513.7	16.8	483.6	91.0	520.5	3.0
592	4095	0.5	14.5111	10.3	0.814	10.5	0.086	2.1	0.2	529.7	10.9	604.5	47.8	896.1	212.2	529.7	10.9
205	32623	1.8	17.1488	2.4	0.711	2.5	0.088	0.6	0.2	546.3	2.9	545.3	10.4	541.5	52.5	546.3	2.9
210	37165	3.4	13.1458	1.5	1.936	3.6	0.185	3.2	0.9	1092.1	32.4	1093.7	23.9	1096.9	30.3	1096.9	30.3
275	6360	2.8	15.4413	3.8	0.742	6.8	0.083	5.7	0.8	514.3	28.0	563.3	29.6	766.6	80.8	514.3	28.0
192	19293	3.3	17.2240	3.2	0.691	4.2	0.086	2.7	0.6	533.5	14.0	533.2	17.6	532.0	70.9	533.5	14.0
218	18248	2.2	17.3406	1.9	0.688	1.9	0.087	0.5	0.3	534.9	2.6	531.6	8.1	517.2	41.3	534.9	2.6
461	81533	7.2	13.4162	0.7	1.812	1.0	0.176	0.7	0.7	1047.0	6.6	1049.9	6.2	1056.1	13.5	1056.1	13.5
520	39883	2.5	14.7808	3.8	1.097	10.1	0.118	9.3	0.9	716.8	63.2	752.0	53.6	858.0	79.3	716.8	63.2
344	24485	2.4	16.4243	3.4	0.697	3.6	0.083	1.0	0.3	514.0	5.0	536.8	14.8	635.2	73.3	514.0	5.0
621	59398	3.7	16.5096	1.1	0.871	4.1	0.104	4.0	1.0	639.3	24.3	636.0	19.6	624.0	24.4	639.3	24.3
125	3978	1.0	15.6868	4.2	0.759	5.4	0.086	3.4	0.6	533.8	17.3	573.3	23.7	733.3	89.4	533.8	17.3
230	49345	1.6	12.8766	3.2	2.179	3.3	0.203	0.5	0.2	1193.9	5.4	1174.2	22.8	1138.2	64.3	1138.2	64.3
783	19233	2.7	13.5198	2.1	0.855	4.4	0.084	3.9	0.9	519.0	19.6	627.4	20.8	1040.5	41.4	519.0	19.6

Appendix A Cont.: U-Pb detrital zircon geochronologic analyses by Laser-Ablation Multicollector ICP Mass Spectrometry

			Isotope ratios							Apparent ages (Ma)							
U (ppm)	206Pb 204Pb	U/Th	206Pb* 207Pb*	± (%)	207Pb* 235U*	± (%)	206Pb* 238U	± (%)	error corr.	206Pb* 238U*	± (Ma)	207Pb* 235U	± (Ma)	206Pb* 207Pb*	± (Ma)	**Best age** (Ma)	± (Ma)
SN (SAL 1659) Cont.																	
377	38230	1.7	17.3919	2.2	0.702	2.4	0.089	1.1	0.4	547.0	5.8	540.0	10.2	510.7	48.0	547.0	5.8
793	142143	5.5	13.4813	1.4	1.788	2.5	0.175	2.1	0.8	1038.6	20.0	1041.1	16.3	1046.3	27.7	1046.3	27.7
478	29588	1.1	13.2700	1.4	1.806	3.0	0.174	2.6	0.9	1033.0	24.9	1047.5	19.3	1078.1	27.8	1078.1	27.8
185	34183	1.6	13.0692	1.2	1.993	2.2	0.189	1.8	0.8	1115.6	18.3	1113.2	14.5	1108.6	23.8	1108.6	23.8
283	30345	3.4	16.4708	1.0	0.863	1.2	0.103	0.5	0.4	632.3	3.0	631.6	5.4	629.1	22.3	632.3	3.0
440	21865	2.0	17.1443	1.6	0.681	3.5	0.085	3.1	0.9	523.6	15.5	527.1	14.3	542.1	35.2	523.6	15.5
447	35830	1.5	9.7224	2.6	3.953	4.3	0.279	3.5	0.8	1585.1	48.8	1624.6	35.2	1676.3	48.1	1676.3	48.1
283	57653	6.7	13.2865	1.6	1.893	2.9	0.182	2.4	0.8	1080.4	24.2	1078.8	19.2	1075.6	31.5	1075.6	31.5
279	30240	3.7	12.9757	1.2	1.890	1.5	0.178	1.0	0.6	1055.4	9.3	1077.7	10.1	1122.9	23.4	1122.9	23.4
613	33603	4.4	17.1244	1.9	0.703	2.3	0.087	1.2	0.5	539.3	6.3	540.3	9.5	544.7	41.8	539.3	6.3
357	57873	4.8	13.1417	1.3	1.943	1.7	0.185	1.1	0.6	1095.2	10.8	1096.0	11.1	1097.5	25.2	1097.5	25.2
275	26898	3.8	14.5183	2.5	1.188	4.4	0.125	3.6	0.8	759.5	25.7	794.8	24.2	895.1	52.3	759.5	25.7
231	38863	1.8	13.3114	2.0	1.890	2.3	0.183	1.1	0.5	1080.7	10.5	1077.7	15.2	1071.8	40.8	1071.8	40.8
113	22868	1.8	13.8937	2.2	1.605	2.5	0.162	1.1	0.5	966.1	10.0	972.0	15.5	985.2	45.0	985.2	45.0
331	18968	2.8	17.0305	2.0	0.710	2.2	0.088	0.8	0.4	541.7	4.4	544.6	9.3	556.6	44.3	541.7	4.4
910	38285	5.0	13.3007	1.6	1.899	1.8	0.183	0.9	0.5	1084.5	9.3	1080.8	12.3	1073.4	32.0	1073.4	32.0
197	13836	1.1	15.6946	3.4	0.929	3.8	0.106	1.7	0.4	647.9	10.6	667.0	18.7	732.2	72.6	647.9	10.6
186	18380	1.6	16.4527	5.6	0.709	5.9	0.085	1.9	0.3	523.6	9.5	544.2	25.0	631.5	121.4	523.6	9.5
205	58034	4.8	13.4696	1.9	1.701	2.1	0.166	1.0	0.5	990.9	9.0	1008.8	13.5	1048.1	37.8	1048.1	37.8
161	28488	2.8	13.5121	2.6	1.849	3.2	0.181	1.9	0.6	1073.4	18.3	1063.0	21.1	1041.7	52.6	1041.7	52.6
207	33148	1.6	10.2123	2.8	3.529	3.7	0.261	2.4	0.7	1496.9	32.1	1533.8	29.2	1584.9	52.4	1584.9	52.4
502	11900	1.7	16.5694	2.2	0.697	2.7	0.084	1.5	0.6	518.3	7.3	536.8	11.1	616.2	48.1	518.3	7.3
458	17018	2.2	17.0691	2.7	0.700	4.2	0.087	3.3	0.8	535.5	16.9	538.6	17.8	551.7	58.6	535.5	16.9
331	17538	3.6	13.2681	2.0	1.688	5.3	0.162	4.9	0.9	970.2	44.0	1003.9	33.7	1078.3	39.8	1078.3	39.8
181	25820	1.3	13.2055	2.5	1.868	2.7	0.179	1.0	0.4	1060.8	9.4	1069.7	17.5	1087.9	49.6	1087.9	49.6
177	9362	5.5	17.7051	5.9	0.633	6.0	0.081	0.6	0.1	503.7	3.0	497.9	23.4	471.3	131.1	503.7	3.0

Appendix A Cont.: U-Pb detrital zircon geochronologic analyses by Laser-Ablation Multicollector ICP Mass Spectrometry

			Isotope ratios							Apparent ages (Ma)							
U (ppm)	206Pb 204Pb	U/Th	206Pb* 207Pb*	± (%)	207Pb* 235U*	± (%)	206Pb* 238U	± (%)	error corr.	206Pb* 238U*	± (Ma)	207Pb* 235U	± (Ma)	206Pb* 207Pb*	± (Ma)	**Best age** (Ma)	± (Ma)
SN (SAL 1659) Cont.																	
646	142660	7.3	13.4089	2.6	1.689	3.3	0.164	2.1	0.6	980.6	19.3	1004.5	21.2	1057.1	51.6	1057.1	51.6
387	44148	2.5	16.9687	1.7	0.680	2.2	0.084	1.5	0.6	517.9	7.2	526.6	9.2	564.6	37.1	517.9	7.2
587	61254	18.4	13.4971	1.5	1.778	1.7	0.174	0.8	0.5	1034.2	7.6	1037.3	10.9	1043.9	29.9	1043.9	29.9
130	17108	3.0	17.2083	4.6	0.695	5.0	0.087	1.8	0.4	536.6	9.3	536.1	20.7	534.0	101.4	536.6	9.3
398	16558	1.9	14.7915	1.6	1.112	4.0	0.119	3.6	0.9	726.2	25.0	758.9	21.2	856.5	32.9	726.2	25.0
120	34360	3.3	13.1405	2.5	1.888	2.6	0.180	0.9	0.3	1066.8	8.5	1077.0	17.5	1097.7	49.9	1097.7	49.9
69	7990	2.7	18.8413	9.0	0.620	9.1	0.085	1.1	0.1	524.6	5.5	490.1	35.3	332.0	204.5	524.6	5.5
124	36696	2.0	13.8264	3.8	1.592	3.9	0.160	0.9	0.2	954.7	7.8	967.1	24.5	995.1	77.7	995.1	77.7
97	23380	2.6	13.5503	2.9	1.802	3.0	0.177	0.8	0.3	1051.2	8.0	1046.3	19.4	1036.0	57.9	1036.0	57.9
750	21562	7.2	13.4540	2.2	1.434	4.7	0.140	4.2	0.9	844.0	33.1	903.1	28.3	1050.4	44.4	1050.4	44.4
63	11844	2.0	13.6918	4.9	1.731	5.0	0.172	1.0	0.2	1022.3	9.5	1020.0	32.1	1015.0	99.0	1015.0	99.0
SN (SAL 1660)																	
519	59316	3.9	16.8542	3.3	0.828	5.2	0.101	4.0	0.8	621.5	23.8	612.5	23.9	579.3	71.5	621.5	23.8
139	9820	1.1	16.1685	3.6	1.032	8.1	0.121	7.2	0.9	736.2	50.3	719.7	41.7	668.9	77.3	736.2	50.3
3098	107864	0.9	15.0632	4.7	1.163	4.9	0.127	1.7	0.3	771.0	12.3	783.3	27.0	818.6	97.2	771.0	12.3
135	9544	1.0	17.3884	5.8	0.675	9.5	0.085	7.5	0.8	526.4	38.0	523.6	38.9	511.1	127.7	526.4	38.0
324	54548	1.2	13.3951	2.0	1.855	3.3	0.180	2.6	0.8	1068.1	25.8	1065.2	21.7	1059.2	40.1	1059.2	40.1
395	44264	1.8	13.5637	2.1	1.572	3.4	0.155	2.7	0.8	927.2	23.4	959.4	21.3	1034.0	42.6	1034.0	42.6
325	27756	3.6	16.8724	3.4	0.707	4.8	0.087	3.3	0.7	534.8	17.1	542.9	20.2	576.9	74.9	534.8	17.1
535	76436	2.5	13.4781	2.6	1.769	2.7	0.173	0.5	0.2	1028.1	4.8	1034.1	17.4	1046.8	53.3	1046.8	53.3
320	16784	4.5	15.4874	3.3	0.978	3.9	0.110	2.0	0.5	672.1	12.8	692.7	19.3	760.3	69.4	672.1	12.8
232	5080	1.4	16.9879	6.1	0.674	6.1	0.083	0.6	0.1	514.1	3.1	523.0	25.1	562.1	133.2	514.1	3.1
177	82490	1.7	8.1926	2.1	5.954	2.1	0.354	0.5	0.2	1952.6	8.4	1969.1	18.6	1986.6	37.0	1986.6	37.0
210	15472	1.6	17.5796	3.4	0.672	4.0	0.086	2.1	0.5	529.8	10.5	521.8	16.4	487.0	75.8	529.8	10.5
205	19904	2.0	17.2152	3.4	0.684	3.5	0.085	0.7	0.2	527.9	3.5	528.9	14.4	533.1	75.0	527.9	3.5

Appendix A Cont.: U-Pb detrital zircon geochronologic analyses by Laser-Ablation Multicollector ICP Mass Spectrometry

			Isotope ratios							Apparent ages (Ma)							
U (ppm)	206Pb 204Pb	U/Th	206Pb* 207Pb*	± (%)	207Pb* 235U*	± (%)	206Pb* 238U	± (%)	error corr.	206Pb* 238U*	± (Ma)	207Pb* 235U	± (Ma)	206Pb* 207Pb*	± (Ma)	**Best age** (Ma)	± (Ma)
SN (SAL 1660) Cont.																	
538	37068	6.1	13.9011	1.8	1.610	2.7	0.162	2.0	0.7	969.8	18.0	974.2	16.9	984.2	36.7	984.2	36.7
300	22088	3.0	15.6617	2.5	0.850	3.5	0.097	2.5	0.7	593.9	14.0	624.5	16.4	736.7	52.9	593.9	14.0
218	17148	3.1	17.5719	5.5	0.635	5.9	0.081	2.0	0.3	502.0	9.8	499.5	23.2	488.0	121.8	502.0	9.8
296	13254	1.9	16.9676	3.2	0.695	3.4	0.085	1.3	0.4	528.7	6.8	535.5	14.2	564.7	68.7	528.7	6.8
260	45728	3.1	16.0461	2.1	0.866	2.8	0.101	1.7	0.6	619.2	10.3	633.5	13.0	685.1	45.5	619.2	10.3
353	23714	1.6	17.5327	3.6	0.645	3.7	0.082	1.0	0.3	508.3	4.8	505.5	14.7	492.9	78.4	508.3	4.8
320	32756	7.6	17.3886	3.0	0.676	3.4	0.085	1.6	0.5	527.4	8.0	524.4	14.0	511.1	66.7	527.4	8.0
578	58016	1.5	16.8416	1.3	0.795	1.9	0.097	1.3	0.7	597.2	7.5	593.8	8.4	580.9	29.0	597.2	7.5
387	27802	2.3	17.2432	1.7	0.653	2.0	0.082	1.0	0.5	506.3	4.8	510.5	8.0	529.6	37.7	506.3	4.8
MH (SAL 1690)																	
1664	64515	1.8	19.8149	2.9	0.202	4.0	0.029	2.7	0.7	184.8	5.0	187.1	6.8	216.5	66.5	184.8	5.0
256	37510	1.4	16.9388	3.5	0.748	4.6	0.092	3.0	0.6	566.9	16.0	567.2	19.9	568.4	76.5	566.9	16.0
1617	39760	1.0	20.0474	2.0	0.203	3.0	0.030	2.2	0.7	187.6	4.0	187.7	5.1	189.5	47.5	187.6	4.0
158	76250	1.8	7.4809	1.2	7.014	5.3	0.381	5.2	1.0	2079.0	91.9	2113.3	47.2	2146.8	20.6	2146.8	20.6
466	91135	1.9	13.4158	2.3	1.840	2.6	0.179	1.1	0.4	1061.5	11.2	1059.7	16.8	1056.1	46.1	1056.1	46.1
257	16470	0.5	15.8741	6.1	0.788	6.2	0.091	0.9	0.2	559.6	5.0	589.8	27.7	708.1	130.1	559.6	5.0
59	5255	1.0	17.7165	15.5	0.352	15.6	0.045	2.1	0.1	284.8	5.9	305.9	41.3	469.9	344.3	284.8	5.9
1009	28330	2.4	17.9321	2.2	0.445	2.7	0.058	1.6	0.6	362.4	5.8	373.5	8.5	443.0	47.8	362.4	5.8
64	73915	1.9	9.7464	3.9	4.301	4.1	0.304	1.1	0.3	1711.4	16.7	1693.6	33.5	1671.7	72.3	1671.7	72.3
142	17295	1.0	21.4505	16.5	0.274	16.7	0.043	2.4	0.1	269.3	6.3	246.0	36.4	29.7	397.7	269.3	6.3
556	50745	1.8	18.8699	4.1	0.418	5.3	0.057	3.3	0.6	358.3	11.4	354.3	15.7	328.5	93.3	358.3	11.4
200	23780	1.2	17.1035	4.7	0.796	4.9	0.099	1.4	0.3	607.4	8.1	594.8	22.3	547.3	103.6	607.4	8.1
249	33135	3.0	15.6730	4.7	1.019	5.4	0.116	2.7	0.5	706.2	18.0	713.2	27.7	735.1	99.2	706.2	18.0
248	56900	0.9	12.2912	1.5	2.351	2.4	0.210	1.9	0.8	1226.5	21.0	1227.8	16.9	1230.1	28.5	1230.1	28.5
185	16790	1.8	16.7531	4.0	0.647	4.3	0.079	1.5	0.4	488.2	7.1	506.9	17.0	592.4	86.2	488.2	7.1
498	111420	2.7	12.8047	3.1	1.995	3.5	0.185	1.8	0.5	1095.9	17.6	1113.9	23.9	1149.3	61.0	1149.3	61.0
483	64220	6.7	16.5065	3.6	0.777	4.5	0.093	2.7	0.6	573.5	14.6	583.9	20.0	624.4	78.5	573.5	14.6
586	68190	2.4	13.6557	2.5	1.635	2.6	0.162	0.7	0.3	967.6	5.9	983.9	16.4	1020.3	51.0	967.6	5.9
177	92530	1.8	5.4084	2.8	10.353	4.9	0.406	4.0	0.8	2197.1	74.7	2466.8	45.3	2697.3	46.3	2697.3	46.3

Appendix A Cont.: U-Pb detrital zircon geochronologic analyses by Laser-Ablation Multicollector ICP Mass Spectrometry

					Isotope ratios							Apparent ages (Ma)					
U (ppm)	206Pb 204Pb	U/Th	206Pb* 207Pb*	± (%)	207Pb* 235U*	± (%)	206Pb* 238U	± (%)	error corr.	206Pb* 238U*	± (Ma)	207Pb* 235U	± (Ma)	206Pb* 207Pb*	± (Ma)	**Best age** (Ma)	± (Ma)
MH (SAL 1690) Cont.																	
345	324805	1.4	5.1283	2.1	14.635	2.2	0.544	0.7	0.3	2801.6	15.7	2791.8	21.3	2784.8	34.9	2784.8	34.9
245	34040	0.9	11.9232	3.6	2.589	3.8	0.224	1.1	0.3	1302.2	13.3	1297.4	27.8	1289.5	70.5	1289.5	70.5
280	6436	1.4	20.4307	8.4	0.184	8.8	0.027	2.6	0.3	173.5	4.4	171.6	13.9	145.2	197.3	173.5	4.4
244	15232	0.8	20.1175	6.7	0.291	7.2	0.042	2.7	0.4	268.0	7.0	259.3	16.5	181.3	155.9	268.0	7.0
164	81666	2.1	3.6480	1.9	25.255	3.5	0.668	3.0	0.8	3298.9	76.7	3318.1	34.3	3329.8	29.4	3329.8	29.4
190	34362	1.3	12.7921	2.8	1.880	2.9	0.174	0.8	0.3	1036.6	7.7	1074.2	19.4	1151.3	56.0	1151.3	56.0
255	131250	1.9	3.8794	2.3	22.983	2.3	0.647	0.5	0.2	3215.1	12.7	3226.2	22.5	3233.1	35.6	3233.1	35.6
82	18550	0.6	12.5683	2.9	2.280	3.7	0.208	2.3	0.6	1217.2	25.5	1206.1	26.0	1186.2	56.9	1186.2	56.9
312	37696	1.5	12.5386	2.2	2.040	4.3	0.185	3.7	0.9	1096.9	37.3	1128.9	29.4	1190.9	43.9	1190.9	43.9
165	64008	2.0	10.3222	1.2	3.616	1.7	0.271	1.2	0.7	1544.5	16.1	1553.1	13.2	1564.9	22.1	1564.9	22.1
335	45666	4.1	5.6052	2.1	9.182	5.6	0.373	5.2	0.9	2044.8	90.9	2356.3	51.3	2638.1	35.0	2638.1	35.0
350	17336	1.6	19.6357	3.8	0.279	4.5	0.040	2.4	0.5	251.1	6.0	249.8	10.1	237.6	88.8	251.1	6.0
1271	19144	2.2	18.9267	3.4	0.278	5.0	0.038	3.8	0.7	241.5	8.9	249.1	11.1	321.8	76.5	241.5	8.9
717	2086	0.5	16.7118	5.1	0.192	8.5	0.023	6.8	0.8	148.1	9.9	178.2	13.9	597.7	110.9	148.1	9.9
267	2974	1.0	21.0058	14.2	0.178	14.2	0.027	0.5	0.0	172.7	0.9	166.6	21.8	79.7	337.8	172.7	0.9
159	76630	3.7	3.4332	2.5	24.704	4.9	0.615	4.2	0.9	3090.5	103.9	3296.6	47.7	3424.4	38.1	3424.4	38.1
201	34334	1.5	14.3330	2.3	1.454	2.7	0.151	1.5	0.6	907.5	13.0	911.6	16.5	921.6	46.9	921.6	46.9
117	46970	1.1	9.4995	1.3	4.482	1.5	0.309	0.9	0.5	1734.7	12.9	1727.6	12.8	1719.0	23.8	1719.0	23.8
321	17486	4.0	14.8173	2.9	1.193	4.0	0.128	2.7	0.7	777.9	20.0	797.6	22.2	852.9	61.1	777.9	20.0
89	14890	1.0	9.5519	4.6	4.363	4.9	0.302	1.6	0.3	1702.4	23.8	1705.3	40.3	1708.9	84.9	1708.9	84.9
704	3372	3.0	15.1186	8.4	0.720	8.5	0.079	1.1	0.1	489.9	5.4	550.7	36.1	810.9	176.1	489.9	5.4
490	13070	2.2	7.0249	1.9	7.163	3.6	0.365	3.0	0.9	2005.7	52.4	2132.0	31.8	2256.0	32.4	2256.0	32.4
292	73164	2.1	8.8390	1.1	5.203	1.8	0.334	1.5	0.8	1855.5	23.4	1853.1	15.4	1850.4	19.4	1850.4	19.4
408	50430	2.9	16.7721	2.3	0.791	3.0	0.096	1.9	0.6	592.0	10.9	591.6	13.6	589.9	50.9	592.0	10.9
59	18312	2.6	8.6662	2.8	5.512	4.8	0.346	3.9	0.8	1917.7	64.0	1902.5	41.0	1886.0	50.4	1886.0	50.4
288	26436	3.4	15.2399	2.0	1.125	2.3	0.124	1.1	0.5	755.4	8.1	765.3	12.3	794.2	41.6	755.4	8.1
415	8036	1.6	16.4276	4.4	0.682	4.5	0.081	0.6	0.1	503.9	2.8	528.2	18.4	634.8	95.4	503.9	2.8
425	102046	2.4	3.3222	1.3	29.818	1.5	0.718	0.7	0.5	3490.3	19.7	3480.8	14.7	3475.4	20.3	3475.4	20.3
392	57266	13.0	17.0867	2.0	0.771	2.2	0.096	1.1	0.5	588.5	6.0	580.5	9.9	549.5	42.8	588.5	6.0
147	16142	2.0	17.7728	5.2	0.633	5.3	0.082	0.8	0.2	505.8	3.9	498.1	20.8	462.9	116.0	505.8	3.9
81	7304	2.0	21.0082	24.3	0.264	24.5	0.040	2.8	0.1	253.9	6.9	237.6	51.9	79.4	585.1	253.9	6.9
210	29642	2.6	13.9355	1.6	1.632	1.9	0.165	1.1	0.6	984.2	9.9	982.6	12.0	979.1	31.7	979.1	31.7
517	63546	1.6	3.4121	2.6	22.746	2.7	0.563	0.9	0.3	2878.5	20.0	3216.1	26.7	3434.0	40.5	3434.0	40.5

Appendix A Cont.: U-Pb detrital zircon geochronologic analyses by Laser-Ablation Multicollector ICP Mass Spectrometry

U (ppm)	206Pb 204Pb	U/Th	206Pb* 207Pb*	± (%)	207Pb* 235U*	± (%)	206Pb* 238U	± (%)	error corr.	206Pb* 238U*	± (Ma)	207Pb* 235U	± (Ma)	206Pb* 207Pb*	± (Ma)	**Best age** (Ma)	± (Ma)
					Isotope ratios							**Apparent ages (Ma)**					
MH (SAL 1690) Cont.																	
125	15880	2.1	18.0962	7.2	0.696	7.3	0.091	1.4	0.2	563.3	7.8	536.3	30.5	422.7	160.1	563.3	7.8
347	7186	0.9	18.1876	4.1	0.318	4.2	0.042	0.7	0.2	264.9	1.7	280.4	10.3	411.5	92.6	264.9	1.7
76	15150	0.8	17.8110	9.0	0.671	9.3	0.087	2.4	0.3	536.2	12.4	521.6	38.1	458.1	200.7	536.2	12.4
200	13140	4.5	9.1284	12.9	1.409	16.2	0.093	9.9	0.6	575.0	54.2	892.8	96.6	1791.9	235.4	1791.9	235.4
679	7060	0.9	19.4197	5.1	0.180	5.1	0.025	0.7	0.1	161.4	1.1	168.1	7.9	263.0	116.7	161.4	1.1
129	5578	0.6	16.0704	6.2	0.778	6.3	0.091	1.4	0.2	559.6	7.5	584.4	28.2	681.9	132.3	559.6	7.5
196	65390	1.9	5.1478	1.4	13.342	2.0	0.498	1.5	0.7	2605.7	31.5	2704.1	19.0	2778.5	22.6	2778.5	22.6
515	24642	83.7	16.7765	1.5	0.759	2.1	0.092	1.4	0.7	569.8	7.7	573.7	9.1	589.3	32.8	569.8	7.7
517	37780	3.5	14.7215	2.2	1.058	2.7	0.113	1.7	0.6	690.0	10.8	732.9	14.2	866.4	44.6	690.0	10.8
405	87858	2.2	13.2266	1.7	1.788	2.7	0.171	2.0	0.8	1020.3	18.9	1041.0	17.3	1084.7	34.9	1084.7	34.9
228	10126	1.4	19.2909	9.4	0.299	9.7	0.042	2.5	0.3	264.1	6.4	265.6	22.7	278.3	214.9	264.1	6.4
314	43372	3.5	16.8366	1.6	0.792	1.7	0.097	0.7	0.4	595.2	3.9	592.4	7.8	581.6	34.5	595.2	3.9
447	59088	3.2	8.8959	2.1	3.822	2.4	0.247	1.0	0.4	1421.0	13.3	1597.5	18.9	1838.7	38.2	1838.7	38.2
300	52766	1.3	13.2719	2.8	1.867	3.6	0.180	2.3	0.6	1065.3	22.4	1069.4	23.7	1077.8	55.4	1077.8	55.4
196	27078	56.3	16.5720	4.1	0.798	4.3	0.096	1.2	0.3	590.1	6.9	595.4	19.3	615.9	88.7	590.1	6.9
370	108964	3.2	13.4524	3.2	1.672	3.2	0.163	0.7	0.2	974.1	6.0	997.9	20.6	1050.6	63.9	1050.6	63.9
294	24936	1.8	16.4473	2.5	0.836	3.1	0.100	1.8	0.6	612.9	10.3	617.1	14.2	632.2	54.1	612.9	10.3
182	19140	2.1	16.9718	3.9	0.761	4.0	0.094	1.1	0.3	577.4	5.8	574.7	17.6	564.2	84.1	577.4	5.8
131	22482	1.2	17.8045	5.1	0.699	6.9	0.090	4.6	0.7	557.4	24.4	538.4	28.7	458.9	113.5	557.4	24.4
240	39476	1.4	9.6114	1.6	4.121	3.1	0.287	2.6	0.9	1627.9	37.4	1658.5	25.0	1697.5	29.5	1697.5	29.5
133	29406	3.3	8.5656	1.7	5.317	2.0	0.330	1.1	0.6	1840.0	18.1	1871.7	17.1	1907.0	29.7	1907.0	29.7
270	12074	2.1	18.4894	3.5	0.438	3.6	0.059	0.8	0.2	368.1	2.9	369.0	11.0	374.6	77.9	368.1	2.9
371	55826	3.9	10.8410	1.1	3.212	2.0	0.253	1.7	0.8	1451.8	22.2	1460.1	15.8	1472.4	21.1	1472.4	21.1
173	16784	1.5	16.8101	2.9	0.768	4.9	0.094	4.0	0.8	576.7	22.0	578.4	21.6	585.0	61.9	576.7	22.0
164	37432	1.4	11.7769	1.8	2.308	2.6	0.197	1.9	0.7	1159.8	20.4	1214.7	18.6	1313.5	34.6	1313.5	34.6
316	70976	1.8	5.1977	1.4	12.943	1.8	0.488	1.1	0.6	2561.7	23.5	2675.5	16.8	2762.7	22.8	2762.7	22.8
205	106040	3.8	3.3658	2.2	25.052	2.7	0.612	1.6	0.6	3076.2	38.9	3310.2	26.4	3455.2	34.0	3455.2	34.0
218	29376	3.4	16.3713	1.8	0.871	2.6	0.103	1.8	0.7	634.6	10.9	636.3	12.1	642.2	39.1	634.6	10.9
181	14506	0.6	16.4903	6.6	0.788	6.6	0.094	0.8	0.1	580.5	4.6	590.0	29.6	626.5	141.7	580.5	4.6
798	49070	6.7	9.0512	1.0	4.424	1.3	0.290	0.8	0.6	1643.7	12.0	1716.9	10.8	1807.4	18.4	1807.4	18.4
287	14510	1.0	19.8699	8.2	0.295	8.2	0.042	0.6	0.1	268.2	1.5	262.3	19.0	210.2	190.5	268.2	1.5
218	65004	4.0	11.1043	2.6	2.679	4.9	0.216	4.2	0.9	1259.5	47.9	1322.7	36.4	1426.7	49.3	1426.7	49.3
305	123894	4.3	7.5332	2.3	6.034	2.6	0.330	1.1	0.4	1836.9	17.7	1980.8	22.5	2134.6	40.8	2134.6	40.8
159	4530	1.6	17.7045	19.2	0.348	19.2	0.045	0.8	0.0	281.7	2.2	303.1	50.4	471.4	428.8	281.7	2.2

Appendix A Cont.: U-Pb detrital zircon geochronologic analyses by Laser-Ablation Multicollector ICP Mass Spectrometry

			Isotope ratios							**Apparent ages (Ma)**							
U (ppm)	206Pb 204Pb	U/Th	206Pb* 207Pb*	± (%)	207Pb* 235U*	± (%)	206Pb* 238U	± (%)	error corr.	206Pb* 238U*	± (Ma)	207Pb* 235U	± (Ma)	206Pb* 207Pb*	± (Ma)	**Best age** (Ma)	± (Ma)
MH (SAL 1690) Cont.																	
290	31474	4.6	16.8536	3.4	0.785	3.7	0.096	1.6	0.4	590.6	9.0	588.3	16.6	579.4	73.1	590.6	9.0
61	7650	2.0	18.7724	11.2	0.705	11.3	0.096	1.6	0.1	590.8	9.0	541.7	47.5	340.3	254.0	590.8	9.0
93	25266	0.6	16.5948	9.8	0.755	10.2	0.091	3.0	0.3	560.3	16.1	570.9	44.6	612.9	211.1	560.3	16.1
427	17278	5.1	16.3406	3.0	0.812	3.3	0.096	1.5	0.4	592.5	8.5	603.7	15.2	646.2	64.1	592.5	8.5
341	27822	1.7	16.6815	2.0	0.798	4.0	0.097	3.5	0.9	594.3	19.6	595.8	18.1	601.6	43.7	594.3	19.6
614	45758	4.3	9.2459	1.8	3.540	3.7	0.237	3.3	0.9	1373.2	40.3	1536.3	29.6	1768.6	33.2	1768.6	33.2
311	31768	1.9	17.1619	2.7	0.729	2.9	0.091	0.9	0.3	560.1	5.0	556.1	12.4	539.9	59.8	560.1	5.0
171	55080	1.6	16.6798	2.7	0.833	3.3	0.101	1.9	0.6	619.0	11.2	615.4	15.1	601.9	57.9	619.0	11.2
160	22352	1.3	14.8671	2.6	0.962	4.4	0.104	3.6	0.8	636.4	21.5	684.5	22.0	845.9	54.9	636.4	21.5
302	35058	1.4	20.0746	4.5	0.278	4.7	0.041	1.5	0.3	256.2	3.7	249.5	10.4	186.3	104.5	256.2	3.7
243	29738	1.7	9.3439	2.4	4.625	2.4	0.313	0.5	0.2	1757.5	7.7	1753.8	20.2	1749.3	43.4	1749.3	43.4
121	10628	0.4	17.5021	5.2	0.750	5.3	0.095	0.9	0.2	586.0	4.9	568.0	23.0	496.8	115.2	586.0	4.9
188	13116	3.0	13.5458	4.6	1.646	4.8	0.162	1.3	0.3	966.2	12.0	988.0	30.2	1036.6	92.7	1036.6	92.7
299	5168	5.0	14.7341	3.8	0.931	6.8	0.100	5.7	0.8	611.6	33.0	668.3	33.5	864.6	79.5	611.6	33.0
464	123230	8.1	8.8500	1.6	5.009	2.7	0.321	2.2	0.8	1797.0	33.9	1820.8	22.5	1848.1	28.0	1848.1	28.0
233	46364	4.6	16.1780	5.1	0.739	5.2	0.087	1.0	0.2	536.2	5.2	561.9	22.6	667.6	110.2	536.2	5.2
436	15418	7.5	15.5635	3.0	0.959	3.7	0.108	2.2	0.6	662.5	13.7	682.7	18.6	749.9	64.2	662.5	13.7
215	16930	2.2	16.8589	2.8	0.688	3.4	0.084	1.9	0.6	520.4	9.6	531.3	14.1	578.7	61.0	520.4	9.6
306	33388	1.0	12.4448	2.8	1.911	3.8	0.172	2.6	0.7	1025.7	24.9	1084.9	25.6	1205.7	55.0	1205.7	55.0
484	42104	3.5	14.4281	3.8	1.311	4.4	0.137	2.2	0.5	828.9	17.2	850.7	25.2	907.9	77.9	828.9	17.2
870	76184	8.7	9.3343	3.1	3.444	7.2	0.233	6.5	0.9	1351.0	79.4	1514.5	56.8	1751.2	56.9	1751.2	56.9
803	26870	1.2	21.0230	4.3	0.166	4.9	0.025	2.3	0.5	160.7	3.6	155.5	7.0	77.8	102.3	160.7	3.6
75	31384	1.9	11.0930	5.9	2.281	8.6	0.184	6.3	0.7	1086.1	62.9	1206.4	61.0	1428.6	112.8	1428.6	112.8
283	87264	2.7	6.7633	2.5	6.385	2.6	0.313	0.7	0.3	1756.4	11.1	2030.2	23.2	2321.3	43.6	2321.3	43.6
137	12904	1.9	14.7226	3.8	1.195	7.2	0.128	6.1	0.8	774.2	44.5	798.3	39.8	866.2	79.2	774.2	44.5
527	21970	1.8	18.5217	6.2	0.442	6.8	0.059	2.8	0.4	371.7	10.0	371.6	21.0	370.6	138.9	371.7	10.0
555	37832	9.9	16.8673	2.1	0.771	3.5	0.094	2.8	0.8	581.3	15.8	580.5	15.5	577.6	44.6	581.3	15.8
144	24224	1.4	14.3484	3.9	1.269	4.2	0.132	1.5	0.4	799.6	11.6	831.9	24.0	919.4	80.9	799.6	11.6
226	55402	3.2	3.1605	1.8	30.496	1.9	0.699	0.6	0.3	3416.9	15.9	3502.9	18.6	3552.5	27.6	3552.5	27.6
514	16568	3.7	14.2259	2.3	1.271	3.6	0.131	2.8	0.8	794.2	21.0	832.7	20.5	937.0	46.4	794.2	21.0
361	17926	0.9	19.3911	3.5	0.295	3.9	0.042	1.8	0.5	262.2	4.6	262.6	9.1	266.4	80.5	262.2	4.6
169	3502	0.6	19.5957	10.7	0.307	10.8	0.044	1.4	0.1	275.2	3.8	271.8	25.8	242.3	247.3	275.2	3.8

Appendix A Cont.: U-Pb detrital zircon geochronologic analyses by Laser-Ablation Multicollector ICP Mass Spectrometry

			Isotope ratios							Apparent ages (Ma)							
U (ppm)	206Pb 204Pb	U/Th	206Pb* 207Pb*	± (%)	207Pb* 235U*	± (%)	206Pb* 238U	± (%)	error corr.	206Pb* 238U*	± (Ma)	207Pb* 235U	± (Ma)	206Pb* 207Pb*	± (Ma)	**Best age** (Ma)	± (Ma)
MH (SAL 1691)																	
2475	78265	0.4	19.5813	2.4	0.212	2.6	0.030	1.0	0.4	191.4	2.0	195.4	4.6	243.9	54.6	191.4	2.0
76	8930	1.6	21.6875	41.3	0.278	41.3	0.044	1.1	0.0	275.8	3.0	249.0	91.5	3.3	1035.0	275.8	3.0
136	39320	3.4	17.2229	6.5	0.677	6.7	0.085	1.5	0.2	523.3	7.5	524.9	27.5	532.1	143.5	523.3	7.5
194	201740	3.3	5.8263	2.4	9.872	2.5	0.417	0.9	0.3	2247.5	16.7	2422.9	23.4	2573.7	39.8	2573.7	39.8
134	114880	2.4	5.7979	3.6	8.245	5.0	0.347	3.4	0.7	1918.9	56.4	2258.3	44.9	2581.8	60.3	2581.8	60.3
124	34325	1.6	17.4525	3.2	0.683	3.4	0.086	0.9	0.3	534.7	4.5	528.8	13.8	503.0	71.2	534.7	4.5
43	23745	2.0	15.8538	19.3	0.763	19.4	0.088	2.5	0.1	541.9	13.1	575.6	85.6	710.8	413.2	541.9	13.1
122	16515	1.0	15.7649	11.8	0.374	11.9	0.043	1.6	0.1	270.1	4.3	322.8	32.9	722.7	250.9	270.1	4.3
168	58350	1.2	16.4004	4.9	0.847	5.0	0.101	0.8	0.2	619.0	4.8	623.2	23.3	638.3	106.3	619.0	4.8
96	21595	1.2	20.4926	13.3	0.261	13.6	0.039	2.9	0.2	245.2	7.0	235.3	28.7	138.1	314.4	245.2	7.0
109	60895	2.4	16.8385	4.7	0.768	4.8	0.094	1.3	0.3	577.8	7.1	578.5	21.4	581.3	101.5	577.8	7.1
495	24030	6.0	15.5436	4.5	0.865	4.7	0.097	1.2	0.3	599.5	6.8	632.6	22.0	752.6	95.7	599.5	6.8
218	129080	8.6	17.1890	3.6	0.734	4.8	0.092	3.2	0.7	564.6	17.4	559.0	20.7	536.4	78.2	564.6	17.4
128	65250	1.4	16.3781	3.7	0.867	3.8	0.103	0.7	0.2	631.6	4.3	633.7	17.9	641.2	80.3	631.6	4.3
60	18280	2.7	16.0957	7.9	0.837	8.0	0.098	1.3	0.2	601.1	7.2	617.6	37.1	678.5	169.5	601.1	7.2
102	17110	1.7	19.5489	14.2	0.262	14.3	0.037	1.4	0.1	235.1	3.1	236.2	30.1	247.7	328.9	235.1	3.1
12	2970	0.5	14.5216	24.8	0.865	25.7	0.091	6.8	0.3	561.9	36.4	632.7	121.6	894.7	519.3	561.9	36.4
309	46629	7.7	5.4427	3.4	10.488	4.1	0.414	2.4	0.6	2233.1	44.4	2478.8	38.2	2686.9	55.9	2686.9	55.9
34	3282	0.8	15.8807	13.9	0.814	14.1	0.094	2.3	0.2	577.6	12.8	604.6	64.1	707.2	296.3	577.6	12.8
310	47055	2.2	16.9578	1.8	0.729	2.0	0.090	0.7	0.4	553.2	3.7	555.7	8.4	566.0	40.1	553.2	3.7
111	12108	1.3	18.0199	14.9	0.345	15.1	0.045	2.5	0.2	284.2	6.9	300.9	39.4	432.2	333.6	284.2	6.9
177	44019	3.5	13.9619	1.8	1.588	2.6	0.161	1.9	0.7	961.4	16.9	965.6	16.4	975.3	37.3	975.3	37.3
212	32895	1.0	14.2386	2.3	1.311	4.1	0.135	3.4	0.8	818.3	26.4	850.4	23.8	935.1	47.2	818.3	26.4
228	24216	1.4	16.9442	2.4	0.784	3.0	0.096	1.8	0.6	593.0	10.3	587.8	13.4	567.8	52.3	593.0	10.3
636	68772	51.8	20.0647	3.6	0.289	5.0	0.042	3.5	0.7	265.6	9.0	257.8	11.3	187.5	82.9	265.6	9.0
221	1608	1.3	14.3398	63.1	0.029	63.2	0.003	4.8	0.1	19.4	0.9	28.9	18.1	920.6	1456.3	19.4	0.9
239	48741	1.8	13.2065	1.6	1.905	1.9	0.182	0.9	0.5	1080.5	9.3	1082.9	12.4	1087.7	32.3	1087.7	32.3
140	121935	3.5	5.0443	1.6	12.237	1.7	0.448	0.7	0.4	2385.0	13.6	2622.7	15.9	2811.8	25.3	2811.8	25.3
151	24999	0.4	16.3701	3.7	0.808	3.8	0.096	0.9	0.2	590.2	5.2	601.1	17.2	642.3	79.2	590.2	5.2
674	168963	17.8	5.3450	7.8	12.077	7.8	0.468	0.6	0.1	2475.5	11.5	2610.4	73.3	2716.7	128.5	2716.7	128.5
408	66915	3.1	13.6233	1.4	1.569	3.4	0.155	3.1	0.9	929.1	26.9	958.1	21.2	1025.1	28.9	1025.1	28.9
425	44454	12.9	15.0150	1.8	1.047	2.8	0.114	2.1	0.8	695.9	13.9	727.3	14.5	825.3	38.5	695.9	13.9
763	151605	22.1	4.4941	1.7	16.444	1.9	0.536	0.9	0.5	2766.6	19.8	2903.0	18.4	2998.9	27.5	2998.9	27.5

Appendix A Cont.: U-Pb detrital zircon geochronologic analyses by Laser-Ablation Multicollector ICP Mass Spectrometry

			Isotope ratios							Apparent ages (Ma)							
U (ppm)	206Pb 204Pb	U/Th	206Pb* 207Pb*	± (%)	207Pb* 235U*	± (%)	206Pb* 238U	± (%)	error corr.	206Pb* 238U*	± (Ma)	207Pb* 235U	± (Ma)	206Pb* 207Pb*	± (Ma)	**Best age (Ma)**	± (Ma)
MH (SAL 1691) Cont.																	
644	278994	16.7	4.6872	1.7	16.277	2.0	0.553	1.1	0.6	2839.0	25.3	2893.2	19.1	2931.1	26.8	2931.1	26.8
284	26487	2.2	16.1811	7.4	0.780	7.8	0.092	2.5	0.3	564.5	13.6	585.4	34.9	667.2	159.3	564.5	13.6
176	5454	0.7	18.8211	8.6	0.328	8.6	0.045	0.9	0.1	282.6	2.4	288.3	21.6	334.4	194.6	282.6	2.4
154	8775	1.0	19.4441	9.4	0.275	9.6	0.039	1.6	0.2	245.4	3.9	246.8	21.0	260.1	217.1	245.4	3.9
269	73251	4.1	14.2454	1.6	1.273	4.2	0.131	3.9	0.9	796.3	29.0	833.5	23.7	934.2	31.8	796.3	29.0
149	67137	2.8	13.2211	4.2	1.867	4.3	0.179	1.0	0.2	1061.9	10.1	1069.6	28.7	1085.5	84.5	1085.5	84.5
276	98370	8.1	4.2090	2.0	14.501	2.3	0.443	1.2	0.5	2362.5	23.9	2783.1	22.2	3103.9	31.9	3103.9	31.9
233	49668	1.3	5.6535	2.5	8.518	4.6	0.349	3.9	0.8	1931.1	65.6	2287.9	42.3	2623.8	41.3	2623.8	41.3
267	37908	2.4	17.8725	5.3	0.294	5.5	0.038	1.6	0.3	240.9	3.7	261.5	12.7	450.4	117.4	240.9	3.7
291	74094	0.8	16.2286	2.4	0.857	2.5	0.101	0.8	0.3	619.6	4.9	628.5	11.7	660.9	50.7	619.6	4.9
240	1029	1.1	22.4871	108.8	0.024	108.8	0.004	3.5	0.0	25.0	0.9	24.0	25.8	-84.6	1184.0	25.0	0.9
203	28779	2.7	16.2437	2.7	0.647	3.2	0.076	1.8	0.5	473.5	8.0	506.6	12.8	659.0	57.8	473.5	8.0
188	36693	1.7	16.8064	3.3	0.746	3.7	0.091	1.7	0.5	561.3	9.4	566.1	16.1	585.5	71.4	561.3	9.4
252	118107	2.5	6.6928	2.9	7.087	3.1	0.344	1.1	0.4	1905.9	18.1	2122.4	27.7	2339.2	49.8	2339.2	49.8
234	46398	1.1	16.5959	2.5	0.824	2.6	0.099	0.9	0.3	609.6	5.2	610.2	12.0	612.8	53.2	609.6	5.2
293	21567	1.5	13.3312	3.4	1.297	4.7	0.125	3.2	0.7	761.9	23.0	844.6	26.7	1068.8	68.0	761.9	23.0
495	67188	3.5	14.3298	2.0	1.393	2.1	0.145	0.7	0.3	871.6	5.3	886.0	12.3	922.0	40.7	871.6	5.3
264	153912	1.7	5.4826	1.4	12.349	1.8	0.491	1.2	0.7	2575.1	25.7	2631.3	17.0	2674.8	22.3	2674.8	22.3
384	20256	1.8	18.4730	4.7	0.313	5.0	0.042	1.5	0.3	264.9	3.8	276.6	12.0	376.6	106.4	264.9	3.8
313	1179	1.0	19.4515	41.6	0.026	41.6	0.004	2.2	0.1	23.1	0.5	25.6	10.5	259.2	994.4	23.1	0.5
275	22065	2.9	16.1562	3.8	0.810	4.8	0.095	2.9	0.6	584.8	16.0	602.7	21.6	670.5	81.2	584.8	16.0
102	19017	1.4	14.0129	3.5	1.565	3.9	0.159	1.7	0.4	951.2	14.9	956.3	24.3	967.8	72.3	967.8	72.3
181	8943	2.0	18.7809	5.6	0.320	5.6	0.044	0.6	0.1	275.3	1.7	282.2	13.8	339.3	125.8	275.3	1.7
374	56112	2.2	14.6409	1.8	1.183	2.9	0.126	2.2	0.8	763.0	16.0	792.8	15.9	877.7	37.9	763.0	16.0
352	37722	2.2	17.1297	2.2	0.657	2.3	0.082	0.7	0.3	505.5	3.4	512.5	9.1	544.0	47.1	505.5	3.4
380	8886	1.5	17.9398	5.6	0.292	5.8	0.038	1.5	0.3	240.2	3.5	259.9	13.2	442.1	124.1	240.2	3.5
209	31773	1.7	15.1475	2.6	1.131	3.3	0.124	2.0	0.6	754.9	13.9	768.1	17.7	806.9	55.3	754.9	13.9
109	124665	0.9	16.9138	4.7	0.770	4.7	0.095	0.6	0.1	582.2	3.1	580.0	20.9	571.7	102.1	582.2	3.1
713	15621	2.6	17.5577	4.1	0.443	4.1	0.056	0.5	0.1	353.7	1.7	372.3	12.9	489.8	90.4	353.7	1.7
414	37005	3.9	13.5358	1.4	1.644	4.5	0.161	4.3	1.0	964.3	38.1	987.1	28.2	1038.1	27.9	1038.1	27.9

Appendix A Cont.: U-Pb detrital zircon geochronologic analyses by Laser-Ablation Multicollector ICP Mass Spectrometry

U (ppm)	206Pb/204Pb	U/Th	206Pb*/207Pb*	± (%)	207Pb*/235U*	± (%)	206Pb*/238U	± (%)	error corr.	206Pb*/238U*	± (Ma)	207Pb*/235U	± (Ma)	206Pb*/207Pb*	± (Ma)	**Best age** (Ma)	± (Ma)
					Isotope ratios							**Apparent ages (Ma)**					
KH (SAL 1700)																	
181	18198	5.7	17.2143	3.5	0.675	3.6	0.084	0.6	0.2	521.5	3.0	523.7	14.6	533.2	77.2	521.5	3.0
510	19815	1.5	14.6457	2.4	1.081	5.9	0.115	5.4	0.9	700.7	35.7	744.1	31.1	877.0	50.6	700.7	35.7
323	41193	1.5	16.7599	1.7	0.802	2.0	0.097	1.0	0.5	599.6	5.6	597.9	9.0	591.5	37.7	599.6	5.6
407	38805	8.1	17.3749	1.7	0.679	2.0	0.086	1.1	0.5	528.9	5.4	525.9	8.3	512.8	37.8	528.9	5.4
377	22944	2.3	16.3262	2.7	0.802	5.1	0.095	4.3	0.9	584.6	24.2	597.8	22.9	648.1	57.0	584.6	24.2
308	32202	11.1	17.0458	3.0	0.680	4.2	0.084	3.0	0.7	520.0	15.1	526.5	17.4	554.7	64.8	520.0	15.1
716	35214	4.2	15.9486	1.6	1.005	1.8	0.116	0.9	0.5	708.9	5.8	706.3	9.1	698.1	33.3	708.9	5.8
328	44409	6.2	17.3241	1.9	0.685	2.1	0.086	1.0	0.5	531.9	5.1	529.5	8.7	519.3	40.7	531.9	5.1
304	34941	7.0	17.1966	1.4	0.686	1.5	0.086	0.5	0.3	529.4	2.5	530.5	6.3	535.5	31.5	529.4	2.5
202	19398	4.7	17.5784	4.5	0.679	4.5	0.087	0.5	0.1	535.1	2.6	526.1	18.5	487.2	98.9	535.1	2.6
514	58119	5.9	16.4057	1.8	0.862	1.9	0.103	0.5	0.3	629.6	3.0	631.4	8.8	637.6	38.9	629.6	3.0
257	33651	7.6	17.0617	2.9	0.683	3.3	0.085	1.5	0.5	523.2	7.7	528.8	13.5	552.7	63.4	523.2	7.7
332	31710	1.5	16.5199	2.4	0.712	3.0	0.085	1.7	0.6	527.8	8.8	546.0	12.6	622.7	52.1	527.8	8.8
269	29730	8.2	17.1490	4.3	0.669	7.8	0.083	6.5	0.8	514.9	32.3	519.9	31.9	541.5	94.6	514.9	32.3
193	19284	6.4	16.8019	2.0	0.740	2.4	0.090	1.4	0.6	556.3	7.6	562.2	10.4	586.1	42.3	556.3	7.6
348	34158	4.3	17.3225	2.6	0.659	3.0	0.083	1.5	0.5	512.5	7.3	513.8	12.1	519.4	57.3	512.5	7.3
177	16869	2.1	17.4339	3.1	0.692	3.3	0.088	0.9	0.3	540.9	4.6	534.2	13.5	505.4	68.9	540.9	4.6
258	25467	1.7	17.0777	2.6	0.710	2.7	0.088	0.9	0.3	543.1	4.9	544.5	11.5	550.6	55.9	543.1	4.9
687	64848	3.2	17.3613	3.8	0.671	4.2	0.085	1.8	0.4	523.1	8.9	521.5	17.0	514.5	82.9	523.1	8.9
366	94611	29.4	13.9304	2.3	1.535	2.9	0.155	1.9	0.6	929.6	16.3	944.6	18.1	979.8	46.1	979.8	46.1
147	2364	0.8	14.2110	4.2	0.829	4.3	0.085	1.0	0.2	528.3	5.0	612.9	20.0	939.1	86.7	528.3	5.0
236	20610	7.6	17.1430	2.2	0.687	2.6	0.085	1.3	0.5	528.6	6.8	531.2	10.6	542.3	47.8	528.6	6.8
482	64041	3.8	17.0898	1.8	0.686	2.2	0.085	1.3	0.6	526.3	6.5	530.6	9.2	549.1	39.6	526.3	6.5
272	27417	8.7	17.0431	2.5	0.711	2.5	0.088	0.5	0.2	543.4	2.6	545.6	10.6	555.0	53.9	543.4	2.6
230	27972	3.0	17.0626	3.4	0.720	4.3	0.089	2.7	0.6	550.3	14.2	550.8	18.4	552.5	73.9	550.3	14.2
236	2862	0.5	13.6832	10.8	0.848	10.8	0.084	1.2	0.1	520.6	6.2	623.3	50.5	1016.2	218.7	520.6	6.2
507	48357	3.7	17.0109	1.7	0.701	1.9	0.086	1.0	0.5	534.5	5.0	539.2	8.1	559.2	36.7	534.5	5.0
429	63000	2.0	15.9959	2.1	0.868	2.9	0.101	2.1	0.7	618.7	12.1	634.6	13.9	691.8	44.8	618.7	12.1
125	21324	1.6	17.0105	3.0	0.691	3.3	0.085	1.4	0.4	527.3	7.2	533.3	13.6	559.2	64.5	527.3	7.2
119	16434	4.4	17.9078	5.2	0.669	5.3	0.087	1.0	0.2	536.8	5.4	519.8	21.8	446.1	116.7	536.8	5.4
357	50529	5.2	17.1240	1.7	0.684	2.2	0.085	1.4	0.6	525.3	7.2	529.0	9.1	544.7	36.6	525.3	7.2
493	20103	2.5	14.3183	24.9	0.872	24.9	0.091	0.5	0.0	559.1	2.7	636.9	118.3	923.7	519.0	559.1	2.7
153	27315	2.2	17.4676	2.8	0.694	3.1	0.088	1.2	0.4	543.1	6.1	535.1	12.8	501.2	62.7	543.1	6.1

Appendix A Cont.: U-Pb detrital zircon geochronologic analyses by Laser-Ablation Multicollector ICP Mass Spectrometry

U (ppm)	206Pb/204Pb	U/Th	206Pb*/207Pb*	± (%)	207Pb*/235U*	± (%)	206Pb*/238U	± (%)	error corr.	206Pb*/238U*	± (Ma)	207Pb*/235U	± (Ma)	206Pb*/207Pb*	± (Ma)	**Best age** (Ma)	± (Ma)
					Isotope ratios					**Apparent ages (Ma)**							
KH (SAL 1700) Cont.																	
252	66318	6.9	13.6342	1.5	1.666	1.8	0.165	0.9	0.5	983.1	8.6	995.7	11.5	1023.5	31.2	1023.5	31.2
168	29175	2.5	17.4416	3.2	0.680	3.3	0.086	0.8	0.2	532.3	4.1	527.0	13.6	504.4	70.8	532.3	4.1
170	34950	6.3	17.2405	2.4	0.689	3.6	0.086	2.7	0.8	532.4	13.7	531.9	14.8	529.9	51.6	532.4	13.7
115	16296	5.2	17.1344	4.7	0.689	4.7	0.086	0.5	0.1	529.7	2.5	532.3	19.6	543.4	102.9	529.7	2.5
387	37797	8.2	16.7457	4.4	0.720	4.5	0.087	0.8	0.2	540.1	3.9	550.4	19.1	593.3	96.3	540.1	3.9
733	10587	1.9	16.1918	1.7	0.854	2.3	0.100	1.5	0.7	616.3	8.9	627.0	10.8	665.8	37.4	616.3	8.9
272	34794	4.1	16.6113	4.5	0.720	5.3	0.087	2.7	0.5	536.2	14.1	550.6	22.4	610.8	97.6	536.2	14.1
251	61293	3.2	13.9808	1.2	1.418	3.6	0.144	3.5	0.9	866.1	28.0	896.6	21.7	972.5	24.1	972.5	24.1
211	30927	3.1	16.9925	4.1	0.716	4.5	0.088	2.0	0.4	545.5	10.6	548.6	19.2	561.5	88.6	545.5	10.6
225	26325	3.0	17.3387	2.3	0.687	2.4	0.086	0.7	0.3	534.5	3.4	531.2	9.9	517.4	50.4	534.5	3.4
208	32763	3.8	17.0725	3.1	0.702	3.7	0.087	2.0	0.5	537.3	10.2	540.0	15.4	551.3	67.5	537.3	10.2
279	25815	1.8	17.1376	2.1	0.679	2.4	0.084	1.2	0.5	522.1	5.9	526.0	9.7	542.9	45.0	522.1	5.9
233	28599	7.6	16.0525	6.7	0.749	6.9	0.087	1.3	0.2	539.1	6.5	567.7	29.8	684.3	143.9	539.1	6.5
367	71370	2.7	9.4412	1.9	3.449	4.4	0.236	3.9	0.9	1366.7	48.4	1515.6	34.3	1730.3	34.5	1730.3	34.5
358	33285	8.8	17.2360	1.9	0.692	2.8	0.086	2.1	0.8	534.8	11.0	534.0	11.8	530.5	41.1	534.8	11.0
294	42219	5.0	16.7119	2.5	0.711	2.7	0.086	1.2	0.4	532.9	5.9	545.4	11.4	597.7	53.1	532.9	5.9
544	20256	1.6	16.7753	3.3	0.704	3.7	0.086	1.6	0.4	529.6	8.1	541.0	15.4	589.5	71.7	529.6	8.1
207	39825	3.9	14.0888	2.1	1.222	3.6	0.125	2.9	0.8	758.3	20.9	810.5	20.2	956.8	43.4	956.8	43.4
481	98292	3.0	15.5566	3.3	0.924	6.8	0.104	6.0	0.9	639.5	36.6	664.6	33.4	750.9	68.9	639.5	36.6
165	48726	1.7	13.1432	1.0	1.914	1.1	0.182	0.5	0.4	1080.2	5.0	1085.9	7.6	1097.3	20.6	1097.3	20.6
240	26100	1.7	17.1446	1.6	0.690	2.0	0.086	1.2	0.6	531.0	6.1	533.1	8.2	542.1	34.5	531.0	6.1
366	42141	7.1	17.3101	1.2	0.698	1.9	0.088	1.4	0.8	541.5	7.3	537.6	7.7	521.0	26.4	541.5	7.3
395	53349	1.5	17.0778	1.9	0.693	2.0	0.086	0.6	0.3	531.1	3.2	534.8	8.4	550.6	41.7	531.1	3.2
175	25986	1.4	17.7410	4.9	0.655	4.9	0.084	0.8	0.2	521.5	4.2	511.5	19.9	466.8	108.0	521.5	4.2
332	44043	1.7	17.5982	2.0	0.661	2.3	0.084	1.1	0.5	522.3	5.4	515.4	9.2	484.7	44.2	522.3	5.4
382	54186	6.5	17.5394	1.5	0.667	1.8	0.085	1.0	0.6	525.2	5.1	519.1	7.5	492.1	33.8	525.2	5.1
765	57894	4.7	16.1707	2.2	0.922	2.7	0.108	1.7	0.6	661.6	10.7	663.2	13.4	668.6	46.3	661.6	10.7
157	23781	2.4	14.1414	2.2	1.533	2.4	0.157	1.1	0.4	941.5	9.3	943.8	14.9	949.2	44.8	949.2	44.8
304	29775	10.8	17.1441	1.3	0.698	1.6	0.087	0.9	0.6	536.9	4.6	537.9	6.6	542.2	28.7	536.9	4.6
226	24042	7.2	17.4447	2.0	0.668	3.0	0.085	2.2	0.7	523.0	10.8	519.5	12.0	504.0	44.7	523.0	10.8
74	12102	4.5	16.4912	2.5	0.897	3.0	0.107	1.6	0.5	657.2	10.1	650.3	14.4	626.4	54.5	657.2	10.1
374	45372	9.1	16.9471	2.2	0.670	5.4	0.082	4.9	0.9	509.9	24.2	520.5	22.0	567.4	48.4	509.9	24.2
307	52743	9.5	17.3181	1.7	0.680	2.7	0.085	2.2	0.8	528.0	11.0	526.5	11.3	520.0	37.1	528.0	11.0

Appendix A Cont.: U-Pb detrital zircon geochronologic analyses by Laser-Ablation Multicollector ICP Mass Spectrometry

U (ppm)	206Pb 204Pb	U/Th	206Pb* 207Pb*	± (%)	**Isotope ratios** 207Pb* 235U*	± (%)	206Pb* 238U	± (%)	error corr.	**Apparent ages (Ma)** 206Pb* 238U*	± (Ma)	207Pb* 235U	± (Ma)	206Pb* 207Pb*	± (Ma)	**Best age** (Ma)	± (Ma)
KH (SAL 1700) Cont.																	
420	39447	1.8	17.4484	1.8	0.678	1.9	0.086	0.7	0.3	530.6	3.3	525.5	7.8	503.6	39.2	530.6	3.3
305	96498	3.1	13.5824	1.4	1.809	2.2	0.178	1.7	0.8	1057.0	16.4	1048.6	14.1	1031.2	27.3	1031.2	27.3
233	20397	3.7	17.0001	3.1	0.694	3.6	0.086	1.9	0.5	529.1	9.5	535.0	15.1	560.6	67.9	529.1	9.5
287	44859	2.2	14.6803	3.6	1.051	7.6	0.112	6.6	0.9	683.6	43.1	729.2	39.4	872.1	75.0	683.6	43.1
486	55617	1.9	17.3087	1.6	0.651	1.9	0.082	1.0	0.5	506.7	4.8	509.4	7.4	521.2	34.5	506.7	4.8
185	22104	1.1	17.4119	1.7	0.637	1.9	0.081	0.9	0.5	499.1	4.4	500.7	7.5	508.2	36.7	499.1	4.4
137	35592	1.6	13.4265	1.9	1.832	2.9	0.178	2.2	0.8	1058.2	21.5	1057.0	19.1	1054.5	38.5	1054.5	38.5
295	86397	5.2	13.7637	4.0	1.573	7.9	0.157	6.8	0.9	940.3	59.3	959.7	49.0	1004.3	81.6	1004.3	81.6
227	16704	2.2	17.6409	3.1	0.655	3.6	0.084	1.9	0.5	518.6	9.6	511.4	14.5	479.3	67.7	518.6	9.6
269	45066	3.5	16.6066	2.6	0.740	3.6	0.089	2.5	0.7	550.1	13.2	562.1	15.7	611.4	56.9	550.1	13.2
247	103968	1.4	13.9998	1.6	1.576	2.2	0.160	1.5	0.7	957.0	13.4	960.9	13.4	969.7	31.6	969.7	31.6
215	42387	3.6	16.6729	1.2	0.837	2.0	0.101	1.6	0.8	621.8	9.2	617.7	9.0	602.7	25.7	621.8	9.2
222	21717	1.7	17.2266	3.2	0.694	3.6	0.087	1.7	0.5	536.3	8.8	535.4	15.2	531.7	70.6	536.3	8.8
50	6321	1.2	17.7868	16.2	0.605	16.4	0.078	2.8	0.2	484.4	12.9	480.3	62.9	461.1	360.8	484.4	12.9
493	50940	12.4	17.1448	2.0	0.712	2.4	0.089	1.2	0.5	546.9	6.4	546.0	10.0	542.0	44.0	546.9	6.4
434	36896	1.7	17.0022	1.6	0.689	1.8	0.085	0.7	0.4	525.4	3.7	532.0	7.4	560.3	35.2	525.4	3.7
276	55878	3.3	14.0400	1.9	1.247	8.8	0.127	8.7	1.0	770.5	62.8	821.9	49.9	963.9	37.8	770.5	62.8
234	23626	3.6	15.8200	7.3	0.731	10.4	0.084	7.4	0.7	519.3	36.7	557.2	44.6	715.4	156.2	519.3	36.7
513	15562	1.4	16.9734	3.1	0.712	3.3	0.088	1.0	0.3	541.4	5.2	545.8	13.7	564.0	67.5	541.4	5.2
236	20358	2.1	17.0440	3.5	0.704	3.7	0.087	1.3	0.4	537.9	6.8	541.1	15.6	554.9	76.0	537.9	6.8
284	87588	7.4	8.3754	1.2	4.899	2.4	0.298	2.1	0.9	1679.3	30.6	1802.0	20.2	1947.2	21.6	1947.2	21.6
335	22106	3.5	16.7250	3.7	0.692	3.9	0.084	1.4	0.3	519.4	6.8	533.8	16.4	596.0	80.3	519.4	6.8
233	49824	4.6	13.2189	3.4	1.566	4.5	0.150	2.9	0.7	901.8	24.6	956.9	27.7	1085.8	68.0	1085.8	68.0
457	11788	4.4	17.1237	3.8	0.690	3.9	0.086	0.7	0.2	529.8	3.6	532.7	16.2	544.8	84.1	529.8	3.6
238	131858	2.3	16.3208	1.6	0.794	2.1	0.094	1.4	0.6	578.9	7.6	593.3	9.6	648.8	35.1	578.9	7.6
242	20196	4.0	17.6914	3.5	0.671	3.5	0.086	0.8	0.2	532.1	4.1	521.1	14.5	473.1	76.5	532.1	4.1
349	11736	1.6	16.9884	3.3	0.693	3.5	0.085	1.1	0.3	528.3	5.4	534.7	14.5	562.0	72.5	528.3	5.4
279	1100	4.4	11.3730	10.0	1.005	10.1	0.083	1.5	0.1	513.2	7.3	706.2	51.5	1380.9	192.9	1380.9	192.9
403	43810	8.9	15.4377	1.5	1.030	1.8	0.115	1.0	0.6	703.6	6.9	718.9	9.3	767.1	30.9	703.6	6.9
157	48650	1.7	17.5753	5.3	0.659	5.4	0.084	0.9	0.2	520.2	4.4	514.2	21.7	487.6	117.2	520.2	4.4
592	39022	1.6	17.2560	1.7	0.641	2.8	0.080	2.2	0.8	497.3	10.7	502.8	11.2	527.9	37.3	497.3	10.7
300	24696	6.2	17.5169	2.1	0.649	2.3	0.082	1.0	0.4	510.9	4.7	508.0	9.2	494.9	46.4	510.9	4.7
317	64304	2.0	13.0617	1.3	1.987	2.0	0.188	1.5	0.7	1111.6	15.3	1111.0	13.6	1109.7	26.8	1109.7	26.8

Appendix A Cont.: U-Pb detrital zircon geochronologic analyses by Laser-Ablation Multicollector ICP Mass Spectrometry

U (ppm)	206Pb 204Pb	U/Th	206Pb* 207Pb*	± (%)	207Pb* 235U*	± (%)	206Pb* 238U	± (%)	error corr.	206Pb* 238U*	± (Ma)	207Pb* 235U	± (Ma)	206Pb* 207Pb*	± (Ma)	**Best age** (Ma)	± (Ma)
					Isotope ratios					**Apparent ages (Ma)**							
KH (SAL 1700) Cont.																	
477	41256	2.4	17.5451	1.2	0.623	2.3	0.079	1.9	0.8	491.7	9.1	491.6	8.8	491.4	26.4	491.7	9.1
1089	14720	2.7	16.6396	1.2	0.698	1.7	0.084	1.2	0.7	521.7	5.9	537.9	6.9	607.1	25.0	521.7	5.9
506	37058	9.4	16.4852	3.0	0.754	3.0	0.090	0.6	0.2	556.5	3.3	570.6	13.3	627.2	64.3	556.5	3.3
446	20994	1.5	17.5605	3.0	0.695	3.2	0.089	1.1	0.3	546.7	5.8	535.8	13.5	489.4	67.1	546.7	5.8
557	55316	13.1	17.2351	2.2	0.714	3.0	0.089	2.0	0.7	551.3	10.6	547.3	12.7	530.6	48.7	551.3	10.6
821	68254	4.1	14.1020	1.6	1.224	4.5	0.125	4.2	0.9	760.6	30.1	811.8	25.2	954.9	33.2	760.6	30.1
1490	6766	1.3	16.2881	3.0	0.633	3.5	0.075	1.8	0.5	464.8	8.1	497.9	13.8	653.1	64.8	464.8	8.1
DN (SAL 1694)																	
11	5160	1.6	14.9157	26.7	1.092	27.3	0.118	5.3	0.2	719.8	36.0	749.4	145.5	839.1	566.5	719.8	36.0
1057	64875	3.1	18.6801	3.0	0.425	3.1	0.058	0.5	0.2	360.6	1.8	359.4	9.2	351.4	68.1	360.6	1.8
380	35570	1.7	16.9526	3.3	0.779	3.4	0.096	0.8	0.2	589.3	4.6	584.7	14.9	566.6	70.8	589.3	4.6
620	176975	2.6	5.3580	2.4	11.076	4.0	0.430	3.2	0.8	2307.6	61.5	2529.5	36.9	2712.7	39.3	2712.7	39.3
163	49870	2.2	12.5044	3.1	2.207	3.7	0.200	2.0	0.5	1176.1	21.9	1183.3	26.0	1196.3	61.4	1196.3	61.4
146	9300	1.7	18.3882	8.9	0.440	9.0	0.059	1.5	0.2	367.4	5.2	370.1	27.9	386.9	199.3	367.4	5.2
202	19580	0.6	16.3472	3.1	0.816	3.4	0.097	1.4	0.4	595.3	8.2	605.8	15.7	645.3	66.9	595.3	8.2
264	30850	2.0	17.5033	4.1	0.667	4.4	0.085	1.4	0.3	524.2	7.0	519.1	17.8	496.6	91.3	524.2	7.0
727	99710	10.0	16.2607	2.3	0.936	2.3	0.110	0.5	0.2	675.0	3.2	670.8	11.4	656.7	48.7	675.0	3.2
215	35160	2.3	16.9257	5.2	0.820	5.4	0.101	1.5	0.3	618.4	9.0	608.1	24.7	570.1	112.8	618.4	9.0
198	15720	1.6	18.8505	17.2	0.312	17.3	0.043	1.6	0.1	269.0	4.2	275.5	41.7	330.9	393.0	269.0	4.2
293	25680	2.9	19.4612	6.7	0.289	6.7	0.041	0.6	0.1	257.8	1.5	257.8	15.2	258.1	153.2	257.8	1.5
205	60365	3.3	16.1499	3.8	0.960	3.9	0.112	0.9	0.2	687.0	6.0	683.3	19.6	671.3	82.0	687.0	6.0
203	83975	2.3	12.5227	4.2	2.272	4.3	0.206	1.0	0.2	1209.6	11.2	1203.8	30.6	1193.4	83.1	1193.4	83.1
154	29385	1.6	19.5361	3.8	0.263	4.1	0.037	1.7	0.4	235.9	4.0	237.2	8.8	249.3	86.8	235.9	4.0
173	79795	1.4	13.4107	4.8	1.855	6.1	0.180	3.8	0.6	1069.5	37.6	1065.3	40.5	1056.8	96.9	1056.8	96.9
87	9560	0.9	22.7639	24.3	0.264	24.3	0.044	1.0	0.0	275.1	2.7	237.9	51.6	-114.6	606.0	275.1	2.7
120	10220	1.2	20.3173	11.4	0.273	11.5	0.040	1.5	0.1	254.5	3.8	245.4	25.2	158.3	268.6	254.5	3.8
130	59785	2.2	17.0443	6.3	0.649	6.4	0.080	0.9	0.1	497.8	4.5	508.2	25.4	554.9	137.5	497.8	4.5
572	62660	2.8	17.5908	5.2	0.648	5.2	0.083	0.6	0.1	511.7	2.8	507.0	20.8	485.6	114.2	511.7	2.8
166	23300	3.2	17.6305	3.7	0.668	3.8	0.085	0.9	0.2	528.6	4.6	519.7	15.3	480.6	80.7	528.6	4.6
296	45010	2.1	17.6686	4.2	0.679	4.3	0.087	0.9	0.2	537.9	4.5	526.2	17.5	475.9	92.1	537.9	4.5
246	107895	2.1	4.3227	3.4	16.419	3.8	0.515	1.6	0.4	2676.9	35.1	2901.5	36.0	3061.3	54.4	3061.3	54.4
37	1660	0.8	26.3482	164.3	0.205	164.4	0.039	4.9	0.0	248.2	11.9	189.7	292.3	-488.5	2226.7	248.2	11.9
513	51115	3.9	16.8512	3.6	0.774	4.4	0.095	2.6	0.6	582.9	14.6	582.2	19.6	579.7	77.6	582.9	14.6

Appendix A Cont.: U-Pb detrital zircon geochronologic analyses by Laser-Ablation Multicollector ICP Mass Spectrometry

U (ppm)	206Pb/204Pb	U/Th	206Pb*/207Pb*	± (%)	**Isotope ratios** 207Pb*/235U*	± (%)	206Pb*/238U	± (%)	error corr.	**Apparent ages (Ma)** 206Pb*/238U*	± (Ma)	207Pb*/235U	± (Ma)	206Pb*/207Pb*	± (Ma)	**Best age** (Ma)	± (Ma)
DN (SAL 1694) Cont.																	
550	64255	16.3	16.6229	3.6	0.803	4.0	0.097	1.6	0.4	595.7	9.2	598.5	17.9	609.2	78.3	595.7	9.2
382	59100	2.8	16.3417	4.2	0.941	4.3	0.111	0.5	0.1	681.3	3.2	673.2	21.0	646.0	90.9	681.3	3.2
243	15860	1.2	20.1225	5.8	0.262	6.5	0.038	2.8	0.4	241.7	6.7	236.1	13.6	180.8	135.5	241.7	6.7
2273	42805	11.9	15.8121	5.7	0.774	5.8	0.089	0.9	0.2	548.0	4.8	581.9	25.7	716.4	121.8	548.0	4.8
275	11765	0.7	19.4003	6.8	0.303	6.8	0.043	0.5	0.1	269.4	1.3	269.0	16.0	265.3	155.2	269.4	1.3
47	92490	2.5	5.4070	2.5	12.454	2.7	0.488	1.0	0.4	2563.6	21.6	2639.2	25.0	2697.7	40.6	2697.7	40.6
115	82450	1.0	13.2278	5.1	1.687	5.3	0.162	1.4	0.3	967.1	12.1	1003.6	33.9	1084.4	103.1	967.1	12.1
25	60295	2.0	5.3264	4.3	13.976	4.3	0.540	0.5	0.1	2783.0	11.3	2748.1	40.8	2722.5	70.4	2722.5	70.4
303	44060	2.6	17.3827	3.0	0.646	3.2	0.081	0.8	0.3	504.5	4.0	505.8	12.6	511.8	66.9	504.5	4.0
164	18580	1.4	17.0889	3.9	0.734	4.1	0.091	1.3	0.3	561.6	7.0	559.1	17.5	549.2	84.1	561.6	7.0
248	35075	1.9	17.0669	6.0	0.628	8.4	0.078	5.9	0.7	482.9	27.2	495.1	32.9	552.0	131.1	482.9	27.2
151	17140	3.0	17.1420	4.5	0.624	6.1	0.078	4.1	0.7	481.5	19.0	492.2	23.7	542.4	98.3	481.5	19.0
438	28765	0.8	20.0716	8.4	0.264	8.4	0.038	0.7	0.1	242.7	1.8	237.5	17.8	186.7	194.7	242.7	1.8
613	108125	4.0	14.5719	3.2	1.296	3.8	0.137	2.1	0.5	827.7	16.2	844.1	21.7	887.5	65.3	827.7	16.2
89	24625	2.0	12.3957	4.7	2.275	4.7	0.205	0.6	0.1	1199.5	6.5	1204.5	33.1	1213.5	91.6	1213.5	91.6
150	151495	1.3	4.3175	2.9	19.483	3.3	0.610	1.6	0.5	3070.3	39.8	3066.0	32.1	3063.2	46.4	3063.2	46.4
80	7265	0.9	23.8113	71.8	0.227	71.8	0.039	1.4	0.0	247.9	3.4	207.7	135.7	-226.8	2086.1	247.9	3.4
81	36730	5.9	16.1111	4.5	0.886	4.6	0.103	1.0	0.2	634.8	6.2	644.0	22.0	676.5	96.1	634.8	6.2
34	6775	1.1	15.6928	16.5	0.703	17.1	0.080	4.4	0.3	496.3	21.1	540.7	71.9	732.4	352.7	496.3	21.1
179	39800	1.1	20.8955	9.9	0.265	10.0	0.040	0.8	0.1	253.9	2.0	238.8	21.2	92.2	236.1	253.9	2.0
37	9680	0.5	17.4713	28.8	0.733	28.9	0.093	1.5	0.1	572.9	7.9	558.6	124.6	500.6	647.1	572.9	7.9
503	26030	1.9	16.4335	6.1	0.739	6.2	0.088	1.0	0.2	544.1	5.4	561.7	26.6	634.0	131.1	544.1	5.4
343	52295	6.4	15.2934	3.7	1.007	3.8	0.112	0.7	0.2	682.8	4.8	707.5	19.2	786.8	77.5	682.8	4.8
123	5455	1.0	18.1888	12.2	0.305	12.6	0.040	3.3	0.3	254.2	8.2	270.2	29.9	411.3	273.2	254.2	8.2
152	41555	92.2	16.3820	4.0	0.775	4.2	0.092	1.4	0.3	568.0	7.7	582.8	18.8	640.7	85.8	568.0	7.7
24	29290	0.9	12.1507	31.4	0.919	31.8	0.081	5.1	0.2	501.8	24.8	661.6	155.8	1252.6	629.8	501.8	24.8
BG (SAL 1654)																	
155	44875	2.3	16.8145	2.7	0.751	3.1	0.092	1.6	0.5	565.0	8.6	568.9	13.7	584.4	58.7	565.0	8.6
103	50715	2.1	17.1430	6.6	0.690	6.7	0.086	1.1	0.2	530.3	5.8	532.6	27.7	542.3	144.0	530.3	5.8
454	212485	5.1	18.1318	2.5	0.462	2.5	0.061	0.5	0.2	380.4	1.8	385.8	8.1	418.4	55.4	380.4	1.8
705	21470	2.4	14.8885	10.2	0.714	12.3	0.077	6.8	0.6	479.1	31.3	547.4	52.0	842.9	213.6	479.1	31.3
1025	5185	1.5	13.3152	17.5	0.609	18.9	0.059	7.1	0.4	368.6	25.5	483.1	72.7	1071.2	354.1	368.6	25.5
236	39695	2.0	13.8721	2.9	1.582	4.3	0.159	3.1	0.7	952.0	27.3	963.0	26.5	988.4	59.4	952.0	27.3

Appendix A Cont.: U-Pb detrital zircon geochronologic analyses by Laser-Ablation Multicollector ICP Mass Spectrometry

			Isotope ratios							Apparent ages (Ma)							
U (ppm)	206Pb 204Pb	U/Th	206Pb* 207Pb*	± (%)	207Pb* 235U*	± (%)	206Pb* 238U	± (%)	error corr.	206Pb* 238U*	± (Ma)	207Pb* 235U	± (Ma)	206Pb* 207Pb*	± (Ma)	**Best age (Ma)**	± (Ma)
BG (SAL 1654) Cont.																	
398	92505	2.0	18.1336	5.5	0.431	6.0	0.057	2.3	0.4	355.4	7.9	363.9	18.2	418.1	122.9	355.4	7.9
36	25720	1.6	11.2919	6.3	2.771	6.9	0.227	2.9	0.4	1318.4	34.8	1347.8	51.6	1394.6	120.2	1394.6	120.2
60	74570	1.2	12.2668	4.0	2.119	4.1	0.189	1.0	0.2	1113.3	10.2	1154.9	28.5	1234.0	78.5	1234.0	78.5
74	39135	1.7	20.5366	21.3	0.262	21.4	0.039	2.6	0.1	246.5	6.4	236.0	45.2	133.1	505.3	246.5	6.4
42	14350	1.7	17.8543	31.2	0.457	31.2	0.059	0.5	0.0	370.6	1.9	382.2	99.6	452.7	707.9	370.6	1.9
23	13455	1.3	16.2005	35.7	0.823	35.7	0.097	0.9	0.0	595.1	5.1	609.8	165.1	664.6	788.3	595.1	5.1
316	119715	3.2	14.0889	3.1	1.458	3.5	0.149	1.7	0.5	895.4	14.3	913.3	21.4	956.8	63.6	895.4	14.3
93	46445	3.1	16.2730	6.2	0.805	6.3	0.095	1.2	0.2	585.2	6.7	599.7	28.6	655.1	133.2	585.2	6.7
169	54290	5.8	13.4842	2.1	1.708	2.2	0.167	0.5	0.2	996.0	4.6	1011.7	14.0	1045.8	43.0	996.0	4.6
343	59475	10.6	16.4038	2.2	0.775	5.1	0.092	4.6	0.9	568.3	24.8	582.4	22.4	637.9	46.9	568.3	24.8
168	183835	2.7	16.2906	2.6	0.829	2.7	0.098	0.5	0.2	602.3	2.9	613.0	12.3	652.7	56.3	602.3	2.9
141	33963	2.1	12.0725	1.4	2.474	3.0	0.217	2.7	0.9	1264.0	30.4	1264.5	21.8	1265.3	27.9	1265.3	27.9
215	17740	2.9	16.8553	1.9	0.747	2.6	0.091	1.8	0.7	563.4	9.7	566.6	11.3	579.2	40.9	563.4	9.7
443	51535	2.2	13.5831	1.9	1.747	2.2	0.172	1.2	0.5	1023.5	11.2	1025.9	14.2	1031.1	37.4	1031.1	37.4
54	7958	0.9	16.6627	15.7	0.799	15.7	0.097	1.3	0.1	594.2	7.2	596.2	71.1	604.1	341.3	594.2	7.2
101	21090	1.5	14.1396	2.9	1.403	3.8	0.144	2.5	0.7	866.5	20.5	890.2	22.8	949.4	59.1	949.4	59.1
286	32150	1.5	13.5626	2.4	1.689	2.7	0.166	1.1	0.4	991.0	10.5	1004.5	16.9	1034.1	48.4	1034.1	48.4
378	40998	1.6	14.7577	2.2	1.152	4.7	0.123	4.2	0.9	749.6	29.4	778.2	25.5	861.2	45.3	749.6	29.4
295	37145	1.8	13.3079	1.5	1.729	3.2	0.167	2.8	0.9	994.8	26.2	1019.3	20.7	1072.4	30.4	1072.4	30.4
332	24650	1.8	17.3237	1.6	0.709	2.3	0.089	1.7	0.7	549.9	8.9	544.0	9.8	519.3	35.4	549.9	8.9
468	20258	1.3	19.8476	3.4	0.285	3.5	0.041	0.9	0.2	258.9	2.2	254.4	8.0	212.7	79.8	258.9	2.2
390	47248	2.4	14.3399	2.4	1.441	3.4	0.150	2.5	0.7	900.0	21.1	906.0	20.6	920.6	48.3	920.6	48.3
294	31568	4.7	16.4969	1.7	0.785	2.5	0.094	1.8	0.7	578.6	10.2	588.3	11.1	625.7	36.3	578.6	10.2
1317	495	4.1	8.3172	10.4	1.305	10.7	0.079	2.4	0.2	488.6	11.4	848.1	61.6	1959.7	186.7	1959.7	186.7
627	188408	5.5	4.6580	1.1	16.425	2.8	0.555	2.6	0.9	2845.5	60.0	2901.9	27.2	2941.2	18.3	2941.2	18.3
118	12783	0.9	14.3266	2.5	1.477	3.0	0.153	1.6	0.5	920.3	14.0	921.0	18.2	922.5	52.0	922.5	52.0
222	41660	2.9	13.3647	2.0	1.695	2.4	0.164	1.3	0.6	980.6	12.2	1006.6	15.2	1063.8	39.5	1063.8	39.5
70	7520	4.1	17.4565	6.0	0.750	6.3	0.095	1.7	0.3	585.0	9.2	568.4	27.2	502.5	133.0	585.0	9.2
421	83610	7.4	12.8101	1.3	1.878	1.5	0.175	0.7	0.5	1036.9	6.7	1073.4	10.0	1148.5	26.4	1148.5	26.4
637	42118	5.5	16.4396	1.0	0.895	1.5	0.107	1.1	0.7	653.5	6.8	648.9	7.2	633.2	22.0	653.5	6.8
299	3343	0.2	16.5153	2.9	0.789	3.8	0.095	2.6	0.7	582.1	14.2	590.6	17.2	623.3	61.7	582.1	14.2
125	11260	1.7	13.0696	1.6	1.958	2.2	0.186	1.5	0.7	1097.3	15.3	1101.1	14.8	1108.5	31.9	1108.5	31.9
134	62395	1.3	4.3567	1.5	16.397	2.3	0.518	1.7	0.7	2691.1	37.4	2900.2	21.9	3048.8	24.5	3048.8	24.5

Appendix A Cont.: U-Pb detrital zircon geochronologic analyses by Laser-Ablation Multicollector ICP Mass Spectrometry

					Isotope ratios							**Apparent ages (Ma)**					
U (ppm)	206Pb 204Pb	U/Th	206Pb* 207Pb*	± (%)	207Pb* 235U*	± (%)	206Pb* 238U	± (%)	error corr.	206Pb* 238U*	± (Ma)	207Pb* 235U	± (Ma)	206Pb* 207Pb*	± (Ma)	**Best age** (Ma)	± (Ma)
BG (SAL 1654) Cont.																	
50	11290	1.7	12.8190	2.4	2.127	3.7	0.198	2.8	0.8	1163.1	29.8	1157.5	25.6	1147.1	48.1	1147.1	48.1
216	8160	1.4	19.7868	9.3	0.272	9.5	0.039	1.8	0.2	246.7	4.3	244.2	20.6	219.9	216.1	246.7	4.3
69	15645	0.6	12.4951	3.5	2.240	3.9	0.203	1.9	0.5	1191.5	20.5	1193.7	27.7	1197.8	68.3	1197.8	68.3
161	18785	4.4	17.0835	4.2	0.709	4.5	0.088	1.6	0.3	543.1	8.2	544.4	19.0	549.9	92.4	543.1	8.2
343	42870	1.2	12.5710	1.1	2.052	3.5	0.187	3.3	0.9	1105.4	33.8	1132.8	24.0	1185.8	22.4	1185.8	22.4
934	223723	1.3	4.5675	2.1	17.018	2.4	0.564	1.2	0.5	2882.0	27.7	2935.8	22.7	2972.9	33.0	2972.9	33.0
788	14683	2.8	11.6156	1.8	2.761	2.9	0.233	2.2	0.8	1348.2	27.1	1345.1	21.5	1340.2	35.2	1340.2	35.2
333	120970	2.0	6.3860	1.3	9.023	2.4	0.418	2.0	0.8	2251.0	37.8	2340.3	21.9	2419.2	22.7	2419.2	22.7
268	10328	1.3	20.4316	4.9	0.259	5.0	0.038	0.7	0.1	242.5	1.5	233.6	10.4	145.1	115.9	242.5	1.5
207	20835	5.6	12.5833	5.6	2.079	6.0	0.190	2.3	0.4	1120.1	23.2	1142.0	41.2	1183.9	110.0	1183.9	110.0
48	4643	2.7	17.8956	7.2	0.705	7.2	0.092	0.8	0.1	564.5	4.3	541.9	30.4	447.6	159.8	564.5	4.3
312	26265	3.1	17.0486	2.5	0.666	3.8	0.082	2.8	0.7	510.4	13.8	518.5	15.3	554.3	54.4	510.4	13.8
186	23103	0.8	17.2842	2.8	0.749	3.8	0.094	2.5	0.7	578.6	13.8	567.7	16.4	524.3	62.0	578.6	13.8
115	9720	2.3	17.2793	4.0	0.759	4.8	0.095	2.6	0.5	585.8	14.4	573.5	20.8	524.9	87.7	585.8	14.4
188	36695	2.3	13.6706	1.6	1.635	2.5	0.162	1.9	0.8	968.2	17.3	983.6	15.6	1018.1	31.6	1018.1	31.6
349	18495	1.6	18.8037	2.8	0.394	3.2	0.054	1.5	0.5	337.2	4.8	337.1	9.1	336.5	63.4	337.2	4.8
411	56065	1.7	16.6432	0.8	0.820	1.2	0.099	0.8	0.7	608.3	4.7	607.9	5.3	606.6	17.8	608.3	4.7
100	9355	0.6	17.4666	6.2	0.749	6.3	0.095	1.0	0.2	584.2	5.8	567.5	27.2	501.3	135.9	584.2	5.8
38	12725	0.7	9.2254	2.5	4.791	2.9	0.321	1.5	0.5	1792.5	22.8	1783.3	24.7	1772.6	46.5	1772.6	46.5
325	62168	1.7	9.2594	2.5	4.361	2.9	0.293	1.4	0.5	1655.9	20.9	1705.0	23.8	1765.9	45.7	1765.9	45.7
209	9538	1.2	20.7393	6.7	0.259	6.8	0.039	1.3	0.2	246.6	3.1	234.1	14.2	109.9	157.3	246.6	3.1
385	41853	3.7	13.2288	1.2	1.879	2.6	0.180	2.4	0.9	1068.3	23.2	1073.6	17.4	1084.3	23.3	1084.3	23.3
1368	14455	0.8	20.1386	1.5	0.200	2.7	0.029	2.3	0.8	185.5	4.1	185.0	4.6	178.9	35.4	185.5	4.1
203	83140	1.8	5.3636	0.9	12.423	1.1	0.483	0.6	0.5	2541.5	12.2	2636.9	10.2	2711.0	15.2	2711.0	15.2
226	7775	1.1	19.6162	9.4	0.277	9.4	0.039	1.2	0.1	249.4	2.9	248.5	20.8	239.8	216.3	249.4	2.9
50	30903	1.2	3.6450	1.0	24.807	1.7	0.656	1.4	0.8	3250.8	35.0	3300.6	16.8	3331.1	16.3	3331.1	16.3
146	17500	3.8	17.3625	3.7	0.714	3.9	0.090	1.4	0.3	555.3	7.2	547.3	16.7	514.4	81.5	555.3	7.2
336	26095	2.7	14.9789	2.3	1.067	3.0	0.116	2.0	0.7	706.9	13.3	737.2	15.8	830.3	47.6	706.9	13.3
102	11458	2.4	18.5697	8.8	0.608	9.3	0.082	2.9	0.3	507.4	14.3	482.3	35.8	364.8	199.7	507.4	14.3
135	18170	7.0	16.2562	5.4	0.795	9.0	0.094	7.2	0.8	577.6	39.6	594.0	40.4	657.3	116.0	577.6	39.6
141	18198	1.7	13.0540	2.9	1.933	4.2	0.183	3.1	0.7	1083.6	30.4	1092.7	28.3	1110.9	58.4	1110.9	58.4
280	30615	7.6	17.3054	3.7	0.710	4.0	0.089	1.6	0.4	550.6	8.6	545.0	16.9	521.6	80.5	550.6	8.6
763	92718	27.4	16.1013	2.0	0.954	7.1	0.111	6.8	1.0	680.7	44.1	680.0	35.2	677.8	42.5	680.7	44.1

Appendix A Cont.: U-Pb detrital zircon geochronologic analyses by Laser-Ablation Multicollector ICP Mass Spectrometry

U (ppm)	206Pb 204Pb	U/Th	206Pb* 207Pb*	± (%)	207Pb* 235U*	± (%)	206Pb* 238U	± (%)	error corr.	206Pb* 238U*	± (Ma)	207Pb* 235U	± (Ma)	206Pb* 207Pb*	± (Ma)	**Best age** (Ma)	± (Ma)
					Isotope ratios							Apparent ages (Ma)					
BG (SAL 1654) Cont.																	
154	4445	0.6	20.4677	7.3	0.261	7.4	0.039	1.1	0.1	244.6	2.6	235.1	15.5	141.0	171.2	244.6	2.6
253	12105	1.0	16.4868	1.9	0.834	3.3	0.100	2.7	0.8	613.1	15.5	616.1	15.1	627.0	41.6	613.1	15.5
533	51063	1.1	17.0325	2.1	0.752	2.4	0.093	1.1	0.5	572.5	6.2	569.3	10.3	556.4	45.0	572.5	6.2
401	101418	3.6	6.7316	0.9	6.279	6.4	0.307	6.3	1.0	1723.8	95.4	2015.5	55.9	2329.3	15.6	2329.3	15.6
138	43863	2.7	9.0752	1.1	4.839	1.4	0.318	1.0	0.7	1782.3	14.8	1791.6	12.2	1802.5	19.8	1802.5	19.8
261	73113	1.8	8.6453	0.9	5.348	1.6	0.335	1.3	0.8	1864.2	21.5	1876.6	13.5	1890.3	15.3	1890.3	15.3
157	13008	0.8	16.8427	3.8	0.762	4.1	0.093	1.4	0.4	573.5	7.9	575.0	17.8	580.8	82.4	573.5	7.9
253	69595	2.4	5.6499	2.7	10.714	4.0	0.439	3.0	0.7	2346.3	58.8	2498.7	37.5	2624.9	45.1	2624.9	45.1
313	24553	1.1	16.9067	2.2	0.753	2.9	0.092	1.9	0.7	569.4	10.4	570.1	12.6	572.6	47.4	569.4	10.4
81	10490	4.9	13.5386	4.4	1.558	4.5	0.153	1.1	0.2	917.7	9.3	953.7	27.9	1037.7	88.3	1037.7	88.3
133	17743	1.3	14.7593	2.5	1.138	3.2	0.122	2.0	0.6	740.8	14.1	771.4	17.4	861.0	52.4	740.8	14.1
878	77015	5.1	16.8058	2.0	0.763	3.0	0.093	2.3	0.7	573.3	12.5	575.8	13.4	585.6	43.8	573.3	12.5
136	23860	5.6	14.1281	2.7	1.339	4.2	0.137	3.1	0.8	828.9	24.4	862.9	24.1	951.1	55.6	951.1	55.6
655	12870	0.9	18.7058	3.5	0.280	3.7	0.038	1.4	0.4	240.1	3.2	250.5	8.3	348.3	78.5	240.1	3.2
336	10930	0.7	20.1550	4.1	0.238	4.3	0.035	1.5	0.3	220.3	3.2	216.6	8.5	177.0	94.8	220.3	3.2
230	16598	1.6	13.9854	2.0	1.174	5.3	0.119	4.9	0.9	725.1	33.5	788.3	28.9	971.8	40.8	971.8	40.8
367	77988	2.3	13.4084	1.9	1.826	2.3	0.178	1.2	0.5	1053.8	12.1	1054.9	14.8	1057.2	38.1	1057.2	38.1
525	76980	11.8	14.6550	3.5	0.989	5.0	0.105	3.5	0.7	644.5	21.4	698.4	25.1	875.8	73.3	644.5	21.4
77	15400	0.9	13.2285	2.9	1.892	2.9	0.181	0.7	0.2	1075.1	7.0	1078.2	19.5	1084.4	57.2	1084.4	57.2
234	21433	1.9	13.7267	2.3	1.571	3.5	0.156	2.7	0.8	937.0	23.7	959.0	22.0	1009.8	46.1	1009.8	46.1
140	18533	1.0	16.9923	3.9	0.768	4.9	0.095	3.0	0.6	582.9	16.6	578.5	21.7	561.6	85.2	582.9	16.6
64	7453	1.6	16.4683	8.5	0.734	8.6	0.088	1.3	0.2	541.7	6.9	558.9	37.0	629.4	183.4	541.7	6.9
CM (SAL 183)																	
107	4694	1.3	16.7602	5.7	0.788	5.8	0.096	1.3	0.2	589.7	7.4	590.1	26.2	591.5	123.7	589.7	7.4
753	24892	25.7	13.6077	4.4	1.695	4.7	0.167	1.7	0.4	997.2	16.1	1006.7	30.0	1027.4	88.2	1027.4	88.2
236	81520	3.7	4.0963	2.4	15.761	4.5	0.468	3.8	0.8	2475.8	78.9	2862.4	43.3	3147.0	38.1	3147.0	38.1
107	15466	1.3	12.5041	2.3	2.311	2.3	0.210	0.5	0.2	1226.8	5.6	1215.8	16.5	1196.3	44.8	1196.3	44.8
664	3760	2.7	13.0139	23.0	0.930	23.9	0.088	6.5	0.3	542.2	33.8	667.4	117.2	1117.1	464.0	542.2	33.8
10	4622	0.8	5.2181	8.0	11.788	8.3	0.446	2.3	0.3	2378.0	45.3	2587.7	77.6	2756.3	130.8	2756.3	130.8
294	63898	1.3	9.7061	0.9	4.214	1.5	0.297	1.2	0.8	1674.8	17.8	1676.8	12.2	1679.3	15.9	1679.3	15.9
585	20796	3.0	16.9011	2.3	0.666	3.2	0.082	2.3	0.7	505.8	11.0	518.2	13.0	573.3	49.3	505.8	11.0
468	60464	4.1	13.7614	1.7	1.660	1.8	0.166	0.5	0.3	988.3	4.6	993.4	11.2	1004.7	34.6	1004.7	34.6
179	44600	3.3	5.9126	2.1	9.026	2.2	0.387	0.5	0.2	2109.2	9.0	2340.7	20.1	2549.0	35.9	2549.0	35.9

Appendix A Cont.: U-Pb detrital zircon geochronologic analyses by Laser-Ablation Multicollector ICP Mass Spectrometry

			Isotope ratios							Apparent ages (Ma)							
U (ppm)	206Pb 204Pb	U/Th	206Pb* 207Pb*	± (%)	207Pb* 235U*	± (%)	206Pb* 238U	± (%)	error corr.	206Pb* 238U*	± (Ma)	207Pb* 235U	± (Ma)	206Pb* 207Pb*	± (Ma)	**Best age (Ma)**	± (Ma)
CM (SAL 183) Cont.																	
249	30974	1.6	16.5356	2.0	0.856	2.2	0.103	0.7	0.3	630.2	4.1	628.1	10.1	620.6	44.2	630.2	4.1
82	5916	1.1	18.8110	9.7	0.615	9.8	0.084	1.0	0.1	519.5	5.1	486.8	37.9	335.7	221.2	519.5	5.1
83	43076	1.3	5.1637	2.3	13.912	3.1	0.521	2.1	0.7	2703.5	45.5	2743.7	28.9	2773.5	36.9	2773.5	36.9
721	123776	4.2	13.1423	2.3	1.875	2.5	0.179	1.1	0.4	1060.1	10.8	1072.4	16.6	1097.5	45.0	1097.5	45.0
211	37018	1.5	12.7645	1.5	2.144	2.0	0.198	1.3	0.7	1167.2	14.2	1163.1	13.8	1155.5	29.6	1155.5	29.6
181	27524	1.5	12.4603	2.4	2.116	3.5	0.191	2.5	0.7	1128.1	25.6	1154.1	23.8	1203.2	47.7	1203.2	47.7
568	2626	1.9	13.6816	3.5	0.980	4.0	0.097	2.0	0.5	598.1	11.6	693.4	20.3	1016.4	70.6	598.1	11.6
129	11342	0.5	17.3711	4.3	0.770	4.4	0.097	1.0	0.2	597.0	5.6	579.9	19.3	513.3	93.6	597.0	5.6
81	11346	4.1	14.1874	3.6	1.364	6.5	0.140	5.4	0.8	846.5	42.8	873.5	38.1	942.5	74.7	846.5	42.8
114	20140	1.7	16.7511	3.2	0.726	3.8	0.088	2.0	0.5	544.7	10.4	554.0	16.1	592.6	69.2	544.7	10.4
647	24304	6.9	13.6797	2.7	1.344	7.3	0.133	6.7	0.9	806.7	51.1	864.8	42.3	1016.7	54.8	806.7	51.1
220	23892	1.4	19.7312	7.6	0.281	7.7	0.040	0.6	0.1	253.9	1.5	251.2	17.0	226.4	176.5	253.9	1.5
359	8708	1.6	18.8740	5.6	0.293	5.7	0.040	1.0	0.2	253.6	2.5	261.0	13.2	328.1	128.0	253.6	2.5
248	56884	1.4	12.6667	1.1	2.149	1.2	0.197	0.5	0.4	1161.5	5.3	1164.8	8.6	1170.8	22.6	1170.8	22.6
434	8198	1.9	16.7885	2.7	0.557	7.2	0.068	6.6	0.9	423.1	27.1	449.6	26.0	587.8	59.5	423.1	27.1
217	72538	2.1	13.3004	1.7	1.863	1.9	0.180	0.7	0.4	1065.5	7.0	1068.1	12.4	1073.5	35.0	1073.5	35.0
120	13870	1.9	17.6236	5.7	0.619	5.8	0.079	0.9	0.2	491.0	4.4	489.3	22.5	481.5	126.3	491.0	4.4
449	47898	1.2	16.8389	1.9	0.769	2.8	0.094	2.0	0.7	578.3	11.1	578.9	12.3	581.3	42.2	578.3	11.1
402	24438	3.3	14.0268	3.9	1.251	4.1	0.127	1.0	0.3	772.2	7.5	823.8	23.0	965.8	80.6	772.2	7.5
152	19750	1.7	17.8926	4.6	0.631	4.6	0.082	0.6	0.1	507.0	2.7	496.4	18.1	447.9	101.9	507.0	2.7
397	39866	1.3	16.8640	1.2	0.780	1.3	0.095	0.5	0.4	587.6	2.9	585.6	5.9	578.0	26.6	587.6	2.9
289	48974	1.0	13.8565	1.6	1.607	1.9	0.162	1.1	0.6	965.2	9.9	973.0	12.2	990.7	32.6	990.7	32.6
393	135090	1.7	9.9542	1.2	3.622	1.4	0.261	0.8	0.6	1497.3	11.1	1554.3	11.3	1632.6	21.4	1632.6	21.4
184	42202	2.4	12.6458	1.4	2.159	2.0	0.198	1.4	0.7	1164.5	15.2	1167.9	14.0	1174.1	28.3	1174.1	28.3
327	130734	1.3	6.2260	1.4	10.091	2.0	0.456	1.4	0.7	2420.4	28.9	2443.1	18.3	2462.1	23.2	2462.1	23.2
77	24654	1.8	17.9449	8.6	0.697	8.9	0.091	1.9	0.2	559.6	10.2	536.9	36.9	441.5	192.7	559.6	10.2
234	6236	4.5	16.1182	3.8	0.795	5.2	0.093	3.6	0.7	573.2	19.7	594.3	23.5	675.5	80.9	573.2	19.7
111	3466	0.9	15.3199	6.9	0.797	6.9	0.089	0.9	0.1	547.2	4.9	595.3	31.2	783.2	144.5	547.2	4.9
209	74922	2.2	10.0495	1.1	3.930	1.2	0.286	0.5	0.4	1623.7	7.2	1619.9	9.7	1614.9	20.3	1614.9	20.3
391	16616	6.0	13.8693	2.7	1.355	2.7	0.136	0.5	0.2	823.7	3.9	869.7	15.8	988.8	53.9	823.7	3.9
160	37414	2.4	17.4742	3.5	0.721	3.5	0.091	0.5	0.1	563.5	2.7	551.2	15.0	500.3	77.0	563.5	2.7
83	15428	0.7	12.7901	1.6	2.081	2.7	0.193	2.1	0.8	1137.7	22.1	1142.5	18.4	1151.6	32.7	1151.6	32.7
188	39388	1.5	12.4816	2.2	2.251	2.5	0.204	1.2	0.5	1195.5	13.2	1197.0	17.6	1199.9	43.2	1199.9	43.2

Appendix A Cont.: U-Pb detrital zircon geochronologic analyses by Laser-Ablation Multicollector ICP Mass Spectrometry

U (ppm)	206Pb 204Pb	U/Th	206Pb* 207Pb*	± (%)	207Pb* 235U*	± (%)	206Pb* 238U	± (%)	error corr.	206Pb* 238U*	± (Ma)	207Pb* 235U	± (Ma)	206Pb* 207Pb*	± (Ma)	**Best age** (Ma)	± (Ma)
					Isotope ratios							**Apparent ages (Ma)**					
CM (SAL 183) Cont.																	
158	119164	1.4	5.5600	2.1	9.471	3.6	0.382	2.9	0.8	2085.3	51.1	2384.8	32.8	2651.5	35.3	2651.5	35.3
397	17360	1.6	18.5579	4.1	0.322	4.3	0.043	1.4	0.3	273.3	3.7	283.3	10.6	366.2	91.3	273.3	3.7
407	134498	1.7	6.9995	0.6	8.159	0.7	0.414	0.5	0.7	2234.0	9.4	2248.8	6.7	2262.2	9.5	2262.2	9.5
185	39882	0.6	10.9857	1.7	3.202	1.8	0.255	0.6	0.3	1464.7	7.3	1457.6	13.6	1447.2	31.7	1447.2	31.7
168	37970	1.0	13.5996	3.1	1.573	3.2	0.155	0.9	0.3	929.6	7.9	959.5	20.2	1028.6	63.1	1028.6	63.1
188	55348	3.7	5.2333	1.8	12.312	2.3	0.467	1.5	0.7	2471.7	31.0	2628.5	21.8	2751.5	28.9	2751.5	28.9
133	67032	2.1	5.5887	1.0	11.196	2.7	0.454	2.5	0.9	2412.2	50.9	2539.6	25.3	2643.0	16.3	2643.0	16.3
227	34704	2.4	13.4026	1.6	1.879	1.7	0.183	0.6	0.3	1081.4	5.7	1073.7	11.3	1058.1	32.4	1058.1	32.4
413	127726	23.9	14.0928	1.7	1.442	2.5	0.147	1.9	0.7	886.4	15.7	906.6	15.1	956.2	34.2	886.4	15.7
94	24972	0.7	15.7420	7.2	0.807	7.3	0.092	1.6	0.2	568.2	8.6	600.8	33.3	725.8	152.2	568.2	8.6
113	18764	2.1	13.3507	4.7	1.783	5.5	0.173	3.0	0.5	1026.5	28.1	1039.1	36.0	1065.9	94.1	1065.9	94.1
353	30868	8.6	13.7921	2.4	1.565	3.3	0.157	2.2	0.7	937.7	19.4	956.5	20.2	1000.1	48.7	937.7	19.4
678	17198	21.2	13.1634	2.3	1.616	2.7	0.154	1.4	0.5	925.1	11.8	976.6	16.6	1094.2	45.5	1094.2	45.5
311	73702	1.2	12.4288	3.0	2.394	3.2	0.216	0.8	0.3	1259.5	9.5	1240.7	22.6	1208.3	59.9	1208.3	59.9
545	10806	11.1	15.7974	3.1	0.921	3.5	0.106	1.7	0.5	646.8	10.7	662.9	17.1	718.4	64.8	646.8	10.7
218	45340	3.4	12.9003	1.5	2.031	1.7	0.190	0.7	0.4	1121.6	7.2	1126.0	11.5	1134.5	30.5	1134.5	30.5
146	9058	5.0	17.5924	2.9	0.671	3.0	0.086	0.9	0.3	529.3	4.4	521.1	12.4	485.4	64.3	529.3	4.4
77	10454	2.4	16.8583	6.6	0.753	6.8	0.092	1.3	0.2	567.7	7.3	569.9	29.6	578.8	144.5	567.7	7.3
347	80458	4.4	6.5398	3.5	6.666	4.5	0.316	2.9	0.6	1770.9	44.1	2068.1	39.9	2378.7	59.7	2378.7	59.7
204	31024	3.0	8.9046	2.5	5.158	2.7	0.333	0.9	0.3	1853.6	14.5	1845.8	22.7	1837.0	45.5	1837.0	45.5
226	51286	2.1	8.3947	1.6	5.015	2.4	0.305	1.8	0.8	1717.7	27.6	1821.9	20.5	1943.1	28.4	1943.1	28.4
81	12640	1.4	16.6531	7.0	0.627	7.7	0.076	3.3	0.4	470.4	14.9	494.1	30.3	605.3	151.9	470.4	14.9
212	29892	1.1	16.7160	3.7	0.722	3.9	0.088	1.2	0.3	540.9	6.1	551.8	16.5	597.2	80.3	540.9	6.1
73	45758	1.5	4.1703	2.2	20.759	2.4	0.628	1.1	0.5	3141.2	27.1	3127.4	23.4	3118.6	34.2	3118.6	34.2
112	36494	1.4	12.8225	4.5	2.005	4.7	0.186	1.2	0.3	1101.9	12.4	1117.0	31.9	1146.6	90.3	1146.6	90.3
253	9162	0.8	19.4214	9.5	0.274	9.6	0.039	1.3	0.1	243.9	3.1	245.7	20.9	262.8	218.0	243.9	3.1
308	67742	3.6	9.9294	1.2	4.003	1.4	0.288	0.6	0.5	1633.1	8.9	1634.9	11.0	1637.2	22.5	1637.2	22.5
239	24622	1.5	13.2507	1.6	1.927	1.8	0.185	1.0	0.5	1095.0	9.9	1090.3	12.3	1081.0	31.1	1081.0	31.1
171	98310	2.0	5.0777	1.0	14.624	2.0	0.539	1.8	0.9	2777.4	39.9	2791.1	19.2	2801.0	15.9	2801.0	15.9
259	33812	1.8	5.0264	1.0	10.654	2.1	0.388	1.8	0.9	2115.4	33.0	2493.4	19.6	2817.6	17.0	2817.6	17.0
19	3030	1.4	19.5457	56.8	0.641	56.9	0.091	3.1	0.1	560.5	16.6	502.8	229.6	248.1	1421.8	560.5	16.6
102	54864	1.5	5.2117	1.3	14.012	1.8	0.530	1.3	0.7	2739.9	28.1	2750.5	17.4	2758.3	22.0	2758.3	22.0
157	39046	1.9	13.4175	2.8	1.657	3.1	0.161	1.5	0.5	963.5	13.6	992.1	19.9	1055.9	55.5	1055.9	55.5

Appendix A Cont.: U-Pb detrital zircon geochronologic analyses by Laser-Ablation Multicollector ICP Mass Spectrometry

			Isotope ratios							Apparent ages (Ma)							
U (ppm)	206Pb 204Pb	U/Th	206Pb* 207Pb*	± (%)	207Pb* 235U*	± (%)	206Pb* 238U	± (%)	error corr.	206Pb* 238U*	± (Ma)	207Pb* 235U	± (Ma)	206Pb* 207Pb*	± (Ma)	**Best age** (Ma)	± (Ma)
CM (SAL 183) Cont.																	
121	10378	2.7	16.5981	3.2	0.737	3.2	0.089	0.5	0.2	547.9	2.6	560.6	13.8	612.5	68.4	547.9	2.6
254	31686	2.4	13.4531	1.6	1.730	1.6	0.169	0.5	0.3	1005.5	4.8	1019.8	10.5	1050.5	31.3	1050.5	31.3
256	52486	1.5	12.9488	1.4	1.963	1.6	0.184	0.7	0.5	1090.6	7.3	1102.8	10.7	1127.0	28.0	1127.0	28.0
88	8444	3.8	15.4308	5.2	0.836	5.6	0.094	2.0	0.4	576.7	11.0	617.1	25.7	768.0	109.5	576.7	11.0
84	37940	0.7	5.4133	1.4	13.048	1.5	0.512	0.6	0.4	2666.4	12.7	2683.1	14.1	2695.8	22.8	2695.8	22.8
798	6036	5.1	12.9864	2.1	1.652	2.4	0.156	1.2	0.5	932.1	10.3	990.2	15.0	1121.3	41.0	1121.3	41.0
116	77616	4.9	4.1201	0.9	20.415	2.4	0.610	2.2	0.9	3070.2	54.5	3111.2	23.4	3137.8	14.9	3137.8	14.9
217	21842	2.8	17.0646	2.8	0.750	3.0	0.093	1.1	0.4	572.4	5.9	568.4	13.2	552.3	62.0	572.4	5.9
311	21862	5.1	17.0462	2.5	0.709	4.2	0.088	3.3	0.8	541.4	17.3	544.0	17.5	554.7	54.2	541.4	17.3
221	97046	1.5	5.2328	1.4	13.883	1.9	0.527	1.3	0.7	2728.3	29.6	2741.8	18.3	2751.6	23.0	2751.6	23.0
155	58610	1.0	8.9589	1.3	4.811	1.5	0.313	0.7	0.5	1753.4	11.1	1786.8	12.6	1826.0	23.8	1826.0	23.8
260	96814	168.2	4.5799	1.4	14.637	1.5	0.486	0.5	0.3	2554.1	10.5	2791.9	13.9	2968.5	22.1	2968.5	22.1
110	12204	0.5	12.5937	2.2	2.158	2.2	0.197	0.5	0.2	1160.0	5.3	1167.8	15.3	1182.3	42.6	1182.3	42.6
243	28200	7.3	17.0340	1.9	0.744	2.0	0.092	0.7	0.3	566.7	3.7	564.6	8.8	556.2	41.6	566.7	3.7
294	60886	1.0	16.3645	4.1	0.771	4.3	0.091	1.3	0.3	564.2	7.2	580.2	19.2	643.1	88.9	564.2	7.2
520	57768	3.0	7.8884	1.5	6.201	2.3	0.355	1.8	0.8	1957.3	29.5	2004.5	20.2	2053.6	26.7	2053.6	26.7
478	20862	0.9	19.7891	4.8	0.304	4.9	0.044	0.8	0.2	274.9	2.0	269.2	11.5	219.6	111.7	274.9	2.0
234	63392	2.3	12.3355	1.9	2.203	2.5	0.197	1.7	0.7	1159.8	18.2	1182.1	17.8	1223.0	37.1	1223.0	37.1
322	20306	4.4	12.7775	4.0	1.818	5.0	0.169	3.0	0.6	1004.0	27.5	1052.1	32.8	1153.5	80.1	1153.5	80.1
325	42438	6.9	14.6712	3.2	1.216	3.6	0.129	1.7	0.5	784.6	12.9	808.1	20.3	873.4	66.1	784.6	12.9
323	29672	11.3	17.1417	2.2	0.735	3.2	0.091	2.3	0.7	563.8	12.6	559.6	13.8	542.5	48.2	563.8	12.6
432	51634	3.2	14.9635	0.8	1.271	1.0	0.138	0.5	0.5	832.8	3.9	832.7	5.6	832.5	17.5	832.8	3.9
239	25198	3.9	17.0905	1.6	0.746	1.8	0.092	0.8	0.4	570.3	4.3	566.0	7.9	549.0	35.8	570.3	4.3
471	4174	1.9	13.1668	3.0	1.511	3.8	0.144	2.3	0.6	868.8	18.9	934.8	22.9	1093.7	59.1	1093.7	59.1
95	9260	3.0	14.1094	3.6	1.341	3.9	0.137	1.3	0.3	828.8	10.4	863.6	22.6	953.8	74.5	828.8	10.4
209	59004	2.2	13.0846	2.1	2.018	2.3	0.191	1.0	0.4	1129.4	9.8	1121.5	15.4	1106.2	41.0	1106.2	41.0
281	33464	1.6	14.9630	1.6	1.146	1.7	0.124	0.7	0.4	755.5	5.2	775.2	9.5	832.5	33.0	755.5	5.2
94	4510	1.2	20.2023	16.5	0.274	16.6	0.040	2.3	0.1	253.7	5.7	245.8	36.3	171.5	386.7	253.7	5.7
204	94054	0.8	4.6917	0.5	15.998	0.7	0.544	0.5	0.7	2801.7	11.6	2876.7	7.0	2929.6	8.4	2929.6	8.4
493	82530	6.6	13.7026	1.9	1.686	2.0	0.168	0.5	0.3	998.8	4.6	1003.4	12.6	1013.4	38.8	1013.4	38.8
88	27316	1.6	13.8566	2.1	1.682	3.0	0.169	2.2	0.7	1006.7	20.6	1001.7	19.3	990.7	42.2	990.7	42.2
517	21102	1.5	12.0410	2.7	2.506	3.0	0.219	1.2	0.4	1276.0	14.1	1273.9	21.4	1270.4	52.5	1270.4	52.5
92	18984	1.4	12.2617	1.8	2.377	2.0	0.211	0.8	0.4	1236.0	9.2	1235.6	14.3	1234.9	35.7	1234.9	35.7

Appendix A Cont.: U-Pb detrital zircon geochronologic analyses by Laser-Ablation Multicollector ICP Mass Spectrometry

					Isotope ratios							Apparent ages (Ma)					
U (ppm)	206Pb 204Pb	U/Th	206Pb* 207Pb*	± (%)	207Pb* 235U*	± (%)	206Pb* 238U	± (%)	error corr.	206Pb* 238U*	± (Ma)	207Pb* 235U	± (Ma)	206Pb* 207Pb*	± (Ma)	**Best age (Ma)**	± (Ma)
CM (SAL 183) Cont.																	
270	50214	3.2	9.4078	2.1	4.545	2.5	0.310	1.2	0.5	1741.2	18.8	1739.2	20.5	1736.8	39.2	1736.8	39.2
565	20084	4.0	16.3901	3.2	0.746	3.6	0.089	1.7	0.5	547.6	9.1	565.8	15.7	639.7	68.1	547.6	9.1
358	51768	4.9	13.0094	1.6	2.012	1.7	0.190	0.5	0.3	1120.6	5.1	1119.6	11.3	1117.8	31.7	1117.8	31.7
529	155238	1.0	4.0373	1.7	18.419	4.6	0.539	4.3	0.9	2780.7	97.6	3011.9	44.6	3170.0	26.5	3170.0	26.5
211	63524	3.9	3.5102	1.7	18.862	2.5	0.480	1.9	0.7	2528.1	39.1	3034.8	24.6	3389.9	27.0	3389.9	27.0
245	25360	1.6	16.1821	2.0	0.956	2.0	0.112	0.5	0.2	685.8	3.3	681.5	10.1	667.1	42.4	685.8	3.3
165	25586	5.2	13.9270	2.0	1.346	4.4	0.136	3.8	0.9	821.9	29.6	865.9	25.4	980.3	41.7	821.9	29.6
242	4820	14.0	7.0508	1.6	6.984	1.8	0.357	0.8	0.4	1968.6	13.4	2109.4	16.2	2249.6	28.4	2249.6	28.4
NBP99-02-17 (SAL 141)																	
228	116840	1.7	5.4310	3.1	11.044	4.3	0.435	2.9	0.7	2328.4	56.7	2526.9	39.7	2690.4	51.6	2690.4	51.6
475	19175	2.8	15.9901	2.5	0.739	5.8	0.086	5.2	0.9	530.3	26.6	562.0	25.0	692.6	53.5	530.3	26.6
182	22535	2.4	7.3925	9.2	2.446	9.5	0.131	2.4	0.3	794.4	17.9	1256.2	68.7	2167.5	160.9	2167.5	160.9
204	15955	2.5	17.8868	5.1	0.455	5.4	0.059	1.5	0.3	370.0	5.5	381.0	17.0	448.7	114.1	370.0	5.5
210	39195	2.8	15.4692	3.1	1.077	4.9	0.121	3.8	0.8	735.3	26.1	742.1	25.6	762.8	65.2	735.3	26.1
137	21115	0.6	17.1525	3.4	0.780	3.8	0.097	1.6	0.4	597.1	8.9	585.6	16.7	541.1	74.9	597.1	8.9
97	12335	5.4	17.6605	4.6	0.699	5.4	0.090	2.8	0.5	553.1	15.1	538.5	22.7	476.9	102.7	553.1	15.1
215	51215	3.0	14.2019	2.6	1.493	3.0	0.154	1.4	0.5	922.1	12.4	927.5	18.2	940.4	53.9	922.1	12.4
91	11210	2.6	17.7088	8.6	0.680	8.8	0.087	1.7	0.2	539.7	8.5	526.7	36.1	470.8	191.0	539.7	8.5
521	75020	4.1	17.2444	1.9	0.718	3.0	0.090	2.4	0.8	554.6	12.5	549.7	12.8	529.4	41.0	554.6	12.5
214	66040	2.3	9.4587	2.3	4.353	3.2	0.299	2.2	0.7	1684.4	32.3	1703.4	26.3	1726.9	42.6	1726.9	42.6
296	71585	4.6	12.9716	2.8	2.044	3.3	0.192	1.7	0.5	1133.6	17.6	1130.1	22.3	1123.5	55.8	1123.5	55.8
134	17670	1.7	16.7687	3.6	0.780	5.1	0.095	3.6	0.7	584.3	20.2	585.5	22.7	590.3	78.3	584.3	20.2
212	6325	2.5	12.1952	11.8	1.436	12.5	0.127	4.1	0.3	770.8	29.8	904.1	74.8	1245.5	231.5	1245.5	231.5
144	15740	1.4	17.3402	3.6	0.578	5.0	0.073	3.5	0.7	452.4	15.1	463.2	18.7	517.2	80.1	452.4	15.1
247	13380	0.9	20.2685	6.1	0.234	6.1	0.034	0.8	0.1	218.1	1.7	213.5	11.8	163.9	141.9	218.1	1.7
116	20410	1.4	17.4737	8.8	0.684	9.1	0.087	2.2	0.2	535.6	11.1	528.9	37.5	500.3	195.0	535.6	11.1
343	77495	2.3	13.6193	2.4	1.405	6.4	0.139	6.0	0.9	837.6	46.7	890.9	38.1	1025.7	49.2	837.6	46.7
300	64325	2.0	13.2214	2.9	1.591	4.1	0.153	2.8	0.7	915.4	24.1	966.8	25.3	1085.4	58.6	1085.4	58.6
381	126840	6.6	10.5279	1.7	3.574	2.3	0.273	1.6	0.7	1555.5	22.5	1543.8	18.5	1527.8	31.3	1527.8	31.3
464	12915	1.1	19.3101	6.1	0.233	7.8	0.033	4.8	0.6	207.4	9.8	213.1	14.9	276.0	140.3	207.4	9.8
401	20450	2.0	18.8957	2.4	0.380	3.3	0.052	2.3	0.7	326.9	7.2	326.7	9.3	325.4	55.5	326.9	7.2
587	7155	1.9	19.4404	8.7	0.117	9.7	0.016	4.1	0.4	105.5	4.3	112.3	10.3	260.5	200.7	105.5	4.3
76	7338	1.8	28.2286	44.2	0.157	44.5	0.032	5.2	0.1	203.5	10.4	147.7	61.2	-675.2	1271.8	203.5	10.4

Appendix A Cont.: U-Pb detrital zircon geochronologic analyses by Laser-Ablation Multicollector ICP Mass Spectrometry

U (ppm)	206Pb 204Pb	U/Th	206Pb* 207Pb*	± (%)	**Isotope ratios** 207Pb* 235U*	± (%)	206Pb* 238U	± (%)	error corr.	**Apparent ages (Ma)** 206Pb* 238U*	± (Ma)	207Pb* 235U	± (Ma)	206Pb* 207Pb*	± (Ma)	**Best age** (Ma)	± (Ma)
NBP99-02-17 (SAL 141) Cont.																	
611	81914	1.8	8.8334	4.3	3.760	7.5	0.241	6.2	0.8	1391.2	77.1	1584.2	60.3	1851.5	77.6	1851.5	77.6
233	36550	2.8	13.6455	1.0	1.698	1.5	0.168	1.2	0.8	1001.4	11.3	1007.9	9.9	1021.8	19.3	1021.8	19.3
400	8344	1.4	16.7653	5.5	0.637	6.7	0.077	3.9	0.6	481.0	17.8	500.5	26.7	590.8	120.3	481.0	17.8
241	15990	2.0	18.0276	2.5	0.596	2.5	0.078	0.6	0.2	483.7	2.6	474.7	9.7	431.2	55.4	483.7	2.6
101	5832	1.4	19.5609	13.6	0.358	13.7	0.051	1.7	0.1	319.6	5.2	311.0	36.6	246.3	313.8	319.6	5.2
260	55200	1.9	9.9055	1.2	3.892	1.8	0.280	1.3	0.7	1589.3	18.3	1612.0	14.5	1641.7	22.8	1641.7	22.8
114	8868	1.1	18.6864	5.8	0.402	5.8	0.055	0.5	0.1	342.4	1.7	343.4	16.9	350.7	131.1	342.4	1.7
171	10050	2.6	17.5777	3.6	0.635	4.5	0.081	2.7	0.6	501.8	12.8	499.2	17.7	487.3	79.8	501.8	12.8
186	13460	3.8	16.6668	6.0	0.650	6.2	0.079	1.4	0.2	487.4	6.6	508.3	24.7	603.5	130.0	487.4	6.6
88	7436	1.7	17.3212	9.4	0.618	9.5	0.078	0.7	0.1	482.3	3.3	488.8	36.7	519.6	207.3	482.3	3.3
412	48604	7.7	17.0008	1.7	0.757	1.9	0.093	0.7	0.4	575.4	4.0	572.4	8.2	560.5	37.4	575.4	4.0
317	698	3.1	9.4698	24.3	1.215	24.3	0.083	0.8	0.0	516.7	4.0	807.5	136.3	1724.8	453.4	1724.8	453.4
355	100614	3.5	9.1609	6.5	3.641	6.8	0.242	2.1	0.3	1396.8	25.7	1558.6	54.1	1785.4	118.1	1785.4	118.1
248	42878	5.6	17.5014	5.1	0.664	5.3	0.084	1.5	0.3	521.3	7.7	516.8	21.6	496.9	112.8	521.3	7.7
80	10604	1.5	16.5857	6.6	0.775	6.6	0.093	0.7	0.1	574.6	3.6	582.7	29.5	614.1	142.9	574.6	3.6
282	82006	4.2	9.8942	3.4	3.740	3.7	0.268	1.4	0.4	1532.6	19.4	1580.0	29.6	1643.8	63.3	1643.8	63.3
83	27622	0.8	8.2364	1.7	6.028	2.0	0.360	1.1	0.6	1982.6	19.5	1979.9	17.6	1977.1	29.6	1977.1	29.6
152	5150	1.3	21.0737	7.5	0.243	8.0	0.037	2.6	0.3	235.4	6.1	221.1	15.8	72.1	179.2	235.4	6.1
174	9004	1.8	14.1798	3.5	1.105	4.0	0.114	1.8	0.5	693.9	11.9	755.8	21.1	943.6	72.2	693.9	11.9
78	34066	2.7	13.4228	4.6	1.817	4.7	0.177	0.9	0.2	1050.2	8.7	1051.7	30.6	1055.1	92.2	1055.1	92.2
41	3156	2.3	14.5138	19.9	0.845	20.0	0.089	1.4	0.1	549.2	7.2	621.8	93.2	895.7	415.4	549.2	7.2
184	4892	3.1	15.4752	5.2	0.837	5.4	0.094	1.5	0.3	579.0	8.2	617.6	25.0	762.0	109.7	579.0	8.2
185	11572	2.3	13.3634	2.9	1.771	3.0	0.172	0.7	0.2	1021.0	6.9	1034.7	19.5	1064.0	58.7	1064.0	58.7
262	29478	2.1	16.4432	2.1	0.887	2.3	0.106	0.9	0.4	648.4	5.4	644.9	11.0	632.7	45.9	648.4	5.4
334	38454	3.0	15.2916	3.0	1.006	3.6	0.112	1.9	0.5	681.6	12.1	706.7	18.1	787.1	63.7	681.6	12.1
289	12064	1.5	17.0586	3.5	0.718	3.6	0.089	0.8	0.2	548.6	4.0	549.5	15.2	553.1	76.5	548.6	4.0
242	21964	2.2	17.4801	3.3	0.684	3.4	0.087	0.7	0.2	536.0	3.8	529.1	13.9	499.6	72.4	536.0	3.8
165	24154	2.1	17.0068	6.9	0.762	7.0	0.094	1.1	0.2	579.1	6.1	575.2	30.8	559.7	151.1	579.1	6.1
124	13936	1.8	19.5872	11.2	0.278	11.2	0.040	0.9	0.1	249.9	2.3	249.3	24.8	243.3	258.1	249.9	2.3
175	56026	1.5	13.0240	2.1	2.005	2.3	0.189	0.8	0.4	1118.2	8.5	1117.3	15.3	1115.5	42.0	1115.5	42.0
NBP94-07-63 (SAL 142)																	
140	17465	2.5	16.8874	2.9	0.791	4.8	0.097	3.8	0.8	596.2	21.7	591.8	21.6	575.0	63.8	596.2	21.7
589	15830	2.2	19.8992	4.8	0.178	6.0	0.026	3.7	0.6	163.3	5.9	166.1	9.2	206.7	110.8	163.3	5.9

Appendix A Cont.: U-Pb detrital zircon geochronologic analyses by Laser-Ablation Multicollector ICP Mass Spectrometry

			Isotope ratios							Apparent ages (Ma)							
U (ppm)	206Pb 204Pb	U/Th	206Pb* 207Pb*	± (%)	207Pb* 235U*	± (%)	206Pb* 238U	± (%)	error corr.	206Pb* 238U*	± (Ma)	207Pb* 235U	± (Ma)	206Pb* 207Pb*	± (Ma)	**Best age (Ma)**	± (Ma)
NBP94-07-63 (SAL 142) Cont.																	
174	15270	0.9	13.8610	2.7	1.679	6.4	0.169	5.8	0.9	1005.4	54.1	1000.6	40.8	990.0	54.9	990.0	54.9
318	32375	4.1	16.4780	5.0	0.760	8.8	0.091	7.3	0.8	560.1	39.1	573.7	38.6	628.1	107.0	560.1	39.1
291	14640	1.9	19.2304	4.5	0.275	5.0	0.038	2.2	0.4	242.8	5.1	246.9	11.0	285.4	103.4	242.8	5.1
406	10125	2.2	15.5311	3.5	0.713	4.3	0.080	2.6	0.6	497.8	12.3	546.4	18.2	754.3	72.9	497.8	12.3
157	9280	1.3	16.6946	2.9	0.639	3.0	0.077	0.7	0.2	480.5	3.4	501.7	11.8	599.9	62.7	480.5	3.4
358	18510	0.9	20.1363	2.7	0.246	4.0	0.036	3.0	0.7	227.8	6.6	223.5	8.0	179.2	62.3	227.8	6.6
612	57095	35.7	16.5018	2.8	0.834	4.1	0.100	3.1	0.7	613.6	17.9	616.0	19.2	625.0	60.6	613.6	17.9
222	24150	1.2	17.1606	4.3	0.606	6.2	0.075	4.4	0.7	469.1	19.7	481.3	23.6	540.0	95.0	469.1	19.7
161	5555	1.4	19.4255	9.2	0.218	10.5	0.031	5.2	0.5	195.2	9.9	200.4	19.2	262.3	211.5	195.2	9.9
156	14030	1.4	17.4315	7.4	0.605	7.5	0.077	1.2	0.2	475.3	5.5	480.6	28.6	505.7	162.2	475.3	5.5
351	72590	6.5	14.3913	2.4	1.212	7.0	0.126	6.6	0.9	767.8	47.7	806.0	39.0	913.2	48.6	767.8	47.7
246	22835	1.3	17.2868	4.5	0.675	4.5	0.085	0.8	0.2	523.8	4.1	523.9	18.5	524.0	97.7	523.8	4.1
190	34360	4.1	14.1895	3.3	1.400	6.2	0.144	5.2	0.8	867.8	42.3	889.0	36.5	942.2	67.0	867.8	42.3
477	9270	1.7	19.5950	8.4	0.130	9.9	0.018	5.2	0.5	118.0	6.1	124.1	11.5	242.3	194.1	118.0	6.1
207	12960	1.7	17.7357	5.6	0.575	6.1	0.074	2.5	0.4	459.6	11.0	461.0	22.6	467.5	123.9	459.6	11.0
170	17245	1.2	17.9828	5.3	0.574	7.4	0.075	5.2	0.7	465.0	23.2	460.3	27.5	436.8	118.3	465.0	23.2
390	15725	1.0	18.9296	5.3	0.237	6.4	0.033	3.6	0.6	206.2	7.3	215.8	12.4	321.4	119.7	206.2	7.3
327	48915	1.8	16.7900	2.2	0.623	4.7	0.076	4.2	0.9	471.2	18.9	491.5	18.3	587.6	47.2	471.2	18.9
382	30150	2.0	15.1232	9.8	0.823	10.7	0.090	4.3	0.4	557.0	23.1	609.6	49.2	810.3	205.5	557.0	23.1
69	13245	1.8	17.2244	10.1	0.721	11.1	0.090	4.7	0.4	556.2	24.9	551.5	47.3	531.9	221.5	556.2	24.9
139	21480	1.6	17.0926	2.8	0.654	3.7	0.081	2.4	0.7	502.9	11.8	511.2	15.0	548.7	61.8	502.9	11.8
250	36145	2.1	17.6615	3.7	0.655	5.6	0.084	4.2	0.7	519.5	21.0	511.7	22.6	476.8	82.8	519.5	21.0
315	4595	2.3	14.2114	9.0	0.794	9.3	0.082	2.1	0.2	507.1	10.3	593.4	41.7	939.0	185.5	507.1	10.3
602	157790	8.9	14.0265	3.0	1.389	9.9	0.141	9.5	1.0	852.0	75.5	884.3	58.6	965.8	60.9	852.0	75.5
348	39235	5.4	13.7768	2.7	1.465	9.4	0.146	9.0	1.0	880.7	73.8	916.1	56.5	1002.4	54.4	880.7	73.8
194	18735	6.0	17.4302	2.8	0.678	4.0	0.086	2.9	0.7	529.8	14.7	525.3	16.4	505.8	60.8	529.8	14.7
246	28828	3.5	16.4390	3.0	0.918	3.2	0.110	0.9	0.3	669.9	6.0	661.6	15.3	633.2	64.9	669.9	6.0
82	7864	2.0	17.6657	11.4	0.720	12.1	0.092	4.1	0.3	568.7	22.3	550.6	51.4	476.2	252.0	568.7	22.3
NBP94-07-63 (SAL 164)																	
144	1448	1.2	11.1986	16.0	0.463	16.1	0.038	2.2	0.1	237.9	5.2	386.2	51.9	1410.5	307.7	237.9	5.2
839	67600	4.9	17.2464	3.9	0.717	4.4	0.090	2.1	0.5	553.5	11.4	548.8	18.8	529.1	85.3	553.5	11.4
255	6480	1.6	18.5708	4.1	0.418	4.3	0.056	1.5	0.3	353.1	5.1	354.7	12.9	364.7	91.5	353.1	5.1
201	14696	2.3	17.4082	3.6	0.680	4.7	0.086	3.0	0.6	530.6	15.0	526.5	19.2	508.6	79.9	530.6	15.0

Appendix A Cont.: U-Pb detrital zircon geochronologic analyses by Laser-Ablation Multicollector ICP Mass Spectrometry

U (ppm)	206Pb/204Pb	U/Th	206Pb*/207Pb*	± (%)	Isotope ratios: 207Pb*/235U*	± (%)	206Pb*/238U	± (%)	error corr.	Apparent ages (Ma): 206Pb*/238U*	± (Ma)	207Pb*/235U	± (Ma)	206Pb*/207Pb*	± (Ma)	**Best age (Ma)**	± (Ma)
NBP94-07-63 (SAL 164) Cont.																	
188	45876	1.0	9.9730	1.2	3.917	3.1	0.283	2.9	0.9	1608.0	40.6	1617.2	25.0	1629.1	22.3	1629.1	22.3
317	23256	14.4	17.4024	2.8	0.681	3.4	0.086	2.0	0.6	531.3	10.2	527.2	14.0	509.3	60.6	531.3	10.2
541	19664	1.5	20.0678	3.3	0.241	3.8	0.035	1.9	0.5	221.9	4.2	218.9	7.5	187.1	76.6	221.9	4.2
268	7686	1.0	16.9379	5.1	0.633	5.2	0.078	0.8	0.2	482.8	3.8	498.0	20.4	568.6	111.3	482.8	3.8
83	2638	2.1	21.2468	58.1	0.114	58.4	0.018	6.1	0.1	112.1	6.8	109.5	60.7	52.6	1508.5	112.1	6.8
91	5150	2.1	17.4181	8.5	0.638	8.5	0.081	0.9	0.1	499.4	4.5	500.8	33.6	507.4	186.3	499.4	4.5
437	8970	1.3	17.4042	5.7	0.636	5.7	0.080	0.8	0.1	497.6	3.7	499.7	22.6	509.1	124.7	497.6	3.7
333	138360	2.4	8.1436	0.9	5.504	1.1	0.325	0.7	0.6	1814.4	10.4	1901.2	9.8	1997.2	16.5	1997.2	16.5
604	3382	1.3	16.2649	7.0	0.424	7.2	0.050	1.4	0.2	314.7	4.1	359.0	21.7	656.1	151.2	314.7	4.1
420	64610	4.1	13.3267	1.4	1.791	1.5	0.173	0.5	0.3	1029.1	4.8	1042.1	9.8	1069.5	28.5	1069.5	28.5
300	14856	1.8	17.2787	3.3	0.586	3.6	0.073	1.3	0.4	457.1	5.8	468.6	13.4	525.0	72.9	457.1	5.8
264	48502	2.8	13.2622	2.1	1.827	2.5	0.176	1.4	0.5	1043.7	13.1	1055.2	16.5	1079.3	42.4	1079.3	42.4
208	7422	1.1	19.0899	8.3	0.249	8.4	0.035	1.1	0.1	218.8	2.4	226.0	17.0	302.2	189.9	218.8	2.4
412	14796	4.9	13.8363	3.9	1.275	5.4	0.128	3.7	0.7	776.0	26.8	834.6	30.5	993.6	79.4	993.6	79.4
171	15836	0.8	17.7297	4.5	0.635	4.5	0.082	0.6	0.1	505.7	2.8	499.0	17.8	468.3	99.3	505.7	2.8
229	11240	1.9	17.0456	5.3	0.644	5.4	0.080	0.6	0.1	493.8	2.9	504.7	21.3	554.7	116.2	493.8	2.9
512	7866	0.8	18.8097	4.8	0.226	5.3	0.031	2.4	0.4	196.0	4.6	207.1	10.0	335.8	107.9	196.0	4.6
158	3078	1.4	27.4637	33.7	0.081	33.8	0.016	2.1	0.1	103.3	2.2	79.2	25.7	-599.9	938.3	103.3	2.2
161	19774	1.3	17.2954	3.8	0.592	3.8	0.074	0.6	0.2	461.8	2.6	472.2	14.4	522.9	82.8	461.8	2.6
62	2078	0.6	17.8030	61.3	0.240	61.3	0.031	1.5	0.0	196.6	2.9	218.3	121.0	459.1	1506.0	196.6	2.9
595	2984	2.5	15.5890	4.7	0.656	5.0	0.074	1.7	0.3	461.5	7.3	512.4	20.1	746.5	99.8	461.5	7.3
209	26208	2.2	13.4597	2.4	1.725	2.4	0.168	0.5	0.2	1003.4	4.6	1018.0	15.6	1049.5	47.9	1049.5	47.9
297	1310	2.4	13.8432	6.1	0.802	6.4	0.080	1.8	0.3	499.0	8.8	597.8	28.9	992.6	124.8	499.0	8.8
196	4890	1.5	21.0298	24.9	0.104	25.3	0.016	4.6	0.2	101.3	4.7	100.3	24.2	77.0	599.7	101.3	4.7
405	60346	4.8	13.7401	1.7	1.600	1.9	0.159	0.9	0.5	953.5	7.6	970.1	11.7	1007.8	33.9	1007.8	33.9
51	1838	0.8	24.6572	61.5	0.171	61.6	0.031	3.5	0.1	194.0	6.6	160.1	91.5	-315.4	1731.3	194.0	6.6
516	11278	1.2	16.9707	2.1	0.667	2.5	0.082	1.4	0.5	508.8	6.8	519.0	10.3	564.3	46.1	508.8	6.8
192	11022	2.0	16.6075	5.6	0.695	6.0	0.084	2.0	0.3	518.3	10.0	535.8	24.9	611.2	121.9	518.3	10.0
246	28388	1.5	17.5797	3.7	0.644	3.8	0.082	0.8	0.2	508.6	4.1	504.7	15.1	487.0	82.0	508.6	4.1
107	6252	3.0	13.1145	2.0	1.758	2.2	0.167	0.8	0.4	996.7	7.8	1030.1	14.0	1101.7	39.9	1101.7	39.9
827	34418	11.4	17.4232	1.6	0.646	2.0	0.082	1.1	0.6	505.8	5.5	506.0	7.8	506.7	35.3	505.8	5.5
365	29368	1.7	17.3813	1.4	0.652	1.6	0.082	0.6	0.4	509.5	2.8	509.9	6.3	512.0	31.9	509.5	2.8
473	2734	13.6	14.9753	5.5	0.693	5.7	0.075	1.5	0.3	467.8	6.6	534.6	23.5	830.8	114.1	467.8	6.6

Appendix A Cont.: U-Pb detrital zircon geochronologic analyses by Laser-Ablation Multicollector ICP Mass Spectrometry

U (ppm)	206Pb 204Pb	U/Th	Isotope ratios 206Pb* 207Pb*	± (%)	207Pb* 235U*	± (%)	206Pb* 238U	± (%)	error corr.	Apparent ages (Ma) 206Pb* 238U*	± (Ma)	207Pb* 235U	± (Ma)	206Pb* 207Pb*	± (Ma)	**Best age** (Ma)	± (Ma)
NBP94-07-63 (SAL 164) Cont.																	
186	26978	2.7	13.7888	2.5	1.505	2.7	0.151	0.9	0.3	903.9	7.8	932.5	16.5	1000.6	51.7	1000.6	51.7
462	9770	3.4	12.9969	2.3	1.516	3.1	0.143	2.1	0.7	861.0	16.8	936.9	19.1	1119.7	46.1	1119.7	46.1
280	11952	2.0	16.9506	3.7	0.637	3.8	0.078	1.0	0.3	486.3	4.7	500.7	15.1	566.9	80.4	486.3	4.7
203	7094	2.0	23.4224	24.4	0.096	24.5	0.016	2.4	0.1	104.4	2.5	93.2	21.8	-185.4	616.2	104.4	2.5
168	33686	1.6	17.9408	3.0	0.614	3.2	0.080	1.0	0.3	495.7	4.7	486.3	12.2	442.0	66.7	495.7	4.7
194	21998	4.6	17.2904	5.7	0.670	5.9	0.084	1.7	0.3	520.2	8.4	520.8	24.1	523.5	124.3	520.2	8.4
381	71200	3.4	17.5449	2.4	0.616	2.4	0.078	0.5	0.2	486.3	2.3	487.2	9.3	491.4	52.1	486.3	2.3
529	47670	1.8	17.9230	2.2	0.582	2.2	0.076	0.5	0.2	470.3	2.3	465.9	8.4	444.2	48.6	470.3	2.3
276	53804	2.8	17.0870	2.1	0.759	2.7	0.094	1.6	0.6	579.5	9.0	573.4	11.8	549.4	46.8	579.5	9.0
205	42616	1.9	17.6502	3.1	0.630	3.7	0.081	2.1	0.5	500.0	9.9	496.1	14.6	478.2	68.8	500.0	9.9
471	58686	2.3	17.9384	2.3	0.577	2.6	0.075	1.3	0.5	466.4	5.9	462.3	9.8	442.3	51.0	466.4	5.9
123	18682	3.9	13.7030	4.3	1.704	4.4	0.169	1.1	0.3	1008.8	10.4	1010.2	28.1	1013.3	86.2	1013.3	86.2
100	5186	1.4	19.1666	14.4	0.184	14.5	0.026	1.9	0.1	163.1	3.1	171.7	22.9	293.0	329.9	163.1	3.1
405	26654	3.7	16.9117	2.6	0.743	2.7	0.091	0.8	0.3	562.5	4.2	564.4	11.6	571.9	55.8	562.5	4.2
196	4752	1.2	19.2811	9.8	0.215	10.0	0.030	2.0	0.2	190.8	3.8	197.6	17.9	279.5	224.5	190.8	3.8
522	19112	2.4	18.5373	4.4	0.432	4.4	0.058	0.5	0.1	363.6	1.8	364.3	13.5	368.7	98.6	363.6	1.8
318	71276	2.1	19.3908	5.8	0.263	5.9	0.037	1.4	0.2	234.5	3.2	237.5	12.6	266.4	132.6	234.5	3.2
230	22458	1.4	17.5023	2.4	0.597	2.7	0.076	1.2	0.4	471.0	5.3	475.4	10.1	496.8	52.8	471.0	5.3
479	45340	2.1	19.5293	3.2	0.266	3.3	0.038	0.8	0.3	238.4	1.9	239.4	7.0	250.1	73.1	238.4	1.9
316	23952	0.9	17.4148	2.7	0.659	3.6	0.083	2.4	0.7	515.7	11.8	514.2	14.5	507.8	58.9	515.7	11.8
385	4950	1.1	17.2396	14.3	0.286	14.5	0.036	2.4	0.2	226.8	5.3	255.7	32.9	530.0	315.7	226.8	5.3
115	11840	2.1	17.0541	6.5	0.656	6.6	0.081	1.1	0.2	502.7	5.2	512.0	26.6	553.7	142.3	502.7	5.2
147	3674	0.7	23.1907	24.0	0.169	24.1	0.028	1.0	0.0	180.9	1.8	158.7	35.4	-160.6	604.8	180.9	1.8
1018	5028	1.5	17.9920	4.4	0.237	4.5	0.031	1.1	0.2	196.5	2.1	216.1	8.8	435.6	97.1	196.5	2.1

Appendix A Cont.: U-Pb detrital zircon geochronologic analyses by Laser-Ablation Multicollector ICP Mass Spectrometry

					Isotope ratios						Apparent ages (Ma)						
U (ppm)	206Pb 204Pb	U/Th	206Pb* 207Pb*	± (%)	207Pb* 235U*	± (%)	206Pb* 238U	± (%)	error corr.	206Pb* 238U*	± (Ma)	207Pb* 235U	± (Ma)	206Pb* 207Pb*	± (Ma)	**Best age** (Ma)	± (Ma)
NBP94-07-63 (SAL 164) Cont.																	
167	12156	1.4	12.9778	3.0	2.071	3.1	0.195	0.7	0.2	1147.9	7.8	1139.2	21.3	1122.6	60.3	1122.6	60.3
432	51256	2.2	13.3306	2.7	1.816	2.9	0.176	1.2	0.4	1042.5	11.2	1051.1	19.1	1068.9	53.9	1068.9	53.9
120	3634	1.3	20.1166	24.1	0.251	24.2	0.037	1.3	0.1	231.7	3.0	227.2	49.2	181.4	569.5	231.7	3.0
195	37862	2.8	15.9048	2.5	0.913	2.6	0.105	0.5	0.2	645.7	3.1	658.8	12.4	704.0	53.6	645.7	3.1
653	34918	2.8	19.3727	6.7	0.113	6.8	0.016	0.7	0.1	101.8	0.7	108.9	7.0	268.5	154.1	101.8	0.7
474	33530	4.7	17.1706	2.0	0.677	2.0	0.084	0.5	0.2	521.9	2.5	525.0	8.4	538.8	43.3	521.9	2.5
474	39824	2.1	15.8413	2.1	0.961	2.5	0.110	1.3	0.5	675.5	8.0	684.1	12.4	712.5	45.6	675.5	8.0
184	16450	3.2	16.6601	2.4	0.736	2.5	0.089	0.5	0.2	549.2	2.7	560.1	10.6	604.4	52.2	549.2	2.7
313	6402	1.9	16.3907	6.8	0.675	7.2	0.080	2.5	0.4	497.3	12.1	523.5	29.5	639.6	145.6	497.3	12.1
155	28316	2.7	17.5438	5.2	0.649	5.2	0.083	0.7	0.1	511.7	3.3	508.1	20.9	491.5	114.3	511.7	3.3
39	748	2.0	19.4582	130.9	0.108	131.0	0.015	4.4	0.0	97.1	4.2	103.7	129.8	258.4	1095.8	97.1	4.2
364	58552	4.8	13.4188	3.7	1.334	10.0	0.130	9.3	0.9	786.7	69.1	860.5	58.3	1055.7	74.3	1055.7	74.3
244	4454	2.0	14.6040	17.0	0.825	17.0	0.087	1.3	0.1	540.2	6.8	610.9	78.2	883.0	353.1	540.2	6.8
371	2546	0.5	18.6429	4.1	0.252	5.1	0.034	3.0	0.6	215.9	6.4	228.1	10.3	355.9	91.6	215.9	6.4
299	2272	3.9	15.2079	3.0	0.842	3.1	0.093	0.8	0.2	572.3	4.2	620.1	14.2	798.6	62.3	572.3	4.2
89	392	1.5	11.7179	47.7	0.206	47.9	0.018	4.2	0.1	111.8	4.7	190.1	83.3	1323.2	984.4	111.8	4.7
NBP94-07-39 (SAL 278)																	
1296	15976	0.5	19.6877	3.4	0.144	4.3	0.021	2.6	0.6	131.5	3.3	136.9	5.5	231.4	78.6	131.5	3.3
668	12740	0.8	20.4557	6.1	0.166	6.6	0.025	2.6	0.4	156.7	4.0	155.8	9.6	142.4	143.5	156.7	4.0
174	1212	2.1	10.6081	4.8	1.063	5.0	0.082	1.5	0.3	506.5	7.1	735.1	26.1	1513.5	90.0	1513.5	90.0
314	7870	2.3	19.2307	4.7	0.304	4.9	0.042	1.0	0.2	268.0	2.7	269.8	11.5	285.4	108.6	268.0	2.7
323	36230	10.1	17.7325	2.4	0.635	2.8	0.082	1.5	0.5	506.2	7.2	499.3	11.2	467.9	53.7	506.2	7.2
146	8960	1.7	20.4107	9.8	0.237	10.0	0.035	2.0	0.2	222.4	4.3	216.0	19.5	147.5	230.5	222.4	4.3
217	9368	1.9	19.1136	8.2	0.380	9.0	0.053	3.8	0.4	330.8	12.1	326.9	25.3	299.3	188.0	330.8	12.1
ELT32-21 (SAL 1640)																	
164	22785	2.4	17.3819	4.0	0.701	4.9	0.088	2.7	0.6	546.0	14.1	539.5	20.3	511.9	88.6	546.0	14.1
185	21115	0.6	17.6126	3.2	0.675	4.0	0.086	2.3	0.6	533.0	11.7	523.6	16.2	482.9	71.4	533.0	11.7
315	33225	1.9	17.1024	1.6	0.686	4.3	0.085	4.0	0.9	526.5	20.2	530.4	17.8	547.4	35.1	526.5	20.2
313	44625	1.3	13.0665	1.1	1.776	6.1	0.168	6.0	1.0	1002.9	55.9	1036.8	39.8	1109.0	21.7	1109.0	21.7
878	11085	2.5	15.6344	4.7	0.704	8.4	0.080	6.9	0.8	495.3	33.0	541.4	35.1	740.3	98.9	495.3	33.0
644	63535	9.3	16.3723	3.5	0.788	4.4	0.094	2.6	0.6	576.9	14.5	590.3	19.6	642.0	75.1	576.9	14.5
31	6140	15.3	17.3918	12.3	0.689	14.0	0.087	6.7	0.5	537.6	34.4	532.5	58.1	510.7	271.4	537.6	34.4
273	37140	3.9	17.1038	2.4	0.753	3.5	0.093	2.6	0.7	575.6	14.3	569.9	15.3	547.3	52.0	575.6	14.3

Appendix A Cont.: U-Pb detrital zircon geochronologic analyses by Laser-Ablation Multicollector ICP Mass Spectrometry

U (ppm)	206Pb 204Pb	U/Th	206Pb* 207Pb*	± (%)	207Pb* 235U*	± (%)	206Pb* 238U	± (%)	error corr.	206Pb* 238U*	± (Ma)	207Pb* 235U	± (Ma)	206Pb* 207Pb*	± (Ma)	**Best age (Ma)**	± (Ma)
					Isotope ratios							**Apparent ages (Ma)**					
ELT32-21 (SAL 1640) Cont.																	
167	26855	1.4	15.4975	3.9	0.933	4.4	0.105	2.0	0.5	643.2	12.4	669.5	21.4	758.9	81.8	643.2	12.4
306	28825	1.6	17.6279	2.1	0.631	3.8	0.081	3.2	0.8	500.4	15.3	496.9	14.9	481.0	46.4	500.4	15.3
488	36870	7.9	17.1974	2.1	0.675	2.2	0.084	0.6	0.3	520.9	3.1	523.6	8.8	535.3	45.3	520.9	3.1
1184	71375	6.6	15.1492	1.5	0.949	4.6	0.104	4.4	0.9	639.2	26.6	677.4	22.8	806.7	31.4	639.2	26.6
261	71695	3.6	13.9399	2.8	1.673	3.4	0.169	2.0	0.6	1007.4	18.3	998.3	21.9	978.5	57.7	978.5	57.7
262	45020	3.4	17.9485	7.8	0.705	7.9	0.092	1.0	0.1	565.9	5.4	541.7	33.0	441.0	173.5	565.9	5.4
223	33440	1.2	17.0036	3.0	0.782	4.8	0.096	3.7	0.8	593.6	21.1	586.7	21.3	560.1	65.7	593.6	21.1
171	23760	2.3	17.1431	4.1	0.751	5.7	0.093	4.0	0.7	575.3	22.0	568.7	24.8	542.3	88.6	575.3	22.0
699	119860	2.0	13.4994	2.6	1.726	3.5	0.169	2.5	0.7	1006.5	22.8	1018.3	22.8	1043.6	51.7	1043.6	51.7
534	27195	2.2	17.6709	2.5	0.612	3.5	0.078	2.5	0.7	487.0	11.7	485.0	13.6	475.6	54.9	487.0	11.7
254	38460	2.0	16.0297	2.7	0.988	5.6	0.115	4.9	0.9	700.7	32.5	697.5	28.2	687.3	58.1	700.7	32.5
165	90965	1.2	4.7925	2.6	15.686	2.7	0.545	0.7	0.3	2805.2	16.8	2857.8	25.3	2895.2	41.4	2895.2	41.4
155	14000	1.2	17.5449	5.8	0.593	6.9	0.075	3.7	0.5	468.8	16.8	472.7	25.9	491.4	127.2	468.8	16.8
620	6885	2.9	14.6676	4.6	0.731	6.4	0.078	4.4	0.7	483.0	20.6	557.3	27.4	873.9	95.4	483.0	20.6
137	17980	2.4	17.0628	3.1	0.699	3.4	0.086	1.4	0.4	534.8	7.3	538.1	14.1	552.5	66.9	534.8	7.3
230	60950	3.5	13.6123	2.6	1.662	2.7	0.164	0.9	0.3	979.6	8.1	994.3	17.2	1026.7	51.8	1026.7	51.8
465	17360	2.8	13.1221	2.6	1.650	2.7	0.157	0.8	0.3	940.0	6.6	989.4	17.1	1100.5	52.1	1100.5	52.1
553	99200	4.9	13.7273	2.0	1.710	2.6	0.170	1.6	0.6	1013.5	14.9	1012.3	16.6	1009.7	41.4	1009.7	41.4
273	40450	1.7	16.9042	6.3	0.814	6.4	0.100	0.8	0.1	613.3	4.4	604.8	29.1	572.9	138.0	613.3	4.4
390	96365	56.0	16.1764	2.2	0.906	3.2	0.106	2.4	0.7	651.5	14.7	655.1	15.5	667.8	46.7	651.5	14.7
223	26775	2.0	18.0499	4.1	0.626	4.4	0.082	1.6	0.4	507.8	7.6	493.6	17.2	428.5	91.9	507.8	7.6
334	66925	3.0	13.2176	4.3	1.904	4.5	0.183	1.1	0.3	1081.0	11.3	1082.6	29.7	1086.0	86.4	1086.0	86.4
227	138595	1.5	6.0403	3.6	10.852	3.6	0.475	0.5	0.1	2507.2	10.4	2510.5	33.6	2513.2	60.2	2513.2	60.2
542	31225	2.6	17.0851	2.9	0.656	3.2	0.081	1.4	0.4	503.8	6.7	512.1	12.9	549.7	63.4	503.8	6.7
234	47785	1.9	13.5864	3.3	1.803	3.5	0.178	1.1	0.3	1054.3	10.2	1046.6	22.8	1030.6	67.3	1030.6	67.3
581	13600	8.2	13.2810	1.3	1.586	1.5	0.153	0.7	0.5	916.6	6.1	964.8	9.1	1076.4	25.7	1076.4	25.7
188	31265	3.0	14.0664	2.5	1.508	2.7	0.154	1.0	0.4	922.4	8.7	933.6	16.5	960.0	51.3	922.4	8.7
254	44455	3.6	13.1394	3.8	1.601	3.9	0.153	0.5	0.1	915.2	4.3	970.5	24.1	1097.9	76.7	1097.9	76.7
204	45440	1.4	11.0693	1.8	2.842	2.9	0.228	2.3	0.8	1324.9	27.7	1366.7	21.8	1432.7	33.6	1432.7	33.6
763	27420	2.3	20.3267	2.4	0.209	3.7	0.031	2.8	0.8	195.4	5.4	192.5	6.5	157.2	56.2	195.4	5.4
72	572	20.3	8.1992	6.7	1.446	6.9	0.086	1.7	0.2	531.9	8.8	908.3	41.6	1985.1	119.7	1985.1	119.7
478	35536	3.5	14.9000	3.2	1.224	8.1	0.132	7.5	0.9	800.9	56.3	811.7	45.5	841.3	66.9	800.9	56.3
987	57968	3.5	13.8293	2.2	1.480	5.5	0.148	5.0	0.9	892.4	41.8	922.4	33.2	994.7	44.7	892.4	41.8

Appendix A Cont.: U-Pb detrital zircon geochronologic analyses by Laser-Ablation Multicollector ICP Mass Spectrometry

					Isotope ratios							Apparent ages (Ma)					
U (ppm)	206Pb 204Pb	U/Th	206Pb* 207Pb*	± (%)	207Pb* 235U*	± (%)	206Pb* 238U	± (%)	error corr.	206Pb* 238U*	± (Ma)	207Pb* 235U	± (Ma)	206Pb* 207Pb*	± (Ma)	**Best age** (Ma)	± (Ma)
ELT32-21 (SAL 1640) Cont.																	
130	16132	2.4	17.2287	6.1	0.718	6.6	0.090	2.4	0.4	554.0	12.8	549.6	27.9	531.3	133.9	554.0	12.8
260	40096	5.6	14.3658	2.6	1.464	4.2	0.153	3.3	0.8	915.4	28.2	915.8	25.6	916.9	54.3	915.4	28.2
480	57400	8.0	14.8810	2.7	1.122	6.2	0.121	5.6	0.9	736.6	39.0	763.7	33.5	844.0	57.0	736.6	39.0
299	37048	1.8	16.2962	4.1	0.762	4.7	0.090	2.3	0.5	556.0	12.0	575.2	20.6	652.0	88.5	556.0	12.0
104	480	4.5	7.3288	2.7	1.511	2.9	0.080	0.9	0.3	497.9	4.5	934.7	17.5	2182.6	47.2	2182.6	47.2
ELT27-14 (SAL 1634)																	
95	33200	1.8	5.6502	3.5	10.493	7.0	0.430	6.1	0.9	2305.7	118.3	2479.3	65.1	2624.8	57.6	2624.8	57.6
133	32512	0.8	8.4244	1.8	5.748	2.0	0.351	0.9	0.5	1940.4	15.8	1938.7	17.6	1936.8	32.2	1936.8	32.2
122	15916	2.5	16.8259	5.3	0.880	5.7	0.107	2.1	0.4	657.9	13.1	641.2	26.9	582.9	114.3	657.9	13.1
147	14196	2.9	16.5534	4.9	0.821	5.1	0.099	1.6	0.3	606.1	9.4	608.7	23.4	618.3	104.8	606.1	9.4
412	38740	3.9	16.8792	3.3	0.788	3.8	0.097	1.8	0.5	593.9	10.3	590.2	16.9	576.1	71.8	593.9	10.3
80	8112	2.1	17.6335	6.0	0.720	6.5	0.092	2.6	0.4	567.7	14.1	550.5	27.7	480.3	132.1	567.7	14.1
283	27128	2.2	16.7896	6.4	0.737	6.4	0.090	1.1	0.2	554.0	5.6	560.6	27.7	587.6	137.9	554.0	5.6
346	32752	1.3	17.0488	4.4	0.783	4.9	0.097	2.2	0.4	595.8	12.4	587.3	21.8	554.3	95.7	595.8	12.4
ELT27-14 (SAL 1635)																	
69	15500	4.4	13.8674	3.4	1.701	3.5	0.171	0.8	0.2	1017.8	7.8	1008.7	22.3	989.1	68.8	989.1	68.8
76	39800	1.8	5.4064	2.1	11.805	3.7	0.463	3.1	0.8	2452.3	62.4	2589.1	34.9	2697.9	35.0	2697.9	35.0
272	23395	1.3	17.5609	3.3	0.652	3.8	0.083	1.9	0.5	514.1	9.3	509.6	15.1	489.4	72.1	514.1	9.3
198	20250	2.1	17.2895	4.9	0.718	6.2	0.090	3.7	0.6	555.5	19.8	549.3	26.1	523.6	107.6	555.5	19.8
383	166010	1.1	3.5148	2.9	23.530	3.1	0.600	1.0	0.3	3029.2	23.0	3249.1	29.8	3387.9	45.4	3387.9	45.4
ELT27-14 (SAL 1637)																	
368	37495	1.2	17.4693	3.5	0.687	4.0	0.087	1.9	0.5	537.9	9.6	530.9	16.5	500.9	77.5	537.9	9.6
193	22520	1.3	16.6531	3.6	0.776	4.4	0.094	2.5	0.6	577.6	13.8	583.2	19.5	605.3	78.4	577.6	13.8
ELT32-20 (SAL 1638)																	
91	48220	8.8	3.8419	3.0	21.411	3.9	0.597	2.5	0.6	3016.2	59.7	3157.4	37.9	3248.4	47.4	3248.4	47.4
82	6124	0.3	15.6738	12.9	0.835	13.4	0.095	3.6	0.3	584.5	20.2	616.3	62.2	735.0	275.1	584.5	20.2
116	39592	2.1	9.9595	2.6	3.917	3.2	0.283	1.8	0.6	1606.3	24.9	1617.3	25.6	1631.6	48.9	1631.6	48.9
178	34216	1.1	10.9853	2.3	3.074	3.4	0.245	2.5	0.7	1412.0	31.6	1426.1	25.8	1447.2	43.0	1447.2	43.0
99	50796	1.7	3.2271	1.7	30.387	1.7	0.711	0.5	0.3	3463.1	13.4	3499.4	17.0	3520.3	25.5	3520.3	25.5
364	44524	1.5	16.8167	3.7	0.805	4.1	0.098	1.7	0.4	603.9	9.6	599.8	18.6	584.1	81.2	603.9	9.6
251	15044	1.1	17.5980	4.8	0.609	6.5	0.078	4.4	0.7	482.5	20.4	482.9	25.0	484.7	106.3	482.5	20.4
64	29796	1.1	10.6253	4.2	3.488	4.3	0.269	1.1	0.2	1534.9	14.6	1524.6	33.9	1510.4	78.6	1510.4	78.6

Appendix A Cont.: U-Pb detrital zircon geochronologic analyses by Laser-Ablation Multicollector ICP Mass Spectrometry

					Isotope ratios							**Apparent ages (Ma)**					
U (ppm)	206Pb 204Pb	U/Th	206Pb* 207Pb*	± (%)	207Pb* 235U*	± (%)	206Pb* 238U	± (%)	error corr.	206Pb* 238U*	± (Ma)	207Pb* 235U	± (Ma)	206Pb* 207Pb*	± (Ma)	**Best age** (Ma)	± (Ma)
RISP (SAL 222)																	
197	21696	2.0	17.5296	4.3	0.662	4.9	0.084	2.4	0.5	520.9	11.9	515.8	19.9	493.3	95.4	520.9	11.9
236	8332	1.1	20.2182	11.2	0.217	11.7	0.032	3.4	0.3	201.9	6.8	199.4	21.1	169.7	261.4	201.9	6.8
281	30408	2.5	16.3407	2.1	0.939	5.6	0.111	5.2	0.9	680.2	33.4	672.3	27.4	646.1	44.6	680.2	33.4
916	67216	3.7	17.1641	3.6	0.652	6.6	0.081	5.5	0.8	503.4	26.5	510.0	26.3	539.6	79.2	503.4	26.5
316	24921	2.1	16.9352	3.3	0.665	3.5	0.082	1.3	0.4	506.3	6.4	517.8	14.4	568.9	71.6	506.3	6.4
132	25371	1.8	17.1850	6.4	0.674	6.7	0.084	1.7	0.3	520.0	8.6	523.2	27.3	536.9	141.0	520.0	8.6
1061	26331	3.0	19.4878	3.8	0.219	4.5	0.031	2.3	0.5	196.4	4.4	200.9	8.2	255.0	88.5	196.4	4.4
210	10413	1.4	15.2701	5.3	0.735	5.9	0.081	2.6	0.4	504.4	12.7	559.4	25.5	790.0	111.8	504.4	12.7
235	61077	3.9	13.5702	1.7	1.747	1.9	0.172	0.7	0.4	1022.6	6.3	1025.9	12.0	1033.0	35.2	1033.0	35.2
215	70206	3.9	13.0881	3.0	1.776	3.3	0.169	1.3	0.4	1004.5	12.1	1036.8	21.1	1105.7	59.6	1105.7	59.6
312	35997	1.6	17.2202	3.8	0.657	3.9	0.082	0.5	0.1	508.2	2.4	512.6	15.6	532.5	84.0	508.2	2.4
404	30027	8.2	14.9851	2.5	1.189	3.6	0.129	2.6	0.7	783.5	19.3	795.6	19.8	829.4	51.3	783.5	19.3
524	6927	1.7	15.8122	3.3	0.626	3.5	0.072	0.9	0.3	446.7	3.8	493.4	13.5	716.4	71.0	446.7	3.8
377	38007	3.6	17.3959	2.5	0.649	3.1	0.082	1.9	0.6	507.1	9.1	507.6	12.5	510.2	55.5	507.1	9.1
203	34155	3.4	17.4056	2.5	0.677	5.0	0.085	4.4	0.9	528.4	22.1	524.7	20.6	509.0	55.2	528.4	22.1
151	22791	2.6	18.3433	7.1	0.620	7.2	0.083	1.1	0.2	511.1	5.3	490.0	27.8	392.4	159.0	511.1	5.3
322	69987	2.3	13.4626	0.8	1.712	1.5	0.167	1.3	0.8	996.3	11.6	1013.0	9.6	1049.1	16.2	1049.1	16.2
200	46767	1.9	17.3541	4.4	0.660	4.9	0.083	2.1	0.4	514.4	10.3	514.6	19.8	515.4	97.5	514.4	10.3

REFERENCES CITED

Alley, R.B., Bindschadler, R.A., 2001, The West Antarctic Sheet and sea-level change: The West Antarctica Ice Sheet: Behavior and Environment: Antarctic Research Series, v. 77, p. 1-11.

Amelin, Yuri, 2005, A tale of early earth told in zircons: Science, v. 310, p. 1914-1915.

Anderson, J. B., Shipp, S. S., Bartek, L. R., Reid, D.E., 1992, Evidence for a grounded ice sheet on the Ross Sea continental shelf during the Late Pleistocene and preliminary paleodrainage reconstruction: Contributions to Antarctic Research: Antarctic Research Series, v. 57, p. 39-62.

Barrett, P.J., 1991, The Devonian to Jurassic Beacon Supergroup of the Transantarctic Mountains and correlatives in other parts of Antarctica. In: Tingey, R.J. (Ed.), The Geology of Antarctica. Oxford University Press, New York, pp. 120-152.

Behrendt, J.C., LeMasurier, W.E., Cooper, A.K., Tessenohn, F., Trehu, A, Damaske, D., 1991, The West Antarctic rift system- A review of geophysical investigations: American Geophysical Union Antarctic Research Series, v. 53, p. 67-112.

Bell, Robin E., 2008, The role of subglacial water in ice-sheet mass balance: Nature Geoscience, v. 1, p. 297-304.

Bennett, V.C., and Fanning, C.M., 1993, A glimpse of the cryptic Gondwana shield: Archean and Proterozoic ages from the central Transantarcitc Mountains: Geological Society of America Abstracts with Programs, v. 25, no. 6, p.49.

Bindschadler, Robert, 1998, What is happening to the West Antarctic Ice Sheet?: American Geophysical Union, v. 79, no. 22, p. 257, 264-265.

Bindschadler, Robert, 1998, Future of the West Antarctic Ice Sheet: Science, v. 282, p. 428-429.

Black, L.P., James, P.R., Harley, S.L., 1983, Geochronology and geological evolution of metamorphic rocks in the Field Islands area, East Antarctica: J. Metamorphic Geology, v. 1, p. 227-303.

Borg, S.G., DePaolo, D.J., Smith, B.M., 1990, Isotopic structure and tectonics of the central Transantarctic Mountains: Journal of Geophysical Research, v. 95, no. B5, p. 6647-6667.

Borg, S.G., Goodge J.W., Bennett V.C., and Depaolo D.J., 1987, Geochemistry of granites and metamorphic rocks: central Transantarctic Mountains: Antarctic Journal, v. 22, p. 21-23.

Campbell, I.H., Reiners, P.W., Allen, C.M, Nicolescu, S., Upadhyay, R., 2005, He-Pb double dating of detrital zircons from the Ganges and Indus Rivers: Implication for quantifying sediment recycling and provenance studies: Earth and Planetary Science Letters, v. 237, p. 402-432.

Conway, H., Hall, B.L., Denton, G.H., Gades, A.M., Waddington, E.D., 1999, Past and future grounding-line retreat of the West Antarctic Ice Sheet: Science, v. 286, p. 280-283.

Davis, M.B., and Blankenship D., 2006, Geology of the Scott-Reedy Glaciers Area, Southern Transantarctic Mountains, Antarctica, GSA Map Series MCH093F, The Geological Society of America, Boulder, CO.

Denton, G.H., Hughes, T.J., 2002, Reconstruction of the Antarctic Ice Sheet at the Last Glacial Maximum, Quaternary Science Reviews, v. 21, p. 193-202.
Doumani, G.A., and Minshew, V.H. (1965). General geology of the Mount Weaver area, Queen Maud Mountains, Antarctica, Antarctic Research Series, vol. 1299.
Elliot, D.H., 1975, Gondwana basins of Antarctica, in K.S.W. Campbell, ed., Gondwana Geology, Australian National University Press, Canberra, Australia, p. 493-536.
Encarnación, J., Fleming, T.H., Elliot, D.H., Eales, J.V., 1996, Synchronous emplacement of Ferrar and Karoo dolerites and the early breakup of Gondwana., Geology, v. 24, p. 535-538.
Fahnestock, Mark, Bamber, Jonathan, 2001, Morphology and surface characteristics of the West Antarctic Ice Sheet: The West Antarctica Ice Sheet: Behavior and Environment: Antarctic Research Series, v. 77, p. 13-27.
Farmer, G. Lang, Licht, Kathy, Swope, R. Jeffrey, Andrews, John, 2006, Isotopic Constraints on the provenance of fine-grained sediment in LGM tills from the Ross Embayment, Antarctica: Earth and Planetary Science Letters, v. 249, p. 90-107.
Faure, G., Eastin R., Ray, P.T., McLellend, D., Shultz, C.H., 1979, Geochronology of igneous and metamorphic rocks, central Transantarctic mountains, in Fourth International Gondwana Symposium, ed. B. Laskar and C.S. Raja Rao, p. 805-813.
Fitzgerald, P.G., and Baldwin, S.L., 2007, Thermochronologic constraints on Jurassic rift flank denudation in the Thiel Mountains, Antarctica: U.S. Geological Survey and The National Academies, USGS of- 2007-1047, Short Research Paper 044.
Gehrels, G., Ruiz, J., in review, U-Th-Pb geochronology of zircon by Laser Ablation-Multicollector ICP Mass Spectrometry at the Arizona LaserChron Center: Journal of Analytical Atomic Spectrometry.
Gehrels, G., Valencia, V., and Pullen, A., 2006, Detrital zircon geochronology by laser-ablation multicollector ICPMS at the Arizona Laserchron Center, in Loszewski, T., and Huff, W., eds., Geochronology: Emerging Opportunities: Paleontological Society Papers, v. 12, pp. 67-76.
Goodge, J.W., 2007, Metamorphism in the Ross orogen and its bearing on Gondwana margin tectonics, in Cloos, M., Carlson, W.D., Gilbert, M.C., Liou, J.G., Sorensen, S.S., eds., Convergent Margin Terrains and Associated Regions: A tribute to W.G. Ernst: Geological Society of America Special paper, v. 419, p. 185-206.
Goodge, J.W., 2006, Transantarctic Mountains: Geology, Encyclopedia of the Antarctic, New York, Routledge Press, 2007, v. 2, p. 1007-1012.
Goodge, J.W., and Fanning C.W., 2002, Precambrian costal history of Nimrod Group, central Transantarctic Mountains: Royal Society of New Zealand Journal, v. 35, p. 43-50.
Goodge, J.W., and Fanning, M.C., 1999, 2.5 b.y. of punctuated Earth history as recorded in a single rock; Geology, v. 27, no. 11, p. 1007-1010.
Goodge, J.W., Fanning, M.C., Bennett, V.C., 2001, U-Pb evidence of ~1.7 Ga crustal tectonism during the Nimrod Orogeny in the Transantarctic Mountains, Antarctia: implications for Proterozoic plate reconstructions: Precambrian Research, v.112, p. 261-288.

Goodge, J.W., Myrow, P., Williams, S., Bowring, S.A., 2002, Age and Provenance of the Beardmore Group, Antarctica: Constraints of Rodiana Supercontinent breakup: Journal of geology, V. 110, p. 393-403.
Goodge, J.W., Williams, I.S., Myrow, P., 2004, Provenance of Neoproterozoic and lower Paleozoic siliciclastic rocks of the central Ross orogen, Antarctica: Detrital record of rift-, passive-, and active-margin sedimentation: Geological Society of America Bulletin, v. 116, no. 9/10, p. 1253-1279.
Grikurov, G.E., 1982, Structure of Antarctica and outline of its evolution, Antarctic Geoscience, University of Wisconsin Press, p. 791-804.
Gyunn, Jerome, 2006, Comparison of detrital zircon age distributions using the K-S test: Department of Geosciences, University of Arizona, Tucson, 10p.
Harrison, T.M., Blinchert-Toft, J., Muller, W., Albarede, F., Holden, P., Mojzsis, S.J., 2005, Heterogeneous hadean hafnium: Evidence of continental crust at 4.5-4.5Ga: Science, v. 310, p. 1947-1950.
Kamenev, E.N., 1982, Antarctica's oldest metamorphic rocks in the Fyfe Hills, Enderby Land, in Craddock, C., ed., Antarctic Geoscience: University of Wisconsin Press, Madison, pp. 505-510
Koroznikova, L., Klutke, C., McKnight, S., Hall, S., 2007, The use of low-toxic heavy suspensions in mineral sands evaluation and zircon fractionation: The Southern African Institute of Mining and Metallurgy, p. 21-29.
Kyle P.R., 1990, McMurdo volcanic group western Ross Embayment. In: LeMasurier, W.E., Thompson, L.W. (Eds.), Volcanoes of the Antarctic Plate and Southern Oceans. American Geophysical Union, Washington, DC, pp. 48-80.
Le Masurier, W.E, Rex, D.C., 1991, The Marie Bryd land volcanic province and its relation to the Cenozoic West Antarctic rift system. In Tingey, R.J. (Ed.), The Geology of Antarctica. Oxford University Press, New York, p. 249-284.
Lee, J.K. W., Williams, I.S., Ellis, D.J., 1997, Pb U The diffusion in natural zircon, Nature, no. 390, p. 159-162.
Licht, Kathy J., Lederer, Jason R., Swope, R. Jeffrey, 2005, Provenance of the LGM glacial till (sand fraction) across the Ross embayment, Antarctica: Quaternary Science Reviews, v. 24, p. 1499-1520.
Ludwig, K.R., 2003, Isoplot 3.00: Berkeley Geochronology Center, Special Publication no. 4, 70 p.
Luyendyk, B.P., Wilson, D.S., Siddoway, C.S., 2003, Eastern margin of the Ross Sea Rift in western Marie Byrd Land, Antarctica: Crustal Structure and tectonic development: Geochemistry Geophysics Geosystems an electronic Journal of th Earth Sciences, v. 4, no. 10, p. 1-25.
Minshew, V. H., 1965, Potassium Argon age from a granite at Mount Wilbur, Queen Maud Range, Antarctica: Science, vol. 150, pp. 741-743.
Mosola, Amanda B., Anderson, John B., 2006, Expansion and rapid retreat of the West Antarctic Ice Sheet in eastern Ross Sea: possible consequence of over-extended ice streams?: Quaternary Science Reviews, v. 25, p. 2177-2196.
Myrow, P.M., Pope, M.C., Goodge, J.W., Fischer, W., Palmer, A.R., 2002, Depositional history of pre-Devonian strata and timing of Ross orogenic tectonism in the central Transantarctic Mountains, Antarctica; Geological Society of America Bulletin, v.114, no. 9, p. 1070-1088.

Oppenheimer, Michael, 1998, Global warming and the stability of the West Antarctic Ice Sheet: Nature, v. 393, p. 325-332.
Pankhurst, R.J., Weaver, S.D., Bradshaw, J.D., Storey, B.C., and Ireland, T.R., 1998, Geochronology and geochemistry of pre-Jurrassic superterranes in Marie Byrd Land, Antarctica, Journal of Geophysical Research, v. 1033, B2: 2529-2547.
Palmer, E.F., and Licht, K.J., 2007, Sand petrography and U/Pb detrital zircon geochronology of late Quaternary tills from the Byrd Glacier and central/western Ross Sea, Antarctica. In Antarctica: A Keystone in a Changing World: Online Proceedings of the 10th ISAES X, edited by A.K. Cooper and C.R. Raymond et al., USGS Open-File Report 2007-1047, Extended Abstract 134.
Ravich, M.G., 1982, The lower Precambrian of Antarctica - review paper, in Craddock, C., ed., Antarctic Geoscience: University of Wisconsin Press, Madison, pp. 65-71.
Reiners, P.W., Spell, T.L., Nicolescu, Stefan, Zanetti, K.A., 2004, Zircon (U-Th)/He thermochronometry: He diffusion and comparisons with 40Ar/39Ar dating: Geochimica et Cosmochimica Acta, v. 68, no. 8, p. 1857-1887.
Rignot, E., Bamber, J.L., Van Den Broeke, M.R., Davis, C., Li, Y., Van De Berg, W.J., Van Meijgaard, E., 2008, Recent Antarctic ice mass loss form radar interferometry and regional climate modeling: Nature Geoscience, v. 1, p. 106-110.
Rooney, S.T., Blankenship, D.D., Alley, R.B., Bently, C.R., 1991, Seismic reflection profiling of a sediment-filled graben beneath ice stream B, West Antarctica. In: Thomson, M.R.A., Crame, J.A., Thompson, J.W. (Eds.), Geological Evolution of Antarctica. Cambridge University Press, New York, pp. 261-265.
Shipp, Stephanie, Anderson, John, Domack, Eugene, 1999, Late Pleistocene-Holocene retreat of the West Antarctic Ice-Sheet system in the Ross Sea: Part 1-Geophysical results: Geological Society of America Bulletin, v. 111, p. 1486-1516.
Siddoway, C.S., 2008, Tectonics of the West Antarctic Rift System: New light on the history and dynamics of distributed intracontinental extension: Antarctica: A Keystone in a Changing World, 10th International symposium on Antarctic Science, p. 91-113.
Siddoway, C.S., Baldwin, S.L., Fitzgerald, P.G., Fanning, M.C., Luyendyk, B.P., 2004, Ross Sea mylonites and the timing of intracontinental extension within the West Antarctic rift system: Geology, v. 32, no. 1, p. 57-60.
Sobotovich, E.V., Kamenev, E.N., Komaristyy, A.A., and Rudnik, V.A., 1976, The oldest rocks in Antarctica (Enderby Land): International Geological Review, vol. 18, pp. 371-388.
Studinger, M., Bell, R.E., Fitzgerald, P.G., Buck, W.R., 2006, Crustal architecture of the Transantarctic Mountains between the Scott and Reedy Glacier region and South Pole from aerogeophysical data: Earth and Planetary Science Letters, v. 250, p. 182 199.
Stump, E., Gehrels, G., Talarico, F., Carosi, R., 2007, Constraints from detrital zircons geochronology on the early deformation of the Ross Orogeny, Transantarctic Mountains, Antarctica: U.S Geological Survey and The National Academies, USGS of-2007-1047, Extended Abstract 166.

Stump, E., 1995, The Ross Orogen of the Transantarctic Mountains, Cambridge University Press, p. 166-215.
Suttner, L.J., 1974, Sedimentary petrographic provinces: an evaluation, *in* Ross, C.A., *ed.,* Paleogeographic Provinces and Provinciality: SEPM Special Publication, v. 21, pp. 1486–1516
ten Brink, U. S., Hackney, R.I.,Bannister, S.,Stern, T.A., Makovsky. Y., (1997), Uplift of the Transantarctic Mountains and the bedrock beneath the East Antarctic ice sheet, J. Geophys. Res., 102, 27,603–27,621.
Tingey, R.J., 1991, The regional geology of Achaean and Proterozoic rocks in Antarctica, in Tingey, R.J., ed. The geology of Antarctica: Oxford Monographs on Geology and Geophysics 17, Clareden Press, p. 1-73.
Tonarini, S. and Rocchi, S., 1994, Geochronology of Cambro-Ordovician intrusives in Northern Victoria Land: A Review: Terra Antarctica, no. 1, p. 46-50.
Tulaczyk, S., Kamb, B., Scherer, R.P., Engelhardt, H.F., 1998, Sedimentary processes at the base of a West Antarctic ice stream: constraints from textural and compositional properties of subglacial debris: Journal of Sedimentary Research, v. 68, no. 3, p. 487-496.
Velicogna, Isebella, Whar, John, 2006, Measurements of time-variable gravity show mass loss in Antarctica: Science, v. 311, p. 1754-1756.
Winberry, Paul L., Anandakrishnan, Sridhar, 2004, Crustal structure of the West Antarctic rift system and Marie Byrd Land hotspot: Geology, v. 32, no. 11, p. 977-980.